UNIVERSITY OF CALIFORNIA

SANTA CRUZ

SYSTEMATIC ANALYSIS OF TWO-COMPONENT SIGNAL TRANSDUCTION SYSTEMS IN VIBRIO CHOLERAE BIOFILM FORMATION AND VIRULENCE

A dissertation submitted in partial satisfaction
of the requirements for the degree of

DOCTOR OF PHILOSOPHY

in

MICROBIOLOGY AND ENVIRONMENTAL TOXICOLOGY

by

Andrew Tak-Tung Cheng

June 2015

The Dissertation of
Andrew T. Cheng is approved:

_____
Professor Fitnat H. Yildiz, Chair

_____
Professor Karen M. Ottemann

_____
Professor Grant A. Hartzog

_____
Professor Victoria Auerbuch-Stone

_____
Tyrus Miller
Vice Provost and Dean of Graduate Studies

TABLE OF CONTENTS

LIST OF FIGURES

Systematic analysis of two-component signal transduction system in *Vibrio cholerae* biofilm formation and virulence

by

Andrew Tak-Tung Cheng

ABSTRACT

Vibrio cholerae, the causative agent of cholera, is a facultative human pathogen that can inhabit aquatic environments and human intestines. Its survival in aquatic habitats is critical for its transmission to humans. However, how *V. cholerae* senses and responds to fluctuating environmental factors experienced during aquatic and intestinal growth remains to be explained.

One way in which *V. cholerae* could sense and respond to changes in the environment is through use of a two-component signal transduction systems (TCS). The TCS can regulate a wide variety of behaviors and processes, including virulence, biofilm formation, stress response, and motility. The prototypical TCS consists of a membrane-bound histidine (HK), which senses environmental signals and a corresponding response regulator (RR), which mediates a cellular response. I investigated the role of each TCS in *V. cholerae* infection and biofilm formation by focusing on RRs, the most downstream component.

First, I performed mutational analysis of all (53) RRs. I generated a set of 53 isogenic RR mutants in *V. cholerae* by deletion analysis. To test whether *V. cholerae* these RRs are involved in virulence, I screened my library of 53 RR deletion mutants in a murine model of infection. In addition to the 13 previously identified RRs that control virulence, I identified an uncharacterized TCS named VxrB (*Vibrio* type six regulator) that is required for intestinal colonization. Transcriptome analysis revealed that VxrB activates type VI secretion system (T6SS) genes, which encode a complex molecular machine to inject effector proteins into target cells. Identification of a new TCS controlling virulence is significant because it fills gaps in our knowledge about *V. cholerae* pathogenesis, contributes to the general understanding of how TCS is regulated and suggests new methods for manipulating pathogenic behavior to improve human health. This could represent a target for developing anti-bacterial strategies.

Regulation of biofilm formation in *V. cholerae* involves several transcriptional regulators and alternative sigma factors, such as RpoN. The exact mechanism by which RpoN impacts biofilm formation is yet to be determined. RpoN functions together with the NtrC family of RR, thus raising the possibility that biofilm formation requires both RpoN and an NtrC family RR. In this study, I analyzed the role of the eight NtrC family RRs in biofilm formation and identified four of these RR's regulating biofilm formation. LuxO

positively regulates biofilm formation. In contrast FlrC, FlrA and NtrC negatively regulate biofilm formation. Consistent with this observation, whole-genome expression profiling and transcriptional reporter assays revealed that expression of the *Vibrio* polysaccharide (*vps*) genes and genes encoding the two positive transcriptional regulators, VpsR and VpsT, is increased in an *ntrC* mutant. Epistasis analysis showed that NtrC acts in parallel with HapR and CRP-cAMP complex, the negative regulators of biofilm formation. This study underscores the importance of NtrC family of response regulators in the regulation of biofilm formation in *V. cholerae*. Furthermore, elucidation of the mechanism for regulation of biofilm formation will provide the foundation for developing novel treatments and prevention strategies against cholera, and will facilitate anti-biofilm interventions.

To examine whether *V. cholerae* TCS signal pathways are involved in biofilm formation, I screened my 53 RR deletion mutants for the expression of *Vibrio* polysaccharide (*vps*) genes and analyzed the ability of these deletion mutants to form three dimensional biofilms in a flow-cell environment. These studies led to the identification of two (*ntrC* and *vxrB*) regulators of *vps* gene expression and five (*ntrC*, *vxrB*, VC1348, *flrC*, and *flrA*) regulators of biofilm formation. Since VxrB has previously been shown to regulate virulence, I wanted to further investigate its role in biofilm formation. VxrB positively

regulates biofilm formation and expression of *vps* genes. This study revealed that expression of biofilm genes and T6SS genes are co-regulated by VxrB.

This study identified critical TCSs regulating virulence and biofilm formation in *V. cholerae* and furthered our knowledge of regulation of environmental adaptation by an important human pathogen.

This work is dedicated to my mother and father.

ACKNOWLEDGEMENTS

First, I would like to thank my advisor, Dr. Fitnat Yildiz, who provided me with many opportunities to follow my passion for microbiology. I am grateful for her enormous support and encouragement through my graduate career. Her dedication and commitment to her student's success is more than exceptional.

This work would not have been possible without my committee members, Dr. Karen Ottemann, Dr. Grant Hartzog, and Dr. Victoria Auerbuch Stone who provided valuable advice and support. I would also like to thank the members of my qualifying exam committee, Dr. Chad Saltikov, Dr. Karen Ottemann, and Dr. Victoria Auerbuch Stone. I am also grateful for the advice and support from other faculty members of the METX department, Dr. Manel Camps, Dr. Donald Smith, and Dr. Russell Flegal.

I had the pleasure and fortunate opportunity to work with many intelligent and talented individuals throughout my time at UC Santa Cruz. I would like to thank the members of the Yildiz Lab, past and present, who provided a supportive atmosphere where I was allowed to thrive. Thank you Dr. General Nick Fong, Dr. Nick Shikuma, Dr. Kivanc Bilecen, Dr. Sinem Beyhan, Dr. Xianxian Liu, Fabian Rivera, Kimberly Davis, Loni Townsley, Dr. Chris Jones, Dr. David Sanchez-Zamorano, Dr. Ana Gallego, Dr. Carmen Schwechheimer,

Jennifer Kateri-Teschler, Jenna Conner, Andrew Rogers, and Brianna Fees. Also, I would like to thank Dr. Roger Linington, Dr. Kelly Peach, Dr. Laura Sanchez, and Dr. Gabriel Navarro for their advice and support on the biofilm inhibitor projects that we collaborated on.

I would like to thank my parents and brothers for their unconditional support and encouragement. Thank you to my friends who supported me through this process.

Finally, thank you to my partner, Shanna Kim, for your compassion and support.

The text of this dissertation includes reprints of the following previously published material:

Cheng AT, Ottemann KO, Yildiz FH. 2015. *Vibrio cholerae* response regulator VxrB controls colonization and regulates the Type VI secretion system. PLoS Pathog. Plos Pathog. 11(5): e1004933. This publication is presented in Chapter 2.

CHAPTER 1: Introduction

Andrew T. Cheng and Fitnat H. Yildiz

Cholera

Cholera is an infectious disease caused by the Gram negative bacterium, *Vibrio cholerae*. *V. cholerae* is a facultative human pathogen that can inhabit fresh water estuaries and human intestines. *V. cholerae* is contracted through the ingestion of contaminated food or water; after ingestion the bacterium colonizes the small intestine and causes severe watery diarrhea and dehydration, which can lead to death if treatment is not administered. The devastating effect of cholera results in 100,000-120,000 deaths annually (1).

Cholerae is a disease of epidemic and pandemic proportions. There have been seven cholera pandemics that have occurred in the past two centuries. Recent epidemics include those in Haiti, Vietnam, and Zimbabwe (2-4). Seasonal outbreaks also occur in many areas around the world where cholera is endemic, including countries in Asia, Africa, and the Americas (5, 6). A number of environmental factors, including rainfall, salinity, temperature and plankton bloom can determine the timing and severity of seasonal outbreaks (7). Classification of *V. cholerae* into various serogroups is based on somatic antigens (O antigens) (8, 9) and further classified into biotypes based on biochemical properties and susceptibility to phages (10). The six previous pandemics were caused by the classical biotype and isolates from the 7th pandemic are of the O1 El Tor biotype. In 1992, cholera was reported in India and Bangladesh, caused by a non-O1 serogroup, called O139

(Bengal) (11). A recent 2011 outbreak in Haiti has affected over half a million people and has taken over 8,000 lives (2). This demonstrates how cholera continues to be a major public health problem.

V. cholerae virulence regulatory network

V. cholerae produces a number of virulence factors which facilitate colonization of the intestine and subsequent disease. Major virulence factors are cholera toxin (CT), which is responsible for production of profuse watery diarrhea, and a type IV pilus called the toxin-coregulated pilus (TCP), which is required for intestinal colonization (12). CT is encoded by the *ctxAB* genes and TCP is encoded by *tcpA-F* genes (13, 14). *V. cholerae* virulence factors are well known to be under extensive transcriptional control. CT and TCP production are controlled by the transcriptional activator ToxT (15, 16). Activation of *ctxAB* and *tcpA* transcription by ToxT is repressed by the histone-like protein (H-NS), which binds to the same DNA region (17-19). Expression of *toxT*, in turn, is controlled by a virulence regulatory cascade involving the membrane-bound transcriptional activators ToxRS and TcpPH. These regulators activate *toxT* transcription directly (20-22). TcpPH expression is activated by the transcriptional activators AphA and AphB (23, 24). The quorum sensing (QS) regulatory system is also linked to the virulence gene regulatory cascade through HapR, the master QS regulator, which represses *aphA* expression (25).

V. cholerae biofilms

Biofilm formation by *V. cholerae* is known to be a key factor in both the environmental persistence and infectivity of the host (26, 27). Furthermore, the formation of biofilm provides protection from grazing predators (28) and from toxic compounds, such as antimicrobial agents and bactericidal agents such as chlorine (29-31). Biofilms also enable horizontal gene transfer, which can contribute to bacterial evolution (32). Finally, the importance of biofilms in *V. cholerae* infectivity was demonstrated by filtering drinking water particles greater than 40 μm in Bangladeshi villages, which decreased infection rates by 48% (33) and by studies of Tamayo et al. who showed that *V. cholerae* biofilm was more infectious than planktonic bacteria (34).

In the natural aquatic environment, *V. cholerae* can be found in a free swimming planktonic state or attached as biofilms on zooplankton, phytoplankton, detritus and other surfaces. Initial attachment to biotic or abiotic surfaces, involves the type IV pili mannose-sensitive hemagglutinin pilus (MSHA) (35) and TCP (14). MSHA facilitates early attachment to abiotic surfaces under non-flow conditions (35). *V. cholerae* can exploit chitin as a carbon and nitrogen source in the marine environment, which makes this organism ecologically important in colonizing chitinous surfaces (36, 37). The single polar flagellum, furnished by *V. cholerae*, is also important for surface colonization and biofilm formation. Mutations in a flagellar structural gene,

flagellin A (*flaA*), resulted in increased exopolysaccharide production (38, 39). Thus, it is critical for cells to attach to a surface before they can begin producing extracellular components of biofilm.

Following initial attachment, cells produce the extracellular matrix, which is essential for the formation of mature three-dimensional biofilms. To form biofilms, *V. cholerae* produces an extracellular matrix composed of proteins, nucleic acids, and a glycoconjugate, termed Vibrio polysaccharide (VPS). VPS is a major portion of the biofilm matrix (31, 40). The VPS biosynthesis genes are found in two clusters on the large chromosome of *V. cholerae* O1 El Tor [*vps*U (VC0916), *vpsA*-*K*, VC0917-27 (*vps*-I cluster); *vpsL*-*Q*, VC0934-9 (*vps*-II cluster)] (40). Matrix proteins are another essential component of biofilm formation in *V. cholerae*. In particular, RbmA, RbmC, and Bap1 are required for maintaining the structural integrity of biofilms (41, 42). Recently, Berk et al. showed that RbmA provides cell-cell adhesion, Bap1 allows the developing biofilm to adhere to the surface, and excreted RbmC contributes to the biofilm components that envelope around the cell along with VPS and Bap1 (43). Finally, extracellular DNA is another component of *V. cholerae* biofilm matrix. Seper et al. have shown that extracellular DNA and nucleases are involved in biofilm architecture, nutrient acquisition, and detachment from bacterial biofilms (44).

V. cholerae biofilm regulatory network

V. cholerae biofilm formation is controlled by a complex regulatory network of transcriptional activators, repressors, alternative RNA polymerase sigma factors, small RNAs (sRNA), and signaling molecules. Coordinated regulation by these factors are critical in the formation of biofilm because formation of biofilms is an energetically costly process (reviewed in (45)).

VpsR is the master regulator of biofilm formation in *V. cholerae*. It is a member of the two-component signal transduction system (TCS) and is required to form biofilms (46). VpsT is another activator of biofilm formation and functions as a response regulator. Detailed description of the function of VpsR and VpsT is presented in the "Two component signal transduction systems in *V. cholerae*" section of this chapter.

Two quorum sensing systems negatively regulate *vps* expression. In *V. cholerae* there are two quorum sensing systems that sense two different small signaling molecules, known as autoinducers, Cholera Autoinducer-1 (CAI-1) and Autoinducer-2 (AI-2) (47, 48). CqsA synthesizes CAI-1 (49) and is sensed by its cognate histidine kinase sensor, CqsS, while LuxS synthesizes AI-2 and is sensed by its cognate sensor LuxPQ (50). At low cell density, where there is a low amount of autoinducers, CqsS and LuxPQ autophosphorylate, and transfer the phosphoryl group to the Hpt protein,

LuxU. As a result, LuxU transfers the phosphate to a RR, LuxO, a member of the activator class of NtrC family of response regulators. Phosphorylated LuxO, together with the alternative sigma factor RpoN, activates the expression of Hfq binding sRNAs that mediates inhibition of translation of the master quorum sensing regulator, HapR (51, 52). HapR is also the major negative regulator of biofilm formation in *V. cholerae*. Disruption of *hapR* causes an increase in biofilm formation (53-55). The presence and quantity of quorum sensing molecules will determine the repression or activation of *hapR* expression, which leads to the modulation of biofilm formation (54, 56).

H-NS is a histone-like protein that modulates nucleoid topology and functions as a transcriptional regulator (57). Wang et al. demonstrated that H-NS negatively controls the expression of biofilm formation (57). When VpsT is bound to *vpsL* promoter region, it prevent H-NS negative regulation on *vps* expression. Nonetheless VpsT can also regulate biofilm formation independently of H-NS (58).

Little is known about the signal and molecular mechanisms that activate VpsR. VpsR has a conserved aspartate in the receiver domain that is necessary for its function, however a histidine kinase capable of phosphorylating VpsR has not been identified. Genetic interaction studies suggest that *vpsR* is epistatic to *vpsT* and that VpsR and VpsT positively

regulate their own and each other's expression (59). In an effort to identify a cognate sensor kinase for VpsR, Shikuma et al. overexpressed all of the orphan HKs in a reporter strain harboring a *vpsL-lacZ* transcriptional fusion at the *lacZ* locus on the *V. cholerae* chromosome. This experiment revealed that overexpression of VC1445 (*vpsS*) activated *vps* expression (60). Furthermore, epistatic analysis showed that VpsR is required for VpsS to activate biofilm gene expression. Overexpression studies of *vpsS* in Δ*cqsS*, Δ*luxQ*, and Δ*cqsS*Δ*luxQ* deletions suggested that CqsS and LuxQ are not required for VpsS to activate *vps* expression. However, VpsS requires quorum sensing regulators, LuxU and LuxO, to activate *vps* gene expression. Furthermore, phosphotransfer assays suggested that VpsS can phosphorylate LuxU, which can transfer the phosphate to LuxO and repress HapR expression via Qrr sRNA. The hybrid histidine kinase, VpsS, therefore activates *vps* expression through the quorum sensing phosphotransfer cascade. The signal(s) sensed by VpsS is currently unknown.

Another important signaling molecule which controls the expression of *vps* genes is the ubiquitous second messenger, cyclic dimeric guanosine monophosphate (c-di-GMP). C-di-GMP controls the life style switch between a free living and biofilm lifestyle (61). Diguanylate cyclases (DGC), which contain GGDEF domains, produce c-di-GMP and c-di-GMP is degraded by phosphodiesterases (PDE), which contain an EAL or HD-GYP domain (62).

V. cholerae genome contains 62 genes predicted to encode proteins containing GGDEF or EAL domains capable of degrading or producing c-di-GMP (63). C-di-GMP is sensed by receptor proteins, including PilZ domain-containing proteins and VpsT, or by c-di-GMP-responsive riboswitches (64-66).

Two-component signal transduction systems of *V. cholerae*

The prototypical two-component signal transduction system (TCS) consists of a membrane-bound histidine kinase (HK), which sense environmental signals and a corresponding response regulator (RR), which mediates a cellular response (67-69). HKs usually possess multiple enzyme activities including autokinase, phosphotransfer, and phosphatase activities. The HK usually contains a highly variable sensory input domain, located at the N-terminal, enabling the HKs to sense a wide variety of stimuli (70). Typically, in response to a stimulus, the C-terminal catalytic and Adenosine Triphosphate (ATP) binding domain will bind to ATP and autophosphorylate the conserved histidine residue found within the dimerization and histidine phosphotransfer domain (DHp). The DHp domain mediates homodimerization and serves as the phosphodonor for a cognate RR. Since many HKs are bifunctional and also dephosphorylate their cognate RR, input signals can stimulate the kinase or phosphatase activity of a HK (68).

RRs typically contain two domains: a receiver domain (REC), located at the N-terminus, and an output or effector domain, located at the C-terminus (68). The REC domain contains a conserved phospho-acceptor aspartate residue and several other conserved amino acids that catalyze the phosphotransfer from a HK. The highly variable effector domains are activated by phosphorylation of the receiver domain and are usually involved with binding DNA. RRs contain DNA binding effector domains, which are classified by a small number of structural families named after extensively characterized members. These subfamilies include the OmpR/PhoB winged-helix domain (70), the NarL/FixJ four-helix helix-turn-helix domain (71), the NtrC/Dct AAA+ ATPase domain fused to a factor of inversion (Fis)-type helix-turn-helix domain (72), and the LytR domain (73). Besides DNA binding domains, RR effector domains may consist of enzymatic domains. Most of the enzymatic domains are involved in the regulation of c-di-GMP, a bacterial secondary messenger molecule (74) which regulates a variety of biological processes such as biofilm formation, virulence, and motility (75). Also, there are enzymatic domains that function as methyltransferases, such as CheB (76). Enzymatic domains within these RRs include GGDEF diguanylate cyclase domains and/or phosphodiesterase domains of the EAL or HD-GYP families. RRs can function as transcriptional activators, repressors, or both or as regulators of the synthesis or degradation of c-di-GMP (77). TCS allows cells

to sense and respond to environmental stimuli by modulating gene transcriptions and/or enzymatic activities.

Phosphorelays are a common variant of the two component signaling paradigm. These more complex cell-signaling pathways usually contain multiple regulatory components, where two or more phosphotransfer events occurring between hybrid HK (which contains both HK and RR domains), Hpt (histidine phosphotransferase) and RR proteins (67). A stimulus activates the autophosphorylation of a hybrid HK at the DHp domain. The phosphoryl group is then passed to a C-terminal receiver domain, similar to that found in RRs. A Hpt protein then transfers the phosphoryl group from the hybrid HK to the cognate RR.

Although cognate HK and RR pairs have been identified in many bacterial species, cross-regulation or cross-talk may occur between non-cognate HKs and RRs and sometimes even within cognate HK and RR pairs (78). Cross-talk occurs when a HK phosphorylates a RR that is not its cognate partner. The presence of multiple paralogous HK/RR proteins makes it possible for cross-phosphorylation. This is distinct from inherent multiple cognate pairs in which one-to-many, many-to-one, and many-to-many relationships occur between HK and RR proteins (Figure 1.1). Phosphotransfer profiling has been able to indicate specific interactions between cognate HKs and RRs (69).

Figure 1.1

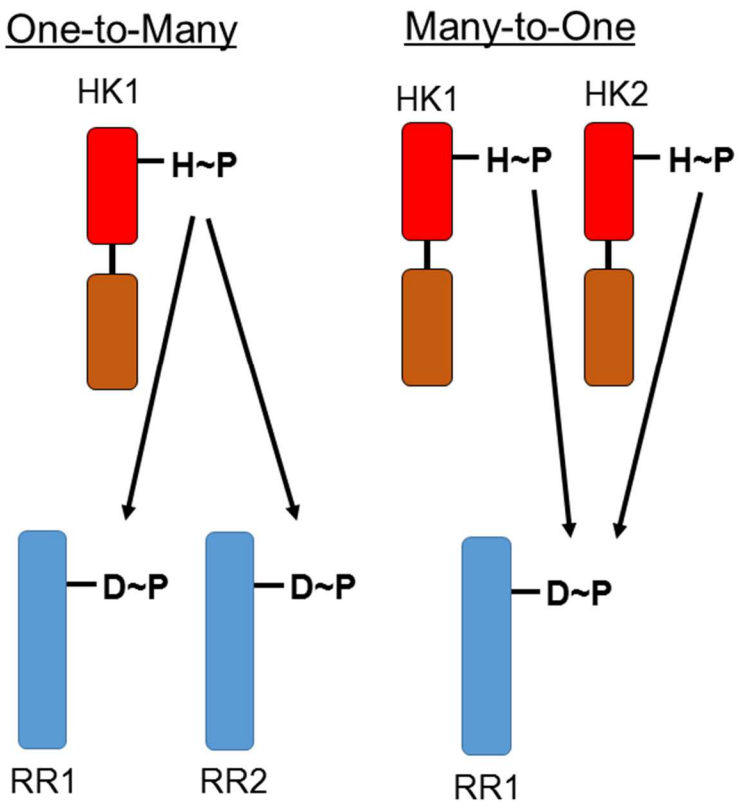

Figure 1.1. Diagram showing how HK and RR can crosstalk during phosphorelay. One-to-many indicates that a HK may phosphorylate multiple RR. Many-to-one indicates that multiple HKs may phosphorylate one RR.

Two-component signal transduction systems in *V. cholerae*

In *V. cholerae*, several TCS that regulate various biological processes have been characterized. These processes include quorum sensing, nutrient availability, biofilm formation, and virulence, and are discussed below.

The genome of the reference strain *V. cholerae* O1 EL Tor N16961 is predicted to encode 43 HK and 49 RR (http://www.ncbi.nlm.nih.gov/Complete_Genomes/RRcensus.html and http://www.p2cs.org). Further analysis of the genome for REC domains identified 4 additional RRs (VpsT, VpsR, QstR, and FlrA). Thus it is predicted that *V. cholerae* O1 EL Tor N16961 genome encodes for 53 putative RRs. A total of 27 out of 53 RR have previously been characterized for their function in *V. cholerae*. Out of the 27 previously characterized RR, 11 of the RRs contain REC domains that control chemotaxis in *V. cholerae* (79-83). Below, I discuss remaining 16 RR that have previously been characterized in *V. cholerae* (Table 1.1). The function of RRs in *V. cholerae* has not been systematically evaluated and their role in critical cellular processes including biofilm formation and virulence has not been examined. Thus, the purpose of this dissertation is to systematically characterize the role of each RR in their ability to form biofilms and cause virulence.

Table 1.1. Currently known functions of all RR in *V. cholerae*

Gene	Name	Function	Reference
VC0396	*qstR*	Competency, Quorum Sensing	(84)
VC0665	*vpsR*	Virulence, Biofilm	(46, 59, 85)
VC0693		Unknown	
VC0719	*phoB*	Virulence, Biofilm	(86, 87)
VC0790	*citB*	Unknown	
VC1021	*luxO*	Virulence, Quorum Sensing, Motility, Biofilm	(51, 88)
VC1050		Unknown	
VC1081		Unknown	
VC1082		Unknown	
VC1086		Unknown	
VC1087		Unknown	
VC1155		Unknown	
VC1213	*varA*	Virulence, Biofilm, Motility	(51, 89-94)
VC1277		Unknown	
VC1320	*carR*	Virulence, Biofilm	(29, 30, 95)
VC1348		Biofilm, Motility	Described in Chapter 4 and (96)
VC1522		Unknown	
VC1604		Unknown	
VC1638		Unknown	
VC1651	*vieB*	Virulence	(97-99)
VC1652	*vieA*	Virulence	(97, 98)
VC1719	*torR*	Unknown	
VC1926	*dct-D1*	Unknown	
VC2135	*flrC*	Virulence, Motility, *vps* gene expression	(100-103)
VC2137	*flrA*	Virulence, Motility, *vps* gene expression	(100-103)
VC2368	*arcA*	Virulence	(104)
VC2692	*cpxR*	Virulence, adaptation to envelope stress and low iron. Antimicrobial resistance	(105-108)
VC2702	*crbR*	Virulence in flies	(109)
VC2714	*ompR*	Unknown	

VC2749	*ntrC*	Biofilm	Described in Chapter 3
VCA0142	*dct-D2*	Unknown	
VCA0210		Biofilm, Motility	(96)
VCA0239		Unknown	
VCA0256		Unknown	
VCA0532		Unknown	
VCA0566	*vxrB*	Virulence, Biofilm	Described in Chapter 2 and 4
VCA0682	*uhpA*	Unknown	
VCA0704	*pgtA*	Unknown	
VCA0850		Unknown	
VCA0952	*vpsT*	Biofilm	(59, 64, 110)
VCA1086		Unknown	
VCA1105		Unknown	

VC0396 (QstR)

Studies have showed a link between natural competence and the environmental niche of *V. cholerae* (32, 111-114). Chitin sensing and degradation, quorum sensing (QS) and carbon catabolite repression contribute to activation of competence (115). When *V. cholerae* is attached to chitinous surfaces, it initiates natural competence to induce natural transformation. Scrudato et al. recently demonstrated that the major regulators of TfoX, which encodes the regulator of competence in *V. cholerae*, and HapR, which is the master quorum sensing regulator, are both involved in the activation of a gene encoding a transcriptional regulator of the LuxR-type family – QstR (Quorum sensing TfoX-dependent regulator) (84).

Strain lacking *qstR* is unable to induce the expression of *comEA* and *comEC*, which encode genes for natural competency (84). As a result, QstR plays a major role in the natural competence and transformation of *V. cholerae*.

VC0665 (VpsR)

VpsR is the major RR of TCS required for expression of *vps* genes and biofilm formation in *V. cholerae* (46). VpsR directly binds to the *vps* promoter region (58). Disruption of *vpsR* leads to a significant decrease in the expression of *vps* genes. VpsR also upregulates extracellular protein secretion genes, which form part of the type II secretion system, matrix protein genes, and *aphA*, which is a major virulence regulator. VpsR-mediated regulation of *aphA* indicates that VpsR may also have a role in pathogenesis (59, 116). Rashid et al. performed *in vivo* studies of VpsR mutants in rabbit ileal loops and demonstrated that VpsR mutants are attenuated in reactogenicity and have a decrease in colonization in the infant mouse model (85).

VC0719 (PhoB)

Phosphate is an essential nutrient for cell growth and function. Phosphate starvation activates a number of genes that ensure the survival of bacterial cells under phosphate deplete growth conditions. Bacterial cells respond to a limitation of inorganic phosphate by synthesizing a number of proteins, many

being involved in the acquisition of phosphate (117). In *E. coli* sensing and responding to phosphate limitation requires PhoR and PhoB, where PhoR is the HK and PhoB is the RR (118). PhoB is part of the OmpR subfamily of RRs, which typically functions as both an activator and repressor to differentially regulate *ompC* and *ompF* that encode outer membrane porin proteins. The genes that are regulated by PhoB comprise the Pho regulon (119). The Pho regulon promoters contain a conserved consensus sequence, the Pho box, which functions as a PhoB-binding site (120).

Similar to *E. coli*, *V. cholerae* also utilizes the PhoBR TCS to adapt to phosphate deplete environments. Permeabilized whole-cell alkaline phosphatase activity assay in *V. cholerae phoB* mutants demonstrated that a functional PhoB protein is essential for the expression of alkaline phosphatase activity (121). Furthermore, competitive assays demonstrated that *V. cholerae* PhoB mutants had reduced colonization ability (121). Furthermore Pratt et al. used mobility gel shift assays and qRT-PCR to show that PhoB binds and represses the *tcpPH* promoter, which encodes the regulator for toxin coregulated pilus (86). PhoB has also been shown to regulate *V. cholerae* motility by activating *acgAB* expression, which encode for c-di-GMP metabolic enzymes (87). It has also been shown that PhoB negatively regulates biofilm formation in *V. cholerae* and represses the expression of *vpsA*, *vpsL*, and *vpsR* (122). Therefore, PhoB regulates a

diverse set of genes that are involved with motility, biofilm, virulence, survival, and adaptation under nutrient limiting conditions.

VC1021 (LuxO)

Quorum sensing is a mechanism that provides cell-cell communication to determine whether they are present in sufficient or critical numbers by producing and detecting signaling molecules (47). The major group of signaling molecules involved in quorum sensing by Gram negative bacteria are related to acyl-homoserine lactones, whereas most Gram positive bacteria communicate using peptides that perform similar cell-density signaling functions. Bacteria use quorum sensing to synchronously control gene expression in response to the cell density (123). As discussed earlier in biofilm regulation section, LuxO is a component of the quorum sensing system of *V. cholerae*. LuxO, a member of the activator class of NtrC family of RR. Phosphorylated LuxO, together with the alternative sigma factor RpoN, activates the expression of sRNAsand prevents translation of HapR (51, 52). As a result, at low cell density, HapR repression leads to increased biofilm production and virulence gene expression (54). However, at high cell density, the HK sensors act as phosphatases and dephosphorylate and inactivate LuxO. Thus, LuxO regulates biofilm formation, cell motility, and virulence gene expression by modulating HapR production.

VC1213 (VarA)

VarA was first identified as a new virulence regulator that positively controls transcription of *tcpA* and the production of CT (89, 91, 124). The VarSA system converges with the *V. cholerae* quorum-sensing systems to regulate the expression of the Qrr sRNAs, and thus, the entire quorum-sensing regulon (93). Strains lacking VarA have colonization defects in mice and reduced fitness in vitro under conditions simulating transmission cycle of V. cholerae (125). Furthermore, Goodier et al. demonstrated that a *varA* mutant was decreased in motility (92). VarSA has been suggested to be involved in biofilm formation via CsrABCD mediated regulation of HapR expression (93, 126). However, these studies do not show any direct evidence demonstrating that VarA regulates *vps* gene expression or biofilm formation. Thus, VarA activates virulence and activates motility through regulation of quorum sensing system.

VC1320 (CarR)

During its lifecycle, *V. cholerae* is exposed to varying levels of calcium. Bilecen et al. investigated the response of *V. cholerae* to changes in extracellular $Ca2^{+}$ levels and identified the TCS *carS* (HK) and *carR* (RR). Analysis of deletion mutants of *carS* and *carR* and overexpression of CarR revealed that *vps* gene expression and biofilm formation are repressed by this TCS system (30). Later, it was reported that CarR confers polymyxin B

resistance by positively regulating expression of the *almEFG* genes, whose products are required for glycine and diglycine modification of lipid A (29). Overall, these studies identified that CarR regulates biofilm formation and antimicrobial peptide resistance in *V. cholerae*.

VC1348 & VCA0210

The second messenger, c-di-GMP, plays an essential role in controlling cellular processes such as motility, biofilm development, and virulence. VC1348 and VCA0210 is predicted to encode a HD-GYP domain that could function as c-di-GMP phosphodiesterases (PDE), which degrade c-di-GMP. McKee et al. showed that overexpression of VC1348 and VCA0210 increases motility and decreases biofilm in *V. cholerae* (96). Furthermore, qRT-PCR analysis showed that VC1348 and VCA0210 transcripts were more abundant in biofilm cells than planktonic cells. Expression of VCA0210 was upregulated in the presence of quorum sensing autoinducers (127). Thus, these RR containing the HD-GYP domain are important for controlling intracellular c-di-GMP levels and also motility and biofilm formation.

VC1651 & VC1652 (VieB & VieA)

The VieSAB system differs from conventional TCS because it encodes one HK, VieS, and two putative RRs, VieA and VieB. VieSAB TCS regulates virulence in *V. cholerae*. RNase protection assays showed a decrease in *toxT*

transcript levels and western blot analysis showed a reduced CT production in *vieSAB* triple mutant, suggesting that the VieSAB system may affect *ctxAB* expression indirectly through *toxT* production (98). Recently, Mitchell et al. showed that VieB negatively regulates the VieSA signal transduction system in *V. cholerae* (99). VieA protein is predicted to contain three conserved domains: an N-terminal domain homologous to phosphoreceiver domains, an EAL domain that has c-di-GMP PDE activity, and a C-terminal HTH DNA binding domain (128). Tischler et al. identified VieA as a TCS RR that represses transcription of *vps* genes by controlling the intracellular concentration of c-di-GMP using an EAL domain that degrades c-di-GMP (129). VieA also regulates *ctxAB* expression indirectly by affecting production of ToxT through cyclic diguanylate (c-di-GMP) signaling (97, 98). *In vitro* phosphorylation assays provided evidence that VieS is the cognate sensor kinase of VieA (128). Quantification of intracellular c-di-GMP and biofilm in *vieS* null mutants showed that VieS negatively regulates biofilm formation by regulating c-di-GMP levels (130). Thus, VieS is involved in the regulation of biofilm production via control of VieA regulation and intracellular levels of c-di-GMP.

VC2135 & VC2137 (FlrC & FlrA)

V. cholerae is equipped with a single polar flagellum. Flagellar transcription and biosynthesis is organized into a four-tired hierarchy (103). FlrA activates

RpoN-dependent transcription of class II genes of the flagellar transcriptional hierarchy (131), which encode components of the MS ring-switch-export apparatus and the TCS, FlrBC (102, 103). Phosphorylated FlrC activates RpoN-dependent transcription of class III genes of the flagellar transcriptional hierarchy (131), which form the basal body-hook and the flagellin, FlaA (100, 101, 103). Transcriptome profiling of Δ*flrA* and Δ*flrC* revealed that *vps* genes were differentially regulated, suggesting that biofilm formation is impacted by these RR (103). Furthermore, FlrA and FlrC are needed to colonize the infant mouse intestine (103). Recently, Srivastava et al. demonstrated that c-di-GMP inhibits motility by binding to FlrA, which represses the ability of FlrA to bind to the promoter of the *flrBC* operon (132). Overall, FlrA and FlrC regulate multiple cellular process in *V. cholerae*, such as motility, virulence, and biofilm formation.

VC2368 (ArcA)

During infection, *V. cholerae* can encounter environments of low oxygen. Bacterial adaptation to growth under oxygen deprivation involves global regulatory systems, like FNR and ArcAB (133-135). Sengupta et al. demonstrated that ArcA functions as a positive regulator of *toxT* expression under both aerobic and anaerobic conditions (104). Furthermore, *arcA* mutant exhibits a reduction in colonization in the infant mouse model.

VC2692 (CpxR)

In *E. coli*, cell envelope stress response is controlled by the TCS made up of the membrane localized sensor HK (CpxA) and the RR (CpxR). The *cpx* TCS in *V. cholerae* has not entirely been explored. Comparison of the *E. coli* and *V. cholerae cpx* loci showed that CpxP and the periplasmic domain of CpxA are about 20% identical (105). Slamti et al. demonstrated that chloride ions and proteins that require periplasmic disulfide bond isomerization specifically activates Cpx TCS pathway (105). Furthermore, deletion of the *cpx* locus did not affect colonization in infant mouse intestine. Recently, transcriptome profiling of Δ*cpxA* (HK) revealed that it promotes the expression of genes involved in antimicrobial resistance; more specifically, Cpx system induces VexAB and VexGH resistance-nodulation-division (RND) efflux system and the cognate outer membrane pore protein, TolC (107). In addition to regulating envelope stress response, Acosta et al. revealed that a major function of the Cpx response in *V. cholerae* is to mediate adaptation to envelope perturbations caused by toxic compounds and the depletion of iron (106). Finally, activation of the *cpx* pathway in *V. cholerae* leads to a decrease in expression of the two major virulence factors, CT and TCP, by modulating the function of cAMP receptor protein (CRP) (108).

VC2702 (CrbR)

The acetate switch is a mechanism where cells increased the expression of the gene encoding acetyl-CoA synthase, which converts acetate and ATP to acetyl-AMP and then reacts with CoA-SH to produce acetyl CoA (136). This mechanism is important for cells to enhance their survival in the absence of nutrients when “scavenging” for acetate. Recently, Hang et al. used a *Drosophila melanogaster* host model to demonstrate that *V. cholerae* CrbSR TCS activates acetate consumption (109). The consumption of acetate within the intestine deactivates host insulin signaling and disrupts fat metabolism. Thus, acetate intake by *V. cholerae* alters host metabolism and CrbR controls the acetate switch in *V. cholerae*.

VCA0952 (VpsT)

VpsT is another positive regulator of biofilm formation. It consists of an N-terminal REC domain and a C-terminal HTH domain. Activity of VpsT positively controlled by c-di-GMP binding. C-di-GMP binding to VpsT is required for DNA association and transcriptional regulation (64). Similarly to VpsR, VpsT binds to the *vps* promoter region to direction control *vps* genes (58).

Conclusion

V. cholerae is environmental pathogen. It is a natural inhabitant of aquatic ecosystems and can colonize human intestine. There are many different

environmental factors that affect *V. cholerae* survival in the environment and also the human intestine. The ability to use TCS to sense and respond to these environmental changes is critical for *V. cholerae* survival and transmission. Thus, a better understanding of the TCS is important for the biology of *V. cholerae*. This work will focus on the systematic characterization of TCS in *V. cholerae* for biofilm formation and virulence.

References

1. **Ali M, Lopez AL, You YA, Kim YE, Sah B, Maskery B, Clemens J.** 2012. The global burden of cholera. Bull World Health Organ **90:**209-218A.

2. **Chin CS, Sorenson J, Harris JB, Robins WP, Charles RC, Jean-Charles RR, Bullard J, Webster DR, Kasarskis A, Peluso P, Paxinos EE, Yamaichi Y, Calderwood SB, Mekalanos JJ, Schadt EE, Waldor MK.** 2011. The origin of the Haitian cholera outbreak strain. N Engl J Med **364:**33-42.

3. **Nguyen BM, Lee JH, Cuong NT, Choi SY, Hien NT, Anh DD, Lee HR, Ansaruzzaman M, Endtz HP, Chun J, Lopez AL, Czerkinsky C, Clemens JD, Kim DW.** 2009. Cholera outbreaks caused by an altered *Vibrio cholerae* O1 El Tor biotype strain producing classical cholera toxin B in Vietnam in 2007 to 2008. J Clin Microbiol **47:**1568-1571.

4. **Mason PR.** 2009. Zimbabwe experiences the worst epidemic of cholera in Africa. J Infect Dev Ctries **3:**148-151.

5. **Alam M, Sultana M, Nair GB, Sack RB, Sack DA, Siddique AK, Ali A, Huq A, Colwell RR.** 2006. Toxigenic Vibrio cholerae in the aquatic environment of Mathbaria, Bangladesh. Appl Environ Microbiol **72:**2849-2855.

6. **Faruque SM, Albert MJ, Mekalanos JJ.** 1998. Epidemiology, genetics, and ecology of toxigenic *Vibrio cholerae*. Microbiol Mol Biol Rev **62:**1301-1314.

7. **Huq A, Sack RB, Nizam A, Longini IM, Nair GB, Ali A, Morris JG, Jr., Khan MN, Siddique AK, Yunus M, Albert MJ, Sack DA, Colwell RR.** 2005. Critical factors influencing the occurrence of *Vibrio cholerae* in the environment of Bangladesh. Appl Environ Microbiol **71:**4645-4654.

8. **Pedersen K, Grisez L, van Houdt R, Tiainen T, Ollevier F, Larsen JL.** 1999. Extended serotyping scheme for *Vibrio anguillarum* with the definition and characterization of seven provisional O-serogroups. Curr Microbiol **38:**183-189.

9. **Shimada T, Sakazaki R.** 1977. Additional serovars and inter-O antigenic relationships of Vibrio cholerae. Jpn J Med Sci Biol **30:**275-277.

10. **Sakazaki R.** 1970. Classification and characteristics of *vibrios*. Public Health Pap **40:**33-37.

11. **Bhattacharya MK, Bhattacharya SK, Garg S, Saha PK, Dutta D, Nair GB, Deb BC, Das KP.** 1993. Outbreak of *Vibrio cholerae* non-O1 in India and Bangladesh. Lancet **341:**1346-1347.

12. **Kaper JB, Morris JG, Jr., Levine MM.** 1995. Cholera. Clin Microbiol Rev **8:**48-86.

13. **Sporecke I, Castro D, Mekalanos JJ.** 1984. Genetic mapping of *Vibrio cholerae* enterotoxin structural genes. J Bacteriol **157:**253-261.

14. **Taylor RK, Miller VL, Furlong DB, Mekalanos JJ.** 1987. Use of *phoA* gene fusions to identify a pilus colonization factor coordinately regulated with cholera toxin. Proc Natl Acad Sci U S A **84:**2833-2837.

15. **DiRita VJ, Parsot C, Jander G, Mekalanos JJ.** 1991. Regulatory cascade controls virulence in *Vibrio cholerae*. Proc Natl Acad Sci U S A **88:**5403-5407.

16. **Higgins DE, Nazareno E, DiRita VJ.** 1992. The virulence gene activator ToxT from *Vibrio cholerae* is a member of the AraC family of transcriptional activators. J Bacteriol **174:**6974-6980.

17. **Yu RR, DiRita VJ.** 2002. Regulation of gene expression in *Vibrio cholerae* by ToxT involves both antirepression and RNA polymerase stimulation. Mol Microbiol **43:**119-134.

18. **Nye MB, Pfau JD, Skorupski K, Taylor RK.** 2000. *Vibrio cholerae* H-NS silences virulence gene expression at multiple steps in the ToxR regulatory cascade. J Bacteriol **182:**4295-4303.

19. **Ghosh A, Paul K, Chowdhury R.** 2006. Role of the histone-like nucleoid structuring protein in colonization, motility, and bile-dependent repression of virulence gene expression in *Vibrio cholerae*. Infect Immun **74:**3060-3064.

20. **Higgins DE, DiRita VJ.** 1994. Transcriptional control of toxT, a regulatory gene in the ToxR regulon of *Vibrio cholerae*. Mol Microbiol **14:**17-29.

21. **Hase CC, Mekalanos JJ.** 1998. TcpP protein is a positive regulator of virulence gene expression in *Vibrio cholerae*. Proc Natl Acad Sci U S A **95:**730-734.

22. **Krukonis ES, Yu RR, Dirita VJ.** 2000. The *Vibrio cholerae* ToxR/TcpP/ToxT virulence cascade: distinct roles for two membrane-localized transcriptional activators on a single promoter. Mol Microbiol **38:**67-84.

23. **Kovacikova G, Lin W, Skorupski K.** 2004. *Vibrio cholerae* AphA uses a novel mechanism for virulence gene activation that involves interaction with the LysR-type regulator AphB at the *tcpPH* promoter. Mol Microbiol **53:**129-142.

24. **Skorupski K, Taylor RK.** 1999. A new level in the *Vibrio cholerae* ToxR virulence cascade: AphA is required for transcriptional activation of the *tcpPH* operon. Mol Microbiol **31:**763-771.

25. **Kovacikova G, Skorupski K.** 2002. Regulation of virulence gene expression in *Vibrio cholerae* by quorum sensing: HapR functions at the *aphA* promoter. Mol Microbiol **46:**1135-1147.

26. **Bina J, Zhu J, Dziejman M, Faruque S, Calderwood S, Mekalanos J.** 2003. ToxR regulon of *Vibrio cholerae* and its expression in *vibrios* shed by cholera patients. Proc Natl Acad Sci U S A **100:**2801-2806.

27. **Faruque SM, Islam MJ, Ahmad QS, Biswas K, Faruque AS, Nair GB, Sack RB, Sack DA, Mekalanos JJ.** 2006. An improved technique for isolation of environmental *Vibrio cholerae* with epidemic potential: monitoring the emergence of a multiple-antibiotic-resistant epidemic strain in Bangladesh. J Infect Dis **193:**1029-1036.

28. **Matz C, McDougald D, Moreno AM, Yung PY, Yildiz FH, Kjelleberg S.** 2005. Biofilm formation and phenotypic variation enhance predation-driven persistence of *Vibrio cholerae*. Proc Natl Acad Sci U S A **102:**16819-16824.

29. **Bilecen K, Fong JC, Cheng A, Jones CJ, Zamorano-Sanchez D, Yildiz FH.** 2015. Polymyxin B Resistance and biofilm formation in

Vibrio cholerae is controlled by the response regulator CarR. Infect Immun doi:10.1128/IAI.02700-14.

30. **Bilecen K, Yildiz FH.** 2009. Identification of a calcium-controlled negative regulatory system affecting *Vibrio cholerae* biofilm formation. Environ Microbiol **11:**2015-2029.

31. **Yildiz FH, Schoolnik GK.** 1999. *Vibrio cholerae* O1 El Tor: identification of a gene cluster required for the rugose colony type, exopolysaccharide production, chlorine resistance, and biofilm formation. Proc Natl Acad Sci U S A **96:**4028-4033.

32. **Meibom KL, Blokesch M, Dolganov NA, Wu CY, Schoolnik GK.** 2005. Chitin induces natural competence in *Vibrio cholerae*. Science **310:**1824-1827.

33. **Colwell RR, Huq A, Islam MS, Aziz KM, Yunus M, Khan NH, Mahmud A, Sack RB, Nair GB, Chakraborty J, Sack DA, Russek-Cohen E.** 2003. Reduction of cholera in Bangladeshi villages by simple filtration. Proc Natl Acad Sci U S A **100:**1051-1055.

34. **Tamayo R, Patimalla B, Camilli A.** 2010. Growth in a biofilm induces a hyperinfectious phenotype in *Vibrio cholerae*. Infect Immun **78:**3560-3569.

35. **Watnick PI, Fullner KJ, Kolter R.** 1999. A role for the mannose-sensitive hemagglutinin in biofilm formation by *Vibrio cholerae* El Tor. J Bacteriol **181:**3606-3609.

36. **Meibom KL, Li XB, Nielsen AT, Wu CY, Roseman S, Schoolnik GK.** 2004. The *Vibrio cholerae* chitin utilization program. Proc Natl Acad Sci U S A **101:**2524-2529.

37. **Nalin DR, Daya V, Reid A, Levine MM, Cisneros L.** 1979. Adsorption and growth of *Vibrio cholerae* on chitin. Infect Immun **25:**768-770.

38. **Watnick PI, Lauriano CM, Klose KE, Croal L, Kolter R.** 2001. The absence of a flagellum leads to altered colony morphology, biofilm development and virulence in *Vibrio cholerae* O139. Mol Microbiol **39:**223-235.

39. **Lauriano CM, Ghosh C, Correa NE, Klose KE.** 2004. The sodium-driven flagellar motor controls exopolysaccharide expression in *Vibrio cholerae*. J Bacteriol **186:**4864-4874.

40. **Fong JC, Syed KA, Klose KE, Yildiz FH.** 2010. Role of *Vibrio* polysaccharide (*vps*) genes in VPS production, biofilm formation and *Vibrio cholerae* pathogenesis. Microbiology **156:**2757-2769.

41. **Fong JC, Yildiz FH.** 2007. The *rbmBCDEF* gene cluster modulates development of rugose colony morphology and biofilm formation in *Vibrio cholerae*. J Bacteriol **189:**2319-2330.

42. **Fong JC, Karplus K, Schoolnik GK, Yildiz FH.** 2006. Identification and characterization of RbmA, a novel protein required for the development of rugose colony morphology and biofilm structure in *Vibrio cholerae*. J Bacteriol **188:**1049-1059.

43. **Berk V, Fong JC, Dempsey GT, Develioglu ON, Zhuang X, Liphardt J, Yildiz FH, Chu S.** 2012. Molecular architecture and assembly principles of *Vibrio cholerae* biofilms. Science **337:**236-239.

44. **Seper A, Fengler VH, Roier S, Wolinski H, Kohlwein SD, Bishop AL, Camilli A, Reidl J, Schild S.** 2011. Extracellular nucleases and extracellular DNA play important roles in *Vibrio cholerae* biofilm formation. Mol Microbiol **82:**1015-1037.

45. **Teschler JK, Zamorano-Sanchez D, Utada AS, Warner CJ, Wong GC, Linington RG, Yildiz FH.** 2015. Living in the matrix: assembly and control of *Vibrio cholerae* biofilms. Nat Rev Microbiol **13:**255-268.

46. **Yildiz FH, Dolganov NA, Schoolnik GK.** 2001. VpsR, a Member of the Response Regulators of the Two-Component Regulatory Systems, Is Required for Expression of *vps* Biosynthesis Genes and EPS(ETr)-Associated Phenotypes in *Vibrio cholerae* O1 El Tor. J Bacteriol **183:**1716-1726.

47. **Waters CM, Bassler BL.** 2005. Quorum sensing: cell-to-cell communication in bacteria. Annu Rev Cell Dev Biol **21:**319-346.

48. **Miller MB, Skorupski K, Lenz DH, Taylor RK, Bassler BL.** 2002. Parallel quorum sensing systems converge to regulate virulence in *Vibrio cholerae*. Cell **110:**303-314.

49. **Kelly RC, Bolitho ME, Higgins DA, Lu W, Ng WL, Jeffrey PD, Rabinowitz JD, Semmelhack MF, Hughson FM, Bassler BL.** 2009. The *Vibrio cholerae* quorum-sensing autoinducer CAI-1: analysis of the biosynthetic enzyme CqsA. Nat Chem Biol **5:**891-895.

50. **Brackman G, Celen S, Baruah K, Bossier P, Van Calenbergh S, Nelis HJ, Coenye T.** 2009. AI-2 quorum-sensing inhibitors affect the starvation response and reduce virulence in several *Vibrio* species, most likely by interfering with LuxPQ. Microbiology **155:**4114-4122.

51. **Lenz DH, Mok KC, Lilley BN, Kulkarni RV, Wingreen NS, Bassler BL.** 2004. The small RNA chaperone Hfq and multiple small RNAs control quorum sensing in *Vibrio harveyi* and *Vibrio cholerae*. Cell **118:**69-82.

52. **Svenningsen SL, Waters CM, Bassler BL.** 2008. A negative feedback loop involving small RNAs accelerates *Vibrio cholerae*'s transition out of quorum-sensing mode. Genes Dev **22:**226-238.

53. **Zhu J, Mekalanos JJ.** 2003. Quorum sensing-dependent biofilms enhance colonization in *Vibrio cholerae*. Dev Cell **5:**647-656.

54. **Hammer BK, Bassler BL.** 2003. Quorum sensing controls biofilm formation in *Vibrio cholerae*. Mol Microbiol **50:**101-104.

55. **Jobling MG, Holmes RK.** 1997. Characterization of *hapR*, a positive regulator of the *Vibrio cholerae* HA/protease gene *hap*, and its identification as a functional homologue of the *Vibrio harveyi luxR* gene. Mol Microbiol **26:**1023-1034.

56. **Liu Z, Stirling FR, Zhu J.** 2007. Temporal quorum-sensing induction regulates *Vibrio cholerae* biofilm architecture. Infect Immun **75:**122-126.

57. **Wang H, Ayala JC, Silva AJ, Benitez JA.** 2012. The histone-like nucleoid structuring protein (H-NS) is a repressor of *Vibrio cholerae* exopolysaccharide biosynthesis (*vps*) genes. Appl Environ Microbiol **78:**2482-2488.

58. **Zamorano-Sanchez D, Fong JC, Kilic S, Erill I, Yildiz FH.** 2015. Identification and characterization of VpsR and VpsT binding sites in *Vibrio cholerae*. J Bacteriol **197:**1221-1235.

59. **Beyhan S, Bilecen K, Salama SR, Casper-Lindley C, Yildiz FH.** 2007. Regulation of rugosity and biofilm formation in *Vibrio cholerae*: comparison of VpsT and VpsR regulons and epistasis analysis of *vpsT*, *vpsR*, and *hapR*. J Bacteriol **189:**388-402.

60. **Shikuma NJ, Fong JC, Odell LS, Perchuk BS, Laub MT, Yildiz FH.** 2009. Overexpression of VpsS, a hybrid sensor kinase, enhances biofilm formation in *Vibrio cholerae*. J Bacteriol **191:**5147-5158.

61. **Hengge R.** 2009. Principles of c-di-GMP signalling in bacteria. Nat Rev Microbiol **7:**263-273.

62. **Romling U, Galperin MY, Gomelsky M.** 2013. Cyclic di-GMP: the first 25 years of a universal bacterial second messenger. Microbiol Mol Biol Rev **77:**1-52.

63. **Beyhan S, Odell LS, Yildiz FH.** 2008. Identification and characterization of cyclic diguanylate signaling systems controlling rugosity in *Vibrio cholerae*. J Bacteriol **190:**7392-7405.

64. **Krasteva PV, Fong JC, Shikuma NJ, Beyhan S, Navarro MV, Yildiz FH, Sondermann H.** 2010. *Vibrio cholerae* VpsT regulates matrix production and motility by directly sensing cyclic di-GMP. Science **327:**866-868.

65. **Pratt JT, Tamayo R, Tischler AD, Camilli A.** 2007. PilZ domain proteins bind cyclic diguanylate and regulate diverse processes in *Vibrio cholerae*. J Biol Chem **282:**12860-12870.

66. **Sudarsan N, Lee ER, Weinberg Z, Moy RH, Kim JN, Link KH, Breaker RR.** 2008. Riboswitches in eubacteria sense the second messenger cyclic di-GMP. Science **321:**411-413.

67. **Gao R, Stock AM.** 2009. Biological insights from structures of two-component proteins. Annu Rev Microbiol **63:**133-154.

68. **Stock AM, Robinson VL, Goudreau PN.** 2000. Two-component signal transduction. Annu Rev Biochem **69:**183-215.

69. **Skerker JM, Prasol MS, Perchuk BS, Biondi EG, Laub MT.** 2005. Two-component signal transduction pathways regulating growth and cell cycle progression in a bacterium: a system-level analysis. PLoS Biol **3:**e334.

70. **Falke JJ, Bass RB, Butler SL, Chervitz SA, Danielson MA.** 1997. The two-component signaling pathway of bacterial chemotaxis: a molecular view of signal transduction by receptors, kinases, and adaptation enzymes. Annu Rev Cell Dev Biol **13:**457-512.

71. **Milani M, Leoni L, Rampioni G, Zennaro E, Ascenzi P, Bolognesi M.** 2005. An active-like structure in the unphosphorylated StyR response regulator suggests a phosphorylation- dependent allosteric activation mechanism. Structure **13:**1289-1297.

72. **Batchelor JD, Doucleff M, Lee CJ, Matsubara K, De Carlo S, Heideker J, Lamers MH, Pelton JG, Wemmer DE.** 2008. Structure and regulatory mechanism of *Aquifex aeolicus* NtrC4: variability and evolution in bacterial transcriptional regulation. J Mol Biol **384:**1058-1075.

73. **Sidote DJ, Barbieri CM, Wu T, Stock AM.** 2008. Structure of the *Staphylococcus aureus* AgrA LytTR domain bound to DNA reveals a beta fold with an unusual mode of binding. Structure **16:**727-735.

74. **Romling U, Gomelsky M, Galperin MY.** 2005. C-di-GMP: the dawning of a novel bacterial signalling system. Mol Microbiol **57:**629-639.

75. **Romling U, Amikam D.** 2006. Cyclic di-GMP as a second messenger. Curr Opin Microbiol **9:**218-228.

76. **Anand GS, Stock AM.** 2002. Kinetic basis for the stimulatory effect of phosphorylation on the methylesterase activity of CheB. Biochemistry **41:**6752-6760.

77. **Tamayo R, Pratt JT, Camilli A.** 2007. Roles of cyclic diguanylate in the regulation of bacterial pathogenesis. Annu Rev Microbiol **61:**131-148.

78. **Yamamoto K, Hirao K, Oshima T, Aiba H, Utsumi R, Ishihama A.** 2005. Functional characterization in vitro of all two-component signal transduction systems from *Escherichia coli*. J Biol Chem **280:**1448-1456.

79. **Boin MA, Austin MJ, Hase CC.** 2004. Chemotaxis in *Vibrio cholerae*. FEMS Microbiol Lett **239:**1-8.

80. **Hyakutake A, Homma M, Austin MJ, Boin MA, Hase CC, Kawagishi I.** 2005. Only one of the five CheY homologs in *Vibrio cholerae* directly switches flagellar rotation. J Bacteriol **187:**8403-8410.

81. **Lee SH, Butler SM, Camilli A.** 2001. Selection for in vivo regulators of bacterial virulence. Proc Natl Acad Sci U S A **98:**6889-6894.

82. **Butler SM, Camilli A.** 2004. Both chemotaxis and net motility greatly influence the infectivity of *Vibrio cholerae*. Proc Natl Acad Sci U S A **101:**5018-5023.

83. **Banerjee R, Das S, Mukhopadhyay K, Nag S, Chakrabortty A, Chaudhuri K.** 2002. Involvement of in vivo induced *cheY-4* gene of *Vibrio cholerae* in motility, early adherence to intestinal epithelial cells and regulation of virulence factors. FEBS Lett **532:**221-226.

84. **Lo Scrudato M, Blokesch M.** 2013. A transcriptional regulator linking quorum sensing and chitin induction to render *Vibrio cholerae* naturally transformable. Nucleic Acids Res **41:**3644-3658.

85. **Rashid MH, Rajanna C, Zhang D, Pasquale V, Magder LS, Ali A, Dumontet S, Karaolis DK.** 2004. Role of exopolysaccharide, the rugose phenotype and VpsR in the pathogenesis of epidemic *Vibrio cholerae*. FEMS Microbiol Lett **230:**105-113.

86. **Pratt JT, Ismail AM, Camilli A.** 2010. PhoB regulates both environmental and virulence gene expression in *Vibrio cholerae*. Mol Microbiol **77:**1595-1605.

87. **Pratt JT, McDonough E, Camilli A.** 2009. PhoB regulates motility, biofilms, and cyclic di-GMP in *Vibrio cholerae*. J Bacteriol **191:**6632-6642.

88. **Zhu J, Miller MB, Vance RE, Dziejman M, Bassler BL, Mekalanos JJ.** 2002. Quorum-sensing regulators control virulence gene expression in *Vibrio cholerae*. Proc Natl Acad Sci U S A **99:**3129-3134.

89. **Jang J, Jung KT, Park J, Yoo CK, Rhie GE.** 2011. The *Vibrio cholerae* VarS/VarA two-component system controls the expression of virulence proteins through ToxT regulation. Microbiology **157:**1466-1473.

90. **Tsou AM, Liu Z, Cai T, Zhu J.** 2011. The VarS/VarA two-component system modulates the activity of the *Vibrio cholerae* quorum-sensing transcriptional regulator HapR. Microbiology **157:**1620-1628.

91. **Wong SM, Carroll PA, Rahme LG, Ausubel FM, Calderwood SB.** 1998. Modulation of expression of the ToxR regulon in *Vibrio cholerae* by a member of the two-component family of response regulators. Infect Immun **66:**5854-5861.

92. **Goodier RI, Ahmer BM.** 2001. SirA orthologs affect both motility and virulence. J Bacteriol **183:**2249-2258.

93. **Lenz DH, Miller MB, Zhu J, Kulkarni RV, Bassler BL.** 2005. CsrA and three redundant small RNAs regulate quorum sensing in *Vibrio cholerae*. Mol Microbiol **58:**1186-1202.

94. **Lenz DH, Bassler BL.** 2007. The small nucleoid protein Fis is involved in *Vibrio cholerae* quorum sensing. Mol Microbiol **63:**859-871.

95. **Herrera CM, Crofts AA, Henderson JC, Pingali SC, Davies BW, Trent MS.** 2014. The *Vibrio cholerae* VprA-VprB Two-Component System Controls Virulence through Endotoxin Modification. MBio **5**.

96. **McKee RW, Kariisa A, Mudrak B, Whitaker C, Tamayo R.** 2014. A systematic analysis of the in vitro and in vivo functions of the HD-GYP domain proteins of *Vibrio cholerae*. BMC Microbiol **14:**272.

97. **Tischler AD, Camilli A.** 2005. Cyclic diguanylate regulates *Vibrio cholerae* virulence gene expression. Infect Immun **73:**5873-5882.

98. **Tischler AD, Lee SH, Camilli A.** 2002. The *Vibrio cholerae vieSAB* locus encodes a pathway contributing to cholera toxin production. J Bacteriol **184:**4104-4113.

99. **Mitchell SL, Ismail AM, Kenrick SA, Camilli A.** 2015. The VieB auxiliary protein negatively regulates the VieSA signal transduction system in *Vibrio cholerae*. BMC Microbiol **15:**59.

100. **Correa NE, Lauriano CM, McGee R, Klose KE.** 2000. Phosphorylation of the flagellar regulatory protein FlrC is necessary for *Vibrio cholerae* motility and enhanced colonization. Mol Microbiol **35:**743-755.

101. **Correa NE, Klose KE.** 2005. Characterization of enhancer binding by the *Vibrio cholerae* flagellar regulatory protein FlrC. J Bacteriol **187:**3158-3170.

102. **Klose KE, Mekalanos JJ.** 1998. Distinct roles of an alternative sigma factor during both free-swimming and colonizing phases of the *Vibrio cholerae* pathogenic cycle. Mol Microbiol **28:**501-520.

103. **Syed KA, Beyhan S, Correa N, Queen J, Liu J, Peng F, Satchell KJ, Yildiz F, Klose KE.** 2009. The *Vibrio cholerae* flagellar regulatory hierarchy controls expression of virulence factors. J Bacteriol **191:**6555-6570.

104. **Sengupta N, Paul K, Chowdhury R.** 2003. The global regulator ArcA modulates expression of virulence factors in *Vibrio cholerae*. Infect Immun **71:**5583-5589.

105. **Slamti L, Waldor MK.** 2009. Genetic analysis of activation of the *Vibrio cholerae* Cpx pathway. J Bacteriol **191:**5044-5056.

106. **Acosta N, Pukatzki S, Raivio TL.** 2015. The *Vibrio cholerae* Cpx Envelope Stress Response Senses and Mediates Adaptation to Low Iron. J Bacteriol **197:**262-276.

107. **Taylor DL, Bina XR, Slamti L, Waldor MK, Bina JE.** 2014. Reciprocal regulation of resistance-nodulation-division efflux systems and the Cpx two-component system in *Vibrio cholerae*. Infect Immun **82:**2980-2991.

108. **Acosta N, Pukatzki S, Raivio TL.** 2015. The Cpx system regulates virulence gene expression in *Vibrio cholerae*. Infect Immun doi:10.1128/IAI.03056-14.

109. **Hang S, Purdy AE, Robins WP, Wang Z, Mandal M, Chang S, Mekalanos JJ, Watnick PI.** 2014. The acetate switch of an intestinal pathogen disrupts host insulin signaling and lipid metabolism. Cell Host Microbe **16:**592-604.

110. **Casper-Lindley C, Yildiz FH.** 2004. VpsT is a transcriptional regulator required for expression of *vps* biosynthesis genes and the development of rugose colonial morphology in *Vibrio cholerae* O1 El Tor. J Bacteriol **186:**1574-1578.

111. **Blokesch M, Schoolnik GK.** 2007. Serogroup conversion of *Vibrio cholerae* in aquatic reservoirs. PLoS Pathog **3:**e81.

112. **Blokesch M, Schoolnik GK.** 2008. The extracellular nuclease Dns and its role in natural transformation of *Vibrio cholerae*. J Bacteriol **190:**7232-7240.

113. **Lo Scrudato M, Blokesch M.** 2012. The regulatory network of natural competence and transformation of *Vibrio cholerae*. PLoS Genet **8:**e1002778.

114. **Blokesch M.** 2012. Chitin colonization, chitin degradation and chitin-induced natural competence of *Vibrio cholerae* are subject to catabolite repression. Environ Microbiol **14:**1898-1912.

115. **Seitz P, Blokesch M.** 2013. Cues and regulatory pathways involved in natural competence and transformation in pathogenic and environmental Gram-negative bacteria. FEMS Microbiol Rev **37:**336-363.

116. **Yildiz FH, Liu XS, Heydorn A, Schoolnik GK.** 2004. Molecular analysis of rugosity in a *Vibrio cholerae* O1 El Tor phase variant. Mol Microbiol **53:**497-515.

117. **Wanner BL.** 1996. Signal transduction in the control of phosphate-regulated genes of *Escherichia coli*. Kidney Int **49:**964-967.

118. **Stock JB, Ninfa AJ, Stock AM.** 1989. Protein phosphorylation and regulation of adaptive responses in bacteria. Microbiol Rev **53:**450-490.

119. **Lee TY, Makino K, Shinagawa H, Amemura M, Nakata A.** 1989. Phosphate regulon in members of the family *Enterobacteriaceae*: comparison of the phoB-phoR operons of *Escherichia coli, Shigella dysenteriae*, and *Klebsiella pneumoniae*. J Bacteriol **171:**6593-6599.

120. **Wanner BL, Chang BD.** 1987. The *phoBR* operon in *Escherichia coli* K-12. J Bacteriol **169:**5569-5574.

121. **von Kruger WM, Humphreys S, Ketley JM.** 1999. A role for the PhoBR regulatory system homologue in the *Vibrio cholerae* phosphate-limitation response and intestinal colonization. Microbiology **145 (Pt 9):**2463-2475.

122. **Sultan SZ, Silva AJ, Benitez JA.** 2010. The PhoB regulatory system modulates biofilm formation and stress response in El Tor biotype *Vibrio cholerae*. FEMS Microbiol Lett **302:**22-31.

123. **Parsek MR, Greenberg EP.** 2005. Sociomicrobiology: the connections between quorum sensing and biofilms. Trends Microbiol **13:**27-33.

124. **Jang J, Jung KT, Yoo CK, Rhie GE.** 2010. Regulation of hemagglutinin/protease expression by the VarS/VarA-CsrA/B/C/D system in *Vibrio cholerae*. Microb Pathog **48:**245-250.

125. **Kamp HD, Patimalla-Dipali B, Lazinski DW, Wallace-Gadsden F, Camilli A.** 2013. Gene fitness landscapes of *Vibrio cholerae* at important stages of its life cycle. PLoS Pathog **9:**e1003800.

126. **Jang J, Jung KT, Yoo CK, Rhie GE.** 2010. Regulation of hemagglutinin/protease expression by the VarS/VarA-CsrA/B/C/D system in *Vibrio cholerae*. Microb Pathog **48:**245-250.

127. **Hammer BK, Bassler BL.** 2009. Distinct sensory pathways in *Vibrio cholerae* El Tor and classical biotypes modulate cyclic dimeric GMP levels to control biofilm formation. J Bacteriol **191:**169-177.

128. **Tamayo R, Tischler AD, Camilli A.** 2005. The EAL domain protein VieA is a cyclic diguanylate phosphodiesterase. J Biol Chem **280:**33324-33330.

129. **Tischler AD, Camilli A.** 2004. Cyclic diguanylate (c-di-GMP) regulates *Vibrio cholerae* biofilm formation. Mol Microbiol **53:**857-869.

130. **Martinez-Wilson HF, Tamayo R, Tischler AD, Lazinski DW, Camilli A.** 2008. The *Vibrio cholerae* hybrid sensor kinase VieS contributes to motility and biofilm regulation by altering the cyclic diguanylate level. J Bacteriol **190:**6439-6447.

131. **Prouty MG, Correa NE, Klose KE.** 2001. The novel sigma(54)- and sigma(28)-dependent flagellar gene transcription hierarchy of *Vibrio cholerae*. Molecular Microbiology **39:**1595-1609.

132. **Srivastava D, Hsieh ML, Khataokar A, Neiditch MB, Waters CM.** 2013. Cyclic di-GMP inhibits *Vibrio cholerae* motility by repressing induction of transcription and inducing extracellular polysaccharide production. Mol Microbiol **90:**1262-1276.

133. **Bauer CE, Elsen S, Bird TH.** 1999. Mechanisms for redox control of gene expression. Annu Rev Microbiol **53:**495-523.

134. **Holman HY, Wozei E, Lin Z, Comolli LR, Ball DA, Borglin S, Fields MW, Hazen TC, Downing KH.** 2009. Real-time molecular monitoring of chemical environment in obligate anaerobes during oxygen adaptive response. Proc Natl Acad Sci U S A **106:**12599-12604.

135. **Sawers G.** 1999. The aerobic/anaerobic interface. Curr Opin Microbiol **2:**181-187.

136. **Wolfe AJ.** 2005. The acetate switch. Microbiol Mol Biol Rev **69**:12-50.

CHAPTER 2: *Vibrio cholerae* response regulator VxrB controls colonization and regulates the Type VI secretion system

Andrew T. Cheng, Karen M. Ottemann, and Fitnat H. Yildiz

Abstract

Two-component signal transduction systems (TCS) are used by bacteria to sense and respond to their environment. TCS are typically composed of a sensor histidine kinase (HK) and a response regulator (RR). The *Vibrio cholerae* genome encodes 52 RR, but the role of these RRs in *V. cholerae* pathogenesis is largely unknown. To identify RRs that control *V. cholerae* colonization, in-frame deletions of each RR were generated and the resulting mutants analyzed using an infant mouse intestine colonization assay. We found that 12 of the 52 RR were involved in intestinal colonization. Mutants lacking one previously uncharacterized RR, VCA0566 (renamed VxrB), displayed a significant colonization defect. Further experiments showed that VxrB phosphorylation state on the predicted conserved aspartate contributes to intestine colonization. The VxrB regulon was determined using whole genome expression analysis. It consists of several genes, including those genes that create the type VI secretion system (T6SS). We determined that VxrB is required for T6SS expression using several in vitro assays and bacterial killing assays, and furthermore that the T6SS is required for intestinal colonization. *vxrB* is encoded in a four gene operon and the other *vxr* operon members also modulate intestinal colonization. Lastly, though Δ*vxrB* exhibited a defect in single-strain intestinal colonization, the Δ*vxrB* strain did not show any *in vitro* growth defect. Overall, our work revealed that

a small set of RRs is required for intestinal colonization and one of these regulators, VxrB affects colonization at least in part through its regulation of T6SS genes.

Introduction

Vibrio cholerae causes the diarrheal disease cholera that affects 3 to 5 million people worldwide every year, resulting in 100,000-120,000 deaths annually (1). *V. cholerae* produces a number of virulence factors which facilitate colonization of the intestine and subsequent disease. Major virulence factors are cholera toxin (CT), which is responsible for production of profuse watery diarrhea, and a type IV pilus called the toxin-coregulated pilus (TCP), which is required for intestinal colonization (2). *V. cholerae* virulence factors are well known to be under extensive transcriptional control. CT and TCP production are controlled by the transcriptional activator ToxT (3, 4). Expression of *toxT*, in turn, is controlled by a virulence regulatory cascade involving the membrane-bound transcriptional activators ToxRS and TcpPH. These two regulators activate *toxT* transcription directly (5-7). TcpPH expression is activated by the transcriptional activators AphA and AphB (8, 9). The quorum sensing (QS) regulatory system is also linked to the virulence gene regulatory cascade through HapR, the master QS regulator, which represses *aphA* expression (10).

Recently, the type VI secretion system (T6SS) has been identified as a new virulence factor in *V. cholerae* (11, 12). T6SSs deliver effector proteins into both eukaryotic and bacterial cells in a contact-dependent manner (12, 13). *V.*

cholerae has one T6SS system with multiple T6SS effectors: VrgG1 and VrgG3 (valine-glycine repeat protein G), which have actin cross-linking activity and peptidoglycan-degrading activity, respectively (14-17); TseL, which has lipase activity (15, 18); and VasX, which perturbs the cytoplasmic membrane of target cells (15, 19). Activity of these effectors is antagonized by corresponding immunity proteins: TsiV3, TsiV1, and TsiV2, respectively, to prevent killing by strains bearing these proteins (15, 16, 20, 21).

The T6SS can be divided into functional sections consisting of the core structural components, the T6SS effector and immunity proteins, and transcriptional regulators. The base of the T6SS apparatus spans the cell envelope, and is a tube within a tube. The inner tube is composed of polymers of the hemolysin coregulated protein (Hcp). The outer tube, also called the contractile sheath, is formed by polymers of VipA and VipB (14, 22). The Hcp inner tube is capped with a spike complex of trimeric VgrG proteins. The effectors are delivered by contraction of the VipA/VipB sheath, which in turn results in ejection of the inner tube along with VgrG and the effectors towards the target cell.

The genes encoding the T6SS components are organized into one large cluster (VCA0105-VCA0124) and two auxiliary clusters (VCA0017-VCA0022 and VC1415-VC1421) (11, 23). A key positive transcriptional regulator of the

V. cholerae T6SS is VasH (VCA0117), which is related to enhancer binding proteins that activate transcription in a σ^{54} (RpoN) dependent manner (24, 25). VasH acts on the T6SS auxiliary clusters and *vgrG3* of the large cluster, but does not affect expression of the structural genes encoded in the large T6SS gene cluster (24, 26). Additionally, Hcp production is positively regulated by the master quorum sensing regulator, HapR, and the global regulator cyclic AMP (cAMP) receptor protein, CRP, and negatively regulated by QS regulator, LuxO, and by global regulator, TsrA, a protein homologous to heat-stable nucleoid-structuring (H-NS) (27, 28). These studies have thus shown that numerous global regulators control T6SS expression, as well as one specific regulator (VasH). VasH, however does not regulate the entire T6SS.

V. cholerae T6SS studies have mainly focused on the *V. cholerae* O37 serogroup V52 strain because it assembles a T6SS apparatus constitutively (11). In this strain, the T6SS is required for cytotoxicity towards *Dictyostelium discoideum* and J774 macrophages, and induces inflammatory diarrhea in the mouse model (29). In *V. cholerae* O1 strain C6706, the T6SS is not constitutively produced and conditions that promote T6SS production are unknown. However, production of T6SS can be achieved in other O1 strains by inactivating mutations in genes encoding the LuxO and TsrA negative regulators. In O1 strains, the T6SS translocates T6SS effectors into

macrophages, and increases fecal diarrhea and intestinal inflammation in infant rabbits (27). It was also shown that the *V. cholerae* O1 C6706 strain T6SS mediates antagonistic interbacterial interactions during intestinal colonization. A strain unable to produce the TsiV3 immunity protein, which provides immunity against the effector VgrG3, exhibited an intestinal colonization defect only when co-infected with strains harboring an intact T6SS locus and VrgG3 (30). Although T6SS is regulated and expressed differently between *V. cholerae* strains, production of this system in multiple strains promotes virulence against both eukaryotic and bacterial cells, suggesting the function is largely conserved but the regulation varies.

Pathogenic bacteria experience varying conditions during infection of human hosts and often use two-component signal transduction systems (TCSs) to monitor their environments (31). TCSs play important roles in the regulation of virulence factors, metabolic adaptation to host environments, and response to numerous environmental stresses including pH, osmolarity, oxygen availability, bile salts, and antimicrobial peptides (32). TCS rely on a phosphorelay-based signal transduction system. The prototypical TCS consists of a membrane-bound histidine kinase (HK), which senses environmental signals, and a corresponding response regulator (RR), which mediates a cellular response. Response regulators are typically multi-domain proteins harboring a conserved receiver domain (REC) and C-terminal output

domain such as DNA-binding, diguanylate cyclase, or methyltransferase (33-35). Upon environmental stimulation, the HK catalyzes an ATP-dependent autophosphorylation reaction on a conserved histidine residue. The phosphoryl group is transferred from the HK to a conserved aspartate residue on the RR, eliciting a conformation change and subsequent cellular response (32, 34, 35).

The *V. cholerae* genome reference genome of O1 EL Tor N16961 strain is predicted to encode 43 HK and 49 RR (http://www.ncbi.nlm.nih.gov/Complete_Genomes/RRcensus.html and http://www.p2cs.org). Further analysis of the genome for REC domains identified 3 additional RRs (VpsT, VpsR, VC0396). Thus it is predicted that *V. cholerae* O1 EL Tor N16961genome encodes for 52 putative RRs. Thirteen of these RRs have been previously characterized and eight have a role in virulence factor production and host colonization: VarA, LuxO, VieA, PhoB, ArcA, FlrC, CarR, and CheY-3 (36-44). VarA and LuxO repress production of quorum sensing regulator, HapR, which represses expression of *aphA* and, in turn, TCP and CT production (36, 37). VieA regulates *ctxAB* expression indirectly by affecting production of ToxT through cyclic diguanylate (c-di-GMP) signaling (38, 39). The RR for phosphate limitation, PhoB, directly controls expression of a key transcriptional regulator, TcpPH, which activates *toxT* transcription (40). The RR ArcA controls adaptation to low oxygen

environment of the intestine and positively controls the expression of *toxT* (41). CarR regulates glycine and diglycine modification of lipid A, confers polymyxin B resistance, and is required for intestinal colonization, although this phenotype is strain dependent (42). FlrC controls flagellar biosynthesis and CheY-3 is needed for control of chemotactic motility (43, 44). Both motility and chemotaxis are known colonization factors for *V. cholerae* (43). Together, these results show these RRs play a role in intestinal colonization have three basic targets: known virulence regulators and concomitant CT and TCP production; lipid A modification enzymes; or motility and chemotaxis. However, 39 out of 52 were not yet analyzed at the time of this study.

To systematically evaluate the role of *V. cholerae* TCSs in intestinal colonization, we generated in-frame deletion mutants of each RR gene and analyzed the *in vivo* colonization phenotypes of the resulting mutants. We found 12 RR were required for wild-type intestinal colonization. One RR in particular had a very strong defect, encoded by genomic locus VCA0566. We determined that VCA0566 (now termed *Vibrio* type six secretion regulator, *vxrB*) controls expression of several genes including the T6SS genes. We used multiple methods to substantiate that VxrB is required for expression of the T6SS *in vitro* and *in vivo*. Lastly, we report that the T6SS are needed for colonization in the *V. cholerae* O1 strain used here.

Materials and Methods

Ethics statement

All animal procedures used were in strict accordance with the NIH *Guide for the Care and Use of Laboratory Animals* (45) and were approved by the UC Santa Cruz Institutional Animal Care and Use Committee (Yildf1206).

Bacterial strains, plasmids, and culture conditions. The bacterial strains and plasmids used in this study are listed in Table 2.1. *Escherichia coli* CC118λpir strains were used for DNA manipulation, and *E. coli* S17-1λpir strains were used for conjugation with *V. cholerae*. In-frame deletion mutants of *V. cholerae* were generated as described earlier (46). All *V. cholerae* and *E. coli* strains were grown aerobically, at 30°C and 37°C, respectively, unless otherwise noted. All cultures were grown in Luria-Bertani (LB) broth (1% Tryptone, 0.5% Yeast Extract, 1% NaCl), pH 7.5, unless otherwise stated. LB agar medium contains 1.5% (wt/vol) granulated agar (BD Difco, Franklin Lakes, NJ). AKI medium contains 0.5% NaCl, 0.3% $NaHCO_3$, 0.4% Yeast Extract, and 1.5% Peptone, as previously described (47). Antibiotics were used at the following concentrations: ampicillin 100 μg/ml; rifampicin 100 μg/ml; gentamicin 50 μg/ml; streptomycin 50 μg/ml.

DNA manipulations. An overlapping PCR method was used to generate in-frame deletion constructs of each RR genes using previously published methods (46). Briefly, a 500-600 bp 5' flanking sequence of the gene, including several nucleotides of the coding region, was PCR amplified using

del-A and del-B primers. del-C and del-D primers were used to amplify the 3' region of the gene including 500-600 bp of the downstream flanking sequence. The two PCR products were joined using the splicing overlap extension technique (48, 49) and the resulting PCR product, which lacks 80% of amino acids, was digested with two restriction enzymes and ligated to similarly-digested pGP704*sacB*28 suicide plasmid. Construction of *vxrB* plasmid harboring point mutations were performed using a similar technique (50) with the following alterations: primers containing the new sequence harboring the point mutations were used in place of the del-B and del-C primers. The deletion constructs were sequenced (UC Berkeley DNA Sequencing Facility, Berkeley, CA) and the clones without any undesired mutations were used. The deletion constructs are listed in Table 2.1.

Table 2.1. Bacterial strains and plasmids used in this study.

Strain or plasmid	Relevant genotype	Source
E. coli strains		
CC118λ*pir*	Δ(*ara-leu*) *araD* Δ*lacX74 galE galK phoA20 thi-1 rpsE rpoB argE*(*Am*) *recA1* λ*pir*	(51)
S17-1λ*pir*	Tp^r Sm^r *recA thi pro* r_K^- m_K^+ RP4::2-Tc::MuKm Tn*7* λ*pir*	(52)
MC4100	F$^-$ *araD139* Δ(*argF-lac*)U169 *rpsL150*(*str^r*) *relA1 deoC1 rbsR fthD5301 fruA25* λ$^-$	Ottemann lab
V. cholerae strains		
FY_VC_0001	*Vibrio cholerae* O1 El Tor A1552, wild type, Rif^r	(53)
FY_VC_0003	Δ*lacZ*, Rif^r	(54)
FY_VC_8327	ΔVC0396 (*qstR*)	This study
FY_VC_2272	ΔVC0665 (*vpsR*)	(55)
FY_VC_8197	ΔVC0693	This study
FY_VC_8162	ΔVC0719 (*phoB*)	This study
FY_VC_8074	ΔVC0790	This study
FY_VC_0192	ΔVC1021 (*luxO*)	This study
FY_VC_8480	ΔVC1050	This study

FY_VC_8329	ΔVC1081	This study
FY_VC_8180	ΔVC1082	This study
FY_VC_1936	ΔVC1086	This study
FY_VC_2760	ΔVC1087	This study
FY_VC_0692	ΔVC1155	This study
FY_VC_8474	ΔVC1213 (*varA*)	This study
FY_VC_4379	ΔVC1277	This study
FY_VC_3282	ΔVC1320 (*carR*)	(56)
FY_VC_8331	ΔVC1348	This study
FY_VC_7998	ΔVC1522	This study
FY_VC_8482	ΔVC1604	This study
FY_VC_8164	ΔVC1638	This study
FY_VC_8706	ΔVC1651 (*vieB*)	This study
FY_VC_0516	ΔVC1652 (*vieA*)	(57)
FY_VC_8166	ΔVC1719 (*torR*)	This study
FY_VC_8243	ΔVC1926 (*dct-D1*)	This study
FY_VC_6286	ΔVC2135 (*flrC*)	This study
FY_VC_8756	ΔVC2692 (*cpxR*)	This study
FY_VC_8708	ΔVC2702 (*crbR*)	This study
FY_VC_8179	ΔVC2714 (*ompR*)	This study
FY_VC_6289	ΔVC2749 (*ntrC*)	This study
FY_VC_8245	ΔVCA0142 (*dct-D2*)	This study
FY_VC_2315	ΔVCA0210	This study
FY_VC_8194	ΔVCA0239	This study
FY_VC_8148	ΔVCA0256	This study
FY_VC_8150	ΔVCA0532	This study
FY_VC_9332	ΔVCA0565 (*vxrA*)	This study
FY_VC_8758	ΔVCA0566 (*vxrB*)	This study
FY_VC_9369	ΔVCA0567 (*vxrC*)	This study
FY_VC_9417	ΔVCA0568 (*vxrD*)	This study
FY_VC_9394	ΔVCA0569 (*vxrE*)	This study
FY_VC_8478	ΔVCA0682 (*uhpA*)	This study
FY_VC_7969	ΔVCA0704 (*pgtA*)	This study
FY_VC_8209	ΔVCA0850	This study
FY_VC_0099	ΔVCA0952 (*vpsT*)	(54)
FY_VC_8841	ΔVCA1086	This study
FY_VC_8154	ΔVCA1105	This study
FY_VC_9460	*vxrB*::D78A	This study
FY_VC_9462	*vxrB*::D78E	This study
FY_VC_9469	SΔ*vxrB*-Tn7::*vxrB*	This study
FY_VC_9952	Δ*vxrB*Δ*hcp1*Δ*hcp2*	This study

FY_VC_9569	ΔVC1415ΔVCA0017 (Δ*hcp1*Δ*hcp2*)	This study
FY_VC_9735	Δ*hcp1*Δ*hcp2*-Tn7-*hcp1*	This study
FY_VC_9737	Δ*hcp1*Δ*hcp2*-Tn7-*hcp2*	This study
FY_VC_9562	ΔVCA0117 (Δ*vasH*)	This study
	ΔVCA0123 (Δ*vgrG3*)	(58)
Plasmids		
pGP704*sacB*28	pGP704 derivative, *mob*/*oriT sacB*, Ap^r	(54)
pFY-0484	pGP704-*sacB28*::ΔVC0396, Ap^r	This study
pFY-1656	pGP704-*sacB28*::ΔVC0693, Ap^r	This study
pFY-1402	pGP704-*sacB28*::ΔVC0719, Ap^r	This study
pFY-1826	pGP704-*sacB28*::ΔVC0790, Ap^r	This study
pFY-0008	pGP704-*sacB28*::ΔVC1021, Ap^r	This study
pFY-1840	pGP704-*sacB28*::ΔVC1050, Ap^r	This study
pFY-0120	pGP704-*sacB28*::ΔVC1081, Ap^r	This study
pFY-1651	pGP704-*sacB28*::ΔVC1082, Ap^r	This study
pFY-1748	pGP704-*sacB28*::ΔVC1086, Ap^r	This study
pFY-0562	pGP704-*sacB28*::ΔVC1087, Ap^r	This study
pFY-0124	pGP704-*sacB28*::ΔVC1155, Ap^r	This study
pFY-1829	pGP704-*sacB28*::ΔVC1213, Ap^r	This study
pFY-0766	pGP704-*sacB28*::ΔVC1277, Ap^r	This study
pFY-0116	pGP704-*sacB28*::ΔVC1348, Ap^r	This study
pFY-1345	pGP704-*sacB28*::ΔVC1522, Ap^r	This study
pFY-1844	pGP704-*sacB28*::ΔVC1604, Ap^r	This study
pFY-1405	pGP704-*sacB28*::ΔVC1638, Ap^r	This study
pFY-1847	pGP704-*sacB28*::ΔVC1651, Ap^r	This study
pFY-1655	pGP704-*sacB28*::ΔVC1719, Ap^r	This study
pFY-1820	pGP704-*sacB28*::ΔVC1926, Ap^r	This study
pFY-1077	pGP704-*sacB28*::ΔVC2135, Ap^r	This study
pFY-1917	pGP704-*sacB28*::ΔVC2692, Ap^r	This study
pFY-1898	pGP704-*sacB28*::ΔVC2702, Ap^r	This study
pFY-1411	pGP704-*sacB28*::ΔVC2714, Ap^r	This study
pFY-1073	pGP704-*sacB28*::ΔVC2749, Ap^r	This study
pFY-1818	pGP704-*sacB28*::ΔVCA0142, Ap^r	This study
pFY-0471	pGP704-*sacB28*::ΔVCA0210, Ap^r	This study
pFY-0115	pGP704-*sacB28*::ΔVCA0239, Ap^r	This study
pFY-1660	pGP704-*sacB28*::ΔVCA0256, Ap^r	This study
pFY-1338	pGP704-*sacB28*::ΔVCA0532, Ap^r	This study
pFY-2117	pGP704-*sacB28*::ΔVCA0565, Ap^r	This study
pFY-1914	pGP704-*sacB28*::ΔVCA0566, Ap^r	This study

pFY-2119	pGP704-*sacB28*::ΔVCA0567, Ap^r	This study
pFY-3075	pGP704-*sacB28*::ΔVCA0568, Ap^r	This study
pFY-2126	pGP704-*sacB28*::ΔVCA0569, Ap^r	This study
pFY-1832	pGP704-*sacB28*::ΔVCA0682, Ap^r	This study
pFY-1311	pGP704-*sacB28*::ΔVCA0704, Ap^r	This study
pFY-440	pGP704-*sacB28*::ΔVCA0850, Ap^r	This study
pFY-1986	pGP704-*sacB28*::ΔVCA1086, Ap^r	This study
pFY-1658	pGP704-*sacB28*::ΔVCA1105, Ap^r	This study
pFY-3563	pGP704-*sacB28*::ΔVCA0566 (D78A), Ap^r	This study
pFY-3565	pGP704-*sacB28*::ΔVCA0566 (D78E), Ap^r	This study
pFY-1041	pGP704-*sacB28*::ΔVC1415, Ap^r	This study
pFY-1042	pGP704-*sacB28*::ΔVCA0017, Ap^r	This study
pFY-1043	pGP704-*sacB28*::ΔVCA0117, Ap^r	This study
pFY-3573	pGP704-Tn7-*vxrB*, Gm^r, Ap^r	This study
pFY-4154	pGP704-Tn7-*hcp1*, Gm^r, Ap^r	This study
pFY-4156	pGP704-Tn7-*hcp2*, Gm^r, Ap^r	This study
pUX-BF13	oriR6K helper plasmid, mob/oriT, provides the Tn7 transposition function in trans, Ap^r	(59)
pMCM11	pGP704::mTn*7*-*gfp*, Gm^r Ap^r	M. Miller and G. Schoolnik

Generation of in-frame deletion mutants and Tn7 complementation strains. The deletion plasmids were maintained in *E. coli* CC118λpir. Biparental matings were carried out with the wild type *V. cholerae* and an *E. coli* S17λpir strain harboring the deletion plasmid. Selection of deletion mutants were done as described (48) and were verified by PCR. The Tn7 complementation *V. cholerae* strains were generated by triparental matings with donor *E. coli* S17λpir carrying pGP704-Tn7 with gene of interest, helper *E. coli* S17λpir harboring pUX-BF13, and *V. cholerae* strains. Transconjugants were selected on thiosulfate-citrate-bile salts-sucrose (TCBS) (BD Difco, Franklin Lakes, NJ) agar medium containing gentamicin at 30°C. The Tn7 complementation *V. cholerae* strains were verified by PCR.

Intestinal colonization assay. An *in vivo* competition assay for intestinal colonization was performed as described previously (60). Briefly, each of the *V. cholerae* mutant strains (*lacZ*$^+$) and the fully virulent wild-type strain (*lacZ*$^-$) were grown to stationary phase at 30°C with aeration in LB broth. Mutant strains and wild-type were mixed at 1:1 ratios in 1x Phosphate Buffered Saline (PBS). The inoculum was plated on LB agar plates containing 5-bromo-4-chloro-3-indoyl-β-D-galactopyranoside (X-gal) to differentiate wild-type and mutant colonies and to determine the input ratios. Approximately, 10^6-10^7 cfu were intragastrically administered to groups of 5-7 anesthetized 5-day old CD-1 mice (Charles River Laboratories, Hollister, CA). After 20 hours

of incubation, the small intestine was removed, weighed, homogenized, and plated on appropriate selective and differential media to enumerate mutant and wild-type cells recovered and to obtain the output ratios. *In vivo* competitive indices were calculated by dividing the small intestine output ratio by the inoculum input ratio of mutant to wild-type strains. For single strain infections, 10^7 cfu of each strain, including wild type ($lacZ^-$), were intragastrically administrated to 5-day old CD-1 mice. After 20 hours of incubation, the small intestine was harvested and plated on selective media as previously described above. Statistical analyses for competition infecitons were performed using Wilcoxon Signed Rank Test. Statistical analyses were performed using Prism 5 software (GraphPad Software, Inc., San Diego, CA) using Wilcoxon Signed Rank Test. P values of <0.05 were determined to be statistically significant.

Reverse Transcription-PCR. RNA was isolated as described below. The reverse transcription reaction to generate cDNA was carried out using the SuperScript III Reverse Transcriptase (Invitrogen, Carlsbad, CA) according to the manufacturer's instructions at 25°C for 5 min, 50°C for 1 h, and 70°C for 15 min using 1 µg of RNA in a 20 µl final volume. The product was used in a PCR using suitable primers, and RNA without RT treatment was used as a negative control.

Real Time PCR. For RT-PCR expression analysis, RNA was isolated as described below. cDNA was synthesized using iScript cDNG Synthesis Kit

(Bio-Rad, Hercules, CA) from 1 µg of total RNA. Real-time PCR was performed using a Bio-Rad CFX1000 thermal cycler and Bio-RAD CFX96 real-time imager with specific primer pairs (designed within the coding region of the target gene) and SsoAdvanced SYBR green supermix (Bio-Rad, Hercules, CA). Results are from two independent experiments peformed in quadruplicate. All samples were normalized to the expression of the housekeeping gene 16S using the Pfaffl method (61). Relative expression was calculated by normalizing expression at Δ*vxrB* by that of wt. Statistical analysis was performed using two-tailed student's t test.

RNA isolation. *V. cholerae* cells were grown aerobically overnight in LB at 37°C, then diluted 1:100 in fresh 10 ml AKI media in borosilicate glass test tubes (diameter, 15mm; height, 150 mm) and incubated at 37°C without shaking for 4 hours. After 4 hours, 10 ml cultures were transferred to 125 ml flasks (for maximal aerated growth on an orbital shaker (250 rpm) for 2 hours. Aliquots (2 ml) of the cultures were collected and centrifuged for 2 min at room temperature. The cell pellets were immediately resuspended in 1 ml of TRIzol (Invitrogen, Carlsbad, CA) and stored at -80°C. Total RNA was isolated according to the manufacturer's instructions. To remove contaminating DNA, total RNA was incubated with RNase-free DNase I (Ambion, Grand Island, NY), and an RNeasy mini kit (Qiagen, Valencia, CA) was used to clean up RNA after DNase digestion. Five micrograms of total

RNA was treated with a MICROBExpress Kit (Ambion, Grand Island, NY) to remove ribosomal RNA, and the efficiency was confirmed by Bioanalyzer analysis (Agilent Technologies, Santa Clara, CA). Three biological replicates were generated for each condition.

cDNA library construction and Illumina HiSeq sequencing. Libraries for RNA-seq were prepared using NEBNext Ultra Directional RNA Library Prep Kit for Illumina (New England Biolabs, Ipswich, MA). Twelve indexed samples were sequenced per single lane using the HiSeq2500 Illumina sequencing platform for 50 bp single reads (UC Davis Genome Center, UC Davis, CA) and subsequently analyzed and visualized via the CLC Genomics Workbench version 7.5 (Qiagen, Valencia, CA). Samples were mapped to the *V. cholerae* genome N16961. Differentially regulated genes were identified as those displaying a fold change with an absolute value of 1.5-fold or greater. Statistical significance was determined by Empirical analysis of Digital Gene Expression (edgeR) test where $p<0.05$ was deemed significant (62).

Analysis of Hcp production and secretion. *V. cholerae* strains were grown to an OD600 of 2.0, and the culture (25 ml) was centrifuged at 20,000 g for 10 min to obtain whole cell pellets. The culture supernatant containing secreted proteins were filtered through 0.22 μ membranes (Millipore, Billerica, Massachusetts) and secreted proteins in the culture supernatant were precipitated with 13% trichloroacetic acid (TCA) overnight at 4°C, pelleted by centrifugation at 47,000 g for 30 min at 4°C, wash with ice cold acetone and

resuspended in 1x PBS containing Complete protease inhibitor (Roche, Basel, Switzerland). Bovine serum albumin (BSA, 100 µg/ml) was added to the culture supernatant prior to TCA precipitation as a control. Protein pellets from whole cell were suspended in 2% sodium dodecyl sulfate (SDS) and protein concentrations were estimated using a Pierce BCA protein assay kit (Thermo Scientific, Rockford, IL). Equal amounts of total protein (20 µg) were loaded onto a SDS 13% polyacrylamide gel electrophoresis (SDS-PAGE). Western blot analyses were performed as described (63) using anti-Hcp polyclonal antiserum provided by the Sun Wai (28), anti-CRP (Neoclone Inc., Madison, WI), and anti-BSA (Santa Cruz Biotech, Santa Cruz, CA). OneMinute Western Blot Stripping Buffer (GM Biosciences, Frederick, MD) was used to remove the Hcp antibodies and the same blot was used again to probe for CRP or BSA. These experiments were conducted with at least three biological replicates.

Bacterial killing assay. Killing assays were performed as described previously (20). Briefly, bacterial strains were grown overnight on LB plates and resuspended in LB broth containing 340 mM NaCl, as *V. cholerae* strain A1552 displayed enhanced interbacterial virulence towards *E. coli* under high osmolarity (58). *V. cholerae* and *E. coli* MC4100 were mixed at a 10:1 ratio and 25 µl was spotted onto LB agar plates containing 340 mM NaCl and incubated at 37°C for 4 hours. Spots were harvested, serially diluted, and plated onto LB plates containing 50 µg/ml of streptomycin to enumerate

surviving *E. coli* prey cells.

***In vitro* competition assay.** The following assay was performed similarly as the intestinal colonization assay except no animal models were used. The *V. cholerae* mutant strains (*lacZ*$^{+}$) and the wild-type strain (*lacZ*$^{-}$) were grown to stationary phase at 30°C with aeration in LB broth. Mutant strains and wild-type were mixed at 1:1 ratios in 1x PBS. The inoculum was plated on LB agar plates containing X-gal to differentiate colonies formed by the wild-type and mutant strains and to determine the input ratios. The inoculum (50 µl) was spotted on to a LB agar plate and incubated at 37°C. After 20-24 hours of incubation, the 50 µl spots were scraped off the agar plate and resuspended in 1x PBS. The resuspension was serial diluted and plated on appropriate selective and differential media to enumerate mutant and wild type cells recovered and to obtain the output ratios. *In vitro* competitive indices were calculated by dividing the output ratio by the inoculum input ratio of mutant to wild type strains. Statistical analyses were performed using Wilcoxon Signed Rank Test.

Results

Multiple RRs impact intestinal colonization.

We have a limited understanding of the *V. cholerae* TCSs and their role in colonization and adaptation to host environments. To evaluate the importance of the 52 TCS RRs in colonization, we generated in-frame deletion mutants in the 40 RR of unknown function. For this analysis, we excluded 12 RR that were either predicted to be involved in chemotaxis (11 CheY, CheV, and CheB proteins) or that we were unable to mutate (VC2368, ArcA) (43, 64). We then analyzed the ability of 40 RR deletion mutants to colonize the small intestine in an *in vivo* competition assay where *in vivo* fitness of a mutant strain is compared to that of wild type strain using the infant mouse infection model (Fig. 2.1A) (60). While the vast majority of mutants—28—were not different from wild type, we identified 12 RR mutants that had a statistically significant colonization difference as compared to wild type (Fig. 2.1A). We focused on 8 mutants with a statistically significant colonization difference and exhibited at least 2-fold difference in CI (Fig. 2.1B). Consistent with previous studies, we identified that ΔVC0719 (*phoB),* ΔVC1021 *(luxO)*, ΔVC1213 (*varA), and* ΔVC2135 *(flrC)* were defective in colonization (36, 37, 40, 44). The competitive indices (CI) for Δ*phoB*, Δ*luxO*, Δ*varA*, and Δ*flrC* were 0.01, 0.02, 0.16, and 0.43, respectively (Fig. 2.1B).

Figure 2.1

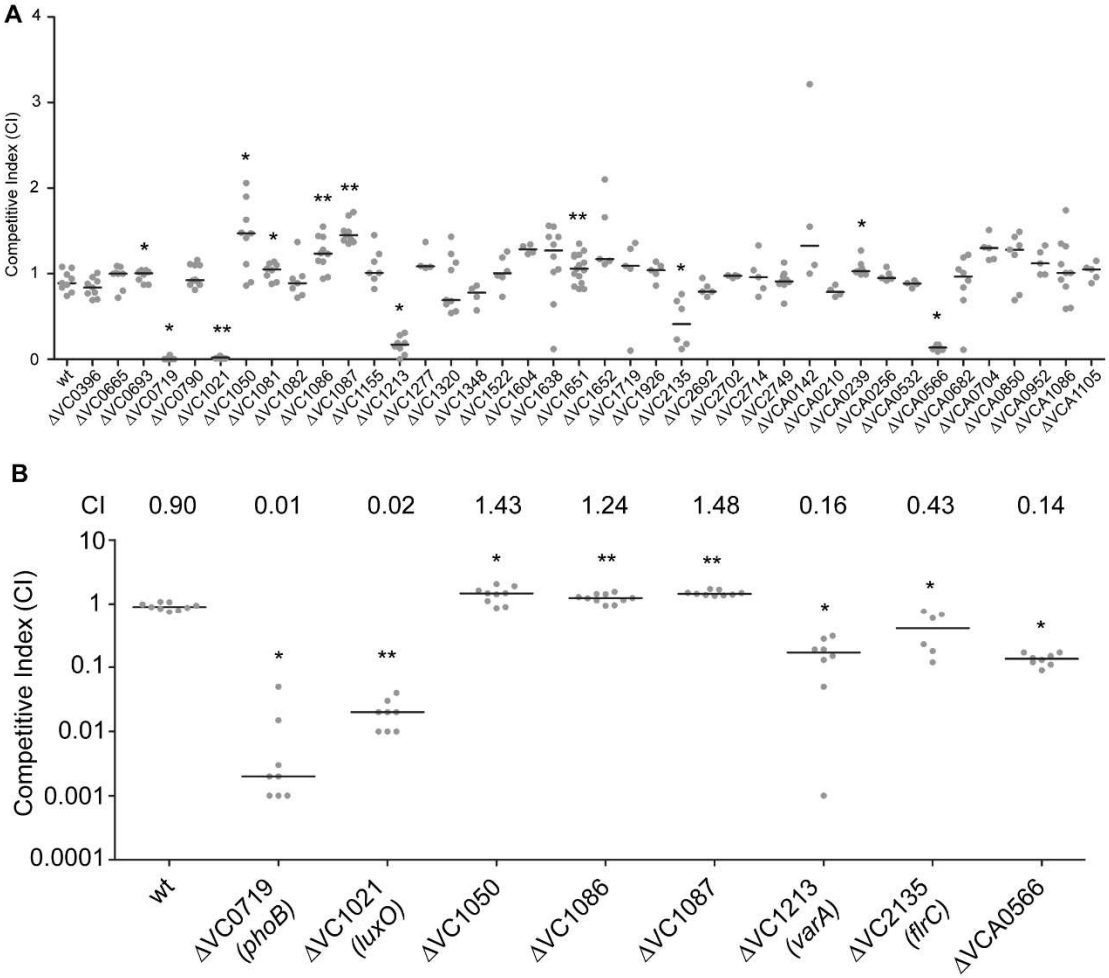
A
Competitive Index (CI)
0
1
2
3
4
wt
ΔVC0396
ΔVC0665
ΔVC0693
ΔVC0719
ΔVC0790
ΔVC1021
ΔVC1050
ΔVC1081
ΔVC1082
ΔVC1086
ΔVC1087
ΔVC1155
ΔVC1213
ΔVC1277
ΔVC1320
ΔVC1348
ΔVC1522
ΔVC1604
ΔVC1638
ΔVC1651
ΔVC1652
ΔVC1719
ΔVC1926
ΔVC2135
ΔVC2692
ΔVC2702
ΔVC2714
ΔVC2749
ΔVCA0142
ΔVCA0210
ΔVCA0239
ΔVCA0256
ΔVCA0532
ΔVCA0566
ΔVCA0682
ΔVCA0704
ΔVCA0850
ΔVCA0952
ΔVCA1086
ΔVCA1105
B
CI
0.90
0.01
0.02
1.43
1.24
1.48
0.16
0.43
0.14
Competitive Index (CI)
10
1
0.1
0.01
0.001
0.0001
wt
ΔVC0719 (phoB)
ΔVC1021 (luxO)
ΔVC1050
ΔVC1086
ΔVC1087
ΔVC1213 (varA)
ΔVC2135 (flrC)
ΔVCA0566

Figure 2.1. Identification of RRs impacting colonization in the infant mouse infection model. (A) Ability of 40 ΔRR mutants in *V. cholerae* strain A1552 to colonize the infant mouse intestine was analyzed using a competition assay with the isogenic wild-type strain. (B) Same data presented in Fig. 1A, expanded to highlight the mutants showing a statistically significant difference in colonization $p<0.05$ and a minimum 1.2-fold change in colonization ability. Competitive index (CI) is defined as the output ratio of mutant to wild-type bacteria divided by the input ratio of mutant to wild-type bacteria. Each symbol represents the CI in an individual mouse; horizontal bars indicate the median. Statistical analysis was carried out using Wilcoxon Signed Rank Test, comparing the CI of each strain to the CI of wt *lacZ*$^{+}$ / wt lacZ^{-} (shown as wt) (*, $p<0.05$; **, $p<0.01$).

Additionally, we identified a set of genes whose absence slightly but statistically significantly enhanced colonization (at least 1.2 fold higher CI), suggesting that inhibition of their expression and activity may be needed for wild-type colonization. These mutants were ΔVC1050, ΔVC1086, and ΔVC1087, which exhibited subtle and enhanced colonization phenotypes with CIs of 1.43, 1.24, and 1.48, respectively (Fig. 2.1B). VC1050 is classified as an Hnr-type RR, (65) but its function is yet to be determined. VC1086 and VC1087 are part of a predicted eight gene operon encompassing VC1080-VC1087. Both VC1086 and VC1087 have domains that suggest they function in cyclic guanylate (c-di-GMP) regulation. Specifically, VC1086 contains an EAL domain with conserved residues required for enzymatic function, while VC1087 harbors an HD-GYP domain, but this domain lacks the conserved residues required for enzymatic activity.

We also identified one RR that was defective for colonization that had not been previously characterized. This mutant, ΔVCA0566, had a colonization defect with a CI of 0.14 (Fig. 2.1). Because this uncharacterized RR was important for colonization, we focused the rest of our studies on this protein.

ΔVCA0566/VxrB impacts colonization.

VCA0566 is the second gene of a predicted five gene operon and had been previously annotated as a RR of the OmpR family. The encoded protein,

which we named VxrB for reasons described below, is 245 amino acids in length with an N-terminal REC domain and a C-terminal winged helix-turn-helix DNA-binding domain (Fig. 2.2B). Previously characterized members of the OmpR family in *V. cholerae* include PhoB, CarR, and ArcA (40-42). Amino acid sequence alignment of the *V. cholerae* RRs in the OmpR family and the previously characterized *E. coli* OmpR (66) was used to identify the aspartate residue that is predicted to be phosphorylated in the REC domain (Fig. 2.2A). Since the phosphorylation state of a RR is likely to determine its activity, we mutated the aspartate residue in the REC domain of VxrB to mimic constitutively active (D78E) and inactive (D78A) versions, as used in other work (66), and replaced the wild-type gene in the chromosome with these altered genes. These mutants were competed against wild type in the infant mouse colonization assay to determine if the phosphorylation state of VxrB is important for colonization. In accordance with our initial colonization screen, Δ*vxrB* displayed a CI of 0.15 (Fig 2.2B). Somewhat surprisingly, the CI for *vxrB*::D78A (inactive form) was 0.53, indicating a modest defect in colonization. This result indicates that the “inactive” form of VxrB does not phenocopy the Δ*vxrB* mutant, suggesting that VxrB D78A is not fully inactive. The CI for *vxrB*::D78E (active form) is 1.07, suggesting that constitutive activation of VxrB does not significantly impair *V. cholerae* (Fig. 2.2B). Collectively, these findings suggest that in vivo phosphorylation of VxrB at D78 is likely to be important for its colonization function, but apparently

perhaps not absolutely required. It is also likely that VxrB may not function by conventional phosphorylation-dependent signal transduction (67).

Figure 2.2

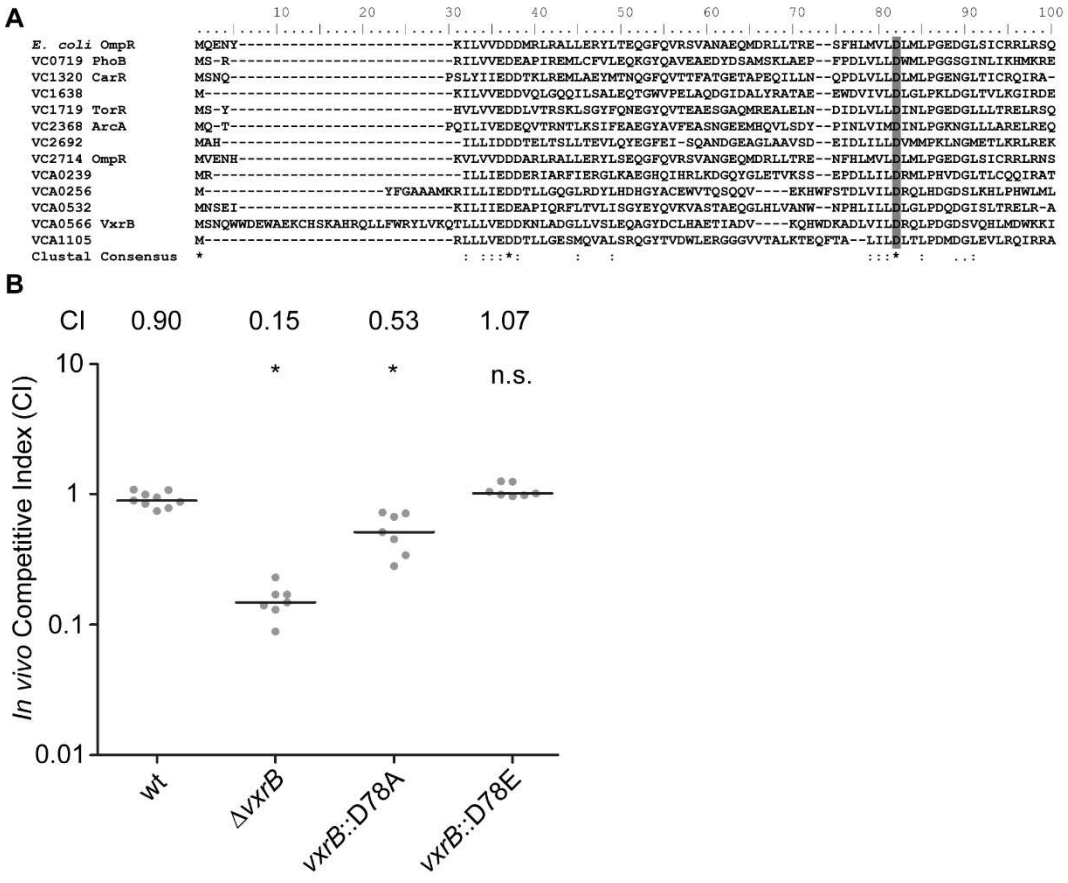
A
10 20 30 40 50 60 70 80 90 100
E. coli OmpR MQENY----------KILVVDDDMRLRALLERYLTEQGFQVRSVANAEQMDRLLTRE--SFHLMVLDLMLPGEDGLSICRRLRSQ
VC0719 PhoB MS-R----------RILVVEDEAPIREMLCFVLEQKGYQAVEAEDYDSAMSKLAEP--FPDLVLLDWMLPGGSGINLIKHMKRE
VC1320 CarR MSNQ----------PSLYIIEDDTKLREMLAEYMTNQGFQVTTFATGETAPEQILLN--QPDLVLLDLMLPGENGLTICRQIRA-
VC1638 M----------KILVVEDDVQLGQQILSALEQTGWVPELAQDGIDALYRATAE--EWDVIVLDLGLPKLDGLTVLKGIRDE
VC1719 TorR MS-Y----------HVLVVEDDLVTRSKLSGYFQNEGYQVTEAESGAQMREALELN--DIDLVLLDINLPGEDGLLLTRELRSQ
VC2368 ArcA MQ-T----------PQILIVEDEQVTRNTLKSIFEAEGYAVFEASNGEEMHQVLSDY--PINLVIMDINLPGKNGLLLARELREQ
VC2692 MAH----------ILLIDDDTELTSLLTEVLQYEGFEI-SQANDGEAGLAAVSD--EIDLILLDVMMPKLNGMETLKRLREK
VC2714 OmpR MVENH----------KVLVVDDDARLRALLERYLSEQGFQVRSVANGEQMDRLLTRE--NFHLMVLDLMLPGEDGLSICRRLRNS
VCA0239 MR----------ILLIEDDERIARFIERGLKAEGHQIHRLKDGQYGLETVKSS--EPDLLILDRMLPHVDGLTLCQQIRAT
VCA0256 M----------YFGAAAMKRILLIEDDTLLGQGLRDYLHDHGYACEWVTQSQQV----EKHWFSTDLVILDRQLHDGDSLKHLPHWLML
VCA0532 MNSEI----------KILIIEDEAPIQRFLTVLISGYEYQVKVASTAEQGLHLVANW--NPHLILLDLGLPDQDGISLTRELR-A
VCA0566 VxrB MSNQWWDEWAEKCHSKAHRQLLFWRYLVKQTLLLVEDDKNLADGLLVSLEQAGYDCLHAETIADV----KQHWDKADLVILDRQLPDGDSVQHLMDWKKI
VCA1105 M----------RLLLVEDDTLLGESMQVALSRQGYTVDWLERGGGVVTALKTEQFTA--LILDLTLPDMDGLEVLRQIRRA
Clustal Consensus * : :::*: : : :::* : ..:
B
CI 0.90 0.15 0.53 1.07
* * n.s.
10
1
0.1
0.01
In vivo Competitive Index (CI)
wt
ΔvxrB
vxrB::D78A
vxrB::D78E

Figure 2.2. The role of the phosphorylation state of VxrB in colonization. (A) Amino acid sequence alignment of the REC domains of the RR proteins belonging to the OmpR family using ClustalW. Numbers above the sequence correspond to the amino acid number of each protein. VC numbers indicate the RR encoded in *V. cholerae* genome. OmpR from *E. coli* was used as a reference to align the aspartate residue that has been shown to be important for phosphorylation (D55A) (66). Highlighted region in gray indicate the aspartate residue that is predicted to be the site of phosphorylation. B) *In vivo* competition assay of a strain harboring the mutated version of *vxrB* on the chromosome. The *vxrB* gene was mutated to convert the aspartate residue predicted to be important for phosphorylation to emulate the inactive (D78A) or active (D78E) state of VxrB. *, $p<0.05$ by the Wilcoxon Signed Rank Test as compared to the CI of wt.

All members of the *vxr* operon contribute to *in vivo* colonization.

The first gene of the *vxr* loci, VCA0565, is annotated as an HK. The other three genes (VCA0567-69) are predicted to encode proteins of unknown function (Fig. 2.3A). We now termed these genes *Vibrio* type six secretion regulator (*vxr*) ABCDE and determined that these genes are co-transcribed using RT-PCR and RNAseq analysis (Fig. 2.3A and Fig. S2.1). The genomic context and organization is conserved in the *Vibrio* species (Figs. S2.2-S2.4) and *vxr* gene products do not share significant sequence similarity with previously characterized proteins.

Figure 2.3

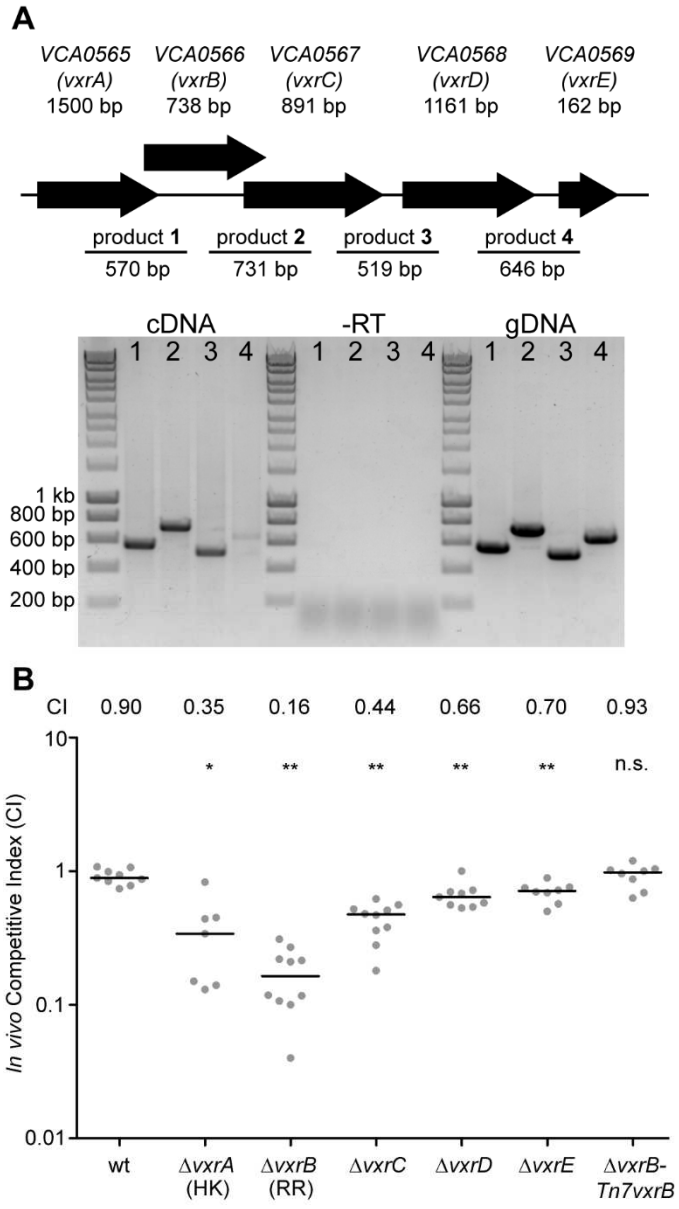
A
VCA0565 (vxrA) 1500 bp
VCA0566 (vxrB) 738 bp
VCA0567 (vxrC) 891 bp
VCA0568 (vxrD) 1161 bp
VCA0569 (vxrE) 162 bp
product 1 570 bp
product 2 731 bp
product 3 519 bp
product 4 646 bp
cDNA
-RT
gDNA
1 2 3 4
1 kb
800 bp
600 bp
400 bp
200 bp
B
CI 0.90 0.35 0.16 0.44 0.66 0.70 0.93
* ** ** ** ** n.s.
In vivo Competitive Index (CI)
10
1
0.1
0.01
wt
ΔvxrA (HK)
ΔvxrB (RR)
ΔvxrC
ΔvxrD
ΔvxrE
ΔvxrB-Tn7vxrB

Figure 2.3. Role of the *vxrABCDE* operon in colonization of the infant mouse model. (A) The top panels shows a schematic representation of the genomic organization of the *vxrABCDE* locus The bottom panel shows the results of RT-PCR analysis designed to determine if *vxrABCDE* genes are cotranscribed. RT-PCR primers designed to amplify intergenic regions are indicated. Products were detected for VCA0565-66 (product 1), VCA0566-67 (product 2), VCA0667-68 (product 3), and VCA0568-69 (product 4) *V. cholerae* genomic DNA template was used for PCR to evaluate primers and amplified product sizes. RT-PCR reaction without reverse transcriptase (-RT) was used as a negative control. (B) Ability of A1552 Δ*vxrA*, Δ*vxrB*, Δ*vxrC*, Δ*vxrD*, Δ*vxrE*, and Δ*vxrB*-Tn7*vxrB* complementation strains to colonize the infant mouse intestine was analyzed using a competition assay with wild-type. Each symbol represents the CI in an individual mouse; horizontal bars indicate the median. *, $p<0.05$; **, $p<0.01$ by the Wilcoxon Signed Rank Test as compared to the CI of wt.

Figure S2.1

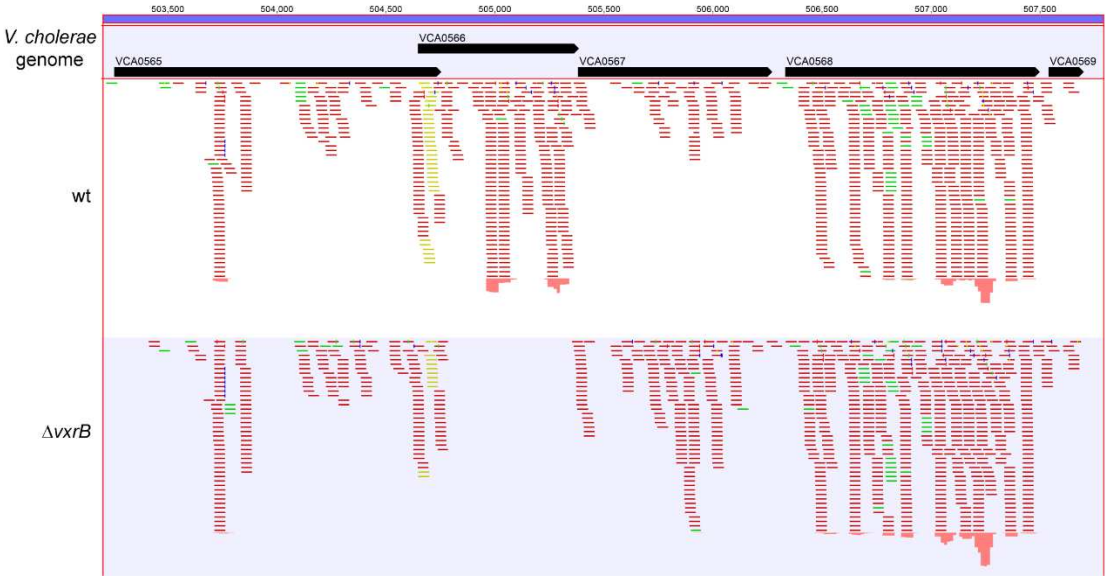
503,500
504,000
504,500
505,000
505,500
506,000
506,500
507,000
507,500
V. cholerae genome
VCA0565
VCA0566
VCA0567
VCA0568
VCA0569
wt
ΔvxrB

Figure S2.1. Confirmation of the predicted operon structure of *vxrABCDE*. RNAseq track reads from wild-type sample. Red and green lines indicate the directionality of the read tracks. Images were prepared by CLC bio version 7.5.1 (Qiagen, Valencia, CA).

Figure S2.2

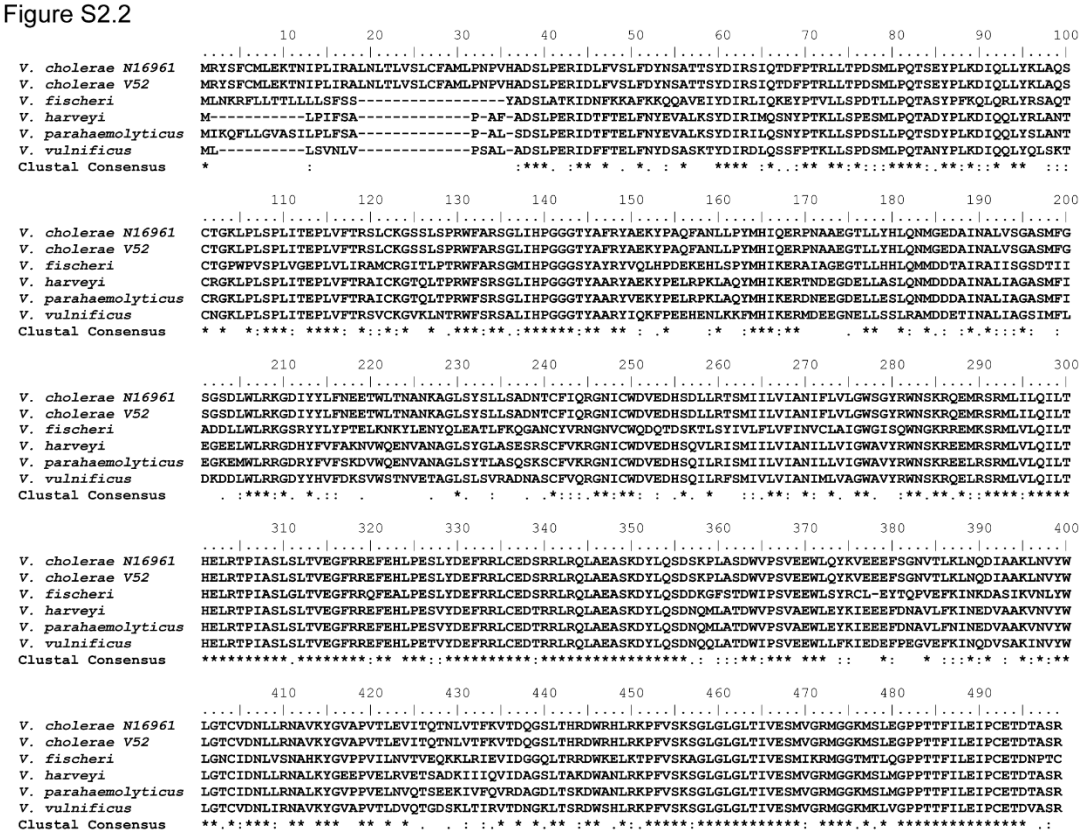
10 20 30 40 50 60 70 80 90 100
V. cholerae N16961 MRYSFCMLEKTNIPLIRALNLTLVSLCFAMLPNPVHADSLPERIDLFVSLFDYNSATTSYDIRSIQTDFPTRLLTPDSMLPQTSEYPLKDIQLLYKLAQS
V. cholerae V52 MRYSFCMLEKTNIPLIRALNLTLVSLCFAMLPNPVHADSLPERIDLFVSLFDYNSATTSYDIRSIQTDFPTRLLTPDSMLPQTSEYPLKDIQLLYKLAQS
V. fischeri MLNKRFLLTTLLLLSFSS----------YADSLATKIDNFKKAFKKQQAVEIYDIRLIQKEYPTVLLSPDTLLPQTASYPFKQLQRLYRSAQT
V. harveyi M----------LPIFSA----------P-AF-ADSLPERIDTFTELFNYEVALKSYDIRIMQSNYPTKLLSPESMLPQTADYPLKDIQQLYRLANT
V. parahaemolyticus MIKQFLLGVASILPLFSA----------P-AL-SDSLPERIDTFTELFNYEVALKSYDIRILQSNYPTKLLSPDSLLPQTSDYPLKDIQQLYSLANT
V. vulnificus ML----------LSVNLV----------PSAL-ADSLPERIDFFTELFNYDSASKTYDIRDLQSSFPTKLLSPDSMLPQTANYPLKDIQQLYQLSKT
Clustal Consensus
110 120 130 140 150 160 170 180 190 200
V. cholerae N16961 CTGKLPLSPLITEPLVFTRSLCKGSSLSPRWFARSGLIHPGGGTYAFRYAEKYPAQFANLLPYMHIQERPNAAEGTLLYHLQNMGEDAINALVSGASMFG
V. cholerae V52 CTGKLPLSPLITEPLVFTRSLCKGSSLSPRWFARSGLIHPGGGTYAFRYAEKYPAQFANLLPYMHIQERPNAAEGTLLYHLQNMGEDAINALVSGASMFG
V. fischeri CTGPWPVSPLVGEPLVLIRAMCRGITLPTRWFARSGMIHPGGGSYAYRYVQLHPDEKEHLSPYMHIKERAIAGEGTLLHHLQMMDDTAIRAIISGSDTII
V. harveyi CRGKLPLSPLITEPLVFTRAICKGTQLTPRWFSRSGLIHPGGGTYAARYAEKYPELRPKLAQYMHIKERTNDEGDELLASLQNMDDDAINALIAGASMFI
V. parahaemolyticus CRGKLPLSPLITEPLVFTRAICKGTQLTPRWFSRSGLIHPGGGTYAARYVEKYPELRPKLAQYMHIKERDNEEGDELLESLQNMDDDAINALIAGASMFI
V. vulnificus CNGKLPLSPLITEPLVFTRSVCKGVKLNTRWFSRSALIHPGGGTYAARYIQKFPEEHENLKKFMHIKERMDEEGNELLSSLRAMDDETINALIAGSIMFL
Clustal Consensus
210 220 230 240 250 260 270 280 290 300
V. cholerae N16961 SGSDLWLRKGDIYYLFNEETWLTNANKAGLSYSLLSADNTCFIQRGNICWDVEDHSDLLRTSMIILVIANIFLVLGWSGYRWNSKRQEMRSRMLILQILT
V. cholerae V52 SGSDLWLRKGDIYYLFNEETWLTNANKAGLSYSLLSADNTCFIQRGNICWDVEDHSDLLRTSMIILVIANIFLVLGWSGYRWNSKRQEMRSRMLILQILT
V. fischeri ADDLLWLRKGSRYYLYPTELKNKYLENYQLEATLFKQGANCYVRNGNVCWQDQTDSKTLSYIVLFLVFINVCLAIGWGISQWNGKRREMKSRMLVLQILT
V. harveyi EGEELWLRRGDHYFVFAKNVWQENVANAGLSYGLASESRSCFVKRGNICWDVEDHSQVLRISMIILVIANILLVIGWAVYRWNSKREEMRSRMLVLQILT
V. parahaemolyticus EGKEMWLRRGDRYFVFSKDVWQENVANAGLSYTLASQSKSCFVKRGNICWDVEDHSQILRISMIILVIANILLVIGWAVYRWNSKREELRSRMLVLQILT
V. vulnificus DKDDLWLRRGDYYHVFDKSVWSTNVETAGLSLSVRADNASCFVQRGNICWDVEDHSQILRFSMIVLVIANIMLVAGWAVYRWNSKRQELRSRMLVLQILT
Clustal Consensus
310 320 330 340 350 360 370 380 390 400
V. cholerae N16961 HELRTPIASLSLTVEGFRREFEHLPESLYDEFRRLCEDSRRLRQLAEASKDYLQSDSKPLASDWVPSVEEWLQYKVEEEFSGNVTLKLNQDIAAKLNVYW
V. cholerae V52 HELRTPIASLSLTVEGFRREFEHLPESLYDEFRRLCEDSRRLRQLAEASKDYLQSDSKPLASDWVPSVEEWLQYKVEEEFSGNVTLKLNQDIAAKLNVYW
V. fischeri HELRTPIASLGLTVEGFRRQFEALPESLYDEFRRLCEDSRRLRQLAEASKDYLQSDDKGFSTDWIPSVEEWLSYRCL-EYTQPVEFKINKDASIKVNLYW
V. harveyi HELRTPIASLSLTVEGFRREFEHLPESVYDEFRRLCEDTRRLRQLAEASKDYLQSDNQMLATDWVPSVAEWLEYKIEEEFDNAVLFKINEDVAAKVNVYW
V. parahaemolyticus HELRTPIASLSLTVEGFRREFEHLPESVYDEFRRLCEDTRRLRQLAEASKDYLQSDNQMLATDWVPSVAEWLEYKIEEEFDNAVLFNINEDVAAKVNVYW
V. vulnificus HELRTPIASLSLTVEGFRREFEHLPETVYDEFRRLCEDTRRLRQLAEASKDYLQSDNQQLATDWIPSVEEWLLFKIEDEFPEGVEFKINQDVSAKINVYW
Clustal Consensus
410 420 430 440 450 460 470 480 490
V. cholerae N16961 LGTCVDNLLRNAVKYGVAPVTLEVITQTNLVTFKVTDQGSLTHRDWRHLRKPFVSKSGLGLGLTIVESMVGRMGGKMSLEGPPTTFILEIPCETDTASR
V. cholerae V52 LGTCVDNLLRNAVKYGVAPVTLEVITQTNLVTFKVTDQGSLTHRDWRHLRKPFVSKSGLGLGLTIVESMVGRMGGKMSLEGPPTTFILEIPCETDTASR
V. fischeri LGNCIDNLVSNAHKYGVPPVILNVTVEQKKLRIEVIDGGQLTRRDWKELKTPFVSKAGLGLGLTIVESMIKRMGGTMTLQGPPTTFILEIPCETDNPTC
V. harveyi LGTCIDNLLRNALKYGEEPVELRVETSADKIIIQVIDAGSLTAKDWANLRKPFVSKSGLGLGLTIVESMVGRMGGKMSLMGPPTTFILEIPCETDTASR
V. parahaemolyticus LGTCIDNLLRNALKYGVPPVELNVQTSEEKIVFQVRDAGDLTSKDWANLRKPFVSKSGLGLGLTIVESMVGRMGGKMSLMGPPTTFILEIPCETDTASR
V. vulnificus LGTCVDNLIRNAVKYGVAPVTLDVQTGDSKLTIRVTDNGKLTSRDWSHLRKPFVSKSGLGLGLTIVESMVGRMGGKMKLVGPPTTFILEIPCETDVASR
Clustal Consensus

Figure S2.2. Multiple sequence alignment of VxrA. Amino acid sequence alignment of the HK, VxrA, to *V. cholerae V52*, *V. fischeri MJ11*, *V. harveyi ATCC BAA-1116, V. parahaemolyticus RIMD 2210633,* and *V.vulnificus YJ016* using ClustalW. Numbers above the sequence correspond to the amino acid number of each protein.

Figure S2.3

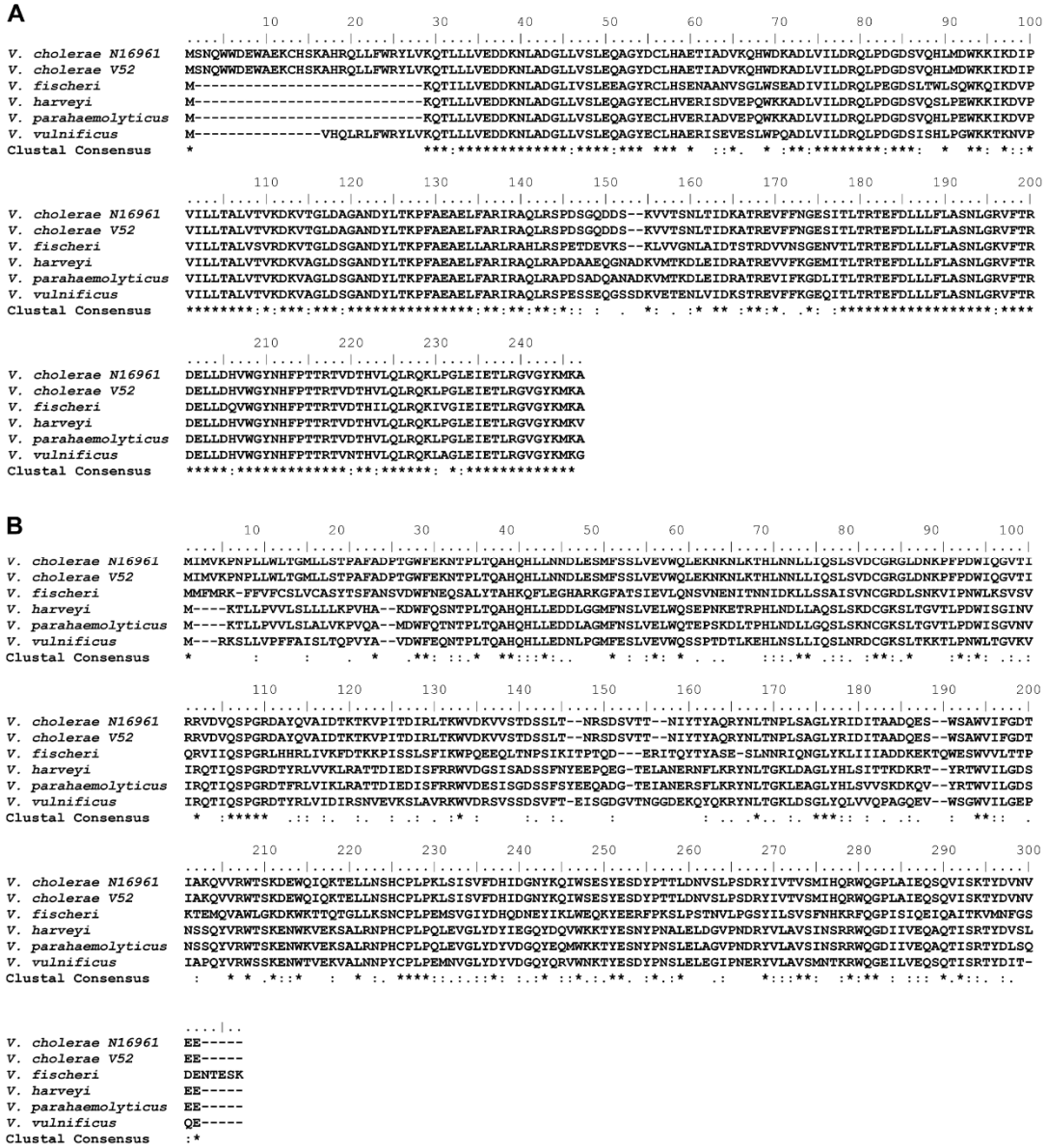
A
V. cholerae N16961
V. cholerae V52
V. fischeri
V. harveyi
V. parahaemolyticus
V. vulnificus
Clustal Consensus
B
V. cholerae N16961
V. cholerae V52
V. fischeri
V. harveyi
V. parahaemolyticus
V. vulnificus
Clustal Consensus

Figure S2.3. Multiple sequence alignment of VxrB and VxrC. (A) Amino acid sequence alignment of the RR, VxrB, and (B) VxrC to *V. cholerae V52*, *V. fischeri MJ11*, *V. harveyi ATCC BAA-1116, V. parahaemolyticus RIMD 2210633,* and *V. vulnificus YJ016* using ClustalW. Numbers above the sequence correspond to the amino acid number of each protein.

Figure S2.4

A

```
                                10        20        30        40        50        60        70        80        90       100
                                ....|....|....|....|....|....|....|....|....|....|....|....|....|....|....|....|....|....|
V. cholerae N16961              MKRIS--LSVGFSLVLTSPLAFSANYAVEARGDAMGGVGVVSGNFLTGPFYNPALVAIYRRNDDAGMILPSIGLSYNDPNDLITDLDKVSDIINQSSKGD
V. cholerae V52                 MKRIS--LSVGFSLVLTSPLAFSANYAVEARGDAMGGVGVVSGNFLTGPFYNPALVAIYRRNDDAGMILPSIGLSYNDPNDLITDLDKVSDIINQSSKGD
V. fischeri                     MKQWIK-IGLLSCATVASSQVSATNFSVDGRIDAMGGAGTAAADYLTGVFYNPALVAIYSRKDDAGLLLPSAGLQVMDQGGMVDDVDQVQKGFSKLANSD
V. harveyi                      MKTQYKILATTMTAALFSGAASAATYAIEARSDAMGGVGTVSASYLTAPFFNPALTAIYRRNDDAGMIVPSFGINYNDQNGLIDEIERIGKL--------
V. parahaemolyticus             MKTQFKILATTITASLFANVASAATYAIEARSDAMGGVGTVSASYLTAPFFNPALTAIYRRNDDAGMIIPSFGISYDDQYDLIDEIERISKL--------
V. vulnificus                   MKLNNRYLYATM---LFCGTANAANYSIEARSDAMGGVGTVSATYLTAPFFNPALAAVYRRNDDAGMLIPSFGITYNDPHDLVDQIDNLGKLIA------
Clustal Consensus               **     :       : .  . ::.:::::.* *****.*..:. :**. *:****.*:* *:****:::** *:   *  .:: :::.: .

                                      110       120       130       140       150       160       170       180       190       200
                                ....|....|....|....|....|....|....|....|....|....|....|....|....|....|....|....|....|....|....|....|
V. cholerae N16961              YSNIGELNKSLTAMQGDVLNAELGGVVAFAIPNQFISANVFGKAYTESFVSPIIDSR-VCADDLCELERAKASSVNAVSVGITELGITLAKYQTFLGQHI
V. cholerae V52                 YSNIGELNKSLTAMQGDVLNAELGGVVAFAIPNQFISANVFGKAYTESFVSPIIDSR-VCADDLCELERAKASSVNAVSVGITELGITLAKYQTFLGQHI
V. fischeri                     PSGAADIENGLRNLNGDALSFSMGAGMAVAIPNRYLSMAFYGKTSVEGITLPDVDALGLPTDPTKPLQLADTTAVGTVALGLAEAGVAFAGYTNFLGQNI
V. harveyi                      -TDPTEIVNSLNAIDGQKMDFDLGGVVAVGIPNKFLSATAYGKLYTESFVEPTIDT--VSGDPLND------SYVRGVSIGVAEAGISLAKYTNFMNQHL
V. parahaemolyticus             -TDVDEIKKSMDAIDGKKMDFDLGGVVAVGIPNKFLSATVYGKLYTESFVQPNVDT--SGADPLTD------SYVQGVSIGVAEAGVSLAKYTNFMNQHL
V. vulnificus                   -AGSPDALPALTAIDGDQLDLELGGALAIGIPNRFLSATIYGKLYTESFITPKV-A--AGPDP-DN------SYVQAVSVSVTEVGVSLAKYQTFLYQHM
Clustal Consensus                :.  :   .:  ::*. :. .:*. :*..***:::*   :**  .*.:  * : :     *          : *  *::.::* *:::* * .*: *::

                                      210       220       230       240       250       260       270       280       290       300
                                ....|....|....|....|....|....|....|....|....|....|....|....|....|....|....|....|....|....|....|....|
V. cholerae N16961              AFGITPKLQRVYTYVYEASLNSYDIKDLRDNGNGETIFNMDAGALWFYGPIRIGFAANNLISREIKTKTITSAV--------SGNPI-SYSYDMKPQYTV
V. cholerae V52                 AFGITPKLQRVYTYVYEASLNSYDIKDLRDNGNGETIFNMDAGALWFYGPIRIGFAANNLISREIKTKTITSAV--------SGNPI-SYSYDMKPQYTV
V. fischeri                     TIGVTPKIQSYLTYTYVEAVNNFDFKDFDKNKTTDNSFNVDVGAVWFYGPWRFAAAGKNLIKNEIETKEITVNFANSQGGGSHGKKTYKYNYELTPTYTA
V. harveyi                      SFGITPKLQRIYTYTYATSFAAFDTKDLRENETAETMFNLDAGALWFFGPYRLGISAKNLIGRDVKTKSFT--Y--------NGDTIQSYEYSMRPVYTV
V. parahaemolyticus             SFGITPKLQRIYTYSYATSFKNFDTKDLREHETAETMFNLDAGALWFFGPYRLGISAKNLIGRDVKTKSFQ--Y--------NTDTIQSYEYSMRPVYTV
V. vulnificus                   AFGVTPKLQRVYTHSFASTFANFDLGDVRENETGETIFNLDAGALWFYGPFRIGVAAKNLIGRDIQTKAYD--F--------NGTSIQSYDYSMRPLYTV
Clustal Consensus               ::*:***:*   *: :  :.  :*  *. .: . :. **:*.**:**:** *:. :.:*** .:::**                    .*.*.: * **.

                                      310       320       330       340       350       360       370       380       390       400
                                ....|....|....|....|....|....|....|....|....|....|....|....|....|....|....|....|....|....|....|....|
V. cholerae N16961              GAGIVADYFTLSVDYDLNEEERYKDFKDNTQMIRVGGEIDIMRQLKLRAGYNKNLAYDNTEGTVTAGIGLSPLNLFQLDLGASYTNENAMGAYINFLASY
V. cholerae V52                 GAGIVADYFTLSVDYDLNEEERYKDFKDNTQMIRVGGEIDIMRQLKLRAGYNKNLAYDNTEGTVTAGIGLSPLNLFQLDLGASYTNENAMGAYINFLASY
V. fischeri                     GVAFMTNYFIVTADLDLNEQERFVGLDDNVQMFRAGAEIDLLYQIQLRGGFKKDLAGTYDD-AFTAGIGFSPLNMFHFDLAAIYSVDSTYGVSVNMAYEY
V. harveyi                      GAGYVADYFSFSVDYDLNEEKKFSTFDDNTQMLRAGFEIDVLRQLALRGGYMTNLARSDDEGTITAGLGLSPLNLIEIDIAARYTNADAMGASINFLATY
V. parahaemolyticus             GAGIVADYFTMSVDYDLNEEKRFSSFDDNTQMIRAGFEIDILRQMALRGGYMKNLARSNDEGTITAGIGLSPLNLIELDISARYTNENAMGASINFLATY
V. vulnificus                   GAGIVADYFTLSVDYDLNEEKKFSSFDDNSQMLRAGFEIDVLRQLQIRGGYMKNMARDVDD-TITAGIGLSPLNLFEVDISARYTNENAMGASINFLATY
Clustal Consensus               *.. :::** .:.* ****::::  :.** **:*.* ***:: *: :*.*: .::*    : :.***:*:****::..*:.* *:  .: *. :*:   *
```

B

```
                                10        20        30        40        50
                                ....|....|....|....|....|....|....|....|....|...
V. cholerae N16961              MFDDLPTLTHAEQQVAVEKIQKLMAEGISTGEAIKIVAQQIREDKKAQNQGTH
V. cholerae V52                 MFDDLPTLTHAEQQVAVEKIQKLMAEGISTGEAIKIVAQQIREDKKAQNQGTH
V. fischeri                     MLD-LPTLTHEEQQQAVEKIQELMRQGVGSGEAIKIISDQIRAEI-AEKEKQR
V. harveyi                      MFDDLPPLSHQEQQQAVERIKELMQKGTSTAEAIKIVAEQIRAEYAAKKQ-D-
V. parahaemolyticus             MFDDLPPISHKEQQEAVERIQELMAKGTSTAEAIKIVADQIRAEYAAKQQGS-
V. vulnificus                   MFDDLPPLSHQEQQRAVEEIQKLMAEGMSTAQAIKIIAEKIRAEHKA--QSAE
Clustal Consensus               *:* **.::* *** ***.*::** :* .:.:****::::** :  *  :
```

Figure S2.4. Multiple sequence alignment of VxrD and VxrE. (A) Amino acid sequence alignment of VxrD, and (B) VxrE to *V. cholerae V52*, *V. fischeri MJ11*, *V. harveyi ATCC BAA-1116, V. parahaemolyticus RIMD 2210633,* and *V. vulnificus YJ016* using ClustalW. Numbers above the sequence correspond to the amino acid number of each protein.

To gain a better understanding of the role of the *vxr* operon in colonization, we investigated whether the cognate HK and other genes in the *vxr* operon also contributed to mouse colonization. In-frame unmarked deletion mutants of *vxrA*, *vxrB, vxrC*, *vxrD*, and *vxrE* (Fig. 2.3B) were generated and analyzed in an *in vivo* competition assay. Each mutant was outcompeted, with CIs of 0.35, 0.16, 0.44, 0.66, and 0.70, respectively (Fig. 2.3B). These findings suggest that while *vxrA and vxrB* genes are critical for colonization in the infant mouse model, contribution of *vxrCDE* genes appears to be minor.

To further confirm the phenotype of Δ*vxrB* colonization defect, a wild type copy of *vxrB* whose expression was driven from its native promoter was inserted into the Tn7 site (located between VC0487 and VC0488) on the chromosome of Δ*vxrB*. *In vivo* competition assay of Δ*vxrB-Tn7vxrB* had a CI of 0.93, similar to wild type levels, where Δ*vxrB* had a CI of 0.16 (Fig. 2.3B). Thus, the Δ*vxrB* colonization defect is restored to wild-type levels by introduction of the wild-type copy of *vxrB*.

VxrB regulates T6SS gene expression.

To gain a better understanding of the contribution of VxrB to *V. cholerae* pathogenesis, we performed high throughput transcriptome sequencing (RNA-seq) analysis to identify the *V. cholerae* genes controlled by VxrB. We used cells grown under virulence inducing AKI conditions, to mimic the

intestinal conditions encountered when we know VxrB is important. 149 genes showed statistically significant differences in gene expression between the wild type and mutant (Tables S2 & S3). Of these, 80 genes were expressed to greater levels in the Δ*vxrB* mutant relative to the wild type (Table S2), while 69 were expressed to lower levels in the Δ*vxrB* mutant relative to wild type (Table S3). Of particular interest was the observation that message abundance of most of the T6SS genes in both the large cluster (VCA0105-VCA0124) and the two auxiliary clusters (VCA0017-VCA0022 and VC1415-VC1421) were less in the VxrB mutant relative to wild type (Table 2.2) (Fig. S5). This finding suggests that VxrB activates expression of the T6SS genes.

Table S2.1. Genes positively regulated by VxrB under AKI conditions

ORF ID[a]	Gene	Fold Down Regulation[b]	p-value	Predicted function
VCA0566	*vxrB*	-21.25	0.00000	Response regulator
VC2662		-6.69	0.00000	Polyhydroxyalkanoic acid synthase
VCA0376		-6.62	0.02888	Hypothetical protein
VCA0105		-4.44	0.00000	PAAR motif
VCA0125		-4.13	0.00000	Prokaryotic membrane lipoprotein lipid attachment site profile
VC0483		-3.83	0.00000	Oxidative stress defense protein
VCA0035		-3.60	0.00000	Phosphatidylglycerophosphatase B
VC1454	*rstA1*	-3.55	0.02341	Putative phage replication protein
VCA0451		-3.55	0.02444	Hypothetical protein
VC0157		-3.28	0.00000	Alkaline serine protease
VC1160		-3.26	0.00000	Glutathione synthase/glutaminyl transferase
VCA0271		-3.19	0.00000	Lambda repressor-like, DNA-binding
VCA0484		-3.18	0.00249	Hypothetical protein

VC1415	*hcp-1*	-3.02	0.00000	T6SS
VCA0106		-2.97	0.00000	T6SS
VCA0017	*hcp-2*	-2.82	0.00000	T6SS
VCA0026		-2.73	0.00000	Hypothetical protein
VCA0112	*fha*	-2.72	0.00000	T6SS
VC1484	*rmf*	-2.70	0.00000	Ribosome modulation factor
VC1962	*nlpE*	-2.64	0.00000	Copper resistance lipoprotein
VCA0140		-2.62	0.00000	Spindolin-related protein
VCA0229	*vctG*	-2.42	0.01903	Iron(III) ABC transporter
VCA0109		-2.39	0.00007	T6SS
VC1162		-2.34	0.00000	Peptidase aspartic lipoprotein
VC2612		-2.31	0.01225	YehU-like superfamily
VCA0113	*vasD*	-2.29	0.00000	T6SS
VC1161		-2.28	0.00000	Gonadoliberin III-related protein
VCA0845		-2.24	0.00000	Hypothetical protein
VC2518		-2.17	0.00000	ABC-type transport resistance to organic solvents
VCA0122	*vasM*	-2.17	0.02985	T6SS
VCA0846		-2.16	0.00000	Putative threonine efflux protein
VCA0365		-2.14	0.00119	Hypothetical protein
VCA0677	*napD*	-2.13	0.00002	Nitrate reductase assembly
VC0255	*rfbT*	-2.12	0.01445	Serotype conversion
VCA0107	*vipA*	-2.11	0.00113	T6SS
VCA0676	*napF*	-2.11	0.00017	Iron-sulfur cluster-binding protein
VC2386		-2.10	0.04729	ATP-binding protein in DNA repair
VC2213	*ompA*	-2.08	0.00000	Outer membrane protein A
VC0248		-2.07	0.03509	Acyl carrier protein
VC1947		-2.07	0.00250	LysR family transcriptional regulator
VCA0108	*vipB*	-2.05	0.00000	T6SS
VCA0116	*clpB-2*	-2.05	0.00000	T6SS
VCA0917		-2.05	0.00000	TetR family transcriptional regulator
VCA0111	*vasB*	-1.99	0.00001	T6SS
VCA0915	*hutD*	-1.97	0.00000	Hemin importer
VCA0121	*vasL*	-1.96	0.00000	T6SS
VCA0120	*vasK*	-1.95	0.00000	T6SS
VCA0114	*vasE*	-1.89	0.00000	T6SS
VC0687	*cstA*	-1.87	0.00000	Carbon starvation protein A
VCA0117	*vasH*	-1.87	0.00000	T6SS
VCA0115	*vasF*	-1.85	0.00001	T6SS
VC2076		-1.81	0.01176	FeoC transcriptional regulator
VCA0119	*vasJ*	-1.77	0.00000	T6SS

VCA0426		-1.76	0.00828	Iron-sulfur protein
VC2548		-1.75	0.00000	Bacterial surface antigen
VC2547		-1.73	0.00000	Hypothetical protein
VC0246	*rfbH*	-1.72	0.00055	Lipopolysaccharide O-antigen transport protein
VCA0124	*tsiV3*	-1.72	0.00144	T6SS
VCA0678	*napA*	-1.65	0.00267	Periplasmic nitrate reductase
VC1207		-1.63	0.00000	Hypothetical protein
VC0259	*rfbV*	-1.62	0.00597	Lipopolysaccharide biosynthesis protein
VC0633	*ompU*	-1.62	0.00000	Outer membrane protein
VC2516		-1.62	0.00168	Anti-sigma factor B antagonist
VC2517		-1.62	0.00000	Toluene tolerance
VC0287	*gntV*	-1.60	0.01846	Thermoresistance gluconokinase
VC1663	*hslJ*	-1.60	0.00000	Heat shock protein
VC1837	*tolA*	-1.60	0.00000	Membrane protein in colicin uptake
VCA0110	*vasA*	-1.59	0.00002	T6SS
VCA0679	*napB*	-1.58	0.00849	Nitrate reductase cytochrome c-type subunit
VC1763		-1.57	0.00019	Chemotaxis protein MotB-related
VC0090	*dinF*	-1.56	0.00000	DNA-damage inducible protein F
VC2221		-1.56	0.00048	Hypothetical protein
VCA0003		-1.56	0.00135	Hypothetical protein
VC0948		-1.55	0.00000	Rare lipoprotein A
VCA0928		-1.55	0.02741	Hypothetical protein
VCA0821		-1.54	0.00000	Hypothetical protein
VC1919	*hupB*	-1.52	0.00018	Histone-like DNA binding protein
VC2401	*murG*	-1.52	0.00465	Glycosyl transferase
VC1270		-1.51	0.00000	Glyoxylase II family protein
VCA0123	*vgrG-3*	-1.50	0.00000	T6SS

[a]ORF IDs are derived from the *V. cholerae* N16961 genome.
[b]Fold change is the Δ*vxrB* mutant relative to the wild-type strain.

Table S2.2. Genes negatively regulated by VxrB under AKI condition

ORF ID[a]	Gene	Fold Up Regulation[b]	p-value	Predicted function
VC1854	*ompT*	3.18	0.00000	Outer membrane porin
VC2215		2.52	0.00000	Cation transport
VC0713		2.39	0.01046	Hypothetical protein
VC2216	*copG*	2.36	0.00000	Copper-binding protein
VC0024		2.31	0.00282	Sulphurtransferase
VC2561	*cysG*	2.31	0.01393	Uroporphyrin-III C-methyltransferase
VC1740		2.22	0.00000	Oxidoreductase, acyl-CoA dehydrogenase
VC1344	*hppD*	2.20	0.00000	4-hydroxyphenylpyruvate dioxygenase
VC1368		2.08	0.00005	Hypothetical protein
VCA0913	*hutB*	2.08	0.01042	Hemin ABC transporter
VC2559	*cysN*	2.01	0.00002	Sulfate adenylate transferase
VCA0766		2.01	0.00063	Cytochrome c554
VC1332		2.00	0.00000	Hypothetical protein
VC1737	*infA*	1.98	0.01954	Initiation factor IF-1
VC1823	*frwB*	1.96	0.00979	PTS system, fructose-specific IIB
VC2231	*fadE*	1.95	0.00000	Oxidoreductase, acyl-CoA dehydrogenase
VCA0260		1.94	0.00000	Cupredoxin
VC1078		1.91	0.00602	Hypothetical protein
VC0784		1.90	0.00000	Sodium/alanine symporter
VCA0350	*blc-2*	1.90	0.00303	Lipoprotein Blc
VCA0812		1.89	0.00000	Leucine aminopeptidase-related protein
VC1345		1.85	0.00000	Oxidoreductase
VC1927	*dctM*	1.83	0.00000	C4-dicarboxylate transport protein
VC1565		1.80	0.00136	Outer membrane efflux protein
VC1542	*ligA-2*	1.78	0.01349	DNA ligase
VC2618	*argD*	1.78	0.00000	Acetylornithine aminotransferase
VC1334		1.77	0.00003	Hypothetical protein
VC2489		1.76	0.01042	TetR family transcriptional regulator
VC1333		1.74	0.00128	Hypothetical protein
VC1741		1.74	0.00390	TetR family transcriptional regulator
VC2558	*cysC*	1.74	0.01196	Adenylylsulfate kinase
VCA0293		1.74	0.00886	Hypothetical protein
VC2617		1.72	0.00000	Arginine/Ornithine succinyltransferase
VCA0567	*vxrC*	1.72	0.00000	Hypothetical protein
VC2705		1.71	0.00000	Sodium/solute symporter

VC1264		1.70	0.00002	Iron-regulated protein A
VC0282		1.68	0.00000	Methyl-accepting chemotaxis protein
VC1528		1.68	0.00565	Periplasmic binding protein-like
VC1318	*ompV*	1.67	0.00002	Outer membrane protein V
VCA0289	*rpmI*	1.67	0.00047	Ribosomal protein L35
VCA0616	*folE*	1.63	0.00057	GTP cyclohydrolase
VC0069		1.62	0.00000	Multidrug resistance protein
VC1928		1.62	0.00014	C4-dicarboxylate transport protein
VC0787		1.61	0.02576	LysR family transcriptional regulator
VC2177		1.61	0.04007	Invasion gene expression up-regulator sirB
VC0706		1.60	0.00239	Sigma-54 modulation protein
VC2704		1.60	0.00000	Sodium symporter
VCA0925	*pyrC*	1.60	0.00001	Dihydroorotase
VC0888		1.58	0.04712	Pseudouridine synthase
VC1293	*aspC*	1.58	0.00004	Aromatic amino acid aminotransferase
VCA0262		1.58	0.00568	Hypothetical protein
VCA0749	*glpC*	1.58	0.00012	Anaerobic glycerol-3-phosphate dehydrogenase
VC1506		1.57	0.00011	Thioesterase
VCA0828	*phhA*	1.57	0.00146	Phenylalanine-4-hydroxylase
VC0302		1.56	0.00371	Transporter
VC1092	*oppB*	1.56	0.00000	Oligopeptide ABC transporter
VC1547		1.53	0.01583	Biopolymer transport protein
VC2758	*fadB*	1.53	0.00000	Fatty oxidation complex
VC0018	*ibpA*	1.52	0.00001	Heat shock protein A
VC1638		1.52	0.02834	OmpR family response regulator
VCA0425		1.52	0.00256	Hypothetical protein
VCA0889		1.52	0.00639	LysR family transcriptional regulator
VC0263		1.51	0.00205	Galactosyl-transferase
VC1897		1.51	0.00044	Hisitidine triad protein
VC2341		1.51	0.00000	Long chain fatty acid CoA ligase
VCA0767		1.51	0.00018	TetR family transcriptional regulator
VCA1002		1.51	0.00884	AzlC family protein
VC0425		1.50	0.00776	Galactose-binding domain-like
VC2669		1.50	0.03708	5-carboxymethyl-2-2hydroxymuconate delta isomerase

[a]ORF IDs are derived from the *V. cholerae* N16961 genome.
[b]Fold change is the Δ*vxrB* mutant relative to the wild-type strain.

Table 2.2. Type VI secretion genes regulated by VxrB

ORF ID	Gene	AKI	
		Fold change	P-value
VCA0105		-4.44	0.00000
VCA0106		-2.97	0.00000
VCA0107	*vipA*	-2.11	0.00113
VCA0108	*vipB*	-2.05	0.00000
VCA0109		-2.39	0.00007
VCA0110	*vasA*	-1.59	0.00002
VCA0111	*vasB*	-1.99	0.00001
VCA0112	*fha*	-2.72	0.00000
VCA0113	*vasD*	-2.29	0.00000
VCA0114	*vasE*	-1.89	0.00000
VCA0115	*vasF*	-1.85	0.00001
VCA0116	*clpB-2*	-2.05	0.00000
VCA0117	*vasH*	-1.87	0.00000
VCA0018	*vasI*	-1.46	0.00612
VCA0119	*vasJ*	-1.77	0.00000
VCA0120	*vasK*	-1.95	0.00000
VCA0121	*vasL*	-1.96	0.00000
VCA0122	*vasM*	-2.17	0.02985
VCA0123	*vgrG-3*	-1.50	0.00000
VCA0124	*tsiV3*	-1.72	0.00144
VCA0017	*hcp2*	-2.82	0.00000
VCA0018	*vgrG-2*	-1.22	0.41237
VCA0019	*vasW*	1.15	0.67767
VCA0020	*vasX*	-1.33	0.11525
VCA0021	*tsiV2*	-1.38	0.11525
VC1415	*hcp1*	-3.02	0.00000
VC1416	*vgrG-1*	-1.12	0.50510
VC1417		-1.44	0.04444
VC1418	*tseL*	-1.29	0.06289

Figure S2.5

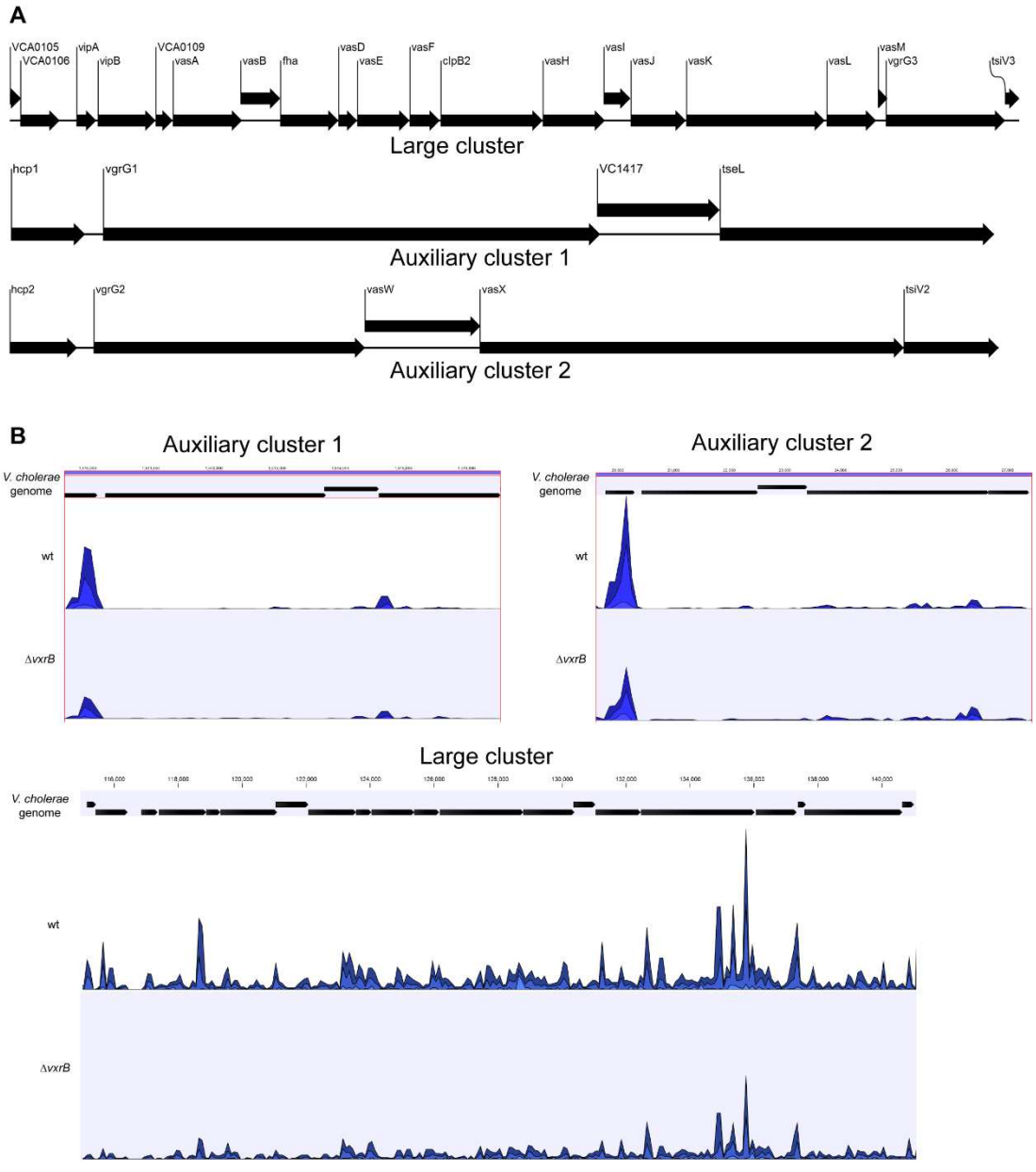
A
VCA0105
VCA0106
vipA
vipB
VCA0109
vasA
vasB
fha
vasD
vasE
vasF
clpB2
vasH
vasI
vasJ
vasK
vasL
vasM
vgrG3
tsiV3
Large cluster
hcp1
vgrG1
VC1417
tseL
Auxiliary cluster 1
hcp2
vgrG2
vasW
vasX
tsiV2
Auxiliary cluster 2
B
Auxiliary cluster 1
Auxiliary cluster 2
V. cholerae genome
wt
ΔvxrB
Large cluster

Figure S2.5. Expression analysis of the T6SS gene clusters. (A) Schematic representation of the major T6SS large gene cluster and auxiliary clusters 1 and 2. (B) RNAseq data showing the coverage of cDNA reads in wild type (wt) and Δ*vxrB* mutant (*vxrB*) over the large cluster and the two auxiliary clusters. Images were prepared by CLC bio version 7.5.1 (Qiagen, Valencia, CA).

VxrB regulates production of T6SS.

To further analyze the role of *vxrB* in T6SS expression and function, we compared the levels of the major T6SS structural component, Hcp, between wild type and ∆*vxrB* mutant *V. cholerae*. Quantitative real-time PCR analysis of *hcp* revealed that the transcript abundance of *hcp* was decreased by 3.7 fold under AKI conditions and 4.1 fold under LB conditions in the ∆*vxrB* mutant relative to wild type (Fig. 2.4A). This finding supports that VxrB regulates expression of *hcp* and is consistent with the RNA-seq analysis. Additionally the levels of the Hcp protein in Δ*vxrB* were lower than wild type, in both whole cell samples and culture supernatants (Fig. 2.4B). We also determined that complementation of the *vxrB* mutation (Δ*vxrB-Tn7vxrB*) restored Hcp to wild-type levels. Because we found lower amounts of Hcp in the supernatant as well as in whole cells, this finding suggests that VxrB is needed to express and secrete Hcp. As negative controls, we included a Δ*hcp1*Δ*hcp2* mutant because it is unable to produce the Hcp proteins (11, 58). As expected, no Hcp production was observed in this mutant. Furthermore, complementation of *hcp1* in the Δ*hcp1*Δ*hcp2* mutant partially restored Hcp levels (Fig. 2.4B). Overall these findings suggest that Hcp production is decreased in Δ*vxrB* mutant.

Figure 2.4

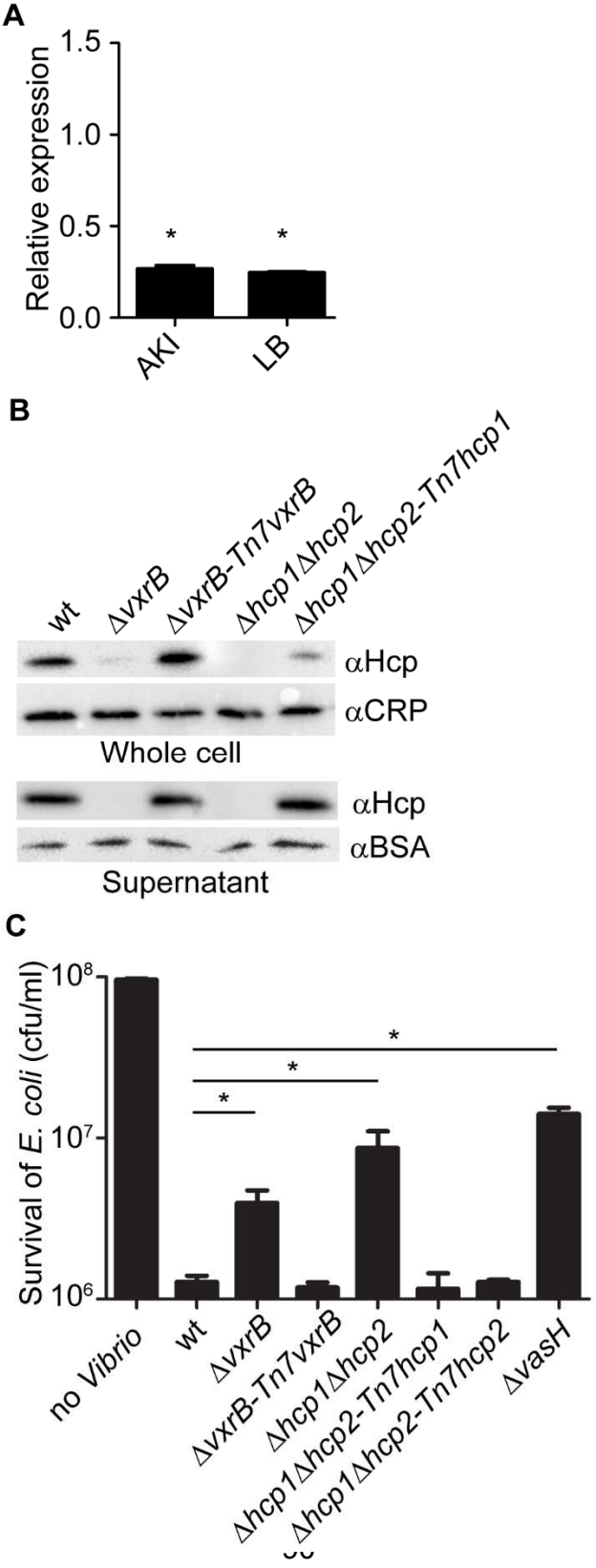
A
Relative expression
1.5
1.0
0.5
0.0
*
*
AKI
LB
B
wt
ΔvxrB
ΔvxrB-Tn7vxrB
Δhcp1Δhcp2
Δhcp1Δhcp2-Tn7hcp1
αHcp
αCRP
Whole cell
αHcp
αBSA
Supernatant
C
Survival of E. coli (cfu/ml)
10^8
10^7
10^6
*
*
*
no Vibrio
wt
ΔvxrB
ΔvxrB-Tn7vxrB
Δhcp1Δhcp2
Δhcp1Δhcp2-Tn7hcp1
Δhcp1Δhcp2-Tn7hcp2
ΔvasH

Figure 2.4. Analysis of Hcp production and secretion in the *vxrB* mutant. (A) Quantitative real-time PCR analysis of *hcp* using total RNA isolated from wild-type and Δ*vxrB* grown in AKI and LB. Experiments were performed using two independent biological replicates, each performed in quadruplicate. The Pfaffl method was used to compare expression levels of *hcp* to 16s rRNA and relative expression was calculated by comparing expression in Δ*vxrB* with that of wt. *, $p<0.05$ by Student's t-test. (B) Hcp production and secretion was analyzed in whole cells and culture supernatants in wild type, Δ*vxrB*, Δ*vxrB::Tn7vxrB*, Δ*hcp1*Δ*hcp2,* and Δ*hcp1*Δ*hcp2*::*Tn7hcp1* strains by immunoblot analysis. Equal amounts of total protein (determined by BCA assay) were loaded onto a SDS 13% polyacrylamide gel. Prior to TCA precipitation and total protein quantification, 100μg/ml of BSA was added to the supernatant. After the blot was probed for Hcp, the blot was stripped of all antibodies using Western Blot Stripping Buffer (GM Biosciences, MD) and the same blot was used to probe for CRP and BSA. The data shown is representative of the results of three independent experiments. (C) Interbacterial killing was analyzed by mixing *V. cholerae* strains and prey *E. coli* strain MC4100 in a 10:1 ratio, followed by incubation on LB agar plates for 4 hours at 30°C and determination of surviving *E. coli* MC4100. The data represent averages and standard deviations of three independent experiments. *, $p<0.05$ by the Student's t-test as compared to the values for interbacterial killing of the wild-type strain.

Next we analyzed whether VxrB was needed for T6SS function, by examining T6SS-mediated interbacterial killing. Killing assays between the *V. cholerae* and the target *E. coli* K-12 strain MC4100 showed that wild-type *V. cholerae* decreased the numbers of *E. coli* compared to control experiments. This killing was dependent on the T6SS, as shown by greater numbers of *E. coli* obtained when incubated with *V. cholerae* Δ*hcp1*Δ*hcp2* mutant and Δ*vasH* mutants, consistent with the findings reported by Ishikawa *et al*. (Fig. 2.4C) (58). This phenotype was complemented by introduction of either *hcp1* or *hcp2* into the Tn7 site on the chromosome. Consistent with our transcriptional and protein analysis presented above, we found that Δ*vxrB* mutants mediated less *E. coli* killing. These findings suggest that T6SS regulation by VxrB contributes to interbacterial killing.

Since VxrB regulates T6SS expression and is required to for intestinal colonization, we next asked whether the T6SS itself is required for intestinal colonization. We performed *in vivo* competition assays of a T6SS null mutant (Δ*hcp1*Δ*hcp2*) against wild type in the infant mouse model. We found that the *in-vivo* CI for Δ*hcp1*Δ*hcp2* was 0.17 (Fig. 2.5A). In addition, Δ*vgrG3* also had an *in-vivo* CI of 0.26 suggesting that T6SS components are important for intestinal colonization (Fig. 2.5A). This suggests that structural components of the T6SS are needed to colonize the intestine. Furthermore, this finding also

suggests that the colonization defect associated with the Δ*vxrB* mutant could be caused by diminished T6SS production. To evaluate this possibility, we tested the *in vivo* competition of Δ*hcp1*Δ*hcp2* against Δ*vxrB* and found that these strains competed nearly equally with each other (Fig. 2.5C). Furthermore, in-vivo CI of Δ*vxrB*Δ*hcp1*Δ*hcp2* triple mutant against Δ*vxrB* was 0.07 and Δ*vxrB*Δ*hcp1*Δ*hcp2* against wt was 0.10. This suggests that in addition to T6SS genes there may be other factors that VxrB may regulate. It is also likely that T6SS expression is not completely abolished by the *vtrB* mutation. Indeed, western analysis (Fig. 2.4B) shows that in *vtrB* mutant Hcp production is reduced but not completely eliminated. Similarly *in vitro* killing assay shows that *vtrB* mutant's interbacterial killing ability is not identical to that of the strain lacking T6SS.

Figure 2.5

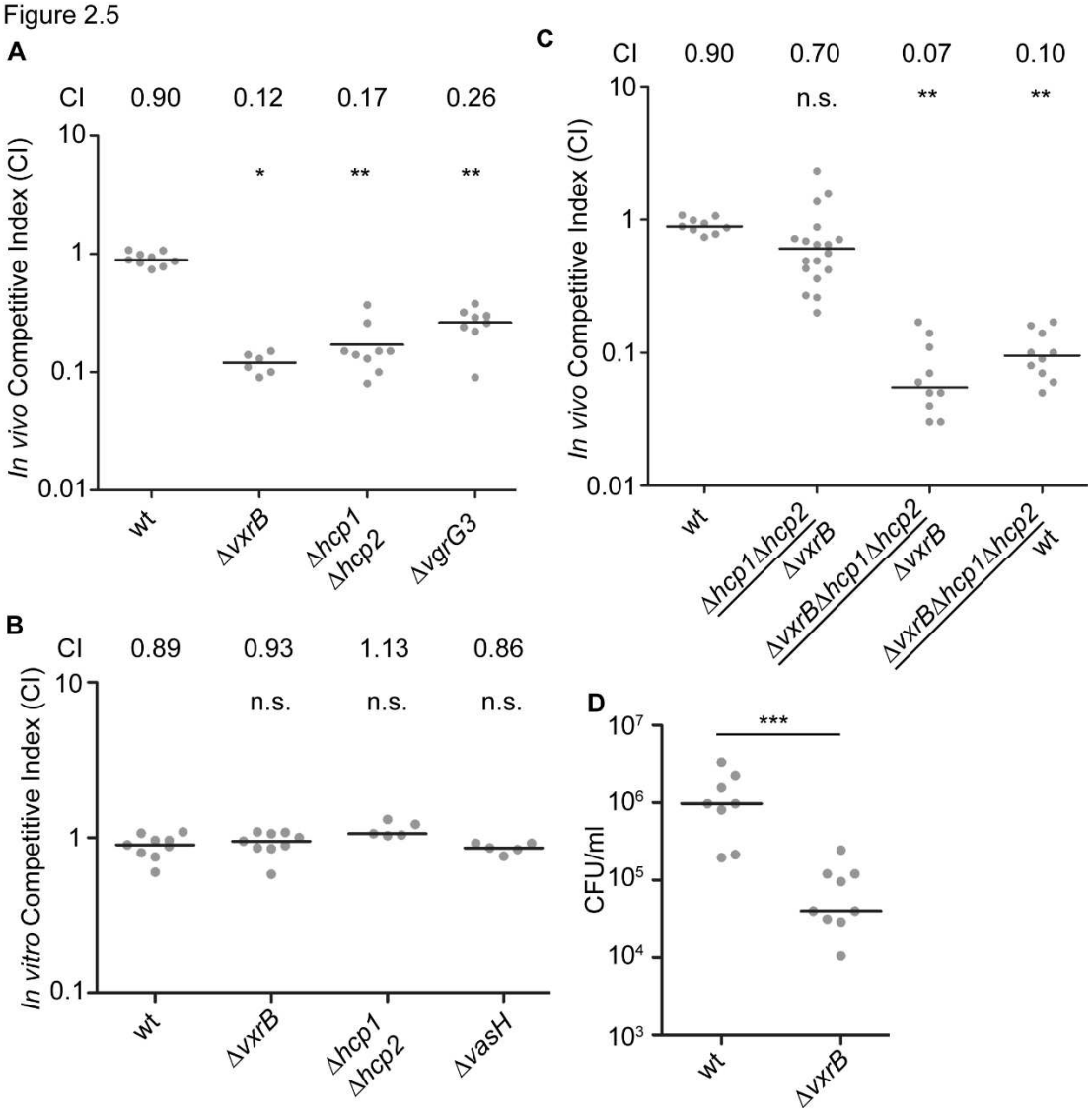
A
CI 0.90 0.12 0.17 0.26
In vivo Competitive Index (CI)
10
1
0.1
0.01
* ** **
wt
ΔvxrB
Δhcp1 Δhcp2
ΔvgrG3
B
CI 0.89 0.93 1.13 0.86
In vitro Competitive Index (CI)
10
1
0.1
n.s. n.s. n.s.
wt
ΔvxrB
Δhcp1 Δhcp2
ΔvasH
C
CI 0.90 0.70 0.07 0.10
In vivo Competitive Index (CI)
10
1
0.1
0.01
n.s. ** **
wt
Δhcp1Δhcp2 ΔvxrB
ΔvxrBΔhcp1Δhcp2 ΔvxrB
ΔvxrBΔhcp1Δhcp2 wt
D
CFU/ml
10^7
10^6
10^5
10^4
10^3
***
wt
ΔvxrB

Figure 2.5. Analysis of the role of T6SS in colonization in the infant mouse in *V. cholerae* O1 EL Tor A1552. (A) Ability of Δ*vxrB*, Δ*vxrB*-Tn7*vxrB,* Δ*hcp1*Δ*hcp2,* Δ*vgrG3*, to colonize the infant mouse intestine was analyzed using a competition assay with isogenic wild-type strain. *, $p<0.05$; **, $p<0.01$ by the Wilcoxon Signed Rank Test as compared to wt (CI of 0.90). (B) *In vitro* competition assay of Δ*vxrB*, Δ*hcp1*Δ*hcp2*, and *ΔvasH*. Strains were grown in LB at 30°C for 20 hours. Statistical analysis was carried out using Wilcoxon Signed Rank Test, comparing the CI of each strain to the CI of wt *lacZ*$^+$ / wt lacZ$^-$ (shown as wt) (CI of 0.98). (C) Ability of Δ*hcp1*Δ*hcp2* to colonize the infant mouse intestine was analyzed using a competition assay with Δ*vxrB*. (D) Ability of wild type and Δ*vxrB* to colonize the infant mouse intestine in single-strain infections. Each symbol represents the CI in an individual mouse; horizontal bars indicate the median. ***, $p<0.001$ by the Student's t-test as compared to the values for colonization of the wild-type strain. n.s. indicates mutants were not significantly different from the wt.

We next asked whether VxrB plays a role in growth in vitro, by performing an *in vitro* competition assay. Δ*vxrB* mutants grew equally well as wild type, suggesting that neither had a competitive advantage over the other *in vitro* (Fig. 2.5B). This outcome suggests that there may be an *in vivo* signal produced in the infant mouse that triggers T6SS activity and colonization. We also performed single-strain colonization assays in the infant mouse model with *ΔvxrB*. There was a 12.7-fold decrease in colonization for Δ*vxrB* compared to wild type (Fig. 2.5D). This finding suggests that the colonization defect by Δ*vxrB* was not solely dependent on wild type, and possibly could be caused by competition with the normal flora or ability of the mutant to adapt to the infection microenvironment.

Discussion

Systematic mutational phenotypic characterization of TCSs has been performed in only a few bacteria, including *Vibrio fischeri*, *E. coli*, *Bacillus subtilis, Streptococcus pneumoniae,* and *Enterococcus faecalis* (68-72). In this study, we systematically analyzed the role of all *V. cholerae* TCS in colonization of the infant mouse small intestine and identified the RRs that play roles in mouse intestinal colonization. Specifically, ΔVC0719 (*phoB*), ΔVC1021 (*luxO*), ΔVC1213 (*varA*), *and* ΔVC2135 (*flrC*), and ΔVCA0566 (*vxrB*) exhibited intestinal colonization defects while ΔVC1050, ΔVC1086, and

ΔVC1087 showed enhanced colonization. Many of the RRs had either no statistically significant defect or minor defects in the infant mouse colonization assay. It remains possible, however, that these RRs have a role in colonization in other infection models.

In vivo transcriptome analysis has been performed on different strains of *V. cholerae* in the infant mouse and rabbit ileal loop infection models. The analysis of the whole genome expression of *V. cholerae* O1 El Tor C6706 cells accumulating in the ceca of orally infected infant rabbits and the intestines of orally infected infant mice revealed that expression of the genes encoding RRs is altered during *in vivo* growth conditions as compared to *in vitro* growth in nutrient broth and that *in vivo* expression of TCS also differed between the model systems (73). In the infant rabbit infection model, expression of seven RR (VC1081, VC1082, VC1155, *vieA*, VC2702 (*crbR*), VCA0210, and VCA1105) was increased and 1 RR (*carR*) was decreased by more than 2-fold significantly in comparison to *V. cholerae* cells grown *in vitro* in nutrient broth. In the infant mouse infection model, expression of 17 RR (*vpsR*, VC1050, VC1081, VC1082, VC1086, VC1087, VC1155, VC1522, *flrC*, *cbrR*, *ompR*, *dct-D2*, *vxrB*, *uhpA*, *vpsT*, VCA1086, and VCA1105) and 9 RR (*qstR, phoB*, VC1348, VC1638, *vieB*, *cpxR*, *ntrC*, VCA0532, *pgtA*) were either decreased and increased significantly by more than 2-fold , respectively, in comparison to *V. cholerae* cells grown *in vitro* in nutrient broth (73). *vxrA* and

vxrB transcript levels were decreased 2 and 3-fold, respectively, in the experiments reported by Mandlik and colleagues, but did not reach statistical significance (73). This work all used the *V. cholerae* O1 El Tor strain C6706, and so it is yet unknown whether *vxrB* expression is similarly regulated in the O1 El Tor A1552 strain used here.

There have been two other studies that analyzed *V. cholerae* infection phenotypes on a global scale, although they did not specifically target RR. Together, these studies and ours suggests there is a set of genes required for intestinal colonization across multiple models. Fu *et al*. used random transposon mutants coupled with insertion site sequencing (Tn-seq) in a rabbit model (30). They identified insertions in two genes — VC1021 (*luxO*) and VC1155—that showed 8-15-fold reduction in colonization, while strains harboring insertions into RRs VC1348, *vieA, vieB, arcA,* VCA0256, *uhpA,* and *pgtA* had less than a 5-fold reduction in colonization ($p<0.001$). Another Tn-seq study using the infant rabbit model identified defects associated with *luxO* and *arcA* as above, and additionally *phoB* and *varA* (74). Combining the results of these studies with ours identifies *luxO*, *phoB*, and *varA*, as required for *in vivo* fitness, and others that are variably identified. Because the Tn-seq work used transposon libraries, it is not known whether all RR were eliminated, so it is possible that their studies missed some critical RR. There are hints in their data, however, that the *vxr* locus is necessary in these other

models as well. While Fu *et al*. did not identify *vxrA* or *vxrB* mutants, they did determine that a strain with an insertion into VCA0567 (*vxrC*) exhibited a 9-fold reduction in colonization ($p<0.0001$) (30). Additionally, Kamp *et al*. found that a strain with a transposon insertion in VCA0565 (*vxrA*) had a disadvantage in fitness (mean fitness value of 0.6) when the bacteria from rabbit cecum fluid was placed into pond water for 48 hours at 30°C (74). Collectively, these studies suggest that the Vxr genes play important roles in *V. cholerae* colonization and environmental dissemination.

Our study revealed that the RR VxrB plays a significant role in colonization and *in vitro* inter-bacterial competition through its ability to regulate expression of T6SS genes. Neither *vxrB* nor any of the *vxrABCDE* operon members show similarity to previously characterized proteins. The *vxr* loci is conserved among the *Vibrio* species *Vibrio parahaemolyticus*, *Vibrio vulnificus, Vibrio harveyi,* and *V. fischeri*. BLAST analysis revealed that VxrA protein exhibits 67-80%, VxrB 79-84%, VxrC 56-68%, VxrD 58-74%, and VxrE 68-81% sequence similarity to the same proteins in other *Vibrio* species (Figs. S2-S4). We also analyzed the predicted structure and function of the VxrCDE proteins using the protein homology/analogy recognition engine (Phyre) (75). While VxrC and VxrE could not be modeled with high confidence and sufficient coverage, VxrD exhibited structural similarity to outer membrane protein transport proteins (100% confidence, 90% coverage).

These analyses suggest that *vxr* genomic loci are a part of the ancestral *Vibrio* genome, and therefore likely have an evolutionarily conserved role in *Vibrio* biology.

Expression and production of T6SS are tightly regulated at the transcriptional and posttranscriptional levels in a variety of bacterial systems (12, 13, 76). Environmental signals such as iron limitation, thermoregulation, salinity, envelope stress, indole, and growth on surfaces regulate T6SS expression (76). In *V. cholerae* A1552, the strain used here, T6SS genes are expressed when cell are grown in high-osmolarity and low temperature conditions (58). A recent study revealed that the *V. cholerae* A1552 T6SS genes are part of the competence regulon and their expression is induced when the bacterium grows on chitinous surfaces in a TfoX-, HapR-, and QstR-dependent manner (77). Our work presented here identified VxrB as a regulator of the T6SS large gene cluster and the two auxiliary clusters. The predicted cognate HK of VxrB, VxrA, does not exhibit similarity to previously characterized sensory domains. The signals that govern expression and activity of VxrAB and how the VxrAB TCS is integrated into the T6SS regulatory network of *V. cholerae* are yet to be determined. We determined that while the wild-type strain has a competitive advantage *in vivo* over Δ*vxrB*, neither strain had a competitive advantage over the other *in vitro*. Furthermore, single infection studies

showed that Δ*vxrB* had a significant colonization defect compared to wild type, suggesting that VxrB could be involved in competition with normal flora. These observations also suggest that there may be an *in vivo* signal produced in the infant mouse that triggers T6SS activity and colonization. Our studies thus provided significant new insights into the regulation of T6SS in *V. cholerae* and provided further support that the T6SS is critical for *V. cholerae* virulence.

Acknowledgements

We thank Sun Nyunt Wai for providing T6SS mutants and anti-Hcp antibodies, UC Davis genome sequencing facility and David Bernick for assisting the RNA-seq analysis, William Sause for help with infection studies, and the Yildiz lab members for their valuable discussions and reading the manuscript.

References

1. **Ali M, Lopez AL, You YA, Kim YE, Sah B, Maskery B, Clemens J.** 2012. The global burden of cholera. Bull World Health Organ **90:**209-218A.

2. **Kaper JB, Morris JG, Jr., Levine MM.** 1995. Cholera. Clin Microbiol Rev **8:**48-86.

3. **DiRita VJ, Parsot C, Jander G, Mekalanos JJ.** 1991. Regulatory cascade controls virulence in *Vibrio cholerae*. Proc Natl Acad Sci U S A **88:**5403-5407.

4. **Higgins DE, Nazareno E, DiRita VJ.** 1992. The virulence gene activator ToxT from *Vibrio cholerae* is a member of the AraC family of transcriptional activators. J Bacteriol **174:**6974-6980.

5. **Higgins DE, DiRita VJ.** 1994. Transcriptional control of toxT, a regulatory gene in the ToxR regulon of *Vibrio cholerae*. Mol Microbiol **14:**17-29.

6. **Hase CC, Mekalanos JJ.** 1998. TcpP protein is a positive regulator of virulence gene expression in *Vibrio cholerae*. Proc Natl Acad Sci U S A **95:**730-734.

7. **Krukonis ES, Yu RR, Dirita VJ.** 2000. The *Vibrio cholerae* ToxR/TcpP/ToxT virulence cascade: distinct roles for two membrane-localized transcriptional activators on a single promoter. Mol Microbiol **38:**67-84.

8. **Kovacikova G, Lin W, Skorupski K.** 2004. *Vibrio cholerae* AphA uses a novel mechanism for virulence gene activation that involves interaction with the LysR-type regulator AphB at the *tcpPH* promoter. Mol Microbiol **53:**129-142.

9. **Skorupski K, Taylor RK.** 1999. A new level in the *Vibrio cholerae* ToxR virulence cascade: AphA is required for transcriptional activation of the *tcpPH* operon. Mol Microbiol **31:**763-771.

10. **Kovacikova G, Skorupski K.** 2002. Regulation of virulence gene expression in *Vibrio cholerae* by quorum sensing: HapR functions at the *aphA* promoter. Mol Microbiol **46:**1135-1147.

11. **Pukatzki S, Ma AT, Sturtevant D, Krastins B, Sarracino D, Nelson WC, Heidelberg JF, Mekalanos JJ.** 2006. Identification of a conserved bacterial protein secretion system in *Vibrio cholerae* using the *Dictyostelium* host model system. Proc Natl Acad Sci U S A **103:**1528-1533.

12. **Ho BT, Dong TG, Mekalanos JJ.** 2014. A view to a kill: the bacterial type VI secretion system. Cell Host Microbe **15:**9-21.

13. **Silverman JM, Brunet YR, Cascales E, Mougous JD.** 2012. Structure and regulation of the type VI secretion system. Annu Rev Microbiol **66:**453-472.

14. **Pukatzki S, Ma AT, Revel AT, Sturtevant D, Mekalanos JJ.** 2007. Type VI secretion system translocates a phage tail spike-like protein into target cells where it cross-links actin. Proc Natl Acad Sci U S A **104:**15508-15513.

15. **Dong TG, Ho BT, Yoder-Himes DR, Mekalanos JJ.** 2013. Identification of T6SS-dependent effector and immunity proteins by Tn-seq in *Vibrio cholerae*. Proc Natl Acad Sci U S A **110:**2623-2628.

16. **Brooks TM, Unterweger D, Bachmann V, Kostiuk B, Pukatzki S.** 2013. Lytic activity of the *Vibrio cholerae* type VI secretion toxin VgrG-3 is inhibited by the antitoxin TsaB. J Biol Chem **288:**7618-7625.

17. **Ma AT, McAuley S, Pukatzki S, Mekalanos JJ.** 2009. Translocation of a *Vibrio cholerae* type VI secretion effector requires bacterial endocytosis by host cells. Cell Host Microbe **5:**234-243.

18. **Russell AB, LeRoux M, Hathazi K, Agnello DM, Ishikawa T, Wiggins PA, Wai SN, Mougous JD.** 2013. Diverse type VI secretion phospholipases are functionally plastic antibacterial effectors. Nature **496:**508-512.

19. **Miyata ST, Kitaoka M, Brooks TM, McAuley SB, Pukatzki S.** 2011. Vibrio cholerae requires the type VI secretion system virulence factor VasX to kill *Dictyostelium discoideum*. Infect Immun **79:**2941-2949.

20. **Miyata ST, Unterweger D, Rudko SP, Pukatzki S.** 2013. Dual expression profile of type VI secretion system immunity genes protects pandemic *Vibrio cholerae*. PLoS Pathog **9:**e1003752.

21. **Unterweger D, Miyata ST, Bachmann V, Brooks TM, Mullins T, Kostiuk B, Provenzano D, Pukatzki S.** 2014. The *Vibrio cholerae* type VI secretion system employs diverse effector modules for intraspecific competition. Nat Commun **5:**3549.

22. **Basler M, Pilhofer M, Henderson GP, Jensen GJ, Mekalanos JJ.** 2012. Type VI secretion requires a dynamic contractile phage tail-like structure. Nature **483:**182-186.

23. **Zheng J, Ho B, Mekalanos JJ.** 2011. Genetic analysis of anti-amoebae and anti-bacterial activities of the type VI secretion system in *Vibrio cholerae*. PLoS One **6:**e23876.

24. **Kitaoka M, Miyata ST, Brooks TM, Unterweger D, Pukatzki S.** 2011. VasH is a transcriptional regulator of the type VI secretion system functional in endemic and pandemic *Vibrio cholerae*. J Bacteriol **193:**6471-6482.

25. **Bernard CS, Brunet YR, Gavioli M, Lloubes R, Cascales E.** 2011. Regulation of type VI secretion gene clusters by sigma54 and cognate enhancer binding proteins. J Bacteriol **193:**2158-2167.

26. **Dong TG, Mekalanos JJ.** 2012. Characterization of the RpoN regulon reveals differential regulation of T6SS and new flagellar operons in *Vibrio cholerae* O37 strain V52. Nucleic Acids Res **40:**7766-7775.

27. **Zheng J, Shin OS, Cameron DE, Mekalanos JJ.** 2010. Quorum sensing and a global regulator TsrA control expression of type VI secretion and virulence in *Vibrio cholerae*. Proc Natl Acad Sci U S A **107:**21128-21133.

28. **Ishikawa T, Rompikuntal PK, Lindmark B, Milton DL, Wai SN.** 2009. Quorum sensing regulation of the two hcp alleles in *Vibrio cholerae* O1 strains. PLoS One **4:**e6734.

29. **Ma AT, Mekalanos JJ.** 2010. In vivo actin cross-linking induced by *Vibrio cholerae* type VI secretion system is associated with intestinal inflammation. Proc Natl Acad Sci U S A **107:**4365-4370.

30. **Fu Y, Waldor MK, Mekalanos JJ.** 2013. Tn-Seq analysis of Vibrio cholerae intestinal colonization reveals a role for T6SS-mediated antibacterial activity in the host. Cell Host Microbe **14:**652-663.

31. **Beier D, Gross R.** 2006. Regulation of bacterial virulence by two-component systems. Curr Opin Microbiol **9:**143-152.

32. **Krell T, Lacal J, Busch A, Silva-Jimenez H, Guazzaroni ME, Ramos JL.** 2010. Bacterial sensor kinases: diversity in the recognition of environmental signals. Annu Rev Microbiol **64:**539-559.

33. **Galperin MY.** 2010. Diversity of structure and function of response regulator output domains. Curr Opin Microbiol **13:**150-159.

34. **Gao R, Stock AM.** 2009. Biological insights from structures of two-component proteins. Annu Rev Microbiol **63:**133-154.

35. **Laub MT, Goulian M.** 2007. Specificity in two-component signal transduction pathways. Annu Rev Genet **41:**121-145.

36. **Jang J, Jung KT, Park J, Yoo CK, Rhie GE.** 2011. The *Vibrio cholerae* VarS/VarA two-component system controls the expression of virulence proteins through ToxT regulation. Microbiology **157:**1466-1473.

37. **Zhu J, Miller MB, Vance RE, Dziejman M, Bassler BL, Mekalanos JJ.** 2002. Quorum-sensing regulators control virulence gene expression in *Vibrio cholerae*. Proc Natl Acad Sci U S A **99:**3129-3134.

38. **Tischler AD, Camilli A.** 2005. Cyclic diguanylate regulates Vibrio cholerae virulence gene expression. Infect Immun **73:**5873-5882.

39. **Tischler AD, Lee SH, Camilli A.** 2002. The *Vibrio cholerae vieSAB* locus encodes a pathway contributing to cholera toxin production. J Bacteriol **184:**4104-4113.

40. **Pratt JT, Ismail AM, Camilli A.** 2010. PhoB regulates both environmental and virulence gene expression in *Vibrio cholerae*. Mol Microbiol **77:**1595-1605.

41. **Sengupta N, Paul K, Chowdhury R.** 2003. The global regulator ArcA modulates expression of virulence factors in *Vibrio cholerae*. Infect Immun **71:**5583-5589.

42. **Bilecen K, Fong JC, Cheng A, Jones CJ, Zamorano-Sanchez D, Yildiz FH.** 2015. Polymyxin B Resistance and biofilm formation in

Vibrio cholerae is controlled by the response regulator CarR. Infect Immun doi:10.1128/IAI.02700-14.

43. **Butler SM, Camilli A.** 2004. Both chemotaxis and net motility greatly influence the infectivity of *Vibrio cholerae*. Proc Natl Acad Sci U S A **101:**5018-5023.

44. **Correa NE, Lauriano CM, McGee R, Klose KE.** 2000. Phosphorylation of the flagellar regulatory protein FlrC is necessary for *Vibrio cholerae* motility and enhanced colonization. Mol Microbiol **35:**743-755.

45. **National Research Council (U.S.). Committee for the Update of the Guide for the Care and Use of Laboratory Animals., Institute for Laboratory Animal Research (U.S.), National Academies Press (U.S.).** 2011. Guide for the care and use of laboratory animals, 8th ed. National Academies Press, Washington, D.C.

46. **Lim B, Beyhan S, Meir J, Yildiz FH.** 2006. Cyclic-diGMP signal transduction systems in *Vibrio cholerae*: modulation of rugosity and biofilm formation. Mol Microbiol **60:**331-348.

47. **Iwanaga M, Yamamoto K, Higa N, Ichinose Y, Nakasone N, Tanabe M.** 1986. Culture conditions for stimulating cholera toxin production by *Vibrio cholerae* O1 El Tor. Microbiol Immunol **30:**1075-1083.

48. **Fong JC, Yildiz FH.** 2007. The *rbmBCDEF* gene cluster modulates development of rugose colony morphology and biofilm formation in *Vibrio cholerae*. J Bacteriol **189:**2319-2330.

49. **Lefebvre B, Formstecher P, Lefebvre P.** 1995. Improvement of the gene splicing overlap (SOE) method. Biotechniques **19:**186-188.

50. **Beyhan S, Bilecen K, Salama SR, Casper-Lindley C, Yildiz FH.** 2007. Regulation of rugosity and biofilm formation in *Vibrio cholerae*: comparison of VpsT and VpsR regulons and epistasis analysis of *vpsT*, *vpsR*, and *hapR*. J Bacteriol **189:**388-402.

51. **Herrero M, de Lorenzo V, Timmis KN.** 1990. Transposon vectors containing non-antibiotic resistance selection markers for cloning and stable chromosomal insertion of foreign genes in gram-negative bacteria. J Bacteriol **172:**6557-6567.

52. **de Lorenzo V, Timmis KN.** 1994. Analysis and construction of stable phenotypes in gram-negative bacteria with Tn5- and Tn10-derived minitransposons. Methods Enzymol **235:**386-405.

53. **Yildiz FH, Liu XS, Heydorn A, Schoolnik GK.** 2004. Molecular analysis of rugosity in a Vibrio cholerae O1 El Tor phase variant. Mol Microbiol **53:**497-515.

54. **Casper-Lindley C, Yildiz FH.** 2004. VpsT is a transcriptional regulator required for expression of vps biosynthesis genes and the development of rugose colonial morphology in *Vibrio cholerae* O1 El Tor. J Bacteriol **186:**1574-1578.

55. **Yildiz FH, Dolganov NA, Schoolnik GK.** 2001. VpsR, a Member of the Response Regulators of the Two-Component Regulatory Systems, Is Required for Expression of vps Biosynthesis Genes and EPS(ETr)-Associated Phenotypes in *Vibrio cholerae* O1 El Tor. J Bacteriol **183:**1716-1726.

56. **Bilecen K, Yildiz FH.** 2009. Identification of a calcium-controlled negative regulatory system affecting *Vibrio cholerae* biofilm formation. Environ Microbiol **11:**2015-2029.

57. **Beyhan S, Tischler AD, Camilli A, Yildiz FH.** 2006. Differences in gene expression between the classical and El Tor biotypes of *Vibrio cholerae* O1. Infect Immun **74:**3633-3642.

58. **Ishikawa T, Sabharwal D, Broms J, Milton DL, Sjostedt A, Uhlin BE, Wai SN.** 2012. Pathoadaptive conditional regulation of the type VI secretion system in *Vibrio cholerae* O1 strains. Infect Immun **80:**575-584.

59. **Bao Y, Lies DP, Fu H, Roberts GP.** 1991. An improved Tn7-based system for the single-copy insertion of cloned genes into chromosomes of gram-negative bacteria. Gene **109:**167-168.

60. **Taylor RK, Miller VL, Furlong DB, Mekalanos JJ.** 1987. Use of *phoA* gene fusions to identify a pilus colonization factor coordinately regulated with cholera toxin. Proc Natl Acad Sci U S A **84:**2833-2837.

61. **Pfaffl MW.** 2001. A new mathematical model for relative quantification in real-time RT-PCR. Nucleic Acids Res **29:**e45.

62. **Robinson MD, McCarthy DJ, Smyth GK.** 2010. edgeR: a Bioconductor package for differential expression analysis of digital gene expression data. Bioinformatics **26:**139-140.

63. **Berk V, Fong JC, Dempsey GT, Develioglu ON, Zhuang X, Liphardt J, Yildiz FH, Chu S.** 2012. Molecular architecture and assembly principles of *Vibrio cholerae* biofilms. Science **337:**236-239.

64. **Butler SM, Camilli A.** 2005. Going against the grain: chemotaxis and infection in *Vibrio cholerae*. Nat Rev Microbiol **3:**611-620.

65. **Galperin MY.** 2006. Structural classification of bacterial response regulators: diversity of output domains and domain combinations. J Bacteriol **188:**4169-4182.

66. **Delgado J, Forst S, Harlocker S, Inouye M.** 1993. Identification of a phosphorylation site and functional analysis of conserved aspartic acid residues of OmpR, a transcriptional activator for *ompF* and *ompC* in *Escherichia coli*. Mol Microbiol **10:**1037-1047.

67. **Ma S, Selvaraj U, Ohman DE, Quarless R, Hassett DJ, Wozniak DJ.** 1998. Phosphorylation-independent activity of the response regulators AlgB and AlgR in promoting alginate biosynthesis in mucoid *Pseudomonas aeruginosa*. J Bacteriol **180:**956-968.

68. **Hussa EA, O'Shea TM, Darnell CL, Ruby EG, Visick KL.** 2007. Two-component response regulators of *Vibrio fischeri*: identification, mutagenesis, and characterization. J Bacteriol **189:**5825-5838.

69. **Kobayashi K, Ogura M, Yamaguchi H, Yoshida K, Ogasawara N, Tanaka T, Fujita Y.** 2001. Comprehensive DNA microarray analysis of *Bacillus subtilis* two-component regulatory systems. J Bacteriol **183:**7365-7370.

70. **Lange R, Wagner C, de Saizieu A, Flint N, Molnos J, Stieger M, Caspers P, Kamber M, Keck W, Amrein KE.** 1999. Domain organization and molecular characterization of 13 two-component systems identified by genome sequencing of *Streptococcus pneumoniae*. Gene **237:**223-234.

71. **Throup JP, Koretke KK, Bryant AP, Ingraham KA, Chalker AF, Ge Y, Marra A, Wallis NG, Brown JR, Holmes DJ, Rosenberg M,**

Burnham MK. 2000. A genomic analysis of two-component signal transduction in *Streptococcus pneumoniae*. Mol Microbiol **35:**566-576.

72. **Yamamoto K, Hirao K, Oshima T, Aiba H, Utsumi R, Ishihama A.** 2005. Functional characterization in vitro of all two-component signal transduction systems from *Escherichia coli*. J Biol Chem **280:**1448-1456.

73. **Mandlik A, Livny J, Robins WP, Ritchie JM, Mekalanos JJ, Waldor MK.** 2011. RNA-Seq-based monitoring of infection-linked changes in *Vibrio cholerae* gene expression. Cell Host Microbe **10:**165-174.

74. **Kamp HD, Patimalla-Dipali B, Lazinski DW, Wallace-Gadsden F, Camilli A.** 2013. Gene fitness landscapes of Vibrio cholerae at important stages of its life cycle. PLoS Pathog **9:**e1003800.

75. **Kelley LA, Sternberg MJ.** 2009. Protein structure prediction on the Web: a case study using the Phyre server. Nat Protoc **4:**363-371.

76. **Bernard CS, Brunet YR, Gueguen E, Cascales E.** 2010. Nooks and crannies in type VI secretion regulation. J Bacteriol **192:**3850-3860.

77. **Borgeaud S, Metzger LC, Scrignari T, Blokesch M.** 2015. Bacterial evolution. The type VI secretion system of *Vibrio cholerae* fosters horizontal gene transfer. Science **347:**63-67.

CHAPTER 3: The role of NtrC family response regulators in *Vibrio cholerae* biofilm formation.

Andrew T. Cheng and Fitnat H. Yildiz

Abstract

Vibrio cholerae, the causative agent of cholera, is a facultative human pathogen. The biofilm growth mode is important in both the intestinal and environmental phases of *V. cholerae*'s life cycle. Regulation of biofilm formation involves several transcriptional regulators and alternative sigma factors. One such factor, the alternative sigma factor, RpoN, positively regulates biofilm formation. However, the exact mechanism by which RpoN impacts biofilm formation is yet to be determined. RpoN functions together with the NtrC family of response regulators (RR), thus raising the possibility that biofilm formation requires both RpoN and an NtrC family response regulator. In this study, we determined the role of the eight NtrC family RRs (LuxO, VC1522, Dct-D1, FlrC FlrA, NtrC, Dct-D2, PgtA) in biofilm formation and identified four of these RRs regulating biofilm formation. LuxO positively regulates biofilm formation. Deletion of *luxO* abolishes formation of typical three dimensional (3-D) biofilm structures, demonstrating that LuxO is required for biofilm formation. In contrast, mutants lacking FlrC, FlrA and NtrC have increased biofilm formation indicating that they function in preventing biofilm formation. In this study, we focused on NtrC. Whole-genome expression profiling and transcriptional reporter assays revealed that expression of the *Vibrio* polysaccharide (*vps*) genes and genes encoding the two positive transcriptional regulators, VpsR and VpsT, is increased in an *ntrC* mutant. Epistasis analysis showed that NtrC acts in parallel with HapR

and CRP-cAMP complex, the negative regulators of biofilm formation. This study underscores the importance of the NtrC family of response regulators in the regulation of biofilm formation in *V. cholerae*.

Introduction

Vibrio cholerae, the causative agent of the severe diarrheal disease cholera, can inhabit fresh water, estuaries, and human intestines. In its natural aquatic environment, *V. cholerae* can be found either as free-swimming planktonic cells or as biofilm-associated cells attached to surfaces (1-3). *V. cholerae*'s ability to form biofilms is critical for its survival in its natural habitats and transmission to the human host. Production of mature biofilms by *V. cholerae* requires extracellular matrix components. A major component of *V. cholerae* biofilm matrix is VPS (*Vibrio* polysaccharide) exopolysaccharide, which is required for the formation of three-dimensional biofilm structures (4, 5). Another major component of *V. cholerae* biofilm is matrix proteins RbmA, RbmC, and Bap1 that mediate cell-cell and cell-surface interactions and provide stability to the biofilm matrix architecture (6-10).

The regulatory network that controls biofilm formation is complex and involves several transcriptional regulators and alternative sigma factors. The primary components of this network consist of two positive transcriptional regulators, VpsT and VpsR and the negative transcriptional regulators HapR, cyclic AMP

(cAMP) receptor protein, and histone-like nucleoid structuring protein (H-NS) (11-18). Finally, alternative sigma factors RpoS and RpoN, have been shown to negatively and positively regulate *vps* gene expression and biofilm formation, respectively (19). However, the exact mechanism by which RpoN impacts biofilm formation is yet to be determined.

RpoN differs from other sigma factors and RpoN-dependent gene expression requires an activator, generally classified as NtrC (nitrogen regulatory protein C) family of response regulators (RR). RRs are part of the two-component signal transduction system (TCS) and their receiver (REC) domain that can be phosphorylated by a sensor histidine kinase (HK), the other component of this signal transduction system (20). Upon environmental stimulation, the sensor HK autophosphorylates at a conserved His residue and transfers the phosphate to a conserved Asp residue on the REC domain of the RR (21). NtrC family RRs have unique domain structure. They harbor an amino-terminal receiver domain (REC), a central RpoN interaction and ATPase Associated with diverse cellular Activities (AAA^+) domain and a C-terminal DNA-binding domain.

NtrC family RR are involved in regulation of diverse cellular processes. In *Salmonella enterica* serovar *Typhimurium* and in *Escherichia coli*, NtrC activates the transcription of genes in response to nitrogen availability (22-

25). Under ammonium limitation, NtrB (HK) is phosphorylated and then transfers the phosphate to the cognate RR, NtrC. Phosphorylated NtrC then activates genes involved in nitrogen metabolism. DNA microarrays and phenotype-arrays studies allowed the detection of all genes/operons under NtrC control (26, 27). NtrBC controls the expression of the *glnALG* operon, where *glnA* encodes glutamine synthetase, *glnL* (also known as *ntrB*) encodes the HK, and *glnG* (also known as *ntrC*) encodes the RR. In addition, NtrBC controls the expression of *glnHPQ,* which encodes for a glutamine transporter; *glnK*, which encodes a trimeric signal-transduction protein (28); *amtB*, which encodes an ammonium uptake protein; and the *nac* gene, which encodes a nitrogen assimilation control protein (27). Approximately 2% of *E. coli's* genome seems to be under NtrC control and about two-thirds of the genes under NtrC control encode for proteins that are involved in scavenging nitrogen-containing compounds.

The *V. cholerae* genome is predicted to encode eight NtrC family RRs: VC1021 (*luxO*), VC1522, VC1926 (*dctD-1*), VC2135 (*flrC*), VC2137 (*flrA*), VC2749 (*ntrC*), VCA0142 (*dctD-2*), and VCA0704 (*pgtA*). (http://www.ncbi.nlm.nih.gov/Complete_Genomes/RRcensus.html and http://www.p2cs.org). In this study, we determined the role of the NtrC family RRs in biofilm formation and expression of *vps* genes. We identified four of these RRs (LuxO, FlrC, FlrA, and NtrC) as regulators of biofilm formation.

Disruption of *luxO* abolishes biofilm structure and null mutants of FlrC, FlrA and NtrC have increased biofilm formation. Epistasis analysis showed that NtrC acts in parallel with HapR and CRP-cAMP, the negative regulators of biofilm formation. This is the first study to comprehensively characterize the role of each NtrC family RRs in *V. cholerae;* and to show negative regulation of biofilm formation by NtrC in *V. cholerae*. This study underscores the importance of NtrC family response regulators in the regulation of biofilm formation in *V. cholerae* and enhances our understanding of how TCS play a role in biofilm formation.

Methods

Bacterial strains, plasmids, and culture conditions. The bacterial strains and plasmids used in this study are listed in Table 3.1. *Escherichia coli* CC118λpir strains were used for DNA manipulation, and *E. coli* S17-1λpir strains were used for conjugation with *V. cholerae*. In-frame deletion mutants of *V. cholerae* were generated as described earlier (29). All *V. cholerae* and *E. coli* strains were grown aerobically, at 30°C and 37°C, respectively, unless otherwise noted. Cells were grown in Luria-Bertani (LB) broth (1% Tryptone, 0.5% Yeast Extract, 1% NaCl), pH 7.5, unless otherwise stated. LB agar medium contains 1.5% (wt/vol) granulated agar (BD Difco, Franklin Lakes, NJ). Concentrations of antibiotics used were as follow: ampicillin 100 μg/ml; rifampicin 100 μg/ml; chloramphenicol 5 μg/ml for *V. cholerae* and 20 μg/ml

for *E. coli*; and gentamicin 50 µg/ml. Cells were also grown in M9 minimal medium lacking NH_4Cl supplemented with minimal essential medium vitamins (10 ml/liter; Gibco, Rockford, IL), 0.75 mM KH_2PO_4, 0.5% glucose and 100 mM of the following L-amino acids: Serine, Arginine, Glutamate, and Glutamine.

DNA manipulations, generation of in-frame deletion mutants and *gfp*-tagged strains. An overlapping PCR method was used to generate in-frame deletion constructs of each RR genes using previously published methods (29). Generation of deletion constructs were previously described (30). *V. cholerae* wild-type and mutant strains were tagged with the green fluorescent protein gene (*gfp*) according to a previously described procedure (6). The *gfp*-tagged *V. cholerae* strains were verified by PCR and examined in flow-cell experiments.

RNA isolation and whole-genome transcriptome profiling. Overnight cultures of *V. cholerae* cells were diluted 1:200 in fresh LB medium and grown aerobically at 30°C to mid-exponential phase. To obtain a homogenous population of exponential-phase cells, mid-exponential phase cultures were diluted 1:200 once more in fresh LB medium and grown aerobically at 30°C to mid-exponential phase (OD_{600} of 0.3 to 0.4). Two milliliter (ml) aliquots were collected and centrifuged for 2 minutes at room temperature. The cell pellets were immediately resuspended in 1 ml of TRIzol reagent (Invitrogen, Carlsbad, CA) and stored at -70°C. Total RNA

from pellets were isolated according to the manufacturer's instructions (Invitrogen, Carlsbad, CA). Total RNA was incubated with RNase-free DNaseI (Ambion, Grand Island, NY) to digest contaminated DNA. Finally, RNeasy mini kit (Invitrogen, Carlsbad, CA) was used to purify total RNA after DNase digestion.

Microarrays used in this study were composed of 70-mer oligonucleotides (designed and synthesized by Illumina, San Diego) representing most of the open reading frames in *V. cholerae* strain N16961 genome and were printed at the University of California, Santa Cruz (31). Whole genome expression analysis was performed using a common reference RNA. Reference RNA was harvested by growing *V. cholerae* overnight in LB, diluting the culture 1:200 in fresh medium, growing the culture to mid-exponential phase of OD_{600} of 0.3 to 0.4. RNA from the test and reference samples were subjected to cDNA synthesis, hybridization, and scanning as described previously (31). Normalized signal ratios were obtained with LOWESS print-tip normalization using the Bioconductor packages (Gentleman, 2004 #15) in the R environment. Differentially regulated genes were determined using three biological replicate and two technical replicates for each treatment, using the Significance of Analysis of Microarrays (SAM) program (32) by using a 1.5% fold difference in gene expression and 3% false discovery rate as cutoff values.

Luminescence assay. Overnight cultures of *V. cholerae* cells were diluted 1:1000 in appropriate medium containing chloramphenicol (5 µg/ml). Then, cells were grown aerobically at 30°C to mid-exponential phase (OD_{600} of 0.3-0.4) and harvested for luminescence reading. Luminescence of cells were read using a Perkin Elmer Victor3 Multi-label Counter (PerkinElmer, Waltham, MA) and is reported as counts min^{-1} ml^{-1}/ OD_{600}. Lux expression is reported as relative light units (RLU). Assays were repeated with three biological replicates. Four technical replicates were measured for all assays. Statistical analysis was performed using two-tailed student's t test.

Spot growth assay. For qualitative analysis of growth, 1 ml of overnight cultures was harvested by centrifugation. The cell pellet was resuspended in 1x PBS and 5 µl of resuspension was added to defined M9 agar containing either L-serine or L-arginine as the only nitrogen source. The plates were incubated at 30°C for *V. cholerae* and 37°C for *E. coli* for 24 hours. Images were taken using Biorad Chemidoc MP (Biorad, Hercules, CA).

β-galactosidase assay. β-galactosidase assays were performed using exponentially grown cultures. *V. cholerae* cells were grown overnight (18 to 20 h) aerobically in LB containing 100 µg/ml of ampicillin medium. Overnight cultures were diluted 1:200 in fresh LB medium with or without arabinose and grown aerobically to an OD_{600} of 0.3 to 0.4. Then, cells were diluted again 1:200 in fresh LB with or without arabinose, grown aerobically to an OD_{600} of 0.3 to 0.4, and then immediately harvested for assays. The β-galactosidase

assays were carried out in MultiScreen 96-well microtiter plates fitted onto a MultiScreen filtration system (Millipore, Billerica, Massachusetts) using a previously described procedure (6).

Flow cell experiments and confocal scanning laser microscopy (CSLM). Flow cells were inoculated by normalizing overnight-grown cultures of *gfp*-tagged *V. cholerae* strains to an OD600 of 0.02 and injecting cells into an Ibidi m-Slide VI0.4 (Ibidi 80601 ; Ibidi LLC, Verona, WI). After inoculation, the bacteria were allowed to adhere at room temperature for 1 h with no flow. Then, flow of 2% (vol/vol) LB (0.2 g/liter tryptone, 0.1 g/liter yeast extract, 1% NaCl) or M9 minimal medium supplemented with different nitrogen sources (NH_4Cl, serine, arginine, glutamate, glutamine) was initiated at a rate of 7.5 ml/h. Confocal laser scanning microscopy (CLSM) images of the biofilms were captured with an LSM 5 PASCAL system (Zeiss, Jena, Germany) using an excitation wavelength of 488 nm and an emission wavelength of 543 nm. Three-dimensional images of the biofilms were reconstructed using Imaris software (Bitplane, Zurich, Switzerland) and quantified using COMSTAT (33).

Table 3.1. Bacterial strains and plasmids used in this study.

Strain or plasmid	Relevant genotype	Source
E. coli strains		
CC118λ*pir*	Δ(*ara-leu*) *araD* Δ*lacX74 galE galK phoA20 thi-1 rpsE rpoB argE*(*Am*) *recA1* λ*pir*	(34)
S17-1λ*pir*	Tp^r Sm^r *recA thi pro* r_K^- m_K^+ RP4::2-Tc::MuKm Tn7 λ*pir*	(35)
K-12 (BW28357)	*lacIp4000*(*lacI*^{q}) *rrnB3* Δ*lacZ4787 hsdR514* Δ(*araBAD*)*567* Δ(*rhaBAD*)*568 rph-1*	(27)
K-12Δ*ntrBC* (BW30011)	*lacIp4000*(*lacI*^{q}) *rrnB3* Δ*lacZ4787 hsdR514* Δ(*araBAD*)*567* Δ(*rhaBAD*)*568 rph-1* Δ(*ntrB-ntrC*)1318	(27)
V. cholerae strains		
FY_VC_0001	*Vibrio cholerae* O1 El Tor A1552, wild type, Rif^r	(19)
FY_VC_0616	*vpsLp-lacZ*, Rif^r	(36)
FY_VC_2272	ΔVC0665 (*vpsR*)	(15)
FY_VC_0192	ΔVC1021 (*luxO*)	(30)
FY_VC_7998	ΔVC1522	(30)
FY_VC_8243	ΔVC1926 (*dct-D1*)	(30)
FY_VC_6286	ΔVC2135 (*flrC*)	(30)
FY_VC_6284	ΔVC2137 (*flrA*)	This study
FY_VC_6289	ΔVC2749 (*ntrC*)	(30)
FY_VC_8245	ΔVCA0142 (*dct-D2*)	(30)
FY_VC_7969	ΔVCA0704 (*pgtA*)	(30)
FY_VC_2407	ΔVC0665 mTn7-*gfp*, Rif^r, Gm^r	This study
FY_VC_8068	ΔVC1021 mTn7-*gfp*, Rif^r, Gm^r	This study
FY_VC_8070	ΔVC1522 mTn7-*gfp*, Rif^r, Gm^r	This study
FY_VC_8319	ΔVC1926 mTn7-*gfp*, Rif^r, Gm^r	This study
FY_VC_8072	ΔVC2135 mTn7-*gfp*, Rif^r, Gm^r	This study
FY_VC_9968	ΔVC2137 mTn7-*gfp*, Rif^r, Gm^r	This study
FY_VC_7061	ΔVC2749 mTn7-*gfp*, Rif^r, Gm^r	This study
FY_VC_8321	ΔVCA0142 mTn7-*gfp*, Rif^r, Gm^r	This study
FY_VC_8064	ΔVCA0704 mTn7-*gfp*, Rif^r, Gm^r	This study
FY_VC_7058	ΔVC2748 (*ntrB*)	This study
FY_VC_7057	Δ*ntrC*Δ*vpsR*	This study
FY_VC_0099	Δ*vpsT*	(14)
FY_VC_7050	Δ*ntrC*Δ*vpsT*	This study
FY_VC_7936	ΔVC2529 (*rpoN*)	This study
FY_VC_7304	Δ*ntrC*Δ*rpoN*	This study
FY_VC_0178	Δ*hapR*	This study
FY_VC_7054	Δ*ntrC*Δ*hapR*	This study
FY_VC_2326	Δ*crp*	(37)
FY_VC_7056	Δ*ntrC*Δ*crp*	This study

FY_VC_7982	ΔVC0497	This study
FY_VC_7984	Δ*ntrC*ΔVC0497	This study
FY_VC_7960	ΔVCA0937	This study
FY_VC_7955	Δ*ntrC*ΔVCA0937	This study
FY_VC_7961	ΔVC2383	This study
FY_VC_7962	Δ*ntrC*ΔVC2383	This study
FY_VC_8478	ΔVCA0682 (*uhpA*)	This study
FY_VC_7960	Δ*ntrC*Δ*uhpA*	This study
FY_VC_1384	ΔVCA0888	This study
FY_VC_7956	Δ*ntrC*ΔVCA0888	This study
FY_VC_8708	ΔVC2702 (*crbR*)	This study
FY_VC_7964	Δ*ntrC*Δ*crbR*	This study
Plasmids		
pGP704*sacB*28	pGP704 derivative, *mob*/*oriT sacB*, Ap^r	(14)
pFY-1070	pGP704-*sacB28*::ΔVC2137, Ap^r	This study
pFY-1422	pGP704-*sacB28*::ΔVC2748, Ap^r	This study
pBBRlux	*luxCDABE*-based promoter fusion vector, Cm^r	(38)
pFY-0950	pBBRlux *vpsL* promoter, Cm^r	(39)
pFY-1323	pBBRlux *glnA* promoter, Cm^r	This study
pFY-0989	pBBRlux *vpsR* promoter, Cm^r	This study
pFY-0988	pBBRlux *vpsT* promoter, Cm^r	This study
pFY-1049	pBBRlux *hapR*, promoter, Cm^r	This study
pBAD/myc-His-B	Arabinose-inducible expression vector with C-terminal myc epitope and six-His tags	Invitrogen
pFY-1648	pBAD/myc-His-B::$ntrBC_{VC}$, Ap^r	This study
pFY-1351	pBAD/myc-His-B::*ntrC*, Ap^r	This study
pFY-1349	pBAD/myc-His-B::$ntrC_{D56A}$, Ap^r	This study
pFY-1350	pBAD/myc-His-B::$ntrC_{D56E}$, Ap^r	This study
pUX-BF13	oriR6K helper plasmid, mob/oriT, provides the Tn7 transposition function in trans, Ap^r	(40)
pMCM11	pGP704::mTn*7*-*gfp*, Gm^r Ap^r	M. Miller and G. Schoolnik

Results

Impact of NtrC family RR on biofilm formation and *vpsL* expression.

Multiple sequence alignment of eight predicted NtrC family RRs in *V. cholerae* showed that these proteins have the conserved domain organization of N-terminal REC domains, central RpoN interaction and AAA^+ ATPase domains, and C-terminal DNA binding domains. However, PgtA (VCA0704) lacks the conserved GAFTGA residues required for RpoN interaction and FlrA lacks the conserved aspartate reside predicted to be phosphorylated (Fig. S3.2). To identify NtrC family RRs that contribute to biofilm formation, we first analyzed biofilm formation by CSLM over time using a flow cell system and GFP-tagged strains. After 48 h of incubation, Δ*luxO* and Δ*rpoN* formed significantly less biofilms and lacked complete three-dimensional biofilm structures (Fig. 3.1A). COMSTAT analysis indicates that Δ*luxO* and Δ*rpoN* have approximately 3-fold decrease in biomass and average thickness compared to wild type (Table 3.2). Other studies have demonstrated that the *luxO* and *rpoN* null mutants failed to produce significant biofilms formation under static conditions at room temperature (15, 41, 42). We determined that Δ*flrC*, Δ*flrA*, and Δ*ntrC* displayed a small, and reproducible, increase in biofilm formation compared to wild type (Fig. 3.1A). COMSTAT analysis showed that Δ*flrC*, Δ*flrA*, and Δ*ntrC* have a 1.3-1.5-fold increase in biomass and average thickness compared to wild type (Table 3.2).

Figure S3.2.

A

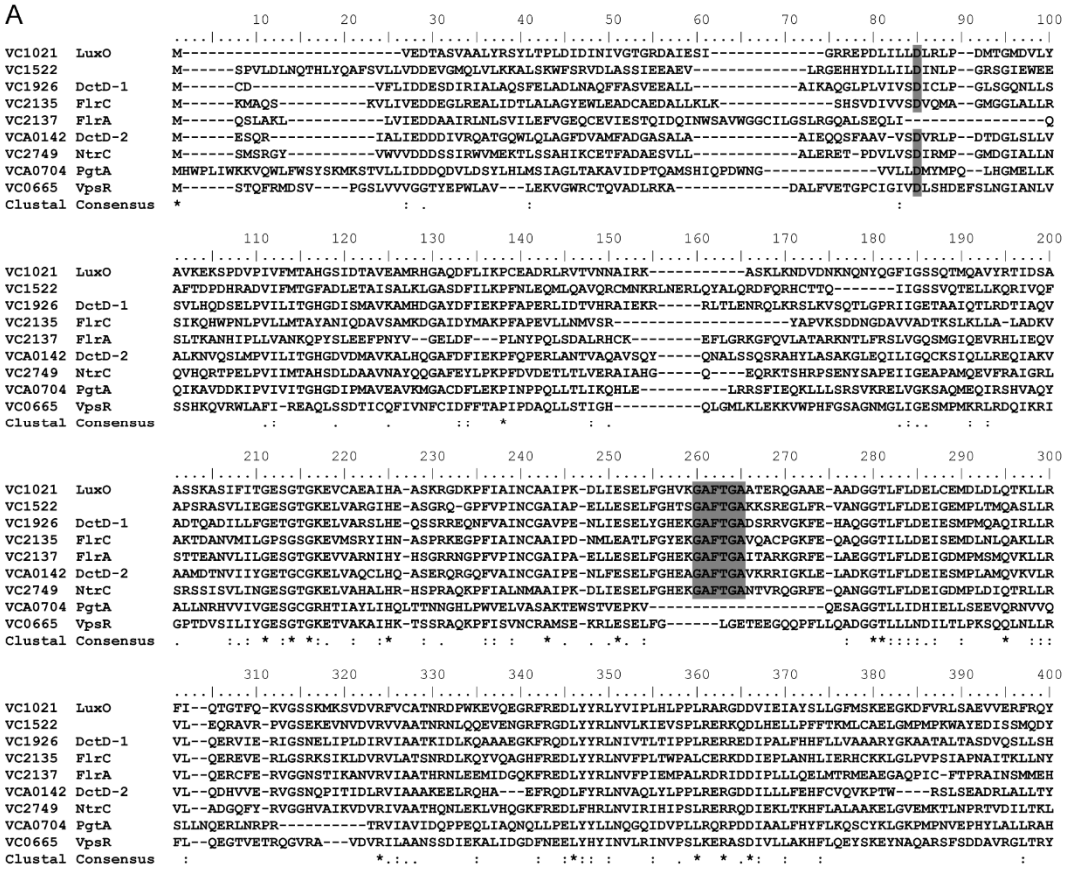
VC1021 LuxO
VC1522
VC1926 DctD-1
VC2135 FlrC
VC2137 FlrA
VCA0142 DctD-2
VC2749 NtrC
VCA0704 PgtA
VC0665 VpsR
Clustal Consensus

Figure S3.2. Multiple sequence alignment of *V. cholerae* NtrC family and VpsR. Amino acid sequence alignment of *V. cholerae* NtrC family RR and VpsR using ClustalW. Highlighted region in gray indicate the aspartate residue (D) that is predicted to be the site of phosphorylation and the GAFTGA region that is required for RpoN interaction. Numbers above the sequence correspond to the amino acid number of each protein.

Figure 3.1

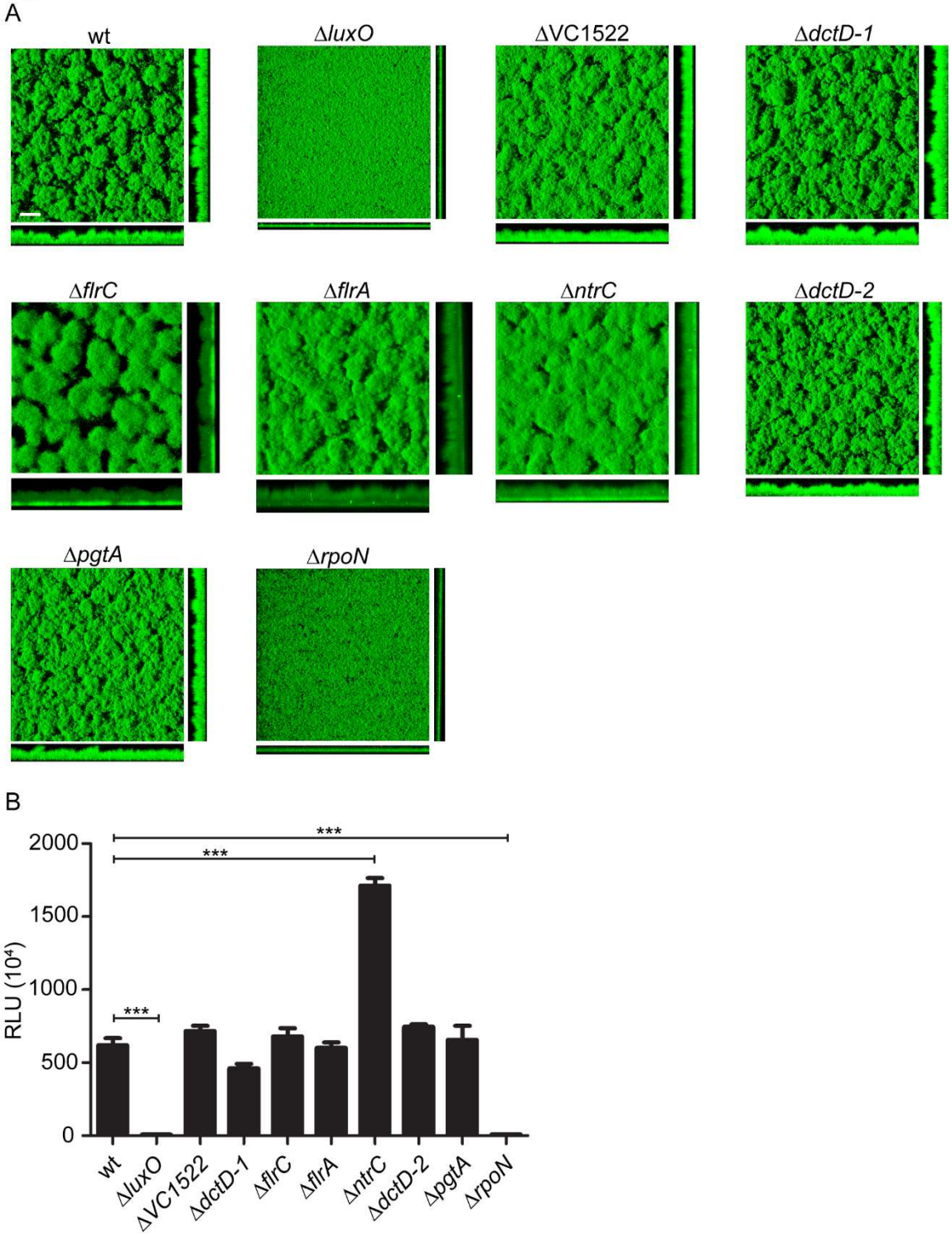
A
wt
ΔluxO
ΔVC1522
ΔdctD-1
ΔflrC
ΔflrA
ΔntrC
ΔdctD-2
ΔpgtA
ΔrpoN
B
RLU (10⁴)
2000
1500
1000
500
0
***
***
***
wt
ΔluxO
ΔVC1522
ΔdctD-1
ΔflrC
ΔflrA
ΔntrC
ΔdctD-2
ΔpgtA
ΔrpoN

Figure 3.1. Analysis of biofilm formation and *vpsL* expression in NtrC family RR deletion mutants. (A) Three dimensional biofilm structures of *gfp* tagged wild type *V. cholerae* (wt), Δl*uxO*, ΔVC1522, Δ*dctD-1*, Δ*flrC*, Δ*flrA*, Δ*ntrC*, Δ*dctD-2*, Δ*pgtA*, and Δ*rpoN* after 48 hours of incubation in flow-cell chambers. Images of horizontal (xy) and vertical (xz) projections of biofilms are shown. The results shown are from one representative experiment of three independent experiments. Scale bars = 30 μm. (B) Expression of P_{vpsL}-*luxCADBE* (pFY_3406) in wild type, Δl*uxO*, ΔVC1522, Δ*dctD-1*, Δ*flrC*, Δ*flrA*, Δ*ntrC*, Δ*dctD-2*, Δ*pgtA*, and Δ*rpoN*. The graph represents the average and standard deviation of relative light units (RLU) obtained from four technical replicates from three independent biological samples. RLU is reported in luminescence counts min^{-1} ml^{-1}/OD_{600}. A two-tailed unpaired t-test was used to compare the expression between wild type and deletion mutants. *** p< 0.001.

Table 3.2. COMSTAT analysis of biofilms of NtrC family ΔRR strains at 48 hours[a]

Strain	Biomass (μm^3)	Average thickness (μm)	Maximum thickness (μm)
wt	17.1 (2.6)	19.0 (2.6)	22.1 (2.4)
Δ*luxO*	6.0 (0.2)	5.4 (0.6)	5.7 (0.6)
ΔVC1522	16.8 (1.9)	19.5 (0.2)	19.5 (0.2)
Δ*dctD-1*	13.5 (4.0)	16.0 (0.8)	23.9 (1.4)
Δ*flrC*	21.8 (0.6)	29.0 (0.7)	31.0 (1.9)
Δ*flrA*	22.4 (0.8)	24.0 (0.8)	35.0 (1.8)
Δ*ntrC*	22.6 (0.6)	25.3 (1.3)	26.7 (2.5)
Δ*dctD-2*	13.9 (1.3)	17.0 (0.8)	22.7 (5.2)
Δ*pgtA*	18.6 (1.3)	20.2 (1.4)	23.2 (0.4)
Δ*rpoN*	6.4 (0.5)	5.8 (0.6)	7.2 (0.9)

[a]The values are the means (standard deviations) of data from six z-series image stacks.

To understand possible mechanism by which these regulators could impact biofilm formation, we measured the promoter activity of the *vps* genes using a luciferase transcriptional reporter *vpsLp-lux* in wild type *V. cholerae*, Δ*luxO*, ΔVC1522, Δ*dctD-1*, Δ*flrC*, Δ*flrA*, Δ*ntrC*, Δ*dctD-2*, Δ*pgtA*, and Δ*rpoN* (Fig. 2.1B). To measure *vpsL* promoter activity, each strain was grown at 30°C until it reached an OD_{600} of 0.3-0.4 and luminescence was measured. Two mutants, Δ*luxO* and Δ*rpoN*, were found to exhibit 47-fold and 58-fold decrease in *vpsL* promoter activity compared to wild type (Fig. 2.1B). This finding is expected as LuxO has previously been shown to repress the master quorum sensing regulator, HapR, and RpoN has been shown to activate biofilm formation (15, 18, 43). In addition, Δ*ntrC* was found to exhibit a 3-fold increase in *vpsL* promoter activity compared to wild type (Fig. 2.1B).

Collectively, these findings show that LuxO is the only NtrC family RR whose biofilm and *vpsL* expression profile phenocopies that of the strain lacking RpoN, suggesting that RpoN mediates its effect on biofilm formation through NtrC. We determined that while FlrC, FlrA, and NtrC negatively regulated biofilm formation, only NtrC negatively regulated *vpsL* gene expression. Previous studies designed to determine FlrA and FlrC regulons have suggested that FlrA and FlrC negatively regulates biofilm formation, as expression of *vps* genes were negatively regulated by them (44) but

involvement of NtrC in biofilm formation has not been previously reported. Thus we decided to focus this study on the regulation of NtrC of biofilm formation.

V. cholerae NtrC functions similarly as to *E. coli* NtrC

Amino acid sequence alignment of *V. cholerae* NtrC to *E. coli* NtrC and *S. typhimurium* showed a 72.3% identity and 72.6% identity, respectively (Fig. S2.1). To test if *V. cholerae* NtrC functions similarly as to *E. coli*, we performed complementation analysis using an *E. coli* strain lacking Δ*ntrBC*. For these studies we expressed *V. cholerae ntrBC* from an arabinose inducible promoter on the pBAD plasmid (Fig. 3.2A) and analyzed its ability to support growth on M9 agar with L-serine as the only nitrogen source. Wild type *E. coli* containing empty vector (pBAD) can grow on this medium; however, Δ*ntrBC* containing empty vector (pBAD) does not grow very well, indicating that the Δ*ntrBC* mutant has decreased ability to utilize L-serine as a nitrogen source (Fig. 3.2A). When *V. cholerae ntrBC* is introduced into the *E. coli* Δ*ntrBC* strain, growth on M9 agar with L-serine is restored (Fig. 3.2A). These findings suggest that *V. cholerae ntrC* functions similarly as to *E. coli*.

Figure S3.1

A

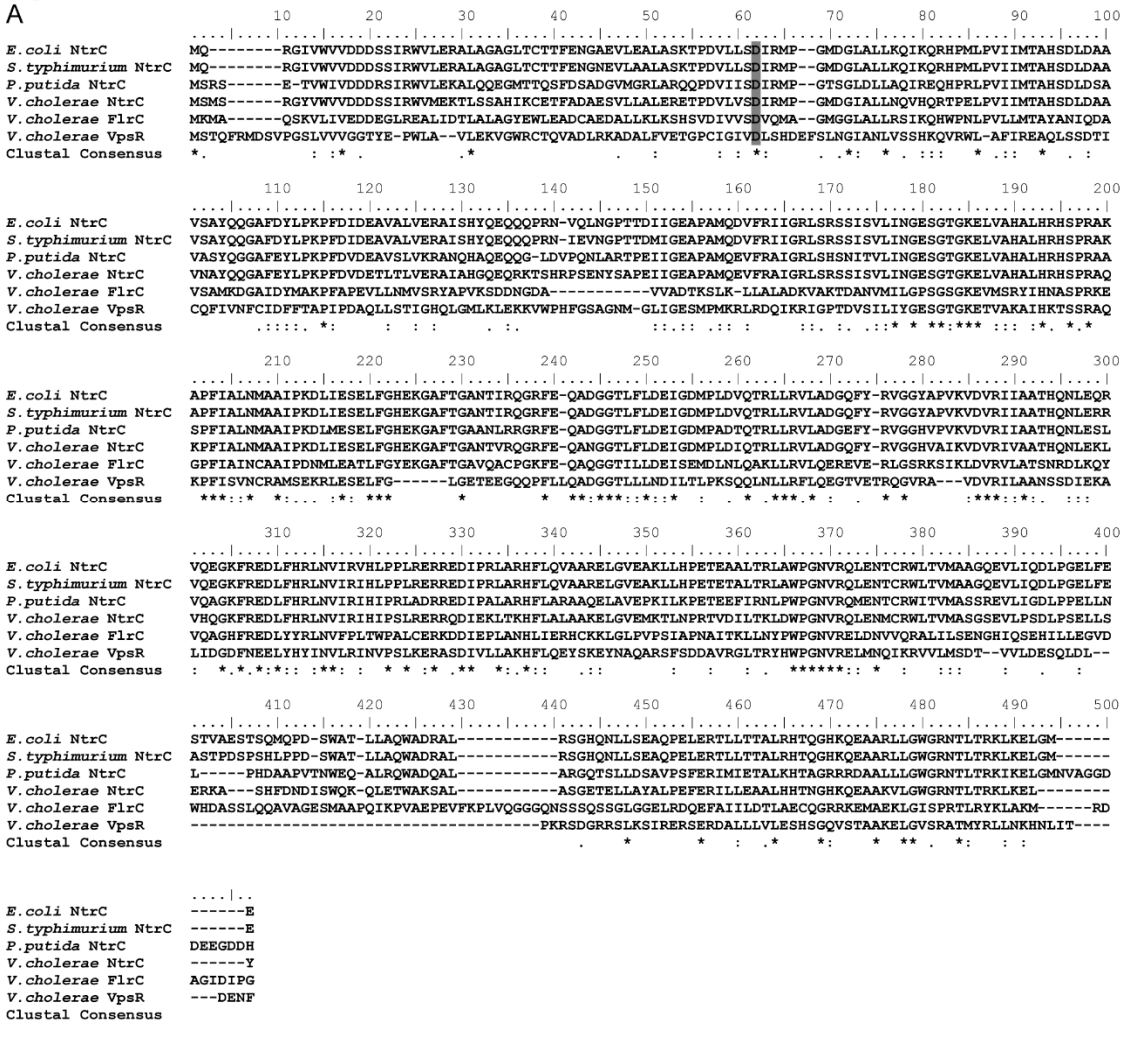
E.coli NtrC
S.typhimurium NtrC
P.putida NtrC
V.cholerae NtrC
V.cholerae FlrC
V.cholerae VpsR
Clustal Consensus

Figure S3.1. Multiple sequence alignment of NtrC, FlrC, and VpsR. Amino acid sequence alignment of *E. coli* NtrC, *S. typhimurium* NtrC, *P. putida* NtrC, *V. cholerae* NtrC, *V. cholerae* FlrC, and *V. cholerae* VpsR using ClustalW. Highlighted region in gray indicate the aspartate residue that is predicted to be the site of phosphorylation. Numbers above the sequence correspond to the amino acid number of each protein.

Figure 3.2

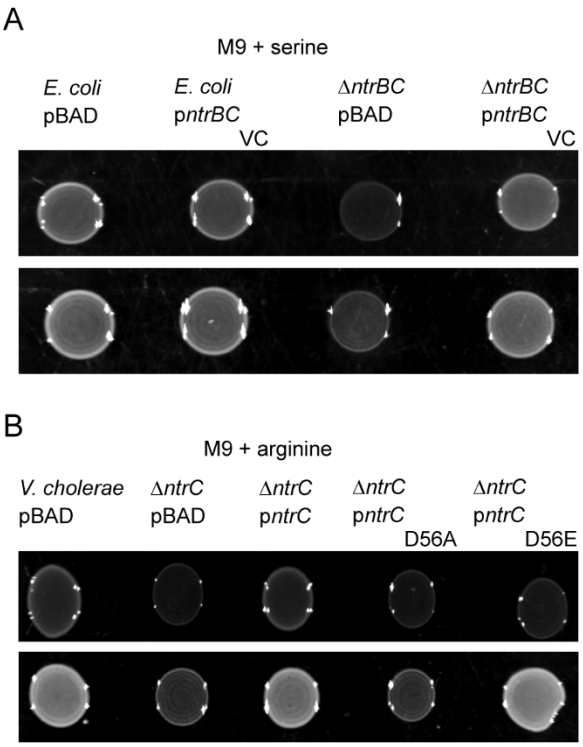
A
M9 + serine
E. coli pBAD
E. coli pntrBC VC
ΔntrBC pBAD
ΔntrBC pntrBC VC
B
M9 + arginine
V. cholerae pBAD
ΔntrC pBAD
ΔntrC pntrC
ΔntrC pntrC D56A
ΔntrC pntrC D56E

Figure 3.2. Function of NtrC in *E. coli* and *V. cholerae*. Images of spot colonies grown on M9 agar supplemented with 100 mM L-serine (A) and 100 mM L-arginine (B) as nitrogen sources after 24 h in 37°C. Colonies were grown under 0% arabinose (top) and 0.1 % arabinose (bottom). (A) Spot colonies of *E. coli* containing empty vector (pBAD), *E. coli* containing *V. cholerae ntrBC* under the control of an arabinose inducible promoter (pBAD-*ntrBC*$_{VC}$), *E. coli* Δ*ntrBC* containing empty vector (pBAD), and *E. coli* Δ*ntrBC* containing *V. cholerae ntrBC* under the control of an arabinose inducible promoter (pBAD-*ntrBC*$_{VC}$). (B) Spot colonies of *V. cholerae* containing empty vector (pBAD), *V. cholerae* Δ*ntrC* containing empty vector (pBAD), *V. cholerae* Δ*ntrC* containing *ntrC* under the control of an arabinose inducible promoter (p*ntrC*), *V. cholerae* Δ*ntrC* harboring a point mutation (D56A) of *ntrC* under the control of an arabinose inducible promoter (p*ntrC*$_{D56A}$), and *V. cholerae* Δ*ntrC* harboring a point mutation (D56E) of *ntrC* under the control of an arabinose inducible promoter (p*ntrC*$_{D56E}$). The *ntrC* gene was mutated to convert the aspartate residue predicted to be important for phosphorylation to emulate the inactive (D56A) or active (D56E) state of NtrC.

Next, we wanted to see if *ntrC* is required to grow under poor nitrogen conditions in *V. cholerae*. For these studies we compared ability of wild type *V. cholerae* and Δ*ntrC* strain to grow on M9 agar with L-arginine as the only nitrogen source, as we determined that L- arginine is a poor nitrogen source for *V. cholerae* Δ*ntrC* (Fig. 3.6A). We determined that increased expression of *ntrC* in a wild type background enhances growth (Fig. 3.2B). Growth of Δ*ntrC* harboring vector pBAD on this medium was impaired (Fig. 3.2B). Introduction of p*ntrC* into the Δ*ntrC* mutant restored the growth defect (Fig. 3.2B). This suggests that NtrC is needed to grow on poor nitrogen sources and the Δ*ntrC* growth defect can be complemented with p*ntrC*.

Figure 3.6

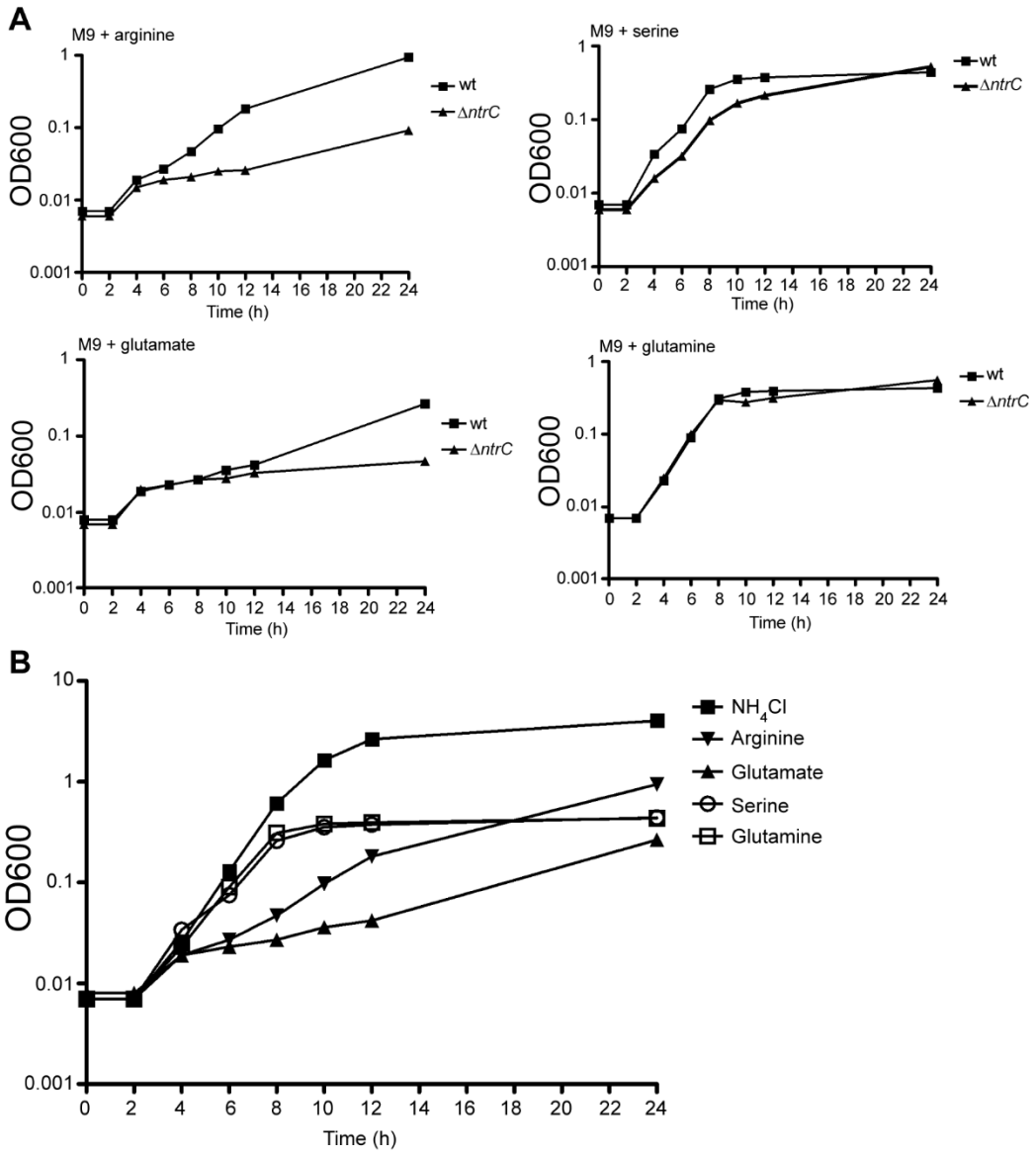
A
M9 + arginine
M9 + serine
M9 + glutamate
M9 + glutamine
OD600
Time (h)
wt
ΔntrC
B
NH4Cl
Arginine
Glutamate
Serine
Glutamine

Figure 3.6. The effect of different nitrogen sources on growth and biofilm formation. (A) Growth curves of wt and Δ*ntrC* mutants grown in M9 media with different amino acids as nitrogen sources: 100 mM arginine, 100 mM glutamate, 100 mM serine, and 100 mM glutamine. Three technical replicates were analyzed and one representative experiment of two independent experiments is shown. (B) Comparison of growth of wt in different nitrogen sources.

Amino acid sequence alignment of NtrC from *E. coli*, *S. tyhpimurium*, *P. putida* and *V. cholerae* VpsR revealed that the aspartate residue D56 of *V. cholerae* NtrC is likely to be the conserved phosphorylation site of the REC domain (Fig. S3.1). Since phosphorylation state of a RR is likely to determine its activity, we mutated the aspartate residue in the REC domain of NtrC to mimic constitutively active (D56A) and inactive (D56E) versions on a plasmid (p*ntrC*$_{D56A}$ and p*ntrC*$_{D56E}$) and introduced the plasmids into the Δ*ntrC* mutant strain. Δ*ntrC* harboring the constitutively inactive (D56A) *ntrC* plasmid did not grow well compared to wild type and Δ*ntrC* harboring the active (D56E) *ntrC* plasmid was able to grow similar to empty vector control strain (Fig. 3.2B). This suggests that *V. cholerae* NtrC is required for growth in poor nitrogen sources, such as L-arginine, and that NtrC phosphorylation at D56 affects the function of NtrC under poor nitrogen conditions.

Impact of NtrC phosphorylation state on *vps* gene expression.

To further characterize the impact of *ntrC* on *vps* gene expression, we utilized a reporter strain with the *vpsL* promoter fused to *lacZ* on the chromosome and analyzed *vpsL* expression using β-galactosidase production as a readout for *vpsL* gene expression. When *ntrC* is overexpressed in a wild type strain background, we saw no changes in *vpsL* expression. A 4.6-fold increase in *vpsL* expression is observed in Δ*ntrC* carrying vector only. Introduction of *ntrC*

restored *vpsL* expression to wild type levels (Fig. 3.3A). Furthermore, we observed that *vpsL* expression is increased by 4-fold when the constitutively (p*ntrC*$_{D56A}$) inactive version of *ntrC* is overexpressed and *vpsL* expression is restored to wild type levels when the constitutively (p*ntrC*$_{D56E}$) active version of *ntrC* is overexpressed (Fig. 3.3A). This data suggests that the Δ*ntrC* phenotype can be complemented and that phosphorylation state of NtrC may play an important role in *vpsL* expression.

Since the phosphorylation state of NtrC may dictate *vpsL* expression, we examined if the cognate HK, NtrB, had an effect on *vpsL* expression. Using a *vpsL*p-*lux* reporter, we observed a slight increase (1.7-fold increase) in *vpsL* expression in Δ*ntrB* compared to wild type (Fig. 3.3B). This suggests that the two-component system NtrBC negatively regulates *vpsL* expression.

Figure 3.3

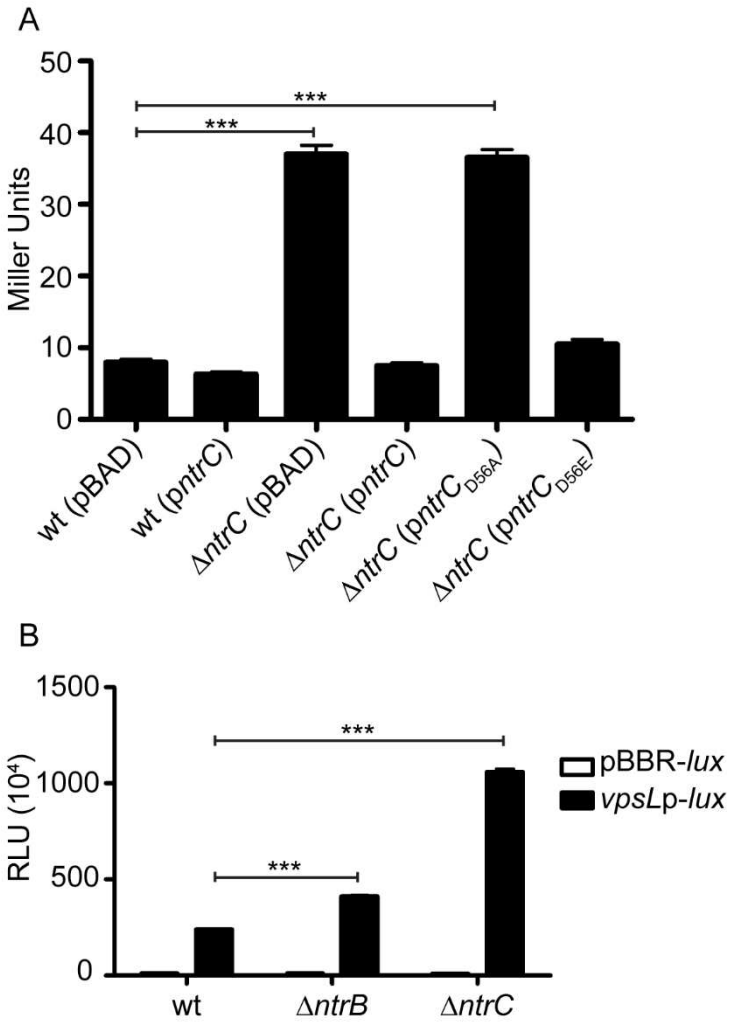
A
50
40
30
20
10
0
Miller Units
***
***
wt (pBAD)
wt (pntrC)
ΔntrC (pBAD)
ΔntrC (pntrC)
ΔntrC (pntrC D56A)
ΔntrC (pntrC D56E)
B
1500
1000
500
0
RLU (10^4)
***
***
pBBR-lux
vpsLp-lux
wt
ΔntrB
ΔntrC

Figure 3.3. The role of the phosphorylation state of NtrC in *vpsL* expression. (A) β-galactosidase assay of *vpsL* expression in a *vpsLp-lacZ* reporter strain containing empty vector (pBAD), *ntrC* under the control of an arabinose inducible promoter (p*ntrC*), Δ*ntrC* containing empty vector (pBAD), Δ*ntrC* containing p*ntrC*, Δ*ntrC* containing a point mutation (D56A) of *ntrC* under the control of an arabinose inducible promoter (p$ntrC_{D56A}$), and Δ*ntrC* containing a point mutation (D56E) of *ntrC* under the control of an arabinose inducible promoter (p$ntrC_{D56E}$). Growth medium was supplemented with 0.1% arabinose to induce expression of *ntrC* and *ntrC* with point mutants. The graph represents the average and standard deviations of four technical replicates. The result of one representative experiment of three biological replicates are shown. (B) Expression of P_{vpsL}-*luxCADBE* (pFY_3406) in wt, Δ*ntrB* and Δ*ntrC*. White bar indicates empty vector (pBBRlux) and black bar indicates *vpsL* expression (*vpsL*p-*lux*). The graph represents the average and standard deviation of relative light units (RLU) obtained from four technical replicates from three independent biological samples. RLU is reported in luminescence counts min^{-1} ml^{-1}/OD_{600}. A two-tailed unpaired T-test was used to compare the expression between wt and deletion mutants. *** $p < 0.001$.

Analysis of the transcriptome profile of NtrC in *V. cholerae*

To understand how NtrC could impact *vps* gene expression, we compared the whole genome expression profile of the wild type strain to the Δ*ntrC* strain using microarray analysis. Transcriptional profiling data were analyzed using SAM software (45). The following criteria were used to define significantly regulated genes: $\leq$ 3% false discovery rate and $\geq$ 1.5-fold transcript abundance differences between the samples. Based on the selection criteria, a total of 172 genes were found to be differentially regulated (132 genes were up-regulated and 40 genes were directly or indirectly down-regulated by NtrC) (Tables 3.3 and 3.4). Biofilm-related genes such as *vpsBCJMN*, *rbmF*, and *bap1* were at least 2-fold up-regulated by NtrC (Table 3.3). Thus, these data confirm our finding that expression of *vps* genes are repressed by NtrC. In addition, expression of type VI secretion genes (T6SS) (VC1417, *vipB*, *hcp1*, *hcp2*) were also found to be negatively regulated by NtrC (Table 3.3). VC1417, *hcp1*, and *hcp2* encode the structural proteins for the T6SS apparatus. VipB, together with VipA, are polymers that form the outer contractile sheath (46, 47). Furthermore, we observed that *glnA* expression was down-regulated 2-fold by NtrC. The *glnA* is the structural gene encoding glutamine synthetase [L-glutamate:ammonia ligase (ADP-forming), EC 6.3.1.2] (22, 48-50). Glutamine synthetase catalyzes glutamine biosynthesis via the condensation of glutamate and ammonia (51).

Table 3.3. Genes negatively regulated by NtrC

ORF ID[a]	Gene	Fold Up Regulation[b]	Predicted function
VCA1028	*ompS*	7.63	Maltoporin
VCA0945	*malE*	5.79	Maltose ABC transporter
VCA0671	VCA0671	4.16	Hypothetical protein
VCA0946	*malK*	3.67	Maltose/maltodextrin ABC transporter
VC1888	*bap1*	3.21	Matrix protein
VCA0994	VCA0994	3.16	Hypothetical protein
VCA0887	VCA0887	3.06	Hypothetical protein
VC0852	*recN*	2.90	DNA repair protein RecN
VCA0014	*malQ*	2.90	4-alpha-glucanotransferase
VCA0944	*malF*	2.86	Maltose ABC transporter
VC0935	*vpsM*	2.84	Exopolysaccharide
VCA0888	VCA0888	2.74	Regulatory functions – LuxR family
VCA1065	VCA1065	2.73	Hypothetical protein
VC2618	*argD*	2.72	Acetylornithine aminotransferase
VCA0732	VCA0732	2.67	Hypothetical protein
VCA0214	*emrD-2*	2.66	Multidrug resistance protein D
VC1415	*hcp-1*	2.65	T6SS
VCA0291	*intI4*	2.64	Site-specific recombinase
VCA0943	*malG*	2.55	Maltose ABC transporter
VC2092	*gltA*	2.51	Citrate synthase
VC1905	*ald*	2.51	Alanine dehydrogenase
VC1184	VC1184	2.44	Central intermediary metabolism
VCA0219	*hlyA*	2.43	Haemolysin
VCA0849	VCA0849	2.41	Hypothetical protein
VC2302	VC2302	2.41	RNA polymerase sigma-70 factor - ECF subfamily
VC0926	*vpsJ*	2.41	Exopolysaccharide
VCA0274	*cah*	2.39	Carbonic anhydrase
VCA0886	*kbl*	2.37	2-amino-3-ketobutyrate coenzyme A ligase
VC0936	*vpsN*	2.36	Exopolysaccharide
VC2345	*serB*	2.35	Phosphoserine phosphatase
VC2481	*serA*	2.35	D-3-phosphoglycerate dehydrogenase
VC0171	VC0171	2.30	Transport and binding proteins

VC1191	VC1191	2.29	Hypothetical protein
VC0162	*ilvC*	2.28	Ketol-acid reductoisomerase
VC1509	*cobB*	2.27	Nicotinate mononucleotide:5_6-dimethylbenzimidazole phosphoribosyltransferase
VCA0787	VCA0787	2.26	Hypothetical protein
VC0026	VC0026	2.20	Zinc-binding alcohol dehydrogenase ||
VC2702	*cbrR*	2.15	Regulatory functions || Other || transcriptional regulator_ LuxR family ||
VC0919	*vpsC*	2.14	Exopolysaccharide
VC1132	*hisG*	2.13	ATP phosphoribosyltransferase
VCA0645	VCA0645	2.12	Hypothetical protein
VC1190	VC1190	2.10	Phosphoribosylaminoimidazole-succinocarboxamide synthase_ putative
VC2155	VC2155	2.09	Hypothetical protein
VC0170	VC0170	2.09	Peptide ABC transporter_ ATP-binding protein
VC1433	VC1433	2.08	Hypothetical protein
VC1812	VC1812	2.07	Hypothetical protein
VCA0885	*tdh*	2.04	Threonine 3-dehydrogenase
VCA0682	*uhpA*	2.02	Transcriptional regulator UhpA
VCA0017	*hcp-2*	2.01	T6SS
VC0895	VC0895	2.01	Hypothetical protein
VC1938	VC1938	2.00	Hypothetical protein
VC0918	*vpsB*	1.99	Exopolysaccharide
VCA0537	VCA0537	1.98	Hypothetical protein
VC0933	*rbmF*	1.98	Matrix protein
VC2748	*ntrB*	1.98	Histidine kinase for nitrogen assimilation
VC0432	*mdh*	1.97	Malate dehydrogenase
VC1119	VC1119	1.95	Oxidoreductase short-chain dehydrogenase
VC0975	VC0975	1.94	Hypothetical protein
VCA0581	VCA0581	1.94	Hypothetical protein
VCA0547	VCA0547	1.93	Hypothetical protein
VCA0574	VCA0574	1.93	Hypothetical protein
VC0135	*lypA*	1.93	Lysophospholipase L2
VC1095	*oppF*	1.92	Oligopeptide ABC transporter

VC1828	VC1828	1.91	Hypothetical protein
VC0328	*rpoB*	1.90	DNA-dependent RNA polymerase
VC2088	*sdhB*	1.90	Succinate dehydrogenase
VC2617	VC2617	1.90	Energy metabolism
VCA0563	*pntA*	1.90	NAD(P) transhydrogenase
VC1417	VC1417	1.90	T6SS
VC1198	VC1198	1.89	Hypothetical protein
VC2448	*pyrG*	1.89	CTP synthase
VC2348	*deoB*	1.89	Phosphopentomutase
VC1534	VC1534	1.88	Hypothetical protein
VC2751	*add*	1.88	Adenosine deaminase
VC1255	*nrdB*	1.86	Ribonucleoside-diphosphate reductase
VC1898	VC1898	1.86	Methyl-accepting chemotaxis protein
VC0667	VC0667	1.86	Oxidoreductase
VC1284	*celF*	1.84	6-phospho-beta-glucosidase
VCA0564	*pntB*	1.82	NAD(P) transhydrogenase
VC2198	*flgD*	1.82	Basal-body rod modification protein
VC1183	VC1183	1.82	Hypothetical protein
VCA1022	VCA1022	1.82	Hypothetical protein
VC2349	*deoA*	1.81	Thymidine phosphorylase
VC2761	VC2761	1.78	Multidrug resistance protein
VC0704	VC0704	1.78	Transport and binding proteins
VC1103	VC1103	1.78	Transport and binding proteins
VC0737	VC0737	1.78	Hypothetical protein
VC1992	*purU*	1.78	Purine ribonucleotide biosynthesis
VCA0763	VCA0763	1.77	Hypothetical protein
VC0019	*avtA*	1.76	Valine-pyruvate aminotransferase
VCA0637	VCA0637	1.76	Central intermediary metabolism
VC2207	VC2207	1.76	Hypothetical protein
VCA0108	*vipB*	1.76	T6SS
VCA0776	VCA0776	1.76	Hypothetical protein
VC1293	*aspC*	1.75	Aspartate aminotransferase
VC2333	VC2333	1.75	Ribosomal protein S6 modification protein
VC0330	*rsd*	1.75	Regulator of sigma D
VCA0100	*pspE*	1.74	Phage shock protein E
VC1516	VC1516	1.74	Energy metabolism
VC1414	VC1414	1.73	Protein fate

VC1138	*hisF*	1.73	HisF protein (cyclase)
VCA1029	*glgX*	1.73	Glycogen operon protein
VCA0249	VCA0249	1.72	Energy metabolism
VCA0239	VCA0239	1.71	Regulatory functions
VC2188	*flaA*	1.70	Flagellin core protein A
VCA0523	VCA0523	1.70	Central intermediary metabolism
VC1059	VC1059	1.70	Central intermediary metabolism
VC2362	*thrC*	1.70	Threonine synthase
VCA0013	*malP*	1.70	Maltodextrin phosphorylase
VC2301	VC2301	1.70	Regulatory functions
VC0039	VC0039	1.70	SpoOM-related protein
VCA0513	VCA0513	1.69	Amino acid biosynthesis
VC0533	*nlpD*	1.68	Lipoprotein
VC1866	*pflB*	1.67	Formate acetyltransferase
VC2036	*asd*	1.67	Aspartate-semialdehyde dehydrogenase
VC2084	*sucD*	1.66	Succinyl-CoA synthase
VC0941	*glyA-1*	1.66	Serine hydroxymethyltransferase
VC2116	*aroC*	1.65	Chorismate synthase
VC2091	*sdhC*	1.65	Succinate dehydrogenase
VCA0264	VCA0264	1.65	Regulatory functions
VC2141	*flaG*	1.65	Flagellin FlaG
VC1302	VC1302	1.65	DNA metabolism
VCA0514	VCA0514	1.64	Hypothetical protein
VC2298	VC2298	1.64	Cell envelope
VC0571	*rpsI*	1.64	Ribosomal protein S9
VC2689	*pfkA*	1.64	6-phosphofructokinase
VCA0986	VCA0986	1.63	Hypothetical protein
VC1937	VC1937	1.63	Hypothetical protein
VCA0867	*ompW*	1.61	Outer membrane protein
VC2358	VC2358	1.61	Hypothetical protein
VC1288	*mdoG*	1.60	Periplasmic glucans biosynthesis protein
VCA0822	VCA0822	1.57	Amino acid biosynthesis

[a]ORF IDs are derived from the *V. cholerae* N16961 genome.
[b]Fold change is the Δ*ntrC* mutant relative to the wild-type strain.

Table 3.4. Genes positively regulated by NtrC

ORF ID[a]	Gene	Fold Down Regulation[b]	Predicted function
VC0053	VC0053	-4.37	Hypothetical protein
VC2171	*uraA*	-3.78	Uracil permease
VC1329	VC1329	-3.75	Opacity protein-related protein
VC1420	VC1420	-3.37	Hypothetical protein
VC1658	*sdaC-2*	-3.16	Serine transporter
VCA0128	*rbsA*	-3.10	Ribose ABC transporter ATP-binding protein
VCA0516	*fruA-2*	-2.94	Fructose-specific IIBC component
VC1822	*frwABC*	-2.77	Fructose-specific IIABC component
VC2383	VC2383	-2.75	Regulatory functions – LysR family
VC1954	VC1954	-2.55	Hypothetical protein
VCA0046	VCA0046	-2.54	Hypothetical protein
VC0265	VC0265	-2.51	Hypothetical protein
VC0615	VC0615	-2.44	Hypothetical protein
VCA0933	VCA0933	-2.42	Regulatory functions
VC0497	VC0497	-2.35	Regulatory functions
VCA0517	*fruK*	-2.34	1-phosphofructokinase
VC0115	VC0115	-2.33	Hypothetical protein
VC1162	VC1162	-2.31	Peptidase aspartic lipoprotein
VC2737	VC2737	-2.30	Hypothetical protein
VC1737	*infA*	-2.24	Initiation factor IF-1
VCA0895	VCA0895	-2.23	Chemotactic transducer-related protein - HDGYP domain
VC1345	VC1345	-2.20	Zinc ABC transporter
VC2081	*znuA*	-2.16	Transport and binding proteins
VC0611	VC0611	-2.15	Energy metabolism
VCA0902	VCA0902	-2.15	Hypothetical protein
VC2746	*glnA*	-2.14	Glutamine synthetase
VC0599	VC0599	-2.13	Hypothetical protein
VC0915	VC0915	-2.10	Hypothetical protein
VC1012	VC1012	-2.07	Energy metabolism
VCA0937	VCA0937	-2.03	Regulatory functions
VC1231	*cdd*	-2.03	Purines pyrimidines nucleosides and nucleotides
VC0728	VC0728	-1.99	Hypothetical protein

VC2385	VC2385	-1.95	DNA metabolism
VC1552	*ugpC*	-1.95	Glycerol-3-phosphate ABC transporter
VC1816	VC1816	-1.91	Hypothetical protein
VC0943	*lipA*	-1.90	Lipoic acid synthetase
VCA0137	*glpT*	-1.85	Glycerol-3-phosphate transporter
VCA0928	VCA0928	-1.82	Hypothetical protein
VC0275	*purD*	-1.80	Phosphoribosylamine-glycine ligase
VC0069	VC0069	-1.69	Transport and binding proteins

[a]ORF IDs are derived from the *V. cholerae* N16961 genome.
[b]Fold change is the Δ*ntrC* mutant relative to the wild-type strain.

Of the genes differentially regulated by NtrC, we choose to focus on genes annotated as transcriptional regulators. We speculated that NtrC could be controlling *vps* expression by regulating the expression of these unknown regulators. We selected 6 regulators (3 up-regulated and 3 down-regulated genes) that had the highest differential expression relative to wild type. The transcriptional regulators that were down-regulated by NtrC were VC2383, VCA0937, and VC0497. VC2383 belongs to the LysR family of transcriptional regulators. VCA0937 is part of the AraC-family transcriptional regulators. VC0497 is predicted to contain a prophage CP4-57 regulatory domain at the N-terminal and putative DNA binding domain at the C-terminal. The transcriptional regulators that were up-regulated by NtrC were VCA0888, VC2702 (*crbR*), and VCA0682 (*uhpA*). VCA0888 belongs to the LuxR-family of DNA binding domains. VC2702 (*crbR*) also belongs to the LuxR-family and contains a signature REC domain for TCS RR. CrbR positively regulates the transcription of acetyl-CoA synthase-1 (ACS-1), which then activates the acetate switch system where bacteria transition from excretion to assimilation of environmental acetate (52). VCA0682 (*uhpA*) also belongs to the LuxR family and is characterized as a RR for regulating hexose-phosphate uptake.

To analyze involvement of these uncharacterized regulators in the regulation of *vpsL* gene expression, we generated single in-frame deletion mutants of

each regulator in a wild type genetic background and also a Δ*ntrC* genetic background. Analysis of *vpsL* gene expression in these mutants revealed that single mutants do not impact *vpsL* gene expression and the double mutants phenocopy *vpsL* expression phenotype of Δ*ntrC* (Fig. S3.3). Collectively, these results show that these regulators do not affect *vpsL* expression.

Figure S3.3

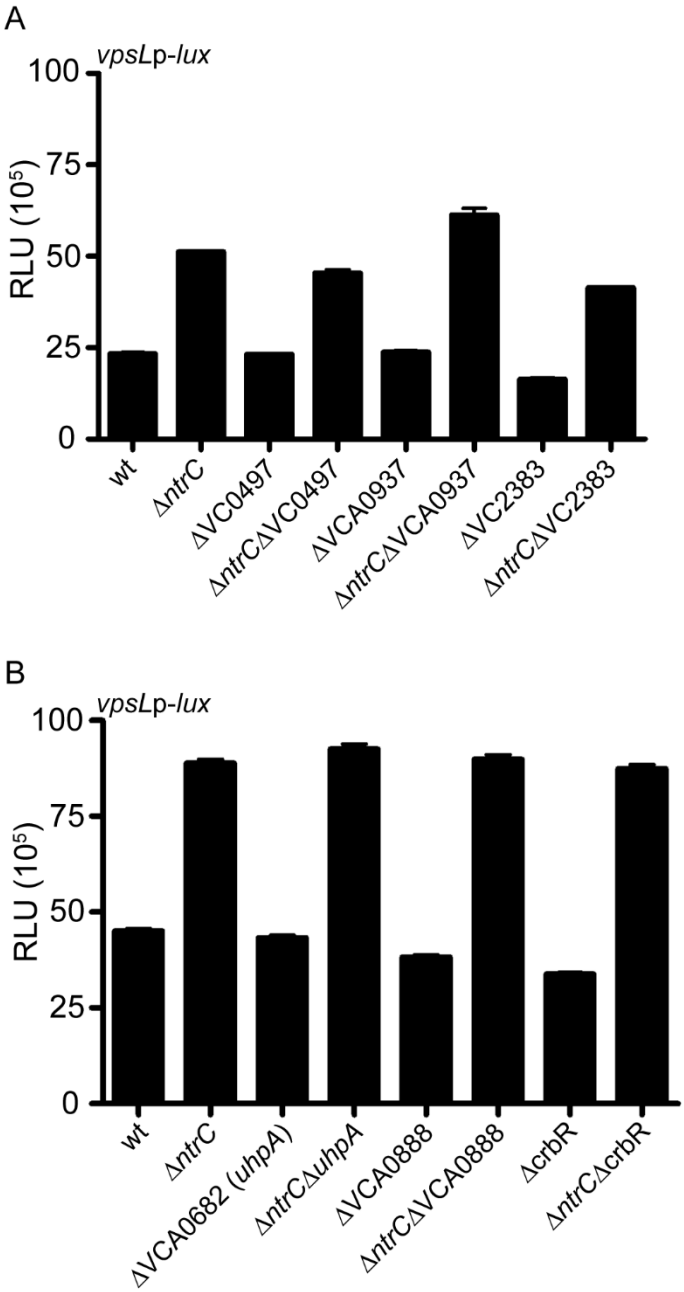
A
vpsLp-lux
100
75
50
25
0
RLU (10^5)
wt
ΔntrC
ΔVC0497
ΔntrCΔVC0497
ΔVCA0937
ΔntrCΔVCA0937
ΔVC2383
ΔntrCΔVC2383
B
vpsLp-lux
100
75
50
25
0
RLU (10^5)
wt
ΔntrC
ΔVCA0682 (uhpA)
ΔntrCΔuhpA
ΔVCA0888
ΔntrCΔVCA0888
ΔcrbR
ΔntrCΔcrbR

Figure S3.3. Analysis of *vpsL* expression in transcriptional regulators whose expression is regulated by NtrC. (A) Expression of P_{vpsL}-*luxCADBE* (pFY_3406) in wt, Δ*ntrC*, ΔVC2383, Δ*ntrC*ΔVC2383, ΔVCA0937, Δ*ntrC*ΔVCA0937, ΔVC0497, and Δ*ntrC*ΔVC0497. (B) Expression of P_{vpsL}-*luxCADBE* (pFY_3406) in wt, Δ*ntrC*, ΔVCA0888, Δ*ntrC*ΔVCA0888, ΔVC2702 (*crbR*), Δ*ntrC*Δ*crbR*, ΔVCA0682 (*uhpA*), and Δ*ntrC*Δ*uhpA*. The graph represents the average and standard deviation of relative light units (RLU) obtained from four technical replicates and three independent biological samples. RLU is reported in luminescence counts min^{-1} ml^{-1}/OD_{600}.

The effect of NtrC on regulators of biofilm formation.

VpsR and VpsT are positive transcriptional regulators of *vps* genes while HapR negatively regulates *vps* genes. To determine if NtrC affects the regulators of *vps* gene expression, we measured expression of each regulator in Δ*ntrC* compared to wild type. As expected, *vpsL* expression is increased 2.6-fold in the Δ*ntrC* mutant compared to wild type (Fig. 3.4A). Expression of *vpsR* and *vpsT* in Δ*ntrC* was increased 1.7 and 2.9-fold, respectively, compared to wild type (Fig. 3.4A). Expression of *hapR* was 1.3-fold higher in Δ*ntrC* compared to wild type (Fig. 3.4A). This was unexpected as HapR negatively regulates *vpsL* gene expression. To better evaluate the impact of NtrC on HapR production, we measured HapR production using western blot analysis. For these studies we generated a strain harboring C-terminally HA tagged version of HapR in wild type and Δ*ntrC*, we probed for HapR using HA antibodies. We did not observe any difference in HapR production based on the western blot (Fig. 3.4B). This suggests that NtrC has no effect on the negative regulator HapR.

Figure 3.4

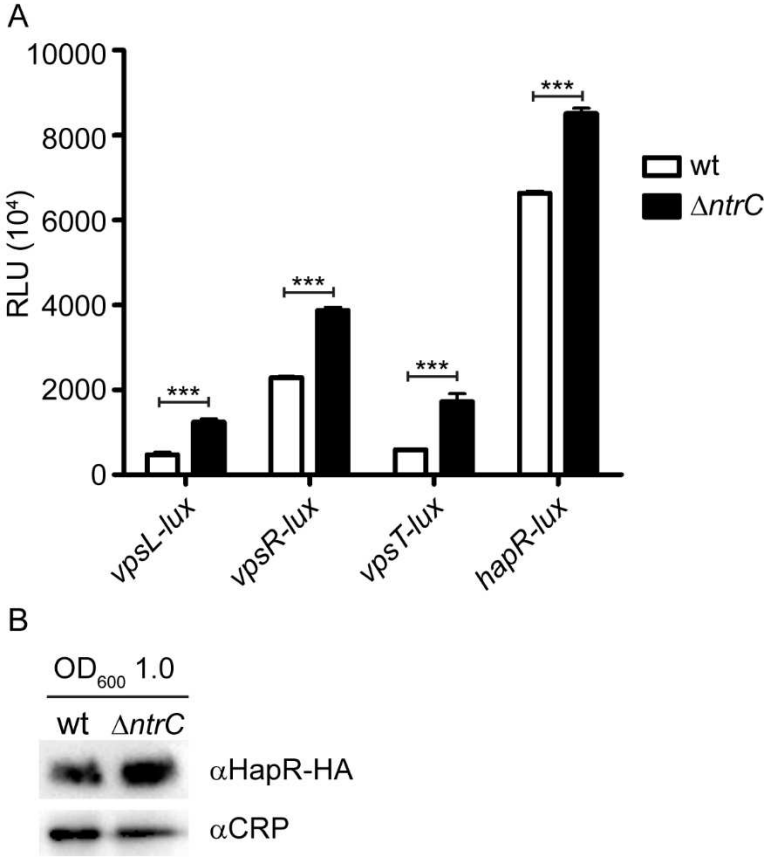
A
10000
8000
6000
4000
2000
0
RLU (10^4)
***
***
***
***
wt
ΔntrC
vpsL-lux
vpsR-lux
vpsT-lux
hapR-lux
B
OD600 1.0
wt
ΔntrC
αHapR-HA
αCRP

Figure 3.4. NtrC negatively regulates *vpsR* and *vpsT* expression. (A) Expression of P_{vpsR}-*luxCADBE*, P_{vpsT}-*luxCADBE*, and P_{hapR}-*luxCADBE* in wt and Δ*ntrC* at exponential growth phase. The graph represents the average and standard deviation of relative light units (RLU) obtained from four technical replicates from three independent biological samples. RLU is reported in luminescence counts min^{-1} ml^{-1}/OD_{600}. A two-tailed unpaired T-test was used to compare the expression between wt and deletion mutants. *** p< 0.001. (B) Western blot of HapR tagged with hemagluttin (HA). HapR production was analyzed in whole cells in wt and Δ*ntrC* strains at early stationary growth phase (OD_{600} 1.0) by immunoblot analysis. In these strains, HapR was tagged with hemagglutinin (HA) at the C-terminal. Equal amounts of total protein (determined by BCA assay) were loaded onto a SDS 13% polyacrylamide gel.

Analysis of epistasis relationships among regulators of *vps* gene expression

To determine the contribution of NtrC to the *vps* regulatory network, we performed an epistasis analysis. As expected, Δ*ntrC* exhibited increased *vpsL* expression, while single deletions of *vpsR*, *vpsT*, and *rpoN* have decreased *vpsL* expression compared to wild type (Fig. 3.5A). Then, Δ*ntrC*Δ*vpsR*, Δ*ntrC*Δ*vpsT*, and Δ*ntrC*Δ*rpoN* showed no significant difference in *vpsL* expression compared to the single deletions (Fig. 3.5A). This suggests that VpsR, VpsT, and RpoN function downstream of NtrC on *vpsL* gene expression. Strains with single deletions of *hapR* and *crp* exhibited an increase in *vpsL* expression compared to wild type (Fig. 3.5B). Δ*ntrC*Δ*hapR* and of Δ*ntrC*Δ*crp* exhibited an increase *vpsL* expression additively when compared to Δ*ntrC* single deletion. This finding suggests that NtrC repressed *vpsL* independently of HapR and CRP.

Figure 3.5

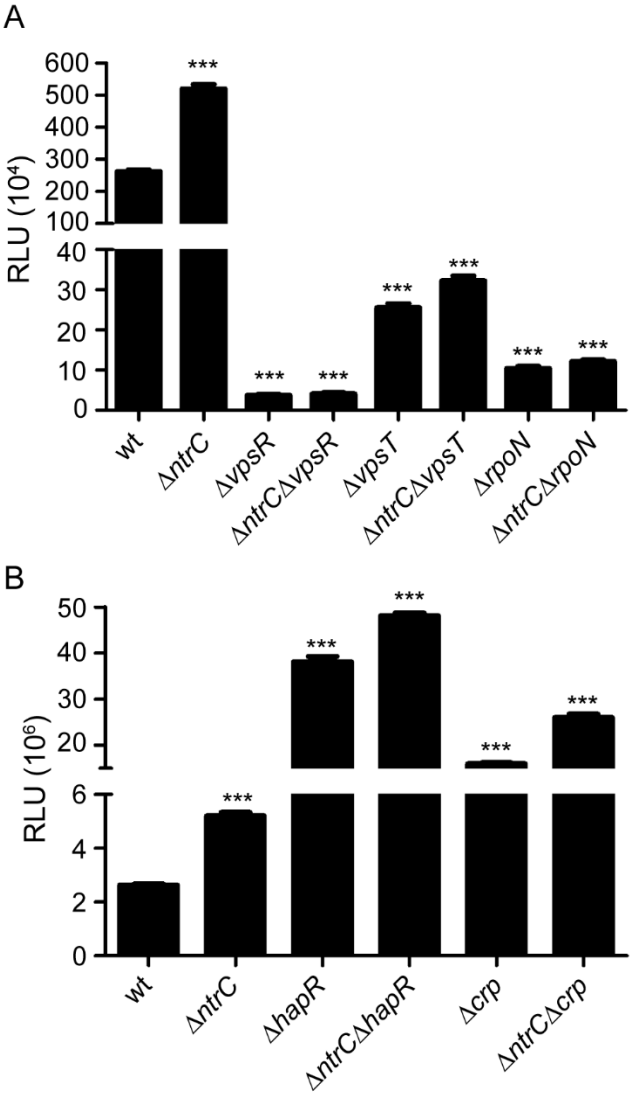
A
RLU (10^4)
600
500
400
300
200
100
40
30
20
10
0
***
wt
ΔntrC
ΔvpsR
ΔntrCΔvpsR
ΔvpsT
ΔntrCΔvpsT
ΔrpoN
ΔntrCΔrpoN
B
RLU (10^6)
50
40
30
20
6
4
2
0
wt
ΔntrC
ΔhapR
ΔntrCΔhapR
Δcrp
ΔntrCΔcrp

Figure 3.5. Epistasis analysis of *ntrC*. (A) Expression of P_{vpsL}-*luxCADBE* (pFY_3406) in wt, Δ*ntrC*, Δ*vpsR*, Δ*ntrC*Δ*vpsR*, Δ*vpsR*, Δ*ntrC*Δ*vpsT*, Δ*rpoN*, and Δ*ntrC*Δ*rpoN*. (B) Expression of P_{vpsL}-*luxCADBE* (pFY_3406) in wt, Δ*ntrC*, Δ*hapR*, Δ*ntrC*Δ*hapR*, Δ*crp*, Δ*ntrC*Δ*crp*. The graph represents the average and standard deviation of relative light units (RLU) obtained from four technical replicates and three independent biological samples. RLU is reported in luminescence counts min^{-1} ml^{-1}/OD_{600}. A two-tailed unpaired T-test was used to compare the expression between wt and deletion mutants. *** $p < 0.001$.

The effect of different nitrogen sources on growth of wild type and *ntrC* mutant

In *E. coli* and *Salmonella* NtrC is critical for growth under nitrogen limiting conditions. Thus, we evaluated the involvement of NtrC in growth under such conditions. We compared growth of *V. cholerae* wild type and Δ*ntrC* in defined M9 media supplemented with 100mM of L-arginine, L-serine, L-glutamate, or L-glutamine as the only nitrogen source (Fig. 3.6A). We selected L-arginine because it has been shown to be a poor nitrogen source for growth in *S. typhimurium* and *E. coli* (53) and L-serine because it has also been shown to be a poor nitrogen source for growth in *Pseudomonas putida* (54). L-glutamine and L-glutamate were tested because they are part of the glutamine biogenesis pathway regulated by NtrC. *V. cholerae* Δ*ntrC* mutant exhibits a growth defect when L-arginine or L-glutamate was used as the sole nitrogen source (Fig. 3.6A). However, there was no growth difference between wild type and Δ*ntrC* when L-serine and L-glutamine was used as the only nitrogen source (Fig. 3.6A). We also compared the growth of wild type in defined M9 media supplemented with 0.1% NH_4Cl, 100mM L-arginine, 100mM L-serine, 100mM L-glutamate, and 100mM L-glutamine (Fig. 3.6B). This suggests that NtrC is also involved in growth under nitrogen limited conditions in *V. cholerae*.

Discussion

V. cholerae is exposed to different environmental stresses in the aquatic environment and the human intestine. The ability to utilize TCS is likely to modulate *V. cholerae*'s ability to sense and respond to these changes in the environment. In this study, we analyzed the role of NtrC family response regulators in biofilm formation, as this family of regulators are necessary for transcriptional activation by RNA polymerase sigma factor RpoN which is required for biofilm formation. There are 8 predicted NtrC type RRs in *V. cholerae* genome: VC1021 (*luxO*), VC1522, VC1926 (*dctD-1*), VC2135 (*flrC*), VC2137 (*flrA*), VC2749 (*ntrC*), VCA0142 (*dctD-2*), and VCA0704 (*pgtA*). Of these, we focused on NtrC. Our major finding was NtrC represses biofilm formation.

VC1522 has not been previously studied in *V. cholerae* and we did not observe any changes in *vps* gene expression and biofilm formation in the absence of VC1552. VC1926 (*dctD-1*) encodes a RR that is homologous to *E. coli* C4-dicarboxylate transport RR. VCA0142 (*dctD-2*) is located on the second chromosome of *V. cholerae* and also encodes for a RR that is also homologous to the *E. coli* C4-dicarboxylate transport RR. In the presence of C4-dicarboxylates, the HK, DctB, is autophosphorylated and transfers the phosphate group to its cognate RR, DctD-1, and activates genes encoding for C4-dicarboxylate transport RR in *E. coli* (55). The activity of the *dct* system is

induced by nitrogen limitation or osmotic stress (56). VCA0704 (*pgtA*) encodes a RR, homologous to *Salmonella typhimurium pgtA,* that controls genes involved in phosphoglycerate transport, such as *pgtP* (57). The phosphoglycerate transport system is used by bacteria for the transport and accumulation of organic phosphates (58). Although strains lacking these regulators did not exhibit any biofilm defect under the conditions utilized in this study, it is still possible that these RR may be involved in biofilm formation under different environmental conditions.

We determined that 4 of the 8 predicted NtrC-type RRs regulate biofilm formation. The first one is LuxO which is part of the quorum sensing regulatory cascade. Previous studies have suggested that LuxO, regulates biofilm formation in *V. cholerae C6706* and *E7046* strains (41). It was shown that LuxO activates the expression of quorum regulatory small RNAs (*qrr* sRNA), where it represses the translation of *hapR* and thus allows biofilm formation to occur at low cell density (59). The findings in this study show similar effects of LuxO on biofilm formation in *V. cholerae A1552*. We also demonstrated that *vpsL* expression and biofilm formation is decreased in Δ*luxO* mutant (Fig. 1). VC2135 (*flrC*) and VC2137 (*flrA*) encodes a RR for flagellar biosynthesis, which is important for biofilm formation (44). FlrA activates RpoN-dependent transcription of class II genes of the flagellar transcriptional hierarchy (60), which encode components of the MS ring-

switch-export apparatus and the TCS, FlrBC (44, 61). Phosphorylated FlrC activates RpoN-dependent transcription of class III genes of the flagellar transcriptional hierarchy (60), which form the basal body-hook and the flagellin, FlaA (44, 62, 63) .This is the first study that demonstrates increased biofilm formation in Δ*flrA* and Δ*flrC* mutants using a flow-cell system (Fig. 3.1A).

Of these RRs, we specifically focused on NtrC as it has not been previously characterized in *V. cholerae*. We determined that *V. cholerae* NtrC, similar to *E. coli* NtrC is critical for growth under nitrogen limiting growth conditions. Further we determined that NtrC negatively regulates biofilm formation and expression of *vps* genes. Our data suggests that NtrC could be repressing *vpsL* expression through VpsR and VpsT. Epistasis analysis suggests that NtrC acts upstream of VpsR and VpsT (Fig. 3.5A). Also, we observed that *vpsR* promoter activity is increased in Δ*ntrC* mutant, suggesting that NtrC is repressing *vpsR* expression. Furthermore, epistasis analysis of the negative regulators of biofilm formation suggests that NtrC could be repressing *vpsL* expression in an independent manner (Fig. 3.5B). Therefore, NtrC regulates *vpsL* expression in parallel with the known negative regulators. It is possible that NtrC may repress *vpsL* expression indirectly via an unidentified regulator, as there are no RpoN binding sites in the regulatory region of *vpsR*.

In this study, we also determined that the ability of NtrC to repress biofilm formation is dependent on its phosphorylation status. We note that our studies were performed in rich medium where cells are not likely to experience nitrogen limitation. In *E. coli*, not only can NtrC be phosphorylated by its cognate HK, NtrB and by acetyl phosphate. Furthermore, NtrC can also be phosphorylated by non-cognate HKs, UhpB (sugar phosphate transporter) and CheA (the chemotaxis modulator protein kinase) (64, 65). Trans-phosphorylation between non-cognate pairs, such as UhpB and NtrC in *E. coli* were detected by *in vitro* phosphorylation assay (66). Phospho-transfer assays demonstrated *in vitro* that CheA catalyzes the ATP-dependent phosphorylation of NtrC (65). Futhermore, cross-talk between CheA and NtrC activated *glnA* transcription from the *glnAp2* promoter has also been reported (65). Our studies showed that, under the conditions we utilized, phenotype of *ntrB* mutant was not identical to that of *ntrC* deletion mutant or NtrC with D56A mutation, suggesting that other factors, besides NtrB, may contribute to NtrC phosphorylation. At present, we do not know which non-cognate HKs or if acetyl phosphate is mediating activation of NtrC and this will be the focus of a future study.

Only a few studies have linked NtrC to biofilm formation in other bacteria. In *P. aeruginosa*, Gallarato et al. revealed that the exopolyphosphatase (Ppx) is involved in biofilm formation and that the gene encoding Ppx is under the

control of two interspaced promoters, dually regulated by nitrogen and phosphate limitation (67). This study showed that *ppx* has two promoters. One is transcribed by RpoN and activated by NtrC, and the other promoter was controlled by sigma-70 and activated by PhoB. Another study showed a link between nitrogen signaling and biofilm formation was carried out in *V. vulnificus*, where NtrC controls biofilm formation by modulating the gene encoding an ADP-glycerol-manno-heptose-6-epimerase, *gmhD*, which is involved with the biosynthesis of an inner core region of the lipopolysaccharide (LPS) (68). *V. vulnificus* mutants lacking *ntrC* produce less biofilm than wild type by crystal violet staining (68). Also, *luxAB* transcriptional fusions with *gmhD* promoter region demonstrated that *gmhD* expression is reduced in *ntrC* deletion mutant, indicating that NtrC positively regulates *gmhD* (69). To our knowledge, our study is first example showing that NtrC is involved in repression of biofilm matrix material. It would be of interest to further characterize how biofilm formation regulated by NtrC under nitrogen limiting conditions.

References

1. **Teschler JK, Zamorano-Sanchez D, Utada AS, Warner CJ, Wong GC, Linington RG, Yildiz FH.** 2015. Living in the matrix: assembly and control of *Vibrio cholerae* biofilms. Nat Rev Microbiol **13:**255-268.

2. **Charles RC, Ryan ET.** 2011. Cholera in the 21st century. Curr Opin Infect Dis **24:**472-477.

3. **Faruque SM, Albert MJ, Mekalanos JJ.** 1998. Epidemiology, genetics, and ecology of toxigenic *Vibrio cholerae*. Microbiol Mol Biol Rev **62:**1301-1314.

4. **Yildiz F, Fong J, Sadovskaya I, Grard T, Vinogradov E.** 2014. Structural characterization of the extracellular polysaccharide from *Vibrio cholerae* O1 El-Tor. PLoS One **9:**e86751.

5. **Yildiz FH, Schoolnik GK.** 1999. *Vibrio cholerae* O1 El Tor: identification of a gene cluster required for the rugose colony type, exopolysaccharide production, chlorine resistance, and biofilm formation. Proc Natl Acad Sci U S A **96:**4028-4033.

6. **Fong JC, Karplus K, Schoolnik GK, Yildiz FH.** 2006. Identification and characterization of RbmA, a novel protein required for the development of rugose colony morphology and biofilm structure in *Vibrio cholerae*. J Bacteriol **188:**1049-1059.

7. **Fong JC, Yildiz FH.** 2007. The *rbmBCDEF* gene cluster modulates development of rugose colony morphology and biofilm formation in *Vibrio cholerae*. J Bacteriol **189:**2319-2330.

8. **Berk V, Fong JC, Dempsey GT, Develioglu ON, Zhuang X, Liphardt J, Yildiz FH, Chu S.** 2012. Molecular architecture and assembly principles of *Vibrio cholerae* biofilms. Science **337:**236-239.

9. **Absalon C, Van Dellen K, Watnick PI.** 2011. A communal bacterial adhesin anchors biofilm and bystander cells to surfaces. PLoS Pathog **7:**e1002210.

10. **Nadell CD, Drescher K, Wingreen NS, Bassler BL.** 2015. Extracellular matrix structure governs invasion resistance in bacterial biofilms. ISME J doi:10.1038/ismej.2014.246.

11. **Zhu J, Mekalanos JJ.** 2003. Quorum sensing-dependent biofilms enhance colonization in *Vibrio cholerae*. Dev Cell **5:**647-656.

12. **Zamorano-Sanchez D, Fong JC, Kilic S, Erill I, Yildiz FH.** 2015. Identification and characterization of VpsR and VpsT binding sites in *Vibrio cholerae*. J Bacteriol **197:**1221-1235.

13. **Wang H, Ayala JC, Silva AJ, Benitez JA.** 2012. The histone-like nucleoid structuring protein (H-NS) is a repressor of *Vibrio cholerae* exopolysaccharide biosynthesis (*vps*) genes. Appl Environ Microbiol **78:**2482-2488.

14. **Casper-Lindley C, Yildiz FH.** 2004. VpsT is a transcriptional regulator required for expression of vps biosynthesis genes and the development of rugose colonial morphology in *Vibrio cholerae* O1 El Tor. J Bacteriol **186:**1574-1578.

15. **Yildiz FH, Dolganov NA, Schoolnik GK.** 2001. VpsR, a Member of the Response Regulators of the Two-Component Regulatory Systems, Is Required for Expression of vps Biosynthesis Genes and EPS(ETr)-Associated Phenotypes in *Vibrio cholerae* O1 El Tor. J Bacteriol **183:**1716-1726.

16. **Beyhan S, Bilecen K, Salama SR, Casper-Lindley C, Yildiz FH.** 2007. Regulation of rugosity and biofilm formation in *Vibrio cholerae*: comparison of VpsT and VpsR regulons and epistasis analysis of *vpsT*, *vpsR*, and *hapR*. J Bacteriol **189:**388-402.

17. **Liang W, Silva AJ, Benitez JA.** 2007. The cyclic AMP receptor protein modulates colonial morphology in *Vibrio cholerae*. Appl Environ Microbiol **73:**7482-7487.

18. **Hammer BK, Bassler BL.** 2003. Quorum sensing controls biofilm formation in *Vibrio cholerae*. Mol Microbiol **50:**101-104.

19. **Yildiz FH, Liu XS, Heydorn A, Schoolnik GK.** 2004. Molecular analysis of rugosity in a Vibrio cholerae O1 El Tor phase variant. Mol Microbiol **53:**497-515.

20. **Gao R, Stock AM.** 2009. Biological insights from structures of two-component proteins. Annu Rev Microbiol **63:**133-154.

21. **Stock AM, Robinson VL, Goudreau PN.** 2000. Two-component signal transduction. Annu Rev Biochem **69:**183-215.

22. **Magasanik B.** 1993. The regulation of nitrogen utilization in enteric bacteria. J Cell Biochem **51:**34-40.

23. **Hirschman J, Wong PK, Sei K, Keener J, Kustu S.** 1985. Products of nitrogen regulatory genes *ntrA* and *ntrC* of enteric bacteria activate *glnA* transcription in vitro: evidence that the *ntrA* product is a sigma factor. Proc Natl Acad Sci U S A **82:**7525-7529.

24. **Hunt TP, Magasanik B.** 1985. Transcription of *glnA* by purified *Escherichia coli* components: core RNA polymerase and the products of *glnF*, *glnG*, and *glnL*. Proc Natl Acad Sci U S A **82:**8453-8457.

25. **van Heeswijk WC, Westerhoff HV, Boogerd FC.** 2013. Nitrogen Assimilation in *Escherichia coli*: Putting Molecular Data into a Systems Perspective. Microbiology and Molecular Biology Reviews **77:**628-695.

26. **Zimmer DP, Soupene E, Lee HL, Wendisch VF, Khodursky AB, Peter BJ, Bender RA, Kustu S.** 2000. Nitrogen regulatory protein C-controlled genes of *Escherichia coli*: scavenging as a defense against nitrogen limitation. Proc Natl Acad Sci U S A **97:**14674-14679.

27. **Zhou L, Lei XH, Bochner BR, Wanner BL.** 2003. Phenotype microarray analysis of *Escherichia coli* K-12 mutants with deletions of all two-component systems. J Bacteriol **185:**4956-4972.

28. **Ninfa AJ, Jiang P.** 2005. PII signal transduction proteins: sensors of alpha-ketoglutarate that regulate nitrogen metabolism. Curr Opin Microbiol **8:**168-173.

29. **Lim B, Beyhan S, Meir J, Yildiz FH.** 2006. Cyclic-diGMP signal transduction systems in *Vibrio cholerae*: modulation of rugosity and biofilm formation. Mol Microbiol **60:**331-348.

30. **Cheng AT, Ottemann KO, Yildiz FH.** 2015. *Vibrio cholerae* response regulator VxrB controls colonization and regulates the Type VI secretion system. PLoS Pathog.

31. **Beyhan S, Tischler AD, Camilli A, Yildiz FH.** 2006. Differences in gene expression between the classical and El Tor biotypes of *Vibrio cholerae* O1. Infect Immun **74:**3633-3642.

32. **Tusher VG, Tibshirani R, Chu G.** 2001. Significance analysis of microarrays applied to the ionizing radiation response. Proc Natl Acad Sci U S A **98:**5116-5121.

33. **Heydorn A, Nielsen AT, Hentzer M, Sternberg C, Givskov M, Ersboll BK, Molin S.** 2000. Quantification of biofilm structures by the novel computer program COMSTAT. Microbiology **146 (Pt 10):**2395-2407.

34. **Herrero M, de Lorenzo V, Timmis KN.** 1990. Transposon vectors containing non-antibiotic resistance selection markers for cloning and stable chromosomal insertion of foreign genes in gram-negative bacteria. J Bacteriol **172:**6557-6567.

35. **de Lorenzo V, Timmis KN.** 1994. Analysis and construction of stable phenotypes in gram-negative bacteria with Tn5- and Tn10-derived minitransposons. Methods Enzymol **235:**386-405.

36. **Shikuma NJ, Yildiz FH.** 2009. Identification and characterization of OscR, a transcriptional regulator involved in osmolarity adaptation in *Vibrio cholerae*. J Bacteriol **191:**4082-4096.

37. **Fong JC, Yildiz FH.** 2008. Interplay between cyclic AMP-cyclic AMP receptor protein and cyclic di-GMP signaling in *Vibrio cholerae* biofilm formation. J Bacteriol **190:**6646-6659.

38. **Hammer BK, Bassler BL.** 2007. Regulatory small RNAs circumvent the conventional quorum sensing pathway in pandemic *Vibrio cholerae*. Proc Natl Acad Sci U S A **104:**11145-11149.

39. **Shikuma NJ, Fong JC, Yildiz FH.** 2012. Cellular levels and binding of c-di-GMP control subcellular localization and activity of the *Vibrio cholerae* transcriptional regulator VpsT. PLoS Pathog **8:**e1002719.

40. **Bao Y, Lies DP, Fu H, Roberts GP.** 1991. An improved Tn7-based system for the single-copy insertion of cloned genes into chromosomes of gram-negative bacteria. Gene **109:**167-168.

41. **Vance RE, Zhu J, Mekalanos JJ.** 2003. A constitutively active variant of the quorum-sensing regulator LuxO affects protease production and biofilm formation in *Vibrio cholerae*. Infect Immun **71:**2571-2576.

42. **Lenz DH, Mok KC, Lilley BN, Kulkarni RV, Wingreen NS, Bassler BL.** 2004. The small RNA chaperone Hfq and multiple small RNAs control quorum sensing in *Vibrio harveyi* and *Vibrio cholerae*. Cell **118:**69-82.

43. **Ng WL, Bassler BL.** 2009. Bacterial quorum-sensing network architectures. Annu Rev Genet **43:**197-222.

44. **Syed KA, Beyhan S, Correa N, Queen J, Liu J, Peng F, Satchell KJ, Yildiz F, Klose KE.** 2009. The *Vibrio cholerae* flagellar regulatory hierarchy controls expression of virulence factors. J Bacteriol **191:**6555-6570.

45. **Tusher VG, Tibshirani R, Chu G.** 2001. Significance analysis of microarrays applied to the ionizing radiation response. Proceedings of the National Academy of Sciences of the United States of America **98:**5116-5121.

46. **Pukatzki S, Ma AT, Revel AT, Sturtevant D, Mekalanos JJ.** 2007. Type VI secretion system translocates a phage tail spike-like protein into target cells where it cross-links actin. Proc Natl Acad Sci U S A **104:**15508-15513.

47. **Basler M, Pilhofer M, Henderson GP, Jensen GJ, Mekalanos JJ.** 2012. Type VI secretion requires a dynamic contractile phage tail-like structure. Nature **483:**182-186.

48. **Kustu SG.** 1974. Mutations Affecting Glutamine-Synthetase Activity in *Salmonella-Typhimurium*. Federation Proceedings **33:**1464-1464.

49. **Pahel G, Rothstein DM, Magasanik B.** 1982. Complex Glna-Glnl-Glng Operon of *Escherichia-Coli*. Journal of Bacteriology **150:**202-213.

50. **McFarland N, McCarter L, Artz S, Kustu S.** 1981. Nitrogen regulatory locus "*glnR*" of enteric bacteria is composed of cistrons *ntrB* and *ntrC*: identification of their protein products. Proc Natl Acad Sci U S A **78:**2135-2139.

51. **Eisenberg D, Gill HS, Pfluegl GM, Rotstein SH.** 2000. Structure-function relationships of glutamine synthetases. Biochim Biophys Acta **1477:**122-145.

52. **Hang S, Purdy AE, Robins WP, Wang Z, Mandal M, Chang S, Mekalanos JJ, Watnick PI.** 2014. The acetate switch of an intestinal pathogen disrupts host insulin signaling and lipid metabolism. Cell Host Microbe **16:**592-604.

53. **Kustu S, Burton D, Garcia E, McCarter L, McFarland N.** 1979. Nitrogen control in *Salmonella*: regulation by the *glnR* and *glnF* gene products. Proc Natl Acad Sci U S A **76:**4576-4580.

54. **Hervas AB, Canosa I, Little R, Dixon R, Santero E.** 2009. NtrC-dependent regulatory network for nitrogen assimilation in *Pseudomonas putida*. J Bacteriol **191:**6123-6135.

55. **Giblin L, Boesten B, Turk S, Hooykaas P, O'Gara F.** 1995. Signal transduction in the *Rhizobium meliloti* dicarboxylic acid transport system. FEMS Microbiol Lett **126:**25-30.

56. **Reid CJ, Poole PS.** 1998. Roles of DctA and DctB in signal detection by the dicarboxylic acid transport system of *Rhizobium leguminosarum*. J Bacteriol **180:**2660-2669.

57. **Yu GQ, Hong JS.** 1986. Identification and nucleotide sequence of the activator gene of the externally induced phosphoglycerate transport system of *Salmonella typhimurium*. Gene **45:**51-57.

58. **Saier MH, Jr., Wentzel DL, Feucht BU, Judice JJ.** 1975. A transport system for phosphoenolpyruvate, 2-phosphoglycerate, and 3-phosphoglycerate in *Salmonella typhimurium*. J Biol Chem **250:**5089-5096.

59. **Lenz DH, Bassler BL.** 2007. The small nucleoid protein Fis is involved in Vibrio cholerae quorum sensing. Mol Microbiol **63:**859-871.

60. **Prouty MG, Correa NE, Klose KE.** 2001. The novel sigma(54)- and sigma(28)-dependent flagellar gene transcription hierarchy of *Vibrio cholerae*. Molecular Microbiology **39:**1595-1609.

61. **Klose KE, Mekalanos JJ.** 1998. Distinct roles of an alternative sigma factor during both free-swimming and colonizing phases of the *Vibrio cholerae* pathogenic cycle. Mol Microbiol **28:**501-520.

62. **Correa NE, Klose KE.** 2005. Characterization of enhancer binding by the *Vibrio cholerae* flagellar regulatory protein FlrC. J Bacteriol **187:**3158-3170.

63. **Correa NE, Lauriano CM, McGee R, Klose KE.** 2000. Phosphorylation of the flagellar regulatory protein FlrC is necessary for *Vibrio cholerae* motility and enhanced colonization. Mol Microbiol **35:**743-755.

64. **Dahl JL, Wei BY, Kadner RJ.** 1997. Protein phosphorylation affects binding of the *Escherichia coli* transcription activator UhpA to the uhpT promoter. J Biol Chem **272:**1910-1919.

65. **Ninfa AJ, Ninfa EG, Lupas AN, Stock A, Magasanik B, Stock J.** 1988. Crosstalk between bacterial chemotaxis signal transduction proteins and regulators of transcription of the Ntr regulon: evidence that nitrogen assimilation and chemotaxis are controlled by a common phosphotransfer mechanism. Proc Natl Acad Sci U S A **85:**5492-5496.

66. **Yamamoto K, Hirao K, Oshima T, Aiba H, Utsumi R, Ishihama A.** 2005. Functional characterization in vitro of all two-component signal transduction systems from *Escherichia coli*. J Biol Chem **280:**1448-1456.

67. **Gallarato LA, Sanchez DG, Olvera L, Primo ED, Garrido MN, Beassoni PR, Morett E, Lisa AT.** 2014. Exopolyphosphatase of *Pseudomonas aeruginosa* is essential for the production of virulence factors, and its expression is controlled by NtrC and PhoB acting at two interspaced promoters. Microbiology **160:**406-417.

68. **Kim HS, Lee MA, Chun SJ, Park SJ, Lee KH.** 2007. Role of NtrC in biofilm formation via controlling expression of the gene encoding an ADP-glycero-manno-heptose-6-epimerase in the pathogenic bacterium, *Vibrio vulnificus*. Mol Microbiol **63:**559-574.

69. **Kim HS, Park SJ, Lee KH.** 2009. Role of NtrC-regulated exopolysaccharides in the biofilm formation and pathogenic interaction of *Vibrio vulnificus*. Mol Microbiol **74:**436-453.

CHAPTER 4: Analysis of *Vibrio cholerae* two-component signal transduction systems for their impact in biofilm formation

Andrew T. Cheng and Fitnat H. Yildiz

Abstract

Vibrio cholerae, the causative agent of cholera, is a facultative human pathogen that grows rapidly within the human intestine and survives for prolonged periods in aquatic habitats. The biofilm growth mode is important in both the intestinal and transmission phases of *V. cholerae*'s life cycle. The ability to sense and respond to the variety of environmental factors inside and outside of the host is commonly regulated by two-component signal transduction systems (TCS). In this work, we successfully constructed in-frame deletion mutants in each of the response regulator (RR) genes. These RR mutants were examined for roles in biofilm formation using a flow-cell system and examined for *vps*, required for production of major biofilm matrix component *Vibrio* polysaccharide, gene expression. This study revealed that deletion of two RRs (VC1348 and VxrB) resulted in decreases in biofilm formation. In addition, we showed that VxrB enhances production of biofilms and expression of *vps* genes and that, the regulation of *vps* genes by VxrB may be controlled by the major transcriptional regulators of biofilm formation, VpsR and VpsT. Finally, transcriptome analysis of Δ*vxrB* showed that genes encoding *vps*, biofilm matrix proteins, and type VI secretion system were positively regulated by VxrB.

Introduction

Vibrio cholerae is the causative agent of the diarrheal disease, cholera. In its natural aquatic environment, *V. cholerae* can be found either as free-swimming planktonic cells or as biofilm-associated cells attached to surfaces (1, 2). *V. cholerae* forms biofilms during the aquatic and intestinal phases of its life cycle (3-5). Biofilms can be defined as surface attached cell aggregates surrounded by an extracellular matrix, typically composed of exopolymeric substances such as exopolysaccahrides, proteins, nucleic acids and lipids (6).

In *V. cholerae*, biofilm formation is controlled by a complex regulatory network and is dependent on the production of biofilm matrix that facilitate cell-cell and cell-surface interactions (7-12) (for most recent review, see (6)). Recent studies have identified the molecular mechanism of these proteins in biofilm development (13-15). To form biofilms, *V. cholerae* produces an extracellular matrix composed of proteins, nucleic acids, and a glycoconjugate, termed *Vibrio* polysaccharide (VPS). VPS is a major portion of the biofilm matrix (7, 9). The polysaccharide portion of VPS has been structurally characterized and has the following structure:-4)-α-GulpNAcAGly3OAc-(1-4)-β-D-Glcp-(1-4)-α-Glcp-(1-4)-α-D-Galp-(1- where α-D-Glc is partially (~20%) replaced with α-D-GlcNAc. α-GulNAcAGly is an amide between 2-acetamido-2-deoxy-α-guluronic acid and glycine (16). The VPS biosynthesis genes are found in two

clusters on the large chromosome of *V. cholerae* O1 El Tor [*vps*U (VC0916), *vpsA-K*, VC0917-27 (*vps*-I cluster); *vpsL-Q*, VC0934-9 (*vps*-II cluster)] (9). Matrix proteins are another essential component of biofilm formation in *V. cholerae*. In particular, RbmA, RbmC, and Bap1 are required for maintaining the structural integrity of biofilms (8, 10). It was recently discovered that RbmA provided cell-cell adhesion; Bap1 allows the developing biofilm to adhere to the surface; RbmC is excreted and contributes to the biofilm components that envelope around the cell along with VPS and Bap1 (13). Together, these major components serve a critical role in the development of a mature biofilm structure. Although important regulators of biofilm formation and their genetic interactions have been examined, little is known regarding the mechanisms by which environmental signals are integrated into the biofilm regulatory network.

Pathogenic bacteria experience varying conditions during infection of human hosts and during growth outside of human host. Bacteria typically use two-component signal transduction systems (TCSs) to sense and respond to different environmental stimuli, such as nutrient availability, pH, bile, osmolarity, and host factors (17-21). The prototypical two-component signal transduction system (TCS) consists of a membrane-bound histidine kinase (HK), which sense environmental signals and functions as a dimer to autophosphorylate at a conserved histidine residue, and a corresponding

response regulator (RR), which catalyzes the transfer of phosphate from the cognate HK to a conserved aspartate residue within the same pathway (22-24). Ultimately, the RR changes its activity based on the phosphorylation state to illicit a cellular response. Typically, RRs contain two functional domains, a REC domain that receives the phosphoryl group and an effector domain, which is typically a DNA binding domain.

The *V. cholerae* genome reference genome of O1 EL Tor N16961 strain is predicted to encode 43 HK and 49 RR (http://www.ncbi.nlm.nih.gov/Complete_Genomes/RRcensus.html and http://www.p2cs.org). Further analysis of the genome for REC domains identified 3 additional RRs (VpsT, VpsR, and VC0396). Thus it is predicted that *V. cholerae* O1 EL Tor N16961 genome encodes for 53 putative RRs. Only 8 RR (*vpsR*, *phoB*, *luxO*, *varA*, *carR*, VC1348, VCA0210, and *vpsT*) have previously been shown to affect biofilm formation by either deletion analysis or overexpression analysis. VpsR and VpsT have been identified to be major positive regulators of biofilm formation (25, 26). PhoB represses biofilm formation and activates motility indirectly through the regulation of c-di-GMP enzymes AcgA and AcgB (27). LuxO positively regulates expression of small regulatory RNAs which in turn represses translation of HapR, the master quorum sensing regulator and repressor of biofilm formation (28, 29). VarA modulates the translation of HapR through a pathway that involves the

regulatory small RNAs CsrBCD that interfere with LuxO-mediated activation of Qrr sRNAs, which as a result affects biofilm formation (30, 31). CarR acts in parallel pathways with HapR and CRP-cAMP to repress biofilm formation and confers polymyxin B resistance by positively regulating expression of genes involved in lipid A modification (19, 32). Finally, VC1348 and VCA0210 are RR that contain HD-GYP domains that degrade c-di-GMP. Biofilm formation decreases when VC1348 and VCA0210 are overexpressed (33).

Since there is little information regarding the role of RRs in biofilm formation in *V. cholerae*, this study systematically analyzed each RR for their role in biofilm formation. This will help eventually to understand which environmental cues control biofilm formation. We determined that VxrB positively regulates biofilm formation and *vpsL*, *vpsR* and *vpsT* gene expression. Transcriptome analysis of Δ*vxrB* showed that the genes encoding *vps* biosynthesis and matrix proteins were down-regulated in comparison to wild type. Interestingly, genes encoding for type VI secretion systems were also down-regulated by VxrB, suggesting that expression of biofilm genes and Type VI secretion system genes are co-regulated.

Materials and Methods

Bacterial strains, plasmids, and culture conditions. The bacterial strains and plasmids used in this study are listed in Table 4.1. *Escherichia coli*

CC118λpir strains were used for DNA manipulation, and *E. coli* S17-1λpir strains were used for conjugation with *V. cholerae*. In-frame deletion mutants of *V. cholerae* were generated as described earlier (34). All *V. cholerae* and *E. coli* strains were grown aerobically, at 30°C and 37°C, respectively, unless otherwise noted. All cultures were grown in Luria-Bertani (LB) broth (1% Tryptone, 0.5% Yeast Extract, 1% NaCl), pH 7.5, unless otherwise stated. LB agar medium contains 1.5% (wt/vol) granulated agar (BD Difco, Franklin Lakes, NJ). Concentrations of antibiotics used were as follow: ampicillin 100 µg/ml; rifampicin 100 µg/ml; chloramphenicol 5 µg/ml for *V. cholerae* and 20 µg/ml for *E. coli*; and gentamicin 50 µg/ml.

DNA manipulations. An overlapping PCR method was used to generate in-frame deletion constructs of each RR genes using previously published methods (34). Briefly, a 500-600 bp 5' flanking sequence of the gene, including several nucleotides of the coding region, was PCR amplified using del-A and del-B primers. del-C and del-D primers were used to amplify the 3' region of the gene including 500-600 bp of the downstream flanking sequence. The two PCR products were joined using the splicing overlap extension technique (10, 35) and the resulting PCR product, which lacks gene sequences encoding approximately 80% of amino acids, was digested with two restriction enzymes and ligated to similarly-digested pGP704*sacB*28 suicide plasmid. Construction of *vtrB* plasmid harboring point mutations were performed using a similar technique (36) with the following alterations:

primers containing the new sequence harboring the point mutations were used in place of the del-B and del-C primers. The deletion constructs were sequenced (UC Berkeley DNA Sequencing Facility, Berkeley, CA) and the clones without any undesired mutations were used.

Generation of in-frame deletion mutants and *gfp*-tagged strains. The deletion plasmids were maintained in *E. coli* CC118λpir. Biparental matings were carried out with the wild type *V. cholerae* and an *E. coli* S17λpir strain harboring the deletion plasmid. Selection of deletion mutants were done as described (10) and were verified by PCR. *V. cholerae* wild-type and mutant strains were tagged with the green fluorescent protein gene (*gfp*) according to a previously described procedure (8). The *gfp*-tagged *V. cholerae* strains were verified by PCR and examined in flow cell experiments.

Luminescence assay. Overnight cultures of *V. cholerae* cells were diluted 1:1000 in appropriate medium containing chloramphenicol (5 μg/ml). Then, cells were grown aerobically at 30°C to mid-exponential phase (OD_{600} of 0.3-0.4) and harvested for luminescence reading. Luminescence was read using a Perkin Elmer Victor3 Multi-label Counter (PerkinElmer) and is reported as counts min^{-1} ml^{-1}/ OD_{600}. Lux expression is reported as relative light units (RLU). Assays were repeated with three biological replicates. Four technical replicates were measured for all assays. Statistical analysis was performed using two-tailed student's t test.

β-Galactosidase assays. β-Galactosidase assays were performed using exponentially grown cultures by first growing *V. cholerae* overnight (18 to 20 h) aerobically in LB medium. The cells were then diluted 1:1000 in fresh LB medium and grown aerobically to an OD_{600} of 0.3 to 0.4 and immediately harvested for the assay. β-Galactosidase assays with cells harboring pBAD plasmids were carried out with overnight cultures grown in the absence of arabinose that were diluted 1:1000 in fresh media with and without 0.2% arabinose. Assays were then performed using TROPIX Kit (Applied Biosystems) according to manufacturer's instructions. Briefly, 10 µl culture lysate was mixed with 70 µl of Galacto reaction buffer diluent containing 1x Galacton Plus and incubated in the dark for 1 h. 100 µl Accelerator II was added and luminescence was immediately measured using a Victor3 Multi-label Counter (PerkinElmer) and lux values were obtained with reading for 0.1 second per well. Each samples were prepared for at least six technical replicates and at least two biological replicates.

Flow cell experiments and confocal scanning laser microscopy (CSLM). Flow cells were inoculated by normalizing overnight-grown cultures of *gfp*-tagged *V. cholerae* strains to an OD600 of 0.02 and injecting cells into an Ibidi m-Slide VI0.4 (Ibidi 80601 ; Ibidi LLC, Verona, WI). After inoculation the bacteria were allowed to adhere at room temperature for 1 h with no flow. Then, flow of 2% (vol/vol) LB (0.2 g/liter trypone, 0.1 g/liter yeast extract, 1% NaCl) was initiated at a rate of 7.5 ml/h and continued for up to 48 h. CLSM

images of the biofilms were captured with an LSM 5 PASCAL system (Zeiss) using an excitation wavelength of 488 nm and an emission wavelength of 543 nm. Three-dimensional images of the biofilms were reconstructed using Imaris software (Bitplane) and quantified using COMSTAT (37).

RNA isolation. Overnight cultures of *V. cholerae* cells were diluted 1:200 in fresh LB medium and grown aerobically at 30°C to mid-exponential phase. To obtain a homogenous population of exponential-phase cells, mid-exponential phase cultures were diluted 1:200 once more in fresh LB medium and grown aerobically at 30°C to mid-exponential phase (OD_{600} of 0.3 to 0.4). Two milliliter (ml) aliquots were collected and centrifuged for 2 minutes at room temperature. The cell pellets were immediately resuspended in 1 ml of TRIzol (Invitrogen, Carlsbad, CA) and stored at -80°C. Total RNA was isolated according to the manufacturer's instructions. To remove contaminating DNA, total RNA was incubated with RNase-free DNase I (Ambion, Grand Island, NY), and an RNeasy mini kit (Qiagen, Valencia, CA) was used to clean up RNA after DNase digestion. Five micrograms of total RNA was treated with a MICROBExpress Kit (Ambion, Grand Island, NY) to remove ribosomal RNA, and the efficiency was confirmed by Bioanalyzer analysis (Agilent Technologies, Santa Clara, CA). Three biological replicates were generated for each condition.

cDNA library construction and Illumina HiSeq sequencing. Libraries for RNA-seq were prepared using NEBNext Ultra Directional RNA Library Prep

Kit for Illumina (New England Biolabs, Ipswich, MA). Twelve indexed samples were sequenced per single lane using the HiSeq2500 Illumina sequencing platform for 50 bp single reads (UC Davis Genome Center, UC Davis, CA) and subsequently analyzed and visualized via the CLC Genomics Workbench version 7.5 (Qiagen, Valencia, CA). Samples were mapped to the *V. cholerae* genome N16961. Differentially regulated genes were identified as those displaying a fold change with an absolute value of 1.5-fold or greater. Statistical significance was determined by Empirical analysis of Digital Gene Expression (edgeR) test where $p<0.05$ was deemed significant (38).

Table 4.1. Bacterial strains and plasmids used in this study.

Strain or plasmid	Relevant genotype	Source
E. coli strains		
CC118λ*pir*	Δ(*ara-leu*) *araD* Δ*lacX74 galE galK phoA20 thi-1 rpsE rpoB argE*(*Am*) *recA1* λ*pir*	(39)
S17-1λ*pir*	Tp^r Sm^r *recA thi pro* r_K^- m_K^+ RP4::2-Tc::MuKm Tn*7* λ*pir*	(40)
MC4100	F$^-$ *araD139* Δ(*argF-lac*)U169 *rpsL150*(*str*^{r}) *relA1 deoC1 rbsR fthD5301 fruA25* λ$^-$	Ottemann lab
V. cholerae strains		
FY_VC_0001	*Vibrio cholerae* O1 El Tor A1552, wild type, Rif^r	(41)
FY_VC_0237	FY_VC_0001 mTn7-gfp, Rif^r, Gm^r	(42)
FY_VC_0616	*vpsLp-lacZ*, Rif^r	(43)
FY_VC_8327	ΔVC0396 (*qstR*)	This study
FY_VC_2272	ΔVC0665 (*vpsR*)	(25)
FY_VC_8197	ΔVC0693	(44)
FY_VC_8162	ΔVC0719 (*phoB*)	(44)
FY_VC_8074	ΔVC0790	(44)
FY_VC_0192	ΔVC1021 (*luxO*)	(44)
FY_VC_8480	ΔVC1050	(44)
FY_VC_8329	ΔVC1081	(44)
FY_VC_8180	ΔVC1082	(44)
FY_VC_1936	ΔVC1086	(44)
FY_VC_2760	ΔVC1087	(44)
FY_VC_0692	ΔVC1155	(44)
FY_VC_8474	ΔVC1213 (*varA*)	(44)
FY_VC_4379	ΔVC1277	(44)
FY_VC_3282	ΔVC1320 (*carR*)	(19)
FY_VC_8331	ΔVC1348	(44)
FY_VC_7998	ΔVC1522	(44)
FY_VC_8482	ΔVC1604	(44)
FY_VC_8164	ΔVC1638	(44)
FY_VC_8706	ΔVC1651 (*vieB*)	(44)
FY_VC_0516	ΔVC1652 (*vieA*)	(45)
FY_VC_8166	ΔVC1719 (*torR*)	(44)
FY_VC_8243	ΔVC1926 (*dct-D1*)	(44)
FY_VC_6286	ΔVC2135 (*flrC*)	(44)
FY_VC_6284	ΔVC2135 (*flrA*)	This study
FY_VC_8756	ΔVC2692 (*cpxR*)	(44)
FY_VC_8708	ΔVC2702 (*cbrR*)	(44)

FY_VC_8179	ΔVC2714 (*ompR*)	(44)
FY_VC_6289	ΔVC2749 (*ntrC*)	(44)
FY_VC_8245	ΔVCA0142 (*dct-D2*)	(44)
FY_VC_2315	ΔVCA0210	(44)
FY_VC_8194	ΔVCA0239	(44)
FY_VC_8148	ΔVCA0256	(44)
FY_VC_8150	ΔVCA0532	(44)
FY_VC_9332	ΔVCA0565 (*vxrA*)	(44)
FY_VC_8758	ΔVCA0566 (*vxrB*)	(44)
FY_VC_8478	ΔVCA0682 (*uhpA*)	(44)
FY_VC_7969	ΔVCA0704 (*pgtA*)	(44)
FY_VC_8209	ΔVCA0850	(44)
FY_VC_0099	ΔVCA0952 (*vpsT*)	(26)
FY_VC_8841	ΔVCA1086	(44)
FY_VC_8154	ΔVCA1105	(44)
FY_VC_8351	Δ*qstR* mTn*7*-*gfp*, Rif^r, Gm^r	This study
FY_VC_2407	Δ*vpsR* mTn*7*-*gfp*, Rif^r, Gm^r	This study
FY_VC_8203	ΔVC0693 mTn*7*-*gfp*, Rif^r, Gm^r	This study
FY_VC_8186	Δ*phoB* mTn*7*-*gfp*, Rif^r, Gm^r	This study
FY_VC_8142	ΔVC0790 mTn*7*-*gfp*, Rif^r, Gm^r	This study
FY_VC_8068	Δ*luxO* mTn*7*-*gfp*, Rif^r, Gm^r	This study
FY_VC_8667	ΔVC1050 mTn*7*-*gfp*, Rif^r, Gm^r	This study
FY_VC_8669	ΔVC1081 mTn*7*-*gfp*, Rif^r, Gm^r	This study
FY_VC_8205	ΔVC1082 mTn*7*-*gfp*, Rif^r, Gm^r	This study
FY_VC_1821	ΔVC1086 mTn*7*-*gfp*, Rif^r, Gm^r	This study
FY_VC_8671	ΔVC1087 mTn*7*-*gfp*, Rif^r, Gm^r	This study
FY_VC_1327	ΔVC1155 mTn*7*-*gfp*, Rif^r, Gm^r	This study
FY_VC_8673	Δ*varA* mTn*7*-*gfp*, Rif^r, Gm^r	This study
FY_VC_8158	ΔVC1277 mTn*7*-*gfp*, Rif^r, Gm^r	This study
FY_VC_3283	Δ*carR* mTn*7*-*gfp*, Rif^r, Gm^r	(19)
FY_VC_8349	ΔVC1348 mTn*7*-*gfp*, Rif^r, Gm^r	This study
FY_VC_8070	ΔVC1522 mTn*7*-*gfp*, Rif^r, Gm^r	This study
FY_VC_8713	ΔVC1604 mTn*7*-*gfp*, Rif^r, Gm^r	This study
FY_VC_8188	ΔVC1638 mTn*7*-*gfp*, Rif^r, Gm^r	This study
FY_VC_8751	Δ*vieB* mTn*7*-*gfp*, Rif^r, Gm^r	This study
FY_VC_8715	Δ*vieA* mTn*7*-*gfp*, Rif^r, Gm^r	This study
FY_VC_8190	Δ*torR* mTn*7*-*gfp*, Rif^r, Gm^r	This study
FY_VC_8319	Δ*dctD-1* mTn*7*-*gfp*, Rif^r, Gm^r	This study
FY_VC_8072	Δ*flrC* mTn*7*-*gfp*, Rif^r, Gm^r	This study
FY_VC_9968	Δ*flrA* mTn*7*-*gfp*, Rif^r, Gm^r	This study
FY_VC_8762	Δ*cpxR* mTn*7*-*gfp*, Rif^r, Gm^r	This study

FY_VC_8749	Δ*cbrR* mTn7-*gfp*, Rif^r, Gm^r	This study
FY_VC_8361	Δ*ompR* mTn7-*gfp*, Rif^r, Gm^r	This study
FY_VC_7061	Δ*ntrC* mTn7-*gfp*, Rif^r, Gm^r	This study
FY_VC_8321	Δ*dctD-2* mTn7-*gfp*, Rif^r, Gm^r	This study
FY_VC_8359	ΔVCA0210 mTn7-*gfp*, Rif^r, Gm^r	This study
FY_VC_8201	ΔVCA0239 mTn7-*gfp*, Rif^r, Gm^r	This study
FY_VC_8168	ΔVCA0256 mTn7-*gfp*, Rif^r, Gm^r	This study
FY_VC_8170	ΔVCA0532 mTn7-*gfp*, Rif^r, Gm^r	This study
FY_VC_8764	Δ*vxrB* mTn7-*gfp*, Rif^r, Gm^r	This study
FY_VC_8719	Δ*uhpA* mTn7-*gfp*, Rif^r, Gm^r	This study
FY_VC_8064	Δ*pgtA* mTn7-*gfp*, Rif^r, Gm^r	This study
FY_VC_9923	ΔVCA0850 mTn7-*gfp*, Rif^r, Gm^r	This study
FY_VC_1739	Δ*vpsT* mTn7-*gfp*, Rif^r, Gm^r	This study
FY_VC_8835	ΔVCA1086 mTn7-*gfp*, Rif^r, Gm^r	This study
FY_VC_8174	ΔVCA1105 mTn7-*gfp*, Rif^r, Gm^r	This study
FY_VC_9217	*vpsLp-lacZ* Δ*vxrB*, Rif^r	This study
FY_VC_9234	Δ*vpsR*Δ*vxrB*, Rif^r	This study
FY_VC_9237	Δ*vpsT*Δ*vxrB*, Rif^r	This study
Plasmids		
pGP704*sacB*28	pGP704 derivative, *mob*/*oriT sacB*, Ap^r	(26)
pUX-BF13	oriR6K helper plasmid, mob/oriT, provides the Tn7 transposition function in trans, Ap^r	(46)
pMCM11	pGP704::mTn*7*-*gfp*, Gm^r Ap^r	M. Miller and G. Schoolnik
pBBRlux	*luxCDABE*-based promoter fusion vector, Cm^r	(47)
pFY-0950	pBBRlux *vpsL* promoter, Cm^r	(48)
pFY-0989	pBBRlux *vpsR* promoter, Cm^r	This study
pFY-0988	pBBRlux *vpsT* promoter, Cm^r	This study
pBAD/myc-His-B	Arabinose-inducible expression vector with C-terminal myc epitope and six-His tags	Invitrogen
pFY-2074	pBAD/*myc*-His-B::*vxrB*, Ap^r	This study

Results

Multiple RRs impact *vps* gene expression and biofilm formation.

There is a limited understanding of the *V. cholerae* TCSs and their role in biofilm formation. To better understand how 53 TCS RRs affect biofilm formation in *V. cholerae*, we generated in-frame deletion mutants in the 41 that we do not yet know how they affect *vps* promoter activity. For this analysis, we excluded 12 RR that were either predicted to be involved in chemotaxis (11 CheY, CheV, and CheB proteins) and that we were unable to mutate (VC2368, ArcA) (49, 50). To identify the specific RR that contributes to *vps* expression, we measured promoter activity of the *vps* genes using a luciferase transcriptional reporter *vpsLp-lux* in wild type *V. cholerae* and 41 strains containing in-frame deletions. In *V. cholerae*, *vpsL* is the first gene in the *vps*-II cluster, which together with the *vps*-I cluster genes, encode proteins that are required for VPS production and biofilm formation. *vpsL* promoter activity was measured at exponential phase (OD_{600} of 0.3) where *vps* expression is at the highest due to the lack of quorum sensing signals. A total of 7 RR mutants had a statistically significant difference and exhibited minimum 2-fold change in *vpsL* promoter activity compared to wild type (Fig 4.1A). We further confirmed that the 7 RR deletion mutants had altered *vpsL* expression relative to that of the wild type (Fig 4.1B). Consistent with previous studies, we identified that ΔVC0665 (*vpsR*), ΔVC1021 (*luxO*), ΔVC1213 (*varA*), and ΔVCA0952 (*vpsT*) had decreased *vpsL* promoter activity 122-fold,

81-fold, 47-fold, and 11 fold, respectively. We also identified that ΔVC1320 (*carR*) and ΔVC2749 (*ntrC*) had increased *vpsL* promoter activity 4-fold and 3-fold, respectively. Interestingly, we observed that ΔVCA0566 (*vxrB*) had a decrease (11-fold) in *vpsL* promoter activity (Figure 4.1B). Recently, we reported that VxrB regulates type VI secretion system and is involved in colonization of *V. cholerae* in the infant mouse model (44).

Figure 4.1

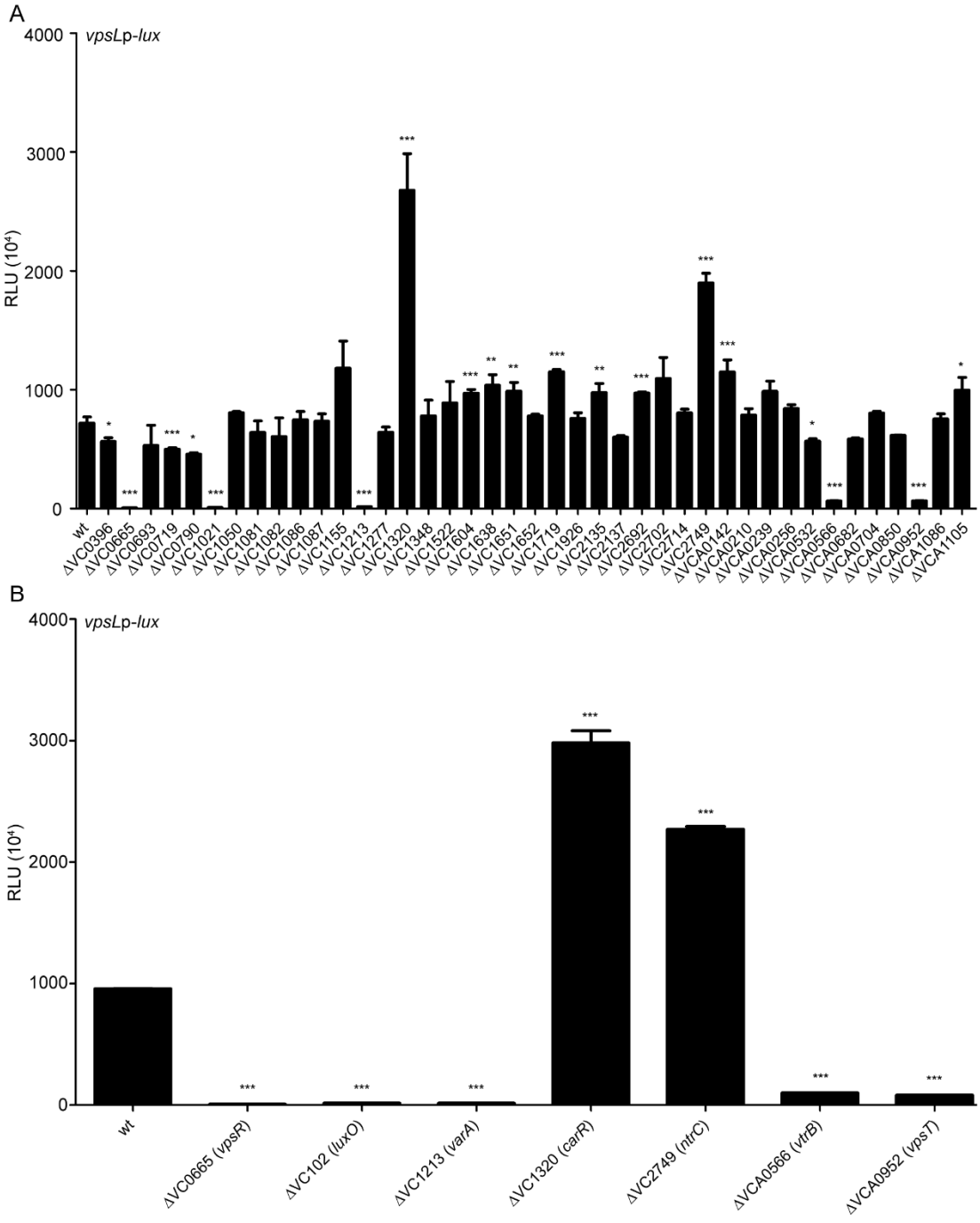
A
vpsLp-lux
RLU (10⁴)
4000
3000
2000
1000
0
wt
ΔVC0396
ΔVC0665
ΔVC0693
ΔVC0719
ΔVC0790
ΔVC1021
ΔVC1050
ΔVC1081
ΔVC1082
ΔVC1086
ΔVC1087
ΔVC1155
ΔVC1213
ΔVC1277
ΔVC1320
ΔVC1348
ΔVC1522
ΔVC1604
ΔVC1638
ΔVC1651
ΔVC1652
ΔVC1719
ΔVC1926
ΔVC2135
ΔVC2137
ΔVC2692
ΔVC2702
ΔVC2714
ΔVC2749
ΔVCA0142
ΔVCA0210
ΔVCA0239
ΔVCA0256
ΔVCA0532
ΔVCA0566
ΔVCA0682
ΔVCA0704
ΔVCA0850
ΔVCA0952
ΔVCA1086
ΔVCA1105
B
vpsLp-lux
RLU (10⁴)
4000
3000
2000
1000
0
wt
ΔVC0665 (vpsR)
ΔVC102 (luxO)
ΔVC1213 (varA)
ΔVC1320 (carR)
ΔVC2749 (ntrC)
ΔVCA0566 (vtrB)
ΔVCA0952 (vpsT)

Figure 4.1. Analysis of *vpsL* expression in RR deletion mutants. (A) Expression of P_{vpsL}-*luxCADBE* (pFY_0950) in 41 ΔRR mutants. (B) Expression of P_{vpsL}-*luxCADBE* (pFY_0950) in Δ*vpsR*, Δ*luxO*, Δ*varA*, Δ*carR*, Δ*ntrC*, Δ*vxrB*, and Δ*vpsT*. The graph represents the average and standard deviation of relative light units (RLU) obtained from four technical replicates from three independent biological samples. RLU is reported in luminescence counts min^{-1} ml^{-1}/OD_{600}. A two-tailed unpaired t-test was used to compare the expression between wt and deletion mutants. * $p< 0.05$, ** $p< 0.01$, *** $p< 0.001$.

To further understand the role of RR in biofilm formation, the 41 deletion mutants were *gfp* labeled and their biofilm forming ability was analyzed using a biofilm flow-cell system. Biofilm images of were captured 48 hours post-inoculation and those images were quantified using COMSTAT analysis (37). Due to the large quantity of deletion mutants to test, we compared a maximum of 5 ΔRR against wild type in a given experimental set-up. We note that there is a variability in biofilms formed by the wild type, in different experiments. Thus, biofilm forming ability of each mutant was compared to biofilm forming ability of wild type control in a given experiment. After screening through 41 deletion mutants, we observed that 8 RR mutants (Δ*ntrC*, Δ*vxrB*, ΔVC1348, Δ*flrC*, Δ*vpsR*, Δ*luxO*, Δ*vpsT*, Δ*flrA*) produced biofilms different than wild-type biofilms (Figs 4.2A-4.2J and Tables 4.2A-4.2J).

Figure 4.2A

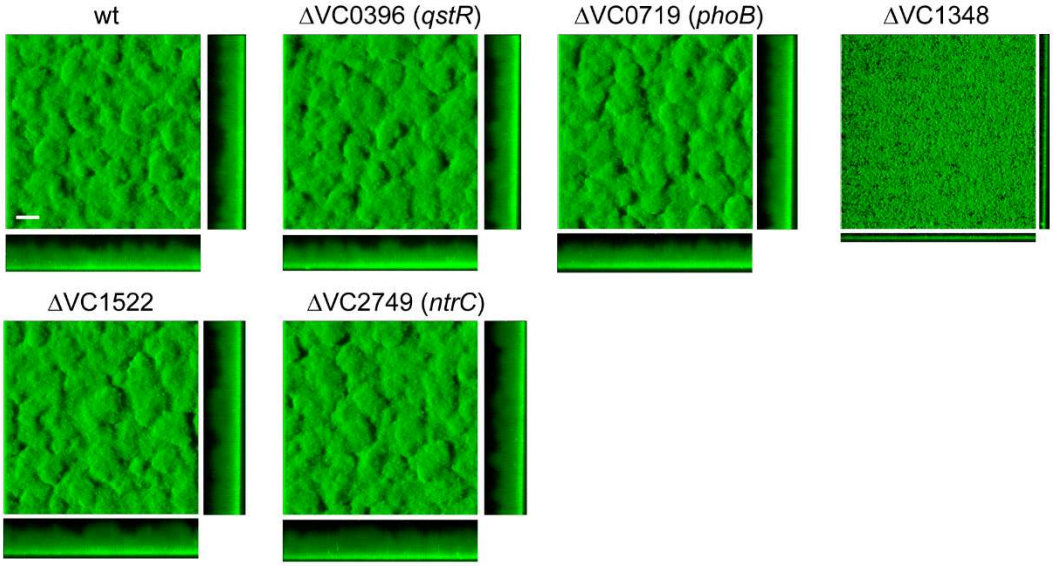

Table 4.2A. COMSTAT analysis of biofilms of wild type and ΔRR strains[a]

Strain	Biomass (μm^3)	Average thickness (μm)	Maximum thickness (μm)
wt	25.77 (0.87)	27.46 (1.45)	41.07 (3.97)
Δ*qstR*	25.32 (2.50)	26.67 (1.13)	38.72 (0.88)
Δ*phoB*	24.18 (0.96)	26.64 (0.74)	39.60 (0.00)
ΔVC1348	2.86 (0.10)	4.85 (0.37)	8.21 (0.51)
ΔVC1522	25.63 (0.99)	26.72 (1.42)	39.89 (0.51)
Δ*ntrC*	32.42 (3.15)	33.62 (1.49)	41.95 (2.03)

[a]The values are the means (standard deviations) of data from six z-series image stacks

Figure 4.2A. Analysis of biofilm formation in RR deletion mutants. Three dimensional biofilm structures of *gfp* tagged wild-type *V. cholerae*, ΔVC0396 (*qstR*), ΔVC0719 (*phoB*), ΔVC1348, ΔVC1522, ΔVC749 (*ntrC*) after 48 hours of incubation in flow-cell chambers. Images of horizontal (xy) and vertical (xz) projections of biofilms are shown. The results shown are from one representative experiment of two independent experiments. Scale bars = 30 μm.

Figure 4.2B

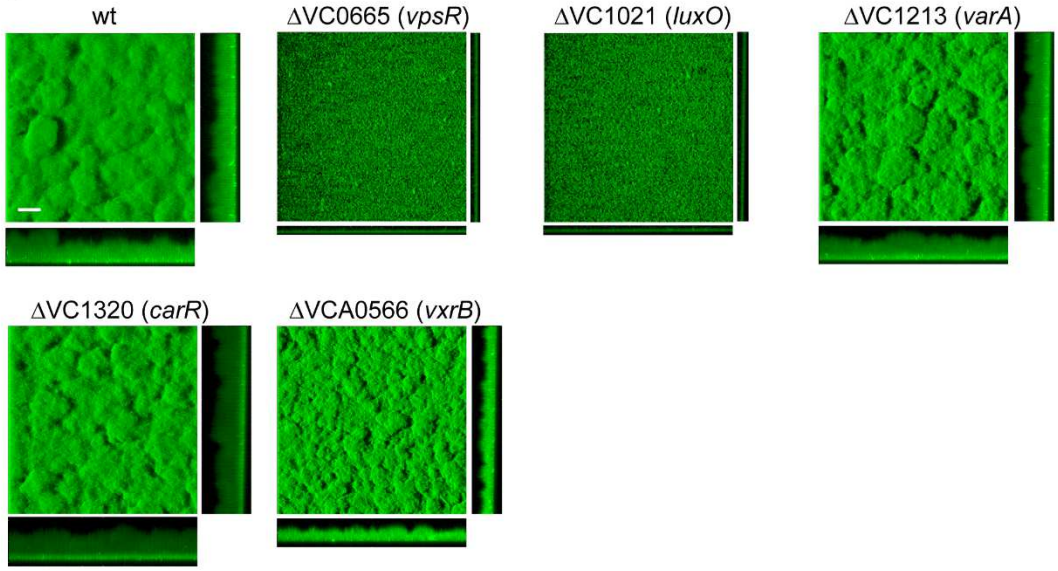

Table 4.2B. COMSTAT analysis of biofilms of wild type and ΔRR strains[a]

Strain	Biomass (μm^3)	Average thickness (μm)	Maximum thickness (μm)
wt	24.37 (0.90)	26.78 (1.39)	41.07 (4.16)
Δ*vpsR*	2.37 (0.21)	3.58 (0.57)	7.63 (1.02)
Δ*luxO*	2.51 (0.06)	4.63 (0.72)	8.80 (0.88)
Δ*varA*	23.12 (2.78)	26.75 (2.49)	40.19 (2.69)
Δ*carR*	22.80 (2.03)	29.85 (1.69)	45.76 (0.88)
Δ*vxrB*	12.52 (0.27)	16.68 (1.05)	29.63 (1.02)

[a]The values are the means (standard deviations) of data from six z-series image stacks

Figure 4.2B. Analysis of biofilm formation in RR deletion mutants. Three dimensional biofilm structures of *gfp* tagged wild-type *V. cholerae*, ΔVC0665 (*vpsR*), ΔVC1021 (*luxO*), ΔVC1213 (*varA*), ΔVC1320 (*carR*), ΔVCA0566 (*vxrB*) after 48 hours of incubation in flow-cell chambers. Images of horizontal (xy) and vertical (xz) projections of biofilms are shown. The results shown are from one representative experiment of two independent experiments. Scale bars = 30 μm.

Figure 4.2C

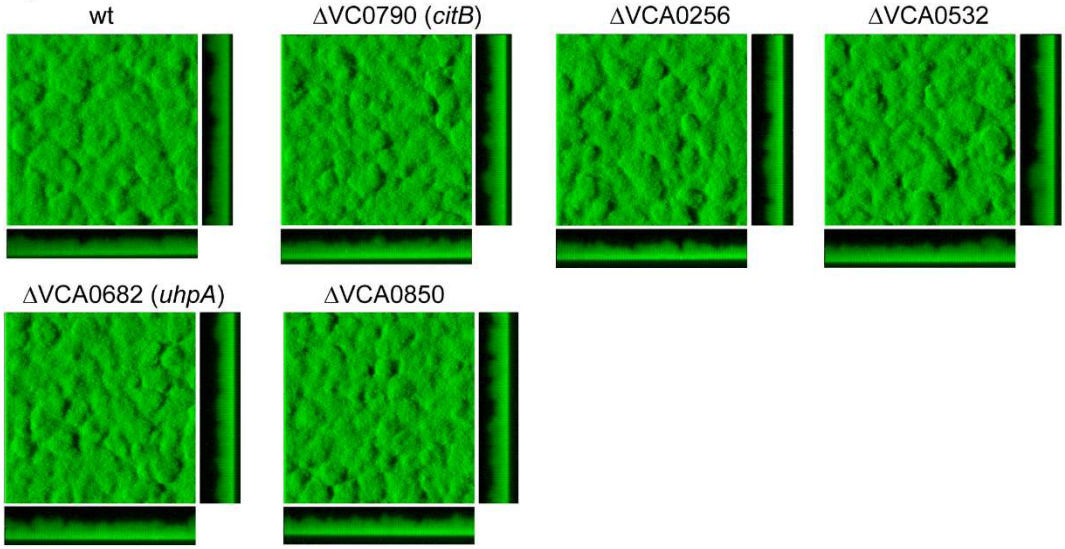

Table 4.2C. COMSTAT analysis of biofilms of wild type and ΔRR strains[a]

Strain	Biomass (μm^3)	Average thickness (μm)	Maximum thickness (μm)
wt	20.99 (0.74)	22.01 (0.55)	29.63 (1.34)
Δ*citB*	22.14 (0.31)	22.74 (0.27)	30.21 (0.51)
ΔVCA0256	20.46 (0.22)	21.25 (0.61)	30.21 (1.02)
ΔVCA0532	21.10 (0.46)	21.44 (0.61)	30.21 (0.51)
Δ*uhpA*	21.33 (0.56)	21.65 (0.73)	29.63 (1.34)
ΔVCA0850	21.16 (0.38)	21.71 (0.85)	30.21 (0.51)

[a]The values are the means (standard deviations) of data from six z-series image stacks

Figure 4.2C. Analysis of biofilm formation in RR deletion mutants. Three dimensional biofilm structures of *gfp* tagged wild-type *V. cholerae*, ΔVC0790 (*citB*), ΔVCA0256, ΔVCA0532, ΔVCA0682 (*uhpA*), ΔVCA0850 after 48 hours of incubation in flow-cell chambers. Images of horizontal (xy) and vertical (xz) projections of biofilms are shown. The results shown are from one representative experiment of two independent experiments. Scale bars = 30 μm.

Figure 4.2D

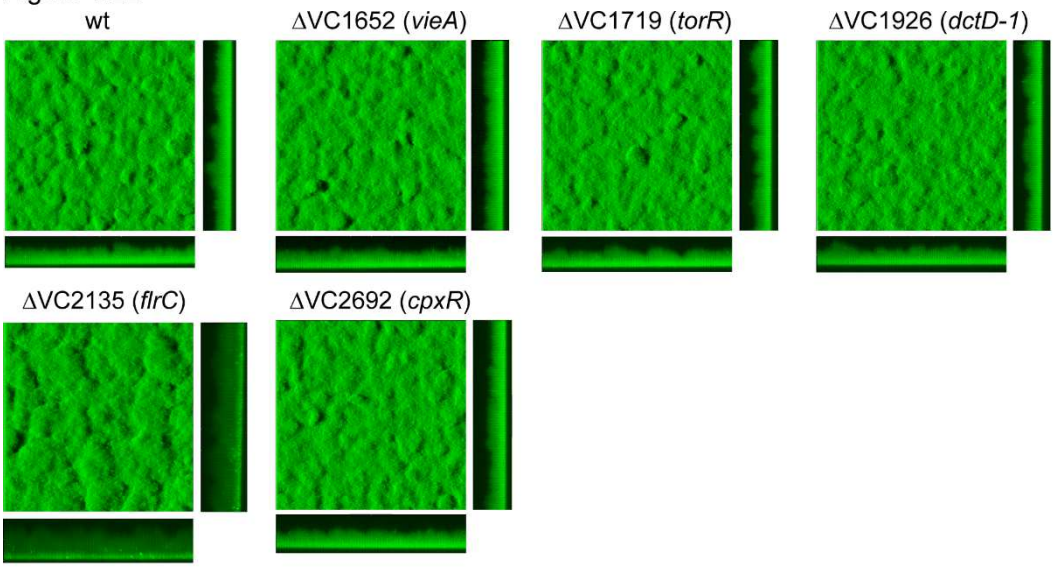

Table 4.2D. COMSTAT analysis of biofilms of wild type and ΔRR strains[a]

Strain	Biomass (μm^3)	Average thickness (μm)	Maximum thickness (μm)
wt	24.01 (0.49)	24.97 (1.00)	41.71 (2.03)
Δ*vieA*	23.56 (0.35)	24.78 (0.40)	41.41 (0.51)
Δ*torR*	22.44 (0.28)	22.93 (0.37)	39.07 (0.51)
Δ*dctD-1*	22.66 (0.22)	22.35 (0.46)	38.19 (0.51)
Δ*flrC*	30.01 (0.78)	30.85 (1.62)	47.89 (2.21)
Δ*cpxR*	23.12 (0.37)	23.49 (0.97)	40.24 (1.76)

[a]The values are the means (standard deviations) of data from six z-series image stacks

Figure 4.2D. Analysis of biofilm formation in RR deletion mutants. Three dimensional biofilm structures of *gfp* tagged wild-type *V. cholerae*, ΔVC1652 (*vieA*), ΔVC1719 (*torR*), ΔVC1926 (*dct-D1*), ΔVC2135 (*flrC*), ΔVC2692 (*cpxR*) after 48 hours of incubation in flow-cell chambers. Images of horizontal (xy) and vertical (xz) projections of biofilms are shown. The results shown are from one representative experiment of two independent experiments. Scale bars = 30 μm.

Figure 4.2E

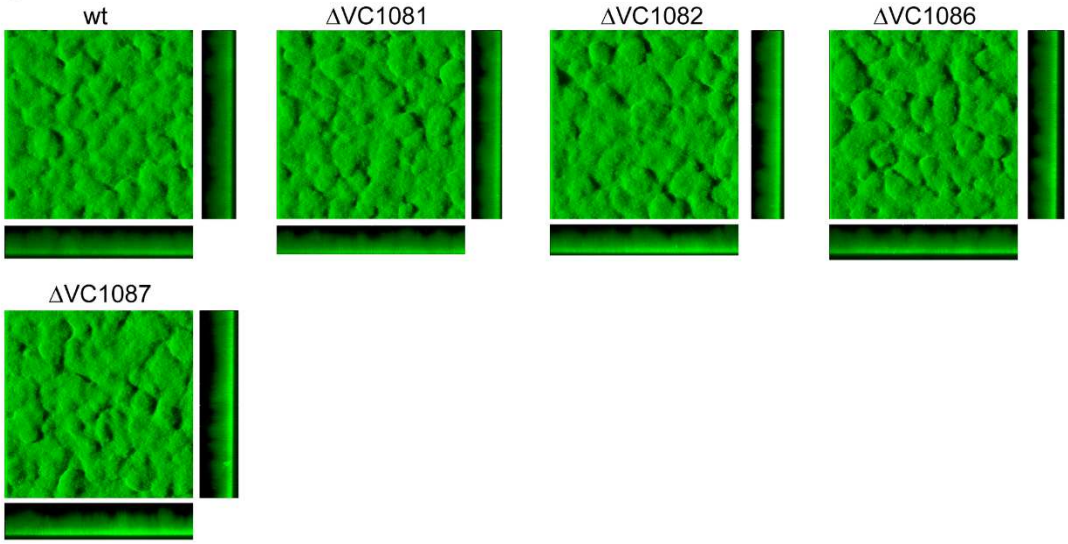

Table 4.2E. COMSTAT analysis of biofilms of wild type and ΔRR strains[a]

Strain	Biomass (μm^3)	Average thickness (μm)	Maximum thickness (μm)
wt	25.87 (1.84)	25.76 (1.64)	33.44 (0.88)
ΔVC1081	26.06 (2.86)	25.80 (3.06)	34.32 (2.33)
ΔVC1082	26.06 (0.94)	25.69 (0.94)	33.44 (0.88)
ΔVC1086	26.54 (0.13)	26.53 (0.13)	34.91 (0.51)
ΔVC1087	24.26 (0.64)	23.90 (0.60)	32.85 (1.83)

[a]The values are the means (standard deviations) of data from six z-series image stacks

Figure 4.2E. Analysis of biofilm formation in RR deletion mutants. (A) Three dimensional biofilm structures of *gfp* tagged wild-type *V. cholerae*, ΔVC1081, ΔVC1082, ΔVC1086, ΔVC1087 after 48 hours of incubation in flow-cell chambers. . Images of horizontal (xy) and vertical (xz) projections of biofilms are shown. The results shown are from one representative experiment of two independent experiments. Scale bars = 30 μm.

Figure 4.2F

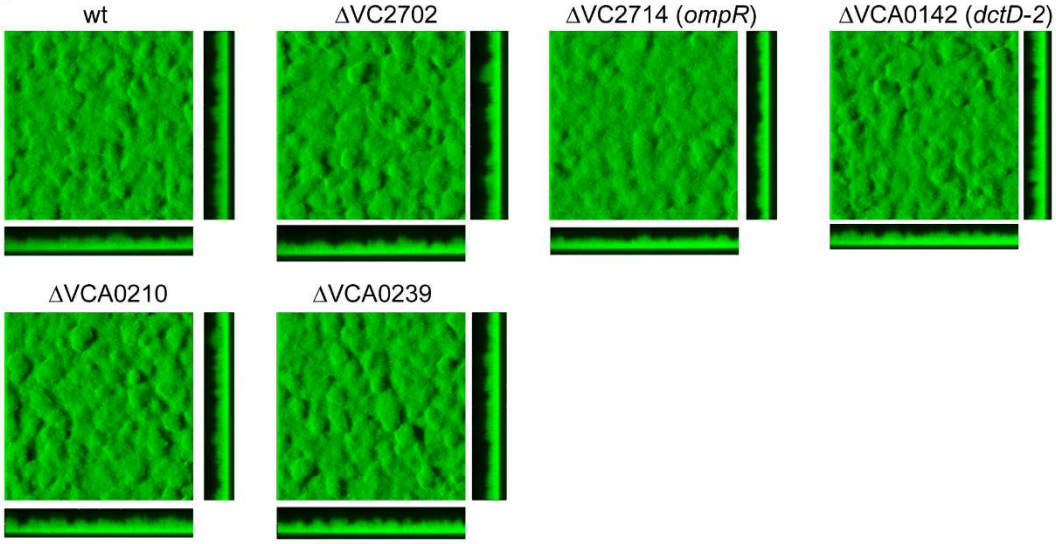

Table 4.2F. COMSTAT analysis of biofilms of wild type and ΔRR strains[a]

Strain	Biomass (μm^3)	Average thickness (μm)	Maximum thickness (μm)
wt	18.79 (4.09)	19.78 (4.76)	27.57 (4.06)
ΔVC2702	22.05 (0.43)	23.40 (0.62)	28.45 (2.03)
Δ*ompR*	18.79 (0.63)	19.49 (0.69)	22.88 (0.00)
Δ*dctD-2*	21.76 (1.10)	22.95 (1.39)	26.99 (2.03)
ΔVCA0210	21.32 (0.49)	22.43 (0.66)	26.99 (1.34)
ΔVCA0239	20.07 (0.81)	20.90 (1.11)	25.52 (2.64)

[a]The values are the means (standard deviations) of data from six z-series image stacks

Figure 4.2F. Analysis of biofilm formation in RR deletion mutants. Three dimensional biofilm structures of *gfp* tagged wild-type *V. cholerae*, ΔVC2702, ΔVC2714 (*ompR*), ΔVCA0142 (*dct-D2*), ΔVCA0210, ΔVCA0239 after 48 hours of incubation in flow-cell chambers. Images of horizontal (xy) and vertical (xz) projections of biofilms are shown. The results shown are from one representative experiment of two independent experiments. Scale bars = 30 μm.

Figure 4.2G

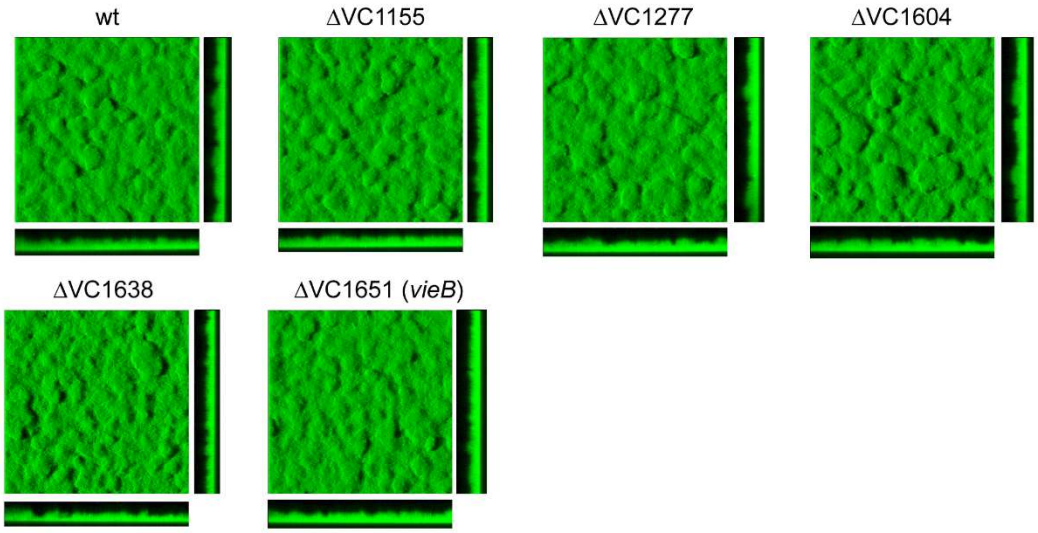

Table 4.2G. COMSTAT analysis of biofilms of wild type and ΔRR strains[a]

Strain	Biomass (μm^3)	Average thickness (μm)	Maximum thickness (μm)
wt	17.49 (0.14)	17.79 (0.41)	22.59 (0.51)
ΔVC1155	17.79 (1.08)	18.59 (1.81)	23.76 (2.33)
ΔVC1277	17.81 (0.40)	17.98 (0.41)	23.47 (1.34)
ΔVC1604	18.38 (0.27)	19.63 (0.15)	27.57 (1.02)
ΔVC1638	14.39 (0.70)	16.60 (0.66)	24.64 (2.33)
Δ*vieB*	18.21 (0.22)	19.27 (0.90)	25.52 (1.76)

[a]The values are the means (standard deviations) of data from six z-series image stacks

Figure 4.2G. Analysis of biofilm formation in RR deletion mutants. Three dimensional biofilm structures of *gfp* tagged wild-type *V. cholerae*, ΔVC1155, ΔVC1277, ΔVC1604, ΔVC1638, ΔVC1651 (*vieB*) after 48 hours of incubation in flow-cell chambers. Images of horizontal (xy) and vertical (xz) projections of biofilms are shown. The results shown are from one representative experiment of two independent experiments. Scale bars = 30 μm.

Figure 4.2H

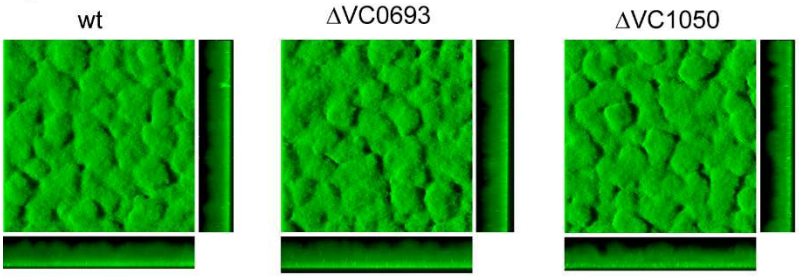

Table 4.2H. COMSTAT analysis of biofilms of wild type and ΔRR strains[a]

Strain	Biomass (μm^3)	Average thickness (μm)	Maximum thickness (μm)
wt	22.04 (1.03)	22.60 (1.57)	33.44 (3.17)
ΔVC0693	22.11 (0.91)	23.32 (0.75)	34.91 (0.51)
ΔVC1050	18.15 (0.77)	19.39 (0.79)	30.51 (0.51)

[a]The values are the means (standard deviations) of data from six z-series image stacks

Figure 4.2H. Analysis of biofilm formation in RR deletion mutants. Three dimensional biofilm structures of *gfp* tagged wild-type *V. cholerae*, ΔVC0693, ΔVC1050 after 48 hours of incubation in flow-cell chambers. Images of horizontal (xy) and vertical (xz) projections of biofilms are shown. The results shown are from one representative experiment of two independent experiments. Scale bars = 30 μm.

Figure 4.2I

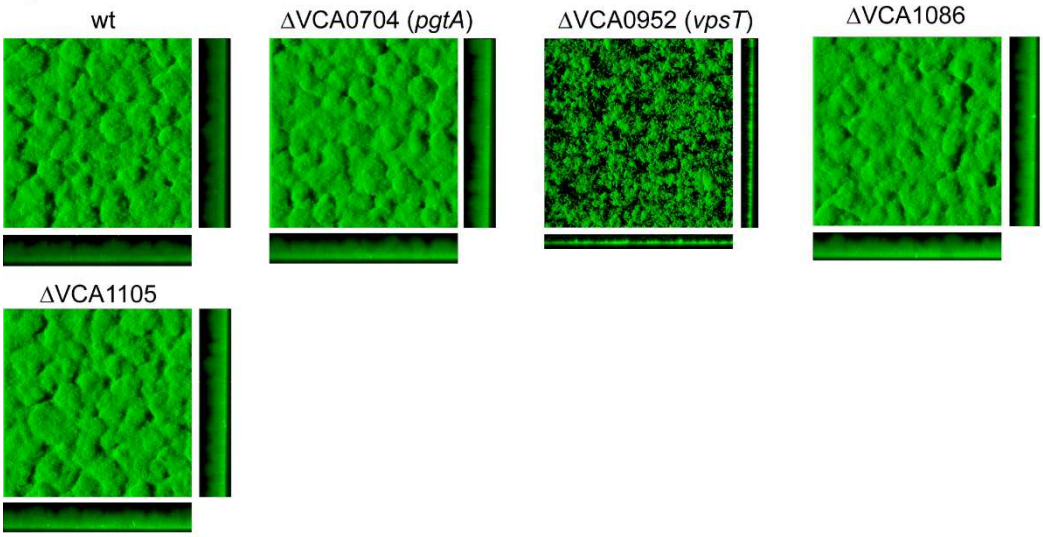

Table 4.2I. COMSTAT analysis of biofilms of wild type and ΔRR strains[a]

Strain	Biomass (μm^3)	Average thickness (μm)	Maximum thickness (μm)
wt	20.94 (2.98)	20.86 (2.67)	27.87 (0.51)
Δ*pgtA*	22.66 (0.50)	22.14 (0.50)	29.63 (1.02)
Δ*vpsT*	4.48 (0.18)	6.14 (0.11)	13.20 (0.88)
ΔVCA1086	22.86 (0.28)	22.26 (0.30)	28.75 (0.51)
ΔVCA1105	22.10 (0.68)	21.51 (0.70)	29.04 (0.00)

[a]The values are the means (standard deviations) of data from six z-series image stacks

Figure 4.2l. Analysis of biofilm formation in RR deletion mutants. Three dimensional biofilm structures of *gfp* tagged wild-type *V. cholerae*, ΔVCA0704 (*pgtA*), ΔVCA0952 (*vpsT*), ΔVCA1086, ΔVCA1105 after 48 hours of incubation in flow-cell chambers. Images of horizontal (xy) and vertical (xz) projections of biofilms are shown. The results shown are from one representative experiment of three independent experiments. Scale bars = 30 μm.

Figure 4.2J

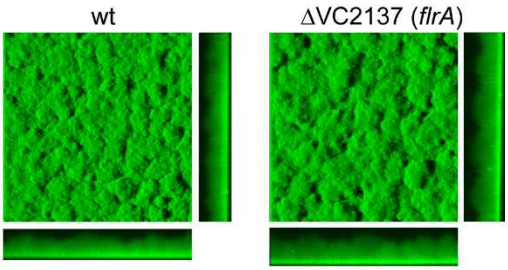

Table 4.2J. COMSTAT analysis of biofilms of wild type and ΔRR strains[a]

Strain	Biomass (μm^3)	Average thickness (μm)	Maximum thickness (μm)
wt	25.43 (0.43)	26.59 (0.37)	35.81 (0.51)
Δ*flrA*	32.45 (0.81)	34.05 (0.77)	44.91 (1.83)

[a]The values are the means (standard deviations) of data from six z-series image stacks

Figure 4.2J. Analysis of biofilm formation in RR deletion mutants. Three dimensional biofilm structures of gfp tagged wild-type *V. cholerae*, ΔVC2137 (*flrA*) after 48 hours of incubation in flow-cell chambers. Images of horizontal (xy) and vertical (xz) projections of biofilms are shown. The results shown are from one representative experiment of two independent experiments. Scale bars = 30 μm.

Comparison of the biofilm forming abilities of each mutant (40 ΔRR) to that of wild type, revealed that 8 ΔRR mutants had a change in biofilm formation. We further confirmed these findings using flow-cell biofilm analysis in Fig 4.3 and Table 4.3. Consistent with our previous findings (chapter 3), we observed an increase in biofilm formation for ΔVC2749 (*ntrC*), ΔVC2135 (*flrC*), and ΔVC2137 (*flrA*) and we also observed a decrease in biofilm formation for ΔVC0665 (*vpsR*), ΔVC1021 (*luxO*), and ΔVCA0952 (*vpsT*) (Fig 4.3 and Table 4.3) (25, 26, 29). Interestingly, these biofilm experiments revealed that ΔVCA0566 (*vxrB*) and ΔVC1348 were decreased in biofilm formation compared to wild type (Fig 4.3 and Table 4.3). VC1348 is a RR which contains a HD-GYP domain that degrades the second messenger cyclic diguanylate (c-di-GMP). It was previously reported that overexpression of VC1348 increases motility and decreases biofilm formation, as measured using crystal violet staining assay (33). This finding is different from our observation that deletion of VC1348 leads to a decrease in biofilm formation.

Since, VxrB has not been studied for its involvement in biofilm formation and the strain lacking *vxrB* showed a decrease in both *vpsLp-lux* activity and biofilm formation (Fig 4.1, 4.3, and Table 4.3), we focused the rest of our studies on this protein.

Figure 4.3

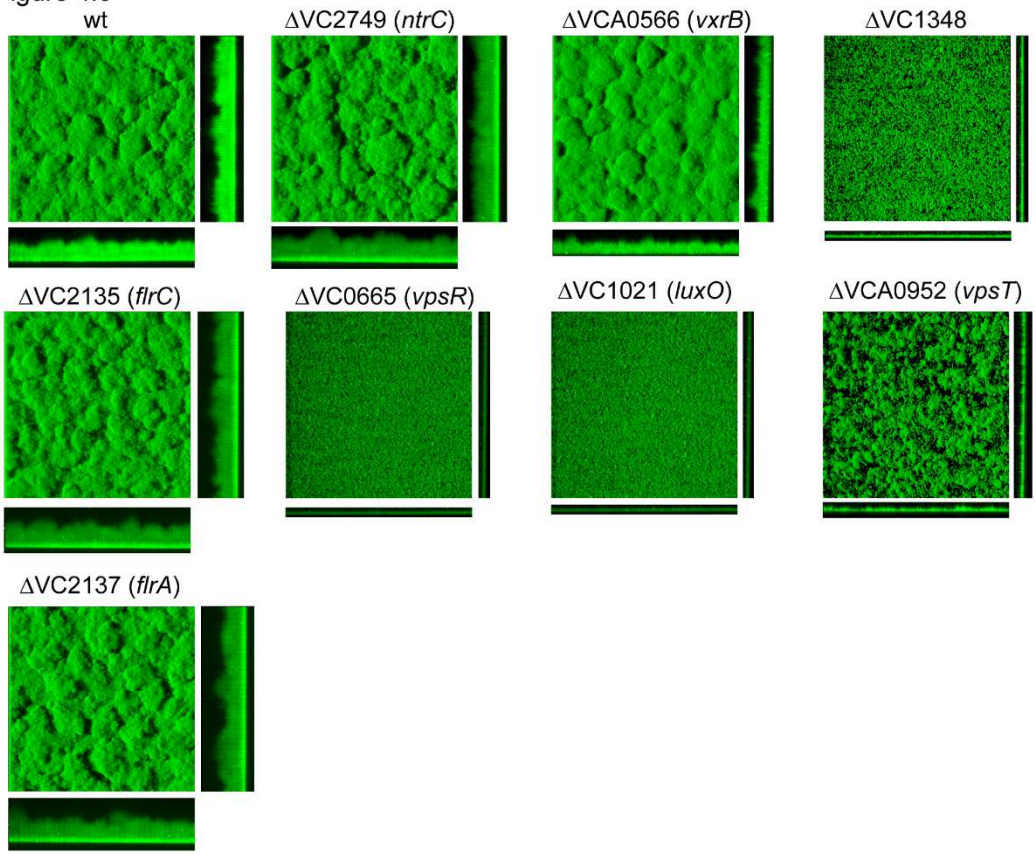

Table 4.3. COMSTAT analysis of biofilms of wild type and ΔRR strains[a]

Strain	Biomass (μm^3)	Average thickness (μm)	Maximum thickness (μm)
wt	24.66 (0.15)	26.47 (0.36)	38.43 (0.51)
Δ*ntrC*	28.19 (1.06)	28.19 (1.41)	39.60 (2.33)
Δ*vxrB*	18.37 (1.44)	18.00 (1.68)	25.81 (0.51)
ΔVC1348	3.45 (0.14)	5.58 (0.78)	8.55 (0.88)
Δ*flrC*	29.84 (0.77)	30.15 (1.42)	42.85 (2.54)
Δ*vpsR*	3.72 (0.12)	3.85 (0.75)	7.22 (1.08)
Δ*luxO*	2.15 (0.08)	4.36 (0.27)	9.80 (0.84)
Δ*vpsT*	4.84 (0.81)	6.41 (0.21)	11.52 (0.88)
Δ*flrA*	30.23 (0.98)	31.12 (0.97)	43.25 (1.97)

[a]The values are the means (standard deviations) of data from six z-series image stacks

Figure 4.3. Analysis of biofilm formation in selected RR deletion mutants. Three dimensional biofilm structures of gfp tagged wild-type V. cholerae, ΔVC2749 (*ntrC*), ΔVCA0566 (*vxrB*), ΔVC1348, ΔVC2135 (*flrC*), ΔVC0665 (*vpsR*), ΔVC1021 (*luxO*), ΔVCA0952 (*vpsT*), and ΔVC2137 (*flrA*) after 48 hours of incubation in flow-cell chambers. Images of horizontal (xy) and vertical (xz) projections of biofilms are shown. The results shown are from one representative experiment of two independent experiments. Scale bars = 30 μm

The VxrAB TCS is important for *vps* gene expression

Recently, we determined that VxrB is required for infant mouse colonization and regulates T6SS gene expression and function (44). In this study, we observed a significant decrease in *vpsL* expression in the Δ*vxrB* mutant. To further confirm that VxrB regulates *vpsL* expression, a wild type (wt) copy of *vxrB* was cloned into an arabinose inducible pBAD expression vector, and the plasmids were introduced individually into a reporter strain harboring a *vpsLp-lacZ* transcriptional fusion at the *lacZ* locus on the *V. cholerae* chromosome. Then, wt and the Δ*vxrB* deletion mutant were assessed to determine *vxrB*'s ability to regulate *vpsL* expression by determining the β-galactosidase activity in cells that were grown for 24 h in the presence or absence of the inducer arabinose. When *vxrB* is expressed in the Δ*vxrB* mutant, we observed that *vpsL* expression is restored to wild type levels without arabinose (Fig 4.4A). We note that the pBAD promoter is leaky, and this finding suggests that the Δ*vxrB* mutant phenotype could be complemented with the basal level of pBAD promoter activity. Furthermore, when expression of *vxrB* is induced with arabinose, we observed that *vpsL* expression increases more than wild type (Fig 4.4A). When *vxrB* is overexpressed in wt background, we observed an increase in *vpsL* expression (Fig. 4.4A). Collectively, these findings suggests that the Δ*vxrB* phenotype can be complemented and that the

phenotype is not caused by polar effects, and that overexpressing *vxrB* can increase *vpsL* expression (Fig 4.4A).

To determine if the cognate sensor histidine kinase (HK), VxrA, plays a role in *vpsL* expression, we measured *vpsL* expression in Δ*vxrA* mutant. We observed a 12-fold decrease in *vpsL* expression compared to wild type (Fig 4.4B). The magnitude of *vpsL* expression was similar in Δ*vxrA* and Δ*vxrB* mutants. This suggests that the HK VxrA is also important in regulating *vpsL* expression. Thus, it would be interesting to observe if phosphorylation activity could affect *vps* gene expression. Further analysis is needed to determine if the phosphorylation state of VxrB is required for regulating *vpsL* expression.

Figure 4.4.

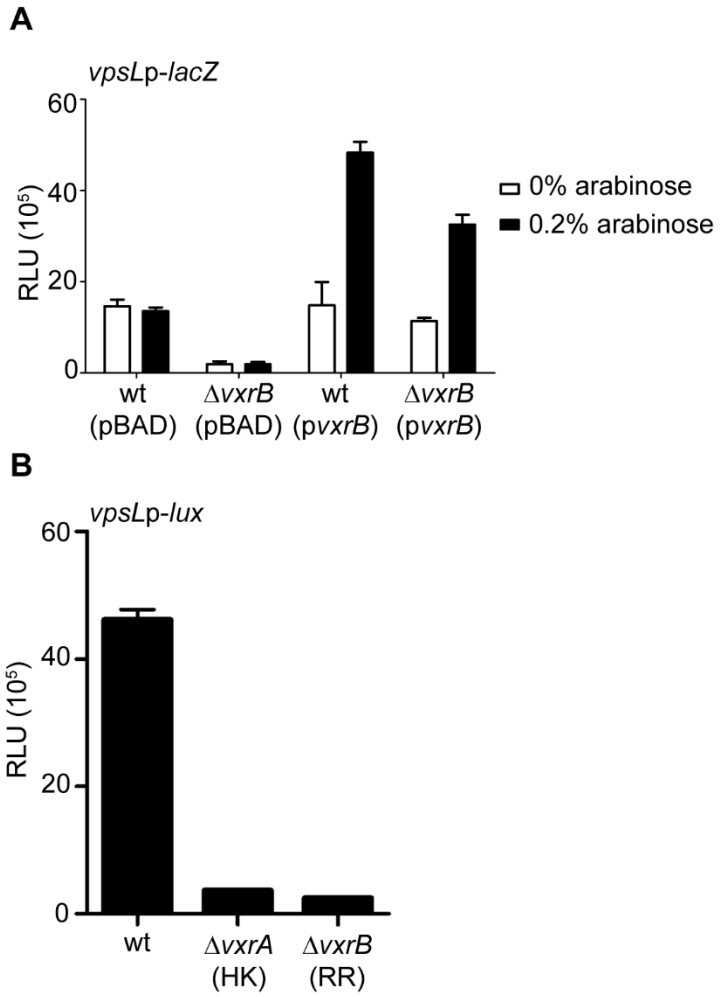
A
vpsLp-lacZ
60
40
20
0
RLU (10^5)
0% arabinose
0.2% arabinose
wt (pBAD)
ΔvxrB (pBAD)
wt (pvxrB)
ΔvxrB (pvxrB)
B
vpsLp-lux
60
40
20
0
RLU (10^5)
wt
ΔvxrA (HK)
ΔvxrB (RR)

Figure 4.4. Analysis of VxrB on *vps* gene expression. (A) β-galactosidase assay was perfomed to evalaute *vpsL* promoter activity in a *vpsLp-lacZ* reporter strain in wild type genetic background (wt) containing empty vector (pBAD), Δ*vxrB* harboring pBAD, wt harboring *vxrB* under the control of an arabinose inducible promoter (pvxrB), and Δ*vxrB* harboring p*vxrB*. 0.2% arabinose was added to the media to induce expression of *vxrB*. The graph represents the average and standard deviation of relative light units (RLU) of four technical replicates. The result of one representative experiment of three biological replicates are shown. (B) Expression of P_{vpsL}-*luxCADBE* in wt, Δ*vxrA* (HK), Δ*vxrB* (RR) at exponential growth phase. The graph represents the average and standard deviation of relative light units (RLU) obtained from four technical replicates from three independent biological samples. RLU is reported in luminescence counts min^{-1} ml^{-1}/OD_{600}. The graph represents the average and standard deviation of relative light units (RLU) obtained from four technical replicates from three independent biological samples. RLU is reported in luminescence counts min^{-1} ml^{-1}/OD_{600}.

The effect of VxrB on regulators of biofilm formation

VpsR and VpsT are the two major positive transcriptional regulators of *vps* genes. To determine if VxrB affects the regulators of *vps* gene expression, we measured the expression of each regulator in the Δ*vxrB* mutant compared to wild type. As expected, *vpsL* expression is decreased 8-fold in the Δ*vxrB* mutant compared to wild type (Fig 4.8B). In addition we observed that *vpsR* and *vpsT* expression decreased 2-fold and 5-fold, respectively (Fig 4.8B). These data suggest that VxrB could regulate *vps* gene expression by regulating the *vps* activators, VpsR and VpsT. Future experiments for investigating how VxrB affects the negative regulators of *vps* gene expression are needed.

Figure 4.5

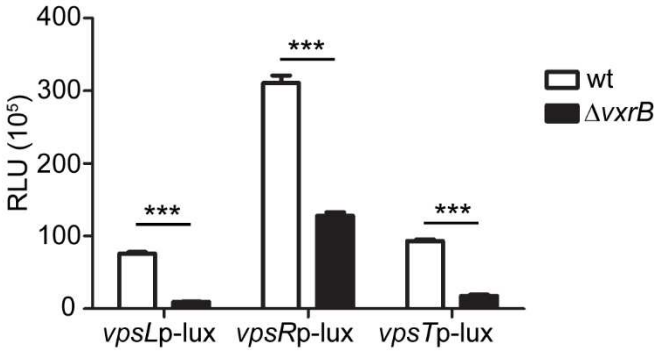
400
300
200
100
0
RLU (10^5)
***
***
***
wt
Δ*vxrB*
*vpsL*p-lux
*vpsR*p-lux
*vpsT*p-lux

Figure 4.5. Analysis of *vxrB* on the expression of the vps regulatory network. Expression of P_{vpsL}-*luxCADBE* P_{vpsR}-*luxCADBE*, and P_{vpsT}-*luxCADBE* in wt and Δ*vxrB* at exponential growth phase. The graph represents the average and standard deviation of relative light units (RLU) obtained from four technical replicates from three independent biological samples. RLU is reported in luminescence counts min^{-1} ml^{-1}/OD_{600}. A two-tailed unpaired T-test was used to compare the expression between wt and deletion mutants. *** $p < 0.001$.

Analysis of epistasis relationships among regulators of *vps* gene expression

To determine the contribution of VxrB to the *vps* regulatory network, we performed an epistasis analysis. As expected, Δ*vxrB*, Δ*vpsR*, and Δ*vpsT* exhibited a decrease in *vpsL* expression (Fig 4.4D). Then, Δ*vxrB*Δ*vpsR* and Δ*vxrB*Δ*vpsT* showed no significant difference in *vpsL* expression compared to the single deletions (Fig 4.4D). This suggests that VpsR and VpsT function downstream of VxrB on *vpsL* expression. Further investigation is needed to determine where *vxrB* is integrated into the *vps* regulatory network.

Figure 4.6

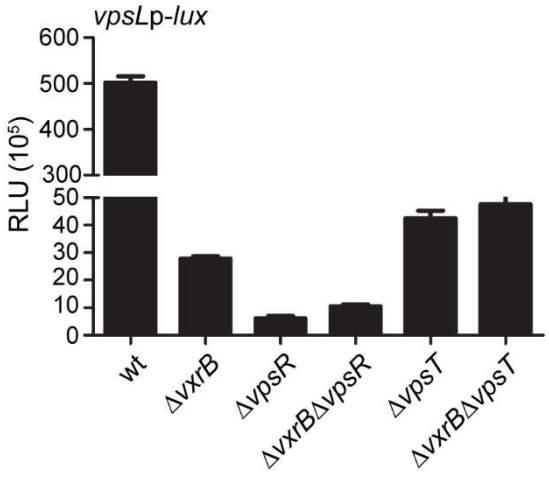
vpsLp-lux
RLU (10^5)
600
500
400
300
50
40
30
20
10
0
wt
ΔvxrB
ΔvpsR
ΔvxrBΔvpsR
ΔvpsT
ΔvxrBΔvpsT

Figure 4.6. Epistasis analysis of vxrB with positive regulators of *vps* genes. Expression of P_{vpsL}-*luxCADBE* in wt, Δ*vxrB*, Δ*vpsR*, Δ*vxrB*Δ*vpsR*, Δ*vpsT*, and Δ*vxrB*Δ*vpsT*. The graph represents the average and standard deviation of relative light units (RLU) obtained from four technical replicates from three independent biological samples. RLU is reported in luminescence counts min^{-1} ml^{-1}/OD_{600}.

Transcriptome profile of VxrB

To gain a better understanding of the contribution of VxrB to *V. cholerae* biofilm formation, we performed high throughput transcriptome sequencing (RNA-seq) analysis to identify the *V. cholerae* genes controlled by VxrB. We used cells grown under LB conditions harvested at exponential growth phase.

For the Δ*vxrB* mutant relative to wild type, a total of 370 genes demonstrated a statistically significant ($p < 0.05$) fold change of ≥1.5 (Tables 4.4 and 4.5). Of these, 157 genes were up-regulated in the Δ*vxrB* mutant relative to the wild type (Table 4.5), while 213 genes were down-regulated (Table 4.3).

Interestingly, we observed that 11 genes encoding *vps* and 5 genes encoding matrix proteins were down-regulated in the RNAseq analysis under LB conditions (Table 4.4). In addition, we observed that 16 genes encoding T6SS were also down-regulated in the RNAseq analysis (Table 4.4). There have been no studies demonstrating that the T6SS affects biofilm formation in *V. cholerae*. Thus, it would be very interesting to further investigate the role of T6SS in biofilm formation in *V. cholerae*.

Table 4.4. Genes activated by VxrB under LB conditions, identified by RNAseq analysis

ORF ID[a]	Gene	Fold Up Regulation[b]	p-value
VCA0566	*vxrB*	-57.31	0.00000
VC0370		-14.27	0.00000
VC2662		-12.5	0.00000
VC1663	*hslJ*	-10.82	0.00000
VC1160		-9.29	0.00000
VCA0003		-9.07	0.00000
VC1162		-8.27	0.00000
VC1161		-7.09	0.00000
VCA0035		-5.62	0.00000
VCA0017	*hcp-2*	-5.13	0.00000
VC1415	*hcp-1*	-4.99	0.00000
VC1687		-3.95	0.00000
VCA0721		-3.54	0.00001
VC0483		-3.46	0.00000
VC1655	*mgtE-1*	-3.28	0.00000
VC0791	*citA*	-3.26	0.00000
VC1115	*bioD*	-3.26	0.00000
VCA0180	*pepT*	-3.2	0.00000
VC0439		-3.18	0.00000
VC1114	*bioC*	-3.07	0.00000
VC0438		-3.06	0.00000
VCA1013		-2.99	0.00000
VC0652		-2.94	0.00000
VCA0115	*vasF*	-2.92	0.00000
VC2371		-2.86	0.00000
VCA0125		-2.86	0.00000
VCA0113	*vasD*	-2.84	0.00000
VCA1012		-2.77	0.00000
VC1731		-2.74	0.00000
VCA0271		-2.74	0.00000
VCA0556		-2.72	0.00004
VCA0784		-2.72	0.00000
VC1947		-2.71	0.00000

VCA0675	*narQ*	-2.65	0.00000
VCA0111	*vasB*	-2.62	0.00000
VCA0112	*fha*	-2.59	0.00000
VC1216		-2.52	0.00000
VCA0718		-2.52	0.00000
VCA0107	*vipA*	-2.51	0.00000
VC1314		-2.44	0.00000
VCA0117	*vasH*	-2.39	0.00000
VCA0565		-2.39	0.00000
VCA0109		-2.37	0.00000
VCA0110	*vasA*	-2.35	0.00000
VCA1032		-2.29	0.00000
VCA0116	*clpB-2*	-2.28	0.00000
VC0026		-2.27	0.00000
VC0918	*vpsB*	-2.26	0.00000
VCA0258		-2.26	0.00000
VCA0946	*malK*	-2.25	0.00000
VC2703		-2.24	0.00000
VCA0108	*vipB*	-2.22	0.00000
VC1962		-2.17	0.00000
VCA0064	*hutR*	-2.14	0.00000
VCA0845		-2.13	0.00000
VCA0867	*ompW*	-2.12	0.00000
VC2077	*feoB*	-2.08	0.00000
VC0919	*vpsC*	-2.07	0.00000
VC2548		-2.07	0.00000
VCA0067		-2.07	0.00000
VC1544	*tonB2*	-2.04	0.00000
VC1343		-2.03	0.00000
VCA0621		-2.03	0.00000
VC0932	*rbmE*	-2.02	0.00000
VCA0114	*vasE*	-2.02	0.00000
VC0928	*rbmA*	-2.01	0.00000
VC1865		-2.01	0.00000
VC2149		-2.01	0.00000
VCA0915	*hutD*	-2.01	0.00000
VCA0917		-2.01	0.00000

VC0920	*vpsD*	-1.99	0.00000
VC1545	*exbD2*	-1.98	0.00000
VC1064		-1.97	0.00000
VC0654		-1.96	0.00000
VC1888	*bap1*	-1.96	0.00000
VC2484		-1.96	0.00000
VC0917	*vpsA*	-1.95	0.00000
VC0206		-1.94	0.01232
VC2078	*feoA*	-1.94	0.00000
VCA0065		-1.94	0.00000
VCA0221	*hlyC*	-1.94	0.03776
VCA0594	*hlx*	-1.94	0.00000
VCA0063	*ptrB*	-1.93	0.00000
VCA0592		-1.93	0.00000
VCA0722		-1.93	0.00063
VC0064	*thiS*	-1.92	0.01401
VC1217		-1.92	0.00000
VCA0026		-1.91	0.00000
VC1433		-1.9	0.00000
VC1973	*menB*	-1.89	0.00000
VCA0719		-1.89	0.00000
VC2667		-1.86	0.00024
VC2286		-1.85	0.00000
VCA0535		-1.85	0.00000
VC0162	*ilvC*	-1.84	0.00000
VC0927	*vpsK*	-1.84	0.00000
VCA0230	*vctC*	-1.84	0.00000
VC2100		-1.83	0.00000
VC0074		-1.82	0.00000
VC2213	*ompA*	-1.82	0.00000
VC2367		-1.81	0.00064
VC2566		-1.81	0.00000
VCA0242		-1.81	0.03581
VCA0910	*tonB1*	-1.81	0.00000
VC0926	*vpsJ*	-1.8	0.00000
VC2212		-1.8	0.00000
VC2368	*fexA*	-1.8	0.00000

VCA0732		-1.8	0.00000
VCA0735		-1.8	0.00000
VC0364	*bfd*	-1.79	0.00285
VC1240		-1.79	0.00001
VC1589	*aldC*	-1.79	0.00000
VC2055	*ccmC*	-1.78	0.00000
VCA0013	*malP*	-1.77	0.00000
VCA0536		-1.77	0.00000
VCA1028	*ompS*	-1.77	0.00000
VC0655		-1.76	0.00000
VC1688		-1.76	0.00217
VC1951	*yecK*	-1.76	0.00000
VC2400	*murC*	-1.76	0.00000
VCA1057		-1.76	0.01360
VC2685	*metF*	-1.75	0.00000
VCA0609		-1.75	0.00000
VCA0677	*napD*	-1.75	0.00000
VCA0860	*malS*	-1.75	0.00000
VCA1019		-1.75	0.00362
VC0204		-1.74	0.00000
VC2448	*pyrG*	-1.74	0.00000
VC1195		-1.73	0.00000
VCA0120	*vasK*	-1.73	0.00000
VC0477	*pgk*	-1.72	0.00000
VC1204	*hutG*	-1.72	0.02789
VCA0803		-1.72	0.00151
VC0470	*dns*	-1.71	0.00000
VC0921	*vpsE*	-1.7	0.00000
VCA0246	*sgaT*	-1.7	0.00570
VCA0754a		-1.7	0.00577
VCA0909	*hutW*	-1.7	0.00000
VC0872		-1.69	0.00000
VC2459	*recO*	-1.69	0.00000
VCA0518	*fruB*	-1.69	0.00000
VC0931	*rbmD*	-1.68	0.00504
VC2401	*murG*	-1.68	0.00001
VC1651	*vieB*	-1.67	0.00000

VC2147		-1.67	0.00000
VCA0725	*modB*	-1.66	0.00017
VC1065		-1.65	0.00017
VC0916	*vpsU*	-1.64	0.00000
VC0930	*rbmC*	-1.64	0.00000
VC1107	*lolA*	-1.64	0.00000
VCA0231		-1.64	0.00000
VC0357		-1.63	0.00000
VC0428		-1.63	0.00000
VC1484	*rmf*	-1.63	0.00000
VC1871		-1.63	0.00000
VC1269		-1.62	0.00000
VC1719	*torR*	-1.62	0.00000
VCA0526		-1.62	0.00000
VCA0726	*modA*	-1.62	0.00000
VCA0927		-1.62	0.03393
VCA0944	*malF*	-1.62	0.00000
VC0934	*vpsL*	-1.61	0.01698
VC1249		-1.61	0.00000
VC2656	*frdA*	-1.61	0.00000
VCA0019	*vasW*	-1.61	0.04156
VCA0511	*nrdD*	-1.61	0.00000
VC0356		-1.6	0.00000
VC1301	*sdaC-1*	-1.6	0.00000
VC1315		-1.6	0.00000
VC1974		-1.59	0.00000
VC2395		-1.59	0.00000
VCA0229	*vctG*	-1.59	0.00000
VC2054	*ccmD*	-1.58	0.00000
VCA0656	*cscK*	-1.58	0.00000
VCA0945	*malE*	-1.58	0.00000
VC2728	*epsI*	-1.57	0.00001
VCA0266		-1.57	0.00005
VCA0653	*scrA*	-1.57	0.00000
VC1207		-1.56	0.00000
VC1652	*vieA*	-1.56	0.00000
VC2408	*ftsL*	-1.56	0.03755

VCA0119	*vasJ*	-1.56	0.00200
VCA0849		-1.56	0.00000
VC1266		-1.55	0.00000
VC1724		-1.55	0.00004
VCA0976		-1.55	0.00018
VC0924	*vpsH*	-1.54	0.00000
VC1051		-1.54	0.04415
VC1475		-1.54	0.03097
VC2145		-1.54	0.00000
VC2406	*murE*	-1.54	0.00000
VCA0023		-1.54	0.00044
VCA0106		-1.54	0.00000
VCA0519	*fruR*	-1.54	0.00000
VCA1030		-1.54	0.00000
VC1049		-1.53	0.00000
VC2033	*adhE*	-1.53	0.00000
VC2547		-1.53	0.00000
VCA0665	*dcuC*	-1.53	0.00000
VC1543		-1.52	0.00000
VC1552	*ugpC*	-1.52	0.03304
VCA0213		-1.52	0.00000
VC0923	*vpsG*	-1.51	0.00001
VCA0676	*napF*	-1.51	0.00000
VC2285		-1.5	0.00000
VCA0257		-1.5	0.00049

[a]ORF IDs are derived from the *V. cholerae* N16961 genome.
[b]Fold change is the Δ*vxrB* mutant relative to the wild type strain.

Table 4.5. Genes repressed by VxrB under LB conditions, identified by RNAseq analysis

ORF ID[a]	Gene	Fold Up Regulation[b]	p-value
VC1793		25.58	0.02162
VCA0363		5.91	0.02147
VC0833	*tcpD*	5.42	0.00054
VC0486		4.68	0.00000
VCA0297		4.15	0.00891
VC0991	*asnB*	3.09	0.00000
VCA0418		2.5	0.00004
VCA0375		2.46	0.00061
VC0382		2.39	0.00144
VCA0317	*blc-1*	2.35	0.00000
VCA0485		2.35	0.00000
VC1448	*rtxB*	2.33	0.00000
VCA0329a		2.31	0.00101
VC1281	*celA*	2.26	0.00002
VCA0431		2.25	0.00027
VCA0381		2.1	0.04484
VC1434	*fnr*	2.06	0.00000
VCA0329b		2.06	0.00004
VCA0348		1.99	0.00000
VCA0427		1.97	0.00293
VC0576	*sspA*	1.93	0.00000
VC1669		1.93	0.00000
VC1420		1.92	0.00568
VCA0319		1.92	0.00003
VC1614		1.91	0.00000
VC0297	*aroQ*	1.9	0.00000
VC2539	*tbpA*	1.89	0.00000
VCA0770		1.87	0.00000
VC1991		1.86	0.00000
VC2473		1.86	0.00000
VC2226	*purM*	1.83	0.00000
VCA0417		1.83	0.00000
VC2708	*gmk*	1.82	0.00000
VCA0334		1.82	0.02520
VCA0340		1.82	0.00106

VCA0503		1.82	0.00000
VC1971	*menE*	1.81	0.00000
VCA0747	*glpA*	1.81	0.00000
VC1540		1.8	0.00000
VC1000	*accD*	1.79	0.00000
VC2489		1.79	0.00021
VC1737	*infA*	1.78	0.00000
VC2415	*pdhR*	1.78	0.00000
VC1854	*ompT*	1.77	0.00000
VCA0308		1.77	0.00001
VC0051	*purK*	1.76	0.00000
VC1422		1.76	0.00000
VCA0285		1.76	0.00031
VCA0387		1.76	0.00000
VC1375		1.75	0.00000
VC1432		1.75	0.00000
VC1579		1.75	0.00000
VC0282		1.74	0.00000
VC1205	*hutI*	1.74	0.00002
VC1904	*lrp*	1.74	0.00000
VCA0380		1.74	0.00897
VC0836	*tcpE*	1.73	0.01433
VCA0201		1.72	0.02818
VC1342		1.71	0.00000
VC1594	*galM*	1.7	0.00000
VC1058		1.69	0.00000
VCA0426		1.69	0.02274
VC0276	*purH*	1.68	0.00002
VC1329		1.68	0.04251
VC2012		1.68	0.00000
VCA0341		1.68	0.00000
VC2311		1.67	0.00000
VC0662	*brnQ*	1.66	0.00000
VC0837	*tcpF*	1.66	0.00001
VCA0330		1.66	0.00000
VCA0338		1.66	0.00228
VCA0745	*glpF*	1.66	0.00038
VC0687		1.65	0.00000
VC0835	*tcpT*	1.65	0.00050
VC2563		1.65	0.00003

VCA0414		1.65	0.02573
VC0238		1.64	0.00281
VC0494	*mshA*	1.64	0.00174
VC0583	*hapR*	1.64	0.00000
VC0757		1.64	0.00000
VC1533		1.64	0.00000
VC2600		1.64	0.00000
VCA0339		1.64	0.00025
VCA0355		1.64	0.00122
VC1853		1.63	0.00040
VCA0316		1.63	0.00007
VCA0790		1.63	0.00042
VC0660	*srmB*	1.62	0.00000
VC0824	*tagD*	1.62	0.00000
VC1103		1.62	0.00001
VC1428	*potA*	1.62	0.00000
VC1741		1.62	0.00960
VC1316		1.61	0.00000
VCA0300	*cat*	1.61	0.00000
VCA0421		1.61	0.00030
VCA0463		1.61	0.00000
VCA0793		1.61	0.03342
VC1151		1.6	0.00000
VC1590	*ilvK*	1.6	0.00012
VC1605a		1.6	0.00004
VCA0010		1.6	0.00001
VCA0389		1.6	0.00001
VC1121		1.59	0.00001
VC2390	*carA*	1.59	0.00000
VC2659	*frdD*	1.59	0.00000
VC0424		1.58	0.00000
VC1649		1.58	0.00000
VC2040		1.58	0.04066
VC2490	*leuA*	1.58	0.00000
VCA0179		1.58	0.00000
VCA0501		1.58	0.00113
VC0607	*glnB-1*	1.57	0.00791
VC1118		1.57	0.00007
VC1264		1.57	0.00000
VC1773		1.56	0.03082

VC1890	*ndh*	1.56	0.00000
VCA0459		1.56	0.00000
VC0985	*htpG*	1.55	0.00000
VC1707		1.55	0.00284
VC2037	*yqkI*	1.55	0.00000
VC2268	*ribH*	1.55	0.00000
VCA0798		1.55	0.00000
VCA1104		1.55	0.00001
VC0623		1.54	0.00000
VC1770		1.54	0.00000
VC2757		1.54	0.00000
VCA0036		1.54	0.00000
VCA0198		1.54	0.00000
VCA0309		1.54	0.00000
VCA0345		1.54	0.01972
VCA0346		1.54	0.00177
VCA0468		1.54	0.00001
VC1031		1.53	0.01138
VC2101		1.53	0.00001
VCA0415		1.53	0.03981
VCA0483		1.53	0.00115
VC1617		1.52	0.00000
VC2031		1.52	0.00000
VC2227	*purN*	1.52	0.00002
VC2669		1.52	0.01126
VCA0367		1.52	0.00016
VCA0554		1.52	0.00000
VCA0974		1.52	0.00000
VC0988		1.51	0.00000
VC1084		1.51	0.00093
VC1713		1.51	0.00007
VCA0356		1.51	0.00039
VCA0458		1.51	0.02925
VC0247	*rfbI*	1.5	0.01136
VC0302		1.5	0.00000
VC1201		1.5	0.00000
VC1413		1.5	0.00000
VC1901	*nhaB*	1.5	0.00000
VCA0464		1.5	0.00000
VCA0482		1.5	0.00228

VCA0892		1.5	0.00000

[a]ORF IDs are derived from the *V. cholerae* N16961 genome.
[b]Fold change is the Δ*vxrB* mutant relative to the wild type strain.

Discussion

Systematic mutational phenotypic characterization of TCSs has been performed in several bacteria, including *Vibrio fischeri*, *E. coli*, *Bacillus subtilis, Streptococcus pneumoniae,* and *Enterococcus faecalis* (51-55). In this study, we systematically analyzed the role of all *V. cholerae* TCS in biofilm formation and identified the RRs that impact biofilm formation and *vps* gene expression. The RRs which were found to be regulating biofilm formation or *vps* gene expression were further characterized. In addition to what was reported in chapter 3, we identified two additional RRs impacting biofilm formation in *V. cholerae* (VC1348 and *vxrB*). VC1348 is predicted to encode a HD-GYP domain that function as c-di-GMP phosphodiesterases (PDE), which degrade c-di-GMP. McKee et al. showed that overexpression of VC1348 increases motility and decreases biofilm formation in *V. cholerae* (33). Furthermore, qRT-PCR analysis showed that VC1348 transcripts were more abundant in biofilm cells than planktonic cells. In our work, we observed that ΔVC1348 had a decrease in biofilm formation (Fig 4.3), suggesting that VC1348 activates biofilm formation. The disparities in these two studies could be due to the differences in biofilm set-ups (flow-cell system versus static chambers, which can lead to accumulation of quorum sensing signals) and the different strains utilized.

VxrB has previously been shown to be required to colonize the infant mouse small intestine and regulate the expression of T6SS (44). This study showed that VxrB activates biofilm formation and *vpsL* expression (Fig. 4.1 and 4.3). Furthermore, overexpression of *vxrB* increased *vpsL* expression and we were able to complement the deletion phenotype (Fig. 4.4A). Additionally, we demonstrated that the cognate HK, VxrA, is also required for *vpsL* promoter activity (Fig. 4.4B). Further analysis of the phosphorylation state of VxrB on regulation of *vpsL* expression and biofilm formation is needed. We showed that VxrB may activate *vps* genes via regulating the expression of *vpsR* and *vpsT* (Fig. 4.5). Epistasis analysis showed that VxrB is regulating *vpsL* expression upstream of VpsR and VpsT (Fig 4.6). Finally, transcriptome profile of *vxrB* showed that *vps* genes and genes encoding matrix proteins were down-regulated in addition to T6SS genes (Table 4.4). Further investigation of how T6SS genes play a role in biofilm formation is needed.

Very few studies have linked T6SS to biofilm formation. In *Pseudomonas aeruginosa* PAO1, Southey-Pillig et al. first identified and confirmed that Hcp took part in the biofilm maturation stage through two-dimensional gel electrophoresis and mass spectrometry (56). Furthermore, Zhang et al. demonstrated that *tssC1*, a gene implicated in T6SS, was important for biofilm-specific antibiotic resistance in *P. aeruginosa* (57). In *Agrobacterium tumefaciens*, Heckel et al. revealed through transcriptome analysis that the

ExoR regulator, an important regulator of biofilm formation, also regulates T6SS (58). Finally, Aubert et al. identified a novel hybrid HK that controls biofilm formation and T6SS in *Burkholderia cencepacia* (59). Inactivation of this hybrid HK, AtsR, led to increased biofilm production and overexpression of *astR* hyper-secreted an Hcp-like protein.

In summary, this is the first study to systematically characterize the RRs of *V. cholerae* for biofilm formation. Additional studies are required to enhance an enhanced understanding of the connections between these RR and their impact on the physiological traits.

References

1. **Charles RC, Ryan ET.** 2011. Cholera in the 21st century. Curr Opin Infect Dis **24:**472-477.

2. **Faruque SM, Albert MJ, Mekalanos JJ.** 1998. Epidemiology, genetics, and ecology of toxigenic *Vibrio cholerae*. Microbiol Mol Biol Rev **62:**1301-1314.

3. **Islam MS, Jahid MIK, Rahman MM, Rahman MZ, Islam MS, Kabir MS, Sack DA, Schoolnik GK.** 2007. Biofilm acts as a microenvironment for plankton-associated *Vibrio cholerae* in the aquatic environment of Bangladesh. Microbiol Immunol **51:**369-379.

4. **Faruque SM, Biswas K, Udden SMN, Ahmad QS, Sack DA, Nair GB, Mekalanos JJ.** 2006. Transmissibility of cholera: In vivo-formed biofilms and their relationship to infectivity and persistence in the environment. Proceedings of the National Academy of Sciences of the United States of America **103:**6350-6355.

5. **Alam M, Sultana M, Nair GB, Siddique AK, Hasan NA, Sack RB, Sack DA, Ahmed KU, Sadique A, Watanabe H, Grim CJ, Huq A, Colwell RR.** 2007. Viable but nonculturable *Vibrio cholerae* O1 in biofilms in the aquatic environment and their role in cholera transmission. Proc Natl Acad Sci U S A **104:**17801-17806.

6. **Teschler JK, Zamorano-Sanchez D, Utada AS, Warner CJ, Wong GC, Linington RG, Yildiz FH.** 2015. Living in the matrix: assembly and control of *Vibrio cholerae* biofilms. Nat Rev Microbiol **13:**255-268.

7. **Yildiz FH, Schoolnik GK.** 1999. *Vibrio cholerae* O1 El Tor: identification of a gene cluster required for the rugose colony type, exopolysaccharide production, chlorine resistance, and biofilm formation. Proc Natl Acad Sci U S A **96:**4028-4033.

8. **Fong JC, Karplus K, Schoolnik GK, Yildiz FH.** 2006. Identification and characterization of RbmA, a novel protein required for the development of rugose colony morphology and biofilm structure in *Vibrio cholerae*. J Bacteriol **188:**1049-1059.

9. **Fong JC, Syed KA, Klose KE, Yildiz FH.** 2010. Role of *Vibrio* polysaccharide (*vps*) genes in VPS production, biofilm formation and *Vibrio cholerae* pathogenesis. Microbiology **156:**2757-2769.

10. **Fong JC, Yildiz FH.** 2007. The *rbmBCDEF* gene cluster modulates development of rugose colony morphology and biofilm formation in *Vibrio cholerae*. J Bacteriol **189:**2319-2330.

11. **Yildiz FH, Visick KL.** 2009. *Vibrio* biofilms: so much the same yet so different. Trends Microbiol **17:**109-118.

12. **Seper A, Fengler VH, Roier S, Wolinski H, Kohlwein SD, Bishop AL, Camilli A, Reidl J, Schild S.** 2011. Extracellular nucleases and extracellular DNA play important roles in *Vibrio cholerae* biofilm formation. Mol Microbiol **82:**1015-1037.

13. **Berk V, Fong JC, Dempsey GT, Develioglu ON, Zhuang X, Liphardt J, Yildiz FH, Chu S.** 2012. Molecular architecture and assembly principles of *Vibrio cholerae* biofilms. Science **337:**236-239.

14. **Absalon C, Van Dellen K, Watnick PI.** 2011. A communal bacterial adhesin anchors biofilm and bystander cells to surfaces. PLoS Pathog **7:**e1002210.

15. **Nadell CD, Drescher K, Wingreen NS, Bassler BL.** 2015. Extracellular matrix structure governs invasion resistance in bacterial biofilms. ISME J doi:10.1038/ismej.2014.246.

16. **Yildiz F, Fong J, Sadovskaya I, Grard T, Vinogradov E.** 2014. Structural characterization of the extracellular polysaccharide from *Vibrio cholerae* O1 El-Tor. PLoS One **9:**e86751.

17. **Beier D, Gross R.** 2006. Regulation of bacterial virulence by two-component systems. Curr Opin Microbiol **9:**143-152.

18. **Calva E, Oropeza R.** 2006. Two-component signal transduction systems, environmental signals, and virulence. Microb Ecol **51:**166-176.

19. **Bilecen K, Yildiz FH.** 2009. Identification of a calcium-controlled negative regulatory system affecting *Vibrio cholerae* biofilm formation. Environ Microbiol **11:**2015-2029.

20. **Shikuma NJ, Davis KR, Fong JN, Yildiz FH.** 2013. The transcriptional regulator, CosR, controls compatible solute biosynthesis and transport, motility and biofilm formation in *Vibrio cholerae*. Environ Microbiol **15:**1387-1399.

21. **Shikuma NJ, Yildiz FH.** 2009. Identification and characterization of OscR, a transcriptional regulator involved in osmolarity adaptation in *Vibrio cholerae*. J Bacteriol **191:**4082-4096.

22. **Gao R, Stock AM.** 2009. Biological insights from structures of two-component proteins. Annu Rev Microbiol **63:**133-154.

23. **Stock AM, Robinson VL, Goudreau PN.** 2000. Two-component signal transduction. Annu Rev Biochem **69:**183-215.

24. **Skerker JM, Prasol MS, Perchuk BS, Biondi EG, Laub MT.** 2005. Two-component signal transduction pathways regulating growth and cell cycle progression in a bacterium: a system-level analysis. PLoS Biol **3:**e334.

25. **Yildiz FH, Dolganov NA, Schoolnik GK.** 2001. VpsR, a Member of the Response Regulators of the Two-Component Regulatory Systems, Is Required for Expression of vps Biosynthesis Genes and EPS(ETr)-Associated Phenotypes in *Vibrio cholerae* O1 El Tor. J Bacteriol **183:**1716-1726.

26. **Casper-Lindley C, Yildiz FH.** 2004. VpsT is a transcriptional regulator required for expression of *vps* biosynthesis genes and the development of rugose colonial morphology in *Vibrio cholerae* O1 El Tor. J Bacteriol **186:**1574-1578.

27. **Pratt JT, McDonough E, Camilli A.** 2009. PhoB regulates motility, biofilms, and cyclic di-GMP in *Vibrio cholerae*. J Bacteriol **191:**6632-6642.

28. **Ng WL, Bassler BL.** 2009. Bacterial quorum-sensing network architectures. Annu Rev Genet **43:**197-222.

29. **Hammer BK, Bassler BL.** 2003. Quorum sensing controls biofilm formation in *Vibrio cholerae*. Mol Microbiol **50:**101-104.

30. **Lenz DH, Mok KC, Lilley BN, Kulkarni RV, Wingreen NS, Bassler BL.** 2004. The small RNA chaperone Hfq and multiple small RNAs

control quorum sensing in *Vibrio harveyi* and *Vibrio cholerae*. Cell **118:**69-82.

31. **Tsou AM, Liu Z, Cai T, Zhu J.** 2011. The VarS/VarA two-component system modulates the activity of the *Vibrio cholerae* quorum-sensing transcriptional regulator HapR. Microbiology **157:**1620-1628.

32. **Bilecen K, Fong JC, Cheng A, Jones CJ, Zamorano-Sanchez D, Yildiz FH.** 2015. Polymyxin B Resistance and biofilm formation in *Vibrio cholerae* is controlled by the response regulator CarR. Infect Immun doi:10.1128/IAI.02700-14.

33. **McKee RW, Kariisa A, Mudrak B, Whitaker C, Tamayo R.** 2014. A systematic analysis of the in vitro and in vivo functions of the HD-GYP domain proteins of *Vibrio cholerae*. BMC Microbiol **14:**272.

34. **Lim B, Beyhan S, Meir J, Yildiz FH.** 2006. Cyclic-diGMP signal transduction systems in *Vibrio cholerae*: modulation of rugosity and biofilm formation. Mol Microbiol **60:**331-348.

35. **Lefebvre B, Formstecher P, Lefebvre P.** 1995. Improvement of the gene splicing overlap (SOE) method. Biotechniques **19:**186-188.

36. **Beyhan S, Bilecen K, Salama SR, Casper-Lindley C, Yildiz FH.** 2007. Regulation of rugosity and biofilm formation in *Vibrio cholerae*: comparison of VpsT and VpsR regulons and epistasis analysis of *vpsT*, *vpsR*, and *hapR*. J Bacteriol **189:**388-402.

37. **Heydorn A, Nielsen AT, Hentzer M, Sternberg C, Givskov M, Ersboll BK, Molin S.** 2000. Quantification of biofilm structures by the novel computer program COMSTAT. Microbiology **146 (Pt 10):**2395-2407.

38. **Robinson MD, McCarthy DJ, Smyth GK.** 2010. edgeR: a Bioconductor package for differential expression analysis of digital gene expression data. Bioinformatics **26:**139-140.

39. **Herrero M, de Lorenzo V, Timmis KN.** 1990. Transposon vectors containing non-antibiotic resistance selection markers for cloning and stable chromosomal insertion of foreign genes in gram-negative bacteria. J Bacteriol **172:**6557-6567.

40. **de Lorenzo V, Timmis KN.** 1994. Analysis and construction of stable phenotypes in gram-negative bacteria with Tn5- and Tn10-derived minitransposons. Methods Enzymol **235:**386-405.

41. **Yildiz FH, Liu XS, Heydorn A, Schoolnik GK.** 2004. Molecular analysis of rugosity in a *Vibrio cholerae* O1 El Tor phase variant. Mol Microbiol **53:**497-515.

42. **Beyhan S, Tischler AD, Camilli A, Yildiz FH.** 2006. Transcriptome and phenotypic responses of *Vibrio cholerae* to increased cyclic di-GMP level. J Bacteriol **188:**3600-3613.

43. **Shikuma NJ, Fong JC, Odell LS, Perchuk BS, Laub MT, Yildiz FH.** 2009. Overexpression of VpsS, a hybrid sensor kinase, enhances biofilm formation in *Vibrio cholerae*. J Bacteriol **191:**5147-5158.

44. **Cheng AT, Ottemann KO, Yildiz FH.** 2015. *Vibrio cholerae* response regulator VxrB controls colonization and regulates the Type VI secretion system. PLoS Pathog.

45. **Beyhan S, Tischler AD, Camilli A, Yildiz FH.** 2006. Differences in gene expression between the classical and El Tor biotypes of *Vibrio cholerae* O1. Infect Immun **74:**3633-3642.

46. **Bao Y, Lies DP, Fu H, Roberts GP.** 1991. An improved Tn7-based system for the single-copy insertion of cloned genes into chromosomes of gram-negative bacteria. Gene **109:**167-168.

47. **Hammer BK, Bassler BL.** 2007. Regulatory small RNAs circumvent the conventional quorum sensing pathway in pandemic Vibrio cholerae. Proc Natl Acad Sci U S A **104:**11145-11149.

48. **Shikuma NJ, Fong JC, Yildiz FH.** 2012. Cellular levels and binding of c-di-GMP control subcellular localization and activity of the *Vibrio cholerae* transcriptional regulator VpsT. PLoS Pathog **8:**e1002719.

49. **Butler SM, Camilli A.** 2004. Both chemotaxis and net motility greatly influence the infectivity of *Vibrio cholerae*. Proc Natl Acad Sci U S A **101:**5018-5023.

50. **Butler SM, Camilli A.** 2005. Going against the grain: chemotaxis and infection in *Vibrio cholerae*. Nat Rev Microbiol **3:**611-620.

51. **Hussa EA, O'Shea TM, Darnell CL, Ruby EG, Visick KL.** 2007. Two-component response regulators of *Vibrio fischeri*: identification, mutagenesis, and characterization. J Bacteriol **189:**5825-5838.

52. **Kobayashi K, Ogura M, Yamaguchi H, Yoshida K, Ogasawara N, Tanaka T, Fujita Y.** 2001. Comprehensive DNA microarray analysis of *Bacillus subtilis* two-component regulatory systems. J Bacteriol **183:**7365-7370.

53. **Lange R, Wagner C, de Saizieu A, Flint N, Molnos J, Stieger M, Caspers P, Kamber M, Keck W, Amrein KE.** 1999. Domain organization and molecular characterization of 13 two-component systems identified by genome sequencing of *Streptococcus pneumoniae*. Gene **237:**223-234.

54. **Throup JP, Koretke KK, Bryant AP, Ingraham KA, Chalker AF, Ge Y, Marra A, Wallis NG, Brown JR, Holmes DJ, Rosenberg M, Burnham MK.** 2000. A genomic analysis of two-component signal transduction in *Streptococcus pneumoniae*. Mol Microbiol **35:**566-576.

55. **Yamamoto K, Hirao K, Oshima T, Aiba H, Utsumi R, Ishihama A.** 2005. Functional characterization in vitro of all two-component signal transduction systems from *Escherichia coli*. J Biol Chem **280:**1448-1456.

56. **Southey-Pillig CJ, Davies DG, Sauer K.** 2005. Characterization of temporal protein production in *Pseudomonas aeruginosa* biofilms. J Bacteriol **187:**8114-8126.

57. **Zhang L, Hinz AJ, Nadeau JP, Mah TF.** 2011. *Pseudomonas aeruginosa tssC1* links type VI secretion and biofilm-specific antibiotic resistance. J Bacteriol **193:**5510-5513.

58. **Heckel BC, Tomlinson AD, Morton ER, Choi JH, Fuqua C.** 2014. *Agrobacterium tumefaciens exoR* controls acid response genes and impacts exopolysaccharide synthesis, horizontal gene transfer, and virulence gene expression. J Bacteriol **196:**3221-3233.

59. **Aubert DF, Flannagan RS, Valvano MA.** 2008. A novel sensor kinase-response regulator hybrid controls biofilm formation and type VI secretion system activity in *Burkholderia cenocepacia*. Infect Immun **76:**1979-1991.

PERSPECTIVES

There has been seven pandemics of cholera caused by pathogenic *Vibrio cholerae* strains (1). Cholera is considered a re-emerging global health problem, as there is a resurgence of cholera cases around the world (2, 3). Therefore, it is important to continue investigating the molecular mechanism of *V. cholerae* pathogenicity and transmission and environmental survival.

Two-component signal transduction systems (TCS) has been widely characterized in bacteria. TCS global characterization studies have been performed in other organisms such as *Vibrio fisheri* and *Enterococcus faecalis*. All RRs in *V. fisheri* have been characterized for their role in bioluminescence, motility, and colonization of squid (4). This study provided a wealth of information regarding the roles of *V. fischeri* RRs in establishing the symbiosis between *V. fischeri* and squid. Phenotypic characterization of *E. faecalis* TCS identified RRs related to antibiotic resistance and environmental stress (5). Therefore, global characterization of TCS can reveal further insights into the molecular players use to regulate critical cellular processes.

TCS are likely to be important for adaptation of *V. cholerae* to different environments. Before my studies, little was known about how TCS affects biofilm formation and virulence of *V. cholerae* at the molecular level. I

characterized all 53 response regulators (RR) in *V. cholerae* for their involvement in virulence and biofilm formation. These studies provided new insights into how *V. cholerae* senses and responds to environmental factors and advanced our knowledge of the mechanism by which *V. cholerae* proliferates in both human hosts and aquatic environments.

My systematic analysis of each RR in *V. cholerae* revealed that there were uncharacterized RRs important for *V. cholerae*'s dual lifestyle as a facultative human pathogen. One of these is VxrB. VxrB controls colonization in the infant mouse model and regulates the type VI secretion system. In addition to virulence, we showed that VxrB plays an important role in biofilm formation. Future work might focus on how the VxrAB TCS facilitates survival and transmission when *V. cholerae* transitions between human and aquatic environments. It will be interesting to determine the signal(s) sensed by the HK, VxrA, which activate VxrB to in turn regulate colonization and/or biofilm formation. Finally, understanding if/how T6SS plays a role in biofilm formation in *V. cholerae* is also important to understand.

Another RR that we found to play a surprising role in biofilm formation in NtC. The identification of NtrC as a repressor of biofilm formation in *V. cholerae* raises interesting questions on how nutrients may affect biofilm formation. Our studies will lead to a further investigation of how carbon-nitrogen ratios impact

biofilm formation. Studies in *Citrobacter* and *Enterobacter* have identified how carbon, nitrogen, and phosphate ratios influence biofilm formation (6). Thus, it is likely that changes in carbon-nitrogen ratios can similarly impact *V. cholerae*'s ability to form biofilms.

Characterizing the role of TCS in biofilm formation and virulence can help develop targets for antimicrobial strategies in *V. cholerae* (7). Drugs that can specifically disrupt a TCS pathway in biofilm formation in *V. cholerae* will be useful when the pathogen leaves the host unable to form biofilms and not survive in the environment. Since cholera victims shed hyper-virulent biofilms during infection (8), these drugs can possibly prevent the spread of hyper-virulent *V. cholerae* biofilms in developing countries and potentially reduce outbreaks.

In summary, our results highlight the importance of a global approach for investigating gene function in *V. cholerae*. These studies have provided valuable information regarding the roles of *V. cholerae* RRs in biofilm formation which will serve as a starting point for understanding the connections between these RR and their impact on the physiological traits.

References

1. **Faruque SM, Albert MJ, Mekalanos JJ.** 1998. Epidemiology, genetics, and ecology of toxigenic *Vibrio cholerae*. Microbiol Mol Biol Rev **62:**1301-1314.

2. **Chin CS, Sorenson J, Harris JB, Robins WP, Charles RC, Jean-Charles RR, Bullard J, Webster DR, Kasarskis A, Peluso P, Paxinos EE, Yamaichi Y, Calderwood SB, Mekalanos JJ, Schadt EE, Waldor MK.** 2011. The origin of the Haitian cholera outbreak strain. N Engl J Med **364:**33-42.

3. **Diaz-Quinonez A, Hernandez-Monroy I, Montes-Colima N, Moreno-Perez A, Galicia-Nicolas A, Martinez-Rojano H, Carmona-Ramos C, Sanchez-Mendoza M, Rodriguez-Martinez JC, Suarez-Idueta L, Jimenez-Corona ME, Ruiz-Matus C, Kuri-Morales P, Centers for Disease C, Prevention.** 2014. Outbreak of *Vibrio cholerae* serogroup O1, serotype Ogawa, biotype El Tor strain--La Huasteca Region, Mexico, 2013. MMWR Morb Mortal Wkly Rep **63:**552-553.

4. **Hussa EA, O'Shea TM, Darnell CL, Ruby EG, Visick KL.** 2007. Two-component response regulators of *Vibrio fischeri*: identification, mutagenesis, and characterization. J Bacteriol **189:**5825-5838.

5. **Hancock LE, Perego M.** 2004. The *Enterococcus faecalis* fsr two-component system controls biofilm development through production of gelatinase. J Bacteriol **186:**5629-5639.

6. **Thompson LJ, Gray V, Lindsay D, von Holy A.** 2006. Carbon : nitrogen : phosphorus ratios influence biofilm formation by Enterobacter cloacae and *Citrobacter freundii*. J Appl Microbiol **101:**1105-1113.

7. **Stephenson K, Hoch JA.** 2002. Two-component and phosphorelay signal-transduction systems as therapeutic targets. Current Opinion in Pharmacology **2:**507-512.

8. **Tamayo R, Patimalla B, Camilli A.** 2010. Growth in a biofilm induces a hyperinfectious phenotype *in Vibrio cholerae*. Infect Immun **78:**3560-3569.